UNIVERSITY OF SALFORD

DEPARTMENT OF AERONAUTICAL AND MECHANICAL ENGINEERING

TRANSIENT RESPONSE PERFORMANCE OF AN ENGINE TURBOCHARGER

BY

SUHAIL ABDUL EMIR, BSc (HONS)(BAGHDAD, IRAQ)

MSc (UMIST)

A THESIS PRESENTED FOR THE

DEGREE OF PHD

MARCH 1981

To My Wife, Hana

and My Two Daughters, Asrah and Ala

C O N T E N T S

	Page
ACKNOWLEDGEMENT	i
SUMMARY	ii
LIST OF FIGURES AND PLATES	iv
NOTATION	viii
COMPUTER PROGRAMS NOMENCLATURE	xi
CHAPTER ONE	
INTRODUCTION	1
1.1 Supercharging	2
1.2 Turbocharging System	5
1.3 Advantages and Disadvantages of turbocharging	8
1.3.1 Advantages	8
1.3.2 Disadvantages	10
CHAPTER TWO	
LITERATURE SURVEY	13
CHAPTER THREE	
EXPERIMENTAL EQUIPMENT	29
3.1 The Experimental Test Rig	29
3.2 Turbocharger	32
3.3 Turbocharger Lubrication System	32
3.4 Combustion Chamber	35
3.5 Pulse Generator	36
CHAPTER FOUR	
INSTRUMENTATION	47
4.1 Pressure Measurements	47

Page

4.2 Mass Flow Rate Measurements 54

4.3 Temperature Measurements 56

4.4 Speed Measurements 58

4.5 Interface Unit 58

CHAPTER FIVE

EXPERIMENTAL PROCEDURE 70

5.1 Pulse Generator Valve Opening Area 70

5.2 Pulse Generator Coefficient of Discharge 78

5.3 Turbocharger Moment of Inertia 86

5.4 Turbocharger Bearing Power Loss 88

5.5 Turbine Exhaust System Flow Losses 93

5.6 Compressor Loading Nozzle Characteristics 93

5.7 Transient Tests 95

CHAPTER SIX

THEORY AND COMPUTATION 105

6.1 Objective 105

6.2 Assumptions 106

6.3 Predicting the Transient Response Performance of the Turbocharger under Non-Pulsating Flow Conditions 106

6.4 Predicting the Transient Response Performance of the Turbocharger under Pulsating Flow Conditions 119

6.4.1 Method 1 119

6.4.2 Method 2 124

Page

6.5 The Flow in the Pipes 128

6.6 Turbocharger Bearing Power Loss 137

6.7 Evaluation of Turbine and Compressor Parameters from Steady State Characteristics 139

6.7.1 Method A 139

6.7.2 Method B 141

6.8 Computer Programs 143

CHAPTER SEVEN

DISCUSSION OF RESULTS 146

7.1 Test Series I 147

7.1.1 Turbine Mass Flow Rate and Pressure Ratio 148

7.1.2 Turbine Inlet Temperature 149

7.1.3 Turbocharger Speed 150

7.1.4 Compressor Mass Flow Rate and Pressure Ratio 151

7.2 Test Series II 152

7.2.1 Experimentally 152

7.2.2 Theoretically 153

7.2.3 Form of the Transients 154

7.2.4 Criteria for Assessing the Results 155

7.2.5 Factors Affecting the Accuracy of the Results 156

7.2.6 Comparison between Experimental and Predicted Results 157

		Page
7.3 General Discussion		159
CHAPTER EIGHT		
CONCLUSIONS		220
CHAPTER NINE		
RECOMMENDATIONS FOR FUTURE WORK		222
REFERENCES		223
APPENDIX 1	UNSTEADY FLOW DISCHARGE COEFFICIENT FOR ORIFICE PLATE	228
APPENDIX 2	MEASURING MASS FLOW RATE BY BS1042	242
APPENDIX 3	TURBINE AND COMPRESSOR STEADY STATE CHARACTERISTICS	243
APPENDIX 4	COMPRESSOR LOADING NOZZLE MASS FLOW CHARACTERISTICS	246
APPENDIX 5	LAGRANGE INTERPOLATION	249
APPENDIX 6	SUBROUTINES	251
	SUBROUTINE TSCHAR	251
	SUBROUTINE TEFFCH	253
	SUBROUTINE CCHAR	254
	SUBROUTINE PIPES	255
	SUBROUTINE CFTINT	256
	SUBROUTINE VAREA	257
APPENDIX 7	FLOW CHARTS	
	PROGRAM "NON-PULSATING"	258
	PROGRAM "PULSATING1"	263
	PROGRAM "PULSATING2"	267
	SUBROUTINES	270

		Page
APPENDIX 8	LISTINGS OF THE PROGRAMS AND SUBROUTINES	
	PROGRAM "NON-PULSATING"	277
	PROGRAM "PULSATING1"	281
	PROGRAM "PULSATING2"	286
	SUBROUTINES	289
APPENDIX 9	COMPUTER PROGRAMS INPUT DATA	
	PROGRAM "PULSATING1" INPUT DATA	298
	PROGRAM "PULSATING2" INPUT DATA	308
	PROGRAM "NON-PULSATING" INPUT DATA	311

A C K N O W L E D G E M E N T S

I wish to express my thanks to my Supervisor, Mr G.P.Mitchell, for his guidance and helpful suggestions throughout the work.

My thanks are also due to Professor J.L.Livesey for his thoughtful help and encouragement and for the provision of research facilities.

I am thankful to the Government of the Republic of Iraq for financial support during the first part of this work.

I should like to thank Mr R.McKissack for his assistance and to the staff of the Thermodynamics, Gas Dynamics and Instrumentation Laboratoriesfor their help especially to Messrs. J.Thorpe, A.Barber and A.Ward.

My thanks are due to Mr A.E.Seaborn who traced some of the figures and Mrs B.A.Rand for typing this thesis.

Finally, I am most grateful to my wife for her unceasing encouragement and patience during the years of study.

SUMMARY

This thesis is concerned with predicting the transient response performance of an exhaust gas turbocharger under pulsating and non-pulsating flow conditions.

Using the measured steady state characteristics of the turbocharger compressor and turbine, theoretical procedures are developed to predict its transient response during rapid variations in the turbine inlet conditions. A computer program has been written for non-pulsating and two other programs for pulsating flow conditions. Each of these programs used a different method of predicting the response. The programs, with their subroutines and the organization of the calculations, and experimental data are presented.

To enable the computer predicted results to be compared with experimental results, an experimental program was carried out on a Holset 3LD turbocharger. The layout and the principal features of the experimental test rig, which is designed to operate the turbocharger from a compressed air supply, are described. The rig may be used to simulate engine exhaust conditions.

The computer predicted results are compared with the experimental ones obtained from tests during pulsating

and non-pulsating operation of the turbocharger. The experimental results and theoretical predictions are found to compare favourably, and the possible causes of discrepancies are suggested. Suggestions are made for further work.

LIST OF FIGURES AND PLATES

FIGURES		Page
1.1	Superchargers	4
3.1	The Experimental Test Rig (Test Series I)	25
3.2	The Experimental Test Rig (Test Series II)	26
3.3	Constructional Arrangement of the Compressor Loading Nozzle	31
3.4	Cross Section of Holset 3LD Turbo-charger	33
3.5	Lubrication Circuit	34
3.6	Diagrammatic Plan View of Pulse Generator	37
3.7	Cross Section Through The Pulse Generator	38
3.8	Non-Return Valve	40
4.1	Diagrammatic Layout of Measuring Instruments (Test Series I)	48
4.2	Diagrammatic Layout of Measuring Instruments (Test Series II)	53
4.3	Wheatstone Bridge Circuit For Measuring Turbine Inlet Temperature	57
4.4	Probe Temperature vs Galvanometer Deflection	59
4.5	Turbocharger Photo-Electric Speed Measurement System	60
4.6	Thermocouple Amplifier Circuit	63
4.7	Pressure Transducer Amplifier Circuit	64
5.1	Diagrammatic Layout of Cam Test Apparatus	71
5.2	Pulse Generator Valve Positions	72
5.3.	Pulse Generator Valve Opening Area	77

Page

5.4 Steady Flow Rig For Measuring Pulse Generator Valve Coefficient of Discharge 81

5.5 Variation of Pulse Generator Valve Coefficient of Discharge with Valve Lift 84

5.6 Measuring Instruments to Measure 90

TEST A: Turbocharger Bearing Power Loss

TEST B: Turbine Exhaust System Flow Losses

TEST C: Compressor Loading Nozzle Mass Characteristic

5.7 Turbocharger Bearing Power Loss vs Turbocharger Speed 92

5.8 Turbine Exhaust System Flow Losses vs Volume Flow Rate 94

5.9 Nozzle Mass Characteristics 96

6.1 Transient Variations at the Turbine Inlet 108

6.2 Superimposition of a transient on the Turbine Mass Characteristics 110

6.3 Turbine Mass Characteristics 111

6.4 Turbine Efficiency Characteristics 113

6.5 Compressor Steady Characteristics 115

6.6 Sequence of predicting turbine and compressor operating points (section 6.3) 120

6.7 Sequence of predicting turbine and compressor operating points (section 6.4.2) 129

6.8 Filling and emptying operations 132

6.9 Interpolation Method - A 140

6.10 Interpolation Method - B 142

Page

TEST SERIES I

7.1-7.3 Turbocharger speed during non-pulsating transient 161-163

7.4-7.6 Turbine mass flow rate during non-pulsating transient 164-166

7.7-7.9 Compressor pressure ratio during non-pulsating transient 167-169

7.10-7.12 Compressor mass flow rate during non-pulsating transient 170-172

7.13-7.15 Turbocharger speed during pulsating transient 173-175

7.16-7.18 Turbine pressure ratio during pulsating transient 176-178

7.19-7.21 Turbine mass flow rate during pulsating transient 179-181

7.22-7.24 Turbine inlet temperature during pulsating transient 182-184

7.25-7.27 Compressor pressure ratio during pulsating transient 185-187

7.28-7.30 Compressor mass flow rate during pulsating transient 188-190

TEST SERIES II

7.31-7.33 Compressor mass flow rate during non-pulsating transient 191-193

7.34-7.36 Compressor pressure ratio during non-pulsating transient 194-196

7.37-7.39 Turbine mass flow rate during non-pulsating transient 197-199

7.40-7.42 Turbocharger speed during non-pulsating transient 200-202

7.43-7.45 Compressor mass flow rate during pulsating transient-25 pulses/sec 203-205

7.46-7.48 Compressor pressure ratio during pulsating transient-25 pulses/sec 206-208

7.49-7.51 Compressor mass flow rate during pulsating transient 38 pulses/sec 209-211

		Page
7.52-7.54	Compressor pressure ratio during pulsating transient 38 pulses/sec	212-214
7.55-7.57	Turbine mass flow rate during pulsating transient 38 pulses/sec	215-217
7.58	Compressor mass flow rate at different permitted error	218
7.59	Compressor pressure ratio at different permitted error	219

PLATES

1.	The Experimental Test Rig	42
2.	The Experimental Test Rig	43
3.	The Turbocharger	44
4.	The Pulse Generator During non-pulsating transient operation	45
5.	The Pulse Generator During pulsating transient operation	46
6.	Instrumentation - Test Series I	65
7.	Instrumentation - Test Series II	66
8.	Orifice plate at turbine exhaust	67
9.	Orifice plate at compressor inlet	68
10.	The resistance wire probe with balanced Wheatstone Bridge	69
11.	Three way valve	102
12.	Sample of the UV recorder trace under pulsating transient test conditions	103
13.	Sample of the UV recorder trace under non-pulsating transient test conditions	104

NOTATION

Symbol	Description	Units
c	Particle velocity of the gas	m/sec
c_d	Coefficient of discharge of the pulse generator valve under steady conditions	
c_{dp}	Coefficient of discharge of the orifice plate under transient conditions	
c_p	Specific heat of air at constant pressure	kJ/kg K
Cpg	Specific heat of gas at constant pressure	kJ/kg K
F	Area	m^2
F_v	Pulse generator valve opening area	m^2
h	Specific enthalpy	kJ/kg
I	Turbocharger moment of inertia	kg m^2
$\dot{m}$	Mass flow rate	kg/sec
N	Rotational speed of turbocharger	rpm
P	Absolute pressure	bar
PW_c	Compressor power input	kW
PW_t	Turbine power output	kW
$\dot{Q}$	Rate of heat transfer	kW
R	Characteristic gas constant	kJ/kg K
T	Absolute temperature	K
$\dot{W}$	Rate of work transfer	kW
V	Exhaust system volume	m^3
u	Specific internal energy in the absence of motion, gravity, etc	kJ/kg

GREEK LETTER SYMBOLS

Symbol	Description	Units
γ	Ratio of specific heats for air	
γ_g	Ratio of specific heats for gas	
η_c	Compressor isentropic efficiency	
η_t	Turbine isentropic efficiency	
η_m	Turbocharger mechanical efficiency	
$\eta_{t/c}$	Overall turbocharger efficiency ($= \eta_m \eta_t \eta_c$)	
ω	Angular velocity of the turbocharger	rad/sec
ρ	Density	kg/m^3
Δt	Small time interval	sec

SUFFICES

a	Orifice plate throat conditions
c	Compressor
e	Orifice plate upstream conditions
isen	Isentropic
n	Conditions of the flow at the instant of calculation
n+1	Conditions of the flow after a time step (Δt)
s	Exhaust system
t	Turbine
u	Conditions immediately upstream of the pulse generator valve
v	Conditions immediately downstream of the pulse generator valve
v_1, v_2, v_3	First, second and third pulse generator valve

z	Compressor loading nozzle
1	Conditions at compressor inlet
2	Conditions at compressor outlet
3	Conditions at turbine inlet
4	Conditions at turbine outlet

COMPUTER PROGRAM NOMENCLATURE

NAME	VARIABLE TYPE	DEFINITION	UNITS
ACDG	ARRAY	C_d, pulse generator valve coefficient of discharge (Input Data)	-
AFG	ARRAY	Pulse generator valve opening area (Input Data)	m^2
AI	REAL	I, turbocharger moment of inertia (Input Data)	kg m^2
AMA	REAL	$\dot{m}_c$, compressor mass flow rate	kg/sec
AMAP	REAL	$\dot{m}_c$, compressor mass flow rate (temporary storage)	kg/sec
AMASTO	REAL	$\dot{m}_c$, compressor mass flow rate (temporary storage)	kg/sec
AMFP	REAL	$\dot{m}_t \sqrt{T_3}/P_3$, turbine mass flow parameter	$kg\sqrt{K}/sec\ bar$
AMG	REAL	$\dot{m}_t$, turbine mass flow rate	kg/sec
AMGTEST	REAL	$\dot{m}_t$, turbine mass flow rate (temporary storage)	kg/sec
ANDRT3	REAL	$N/\sqrt{T_3}$, turbocharger speed parameter	$rpm/\sqrt{K}$
BFG	ARRAY	Pulse generator valve opening area (Input Data)	m^2
BTIME	ARRAY	Pulse generator valve cycle time (Input Data)	sec
CEFF	REAL	η_c, comprssor efficiency	-
CP	REAL	C_p, specific heat at constant pressure (Input Data)	kJ/kg K
CSPED	REAL	N, turbocharger speed	rpm
CSPEDD	ARRAY	N, turbocharger speed (Input Data)	rpm
CSPEDN	REAL	N, turbocharger speed (temporary storage)	rpm
DEN	REAL	ρ, air density	kg/m^3
DENR	REAL	$\rho^{\frac{1}{2}}$, square root of ρ	$(kg/m^3)^{\frac{1}{2}}$

NAME	VARIABLE TYPE	DEFINITION	UNITS
DM	REAL	Increment mass flow rate	kg/sec
DPL	REAL	ΔPL, turbine exhaust system flow losses	bar
Δt	REAL	Δ_t, time step (Input Data)	sec
ERROR	REAL	Permitted error of iterative procedures	-
GAM	REAL	γ, ratio of specific heats (Input Data)	-
GAM1	REAL	$\gamma-1$	-
GASR	REAL	R, characteristic gas constant	kJ/kg K
MEFF	REAL	η_m, turbocharger mechanical efficiency	-
NTM	INTEGER	Number of data points for valve opening areas against valve coefficients of discharge (Input Data)	-
NTN	INTEGER	Number of data points for pulse generator valves cycle time against pulse generator valves opening areas (Input Data)	-
PCN	REAL	$(PW_c)_n$, compressor power	kW
PCNP1	REAL	$(PW_c)_{n+1}$, compressor power after a time step	kW
PG	REAL	P_u, pulse generator input pressure (Input Data)	bar
PTN	REAL	$(PW_t)_n$, turbine power	kW
PTNP1	REAL	$(PW_t)_{n+1}$, turbine power after a time step	kW
PO	REAL	P_o, atmospheric pressure	bar
PTS	REAL	Turbocharger power at steady state condition	kW
PW	REAL	Turbocharger power at transient operation	kW

NAME	VARIABLE TYPE	DEFINITION	UNITS
PWB	REAL	Turbocharger bearing power loss	kW
P2DP1	REAL	P_2/P_1, compressor pressure ratio	-
P3	REAL	P_3, turbine inlet pressure	bar
P3DPO	REAL	P_3/P_4, turbine expansion pressure ratio	-
P3DPOD	ARRAY	P_3/P_4, turbine expansion pressure ratio(Input Data)	-
P3NP1	REAL	$(P_3)_{n+1}$, turbine inlet pressure after a time step	bar
P4	REAL	P_4, turbine outlet pressure	bar
RT3	REAL	$\sqrt{T_3}$, square root of turbine inlet temperature	$\sqrt{K}$
SPDN	REAL	$(N)_n$, turbocharger speed	rpm
SPDNP1	REAL	$(N)_{n+1}$, turbocharger speed after a time step	rpm
STEP	REAL	Increment mass flow rate	kg/S
TCYCLE	REAL	Time required for one pulse generator valve opening cycle	sec
TEFF	REAL	η_t, turbine efficiency	-
TESTIM	REAL	Time interval	sec
TG	REAL	T_u, pulse generator input temperature	K
TIM	REAL	Time at the instant of calculation	sec
TIMED	ARRAY	t, time (Input Data)	sec
TMAX	REAL	t_{max}, calculation time required	sec
TSTART	REAL	Calculation starting time	sec
T1	REAL	T_1, compressor inlet temperature (Input Data)	K

NAME	VARIABLE TYPE	DEFINITION	UNITS
T2	REAL	T_2, compressor outlet temperature	K
T2P	REAL	T_2', compressor isentropic outlet temperature	K
T3	REAL	T_3, turbine inlet temperature	K
T3D	REAL	T_3, turbine inlet temperature (Input Data)	K
T3NP1	REAL	$(T_3)_{n+1}$, turbine inlet temperature after a time step	K
T4	REAL	T_4, turbine outlet temperature	K
T4P	REAL	T_4', turbine isentropic outlet temperature	K
VOLFR4	REAL	Volume Flow rate at the turbine outlet	m^3/sec
VS	REAL	V_s, exhaust system volume	m^3
XA	ARRAY*	$\dot{m}_c$, compressor mass flow rate	kg/sec
XAMFP	ARRAY**	$\dot{m}_t\sqrt{T_3}/P_3$, turbine mass flow parameter	$kg\sqrt{K}/sec\ bar$
XAMO	ARRAY****	$\dot{m}_z/\rho_2^{\frac{1}{2}}$, compressor loading nozzle mass flow rate divided by square root of density	$\frac{kg/sec}{\sqrt{kg/m^3}}$
XCE	ARRAY*	η_c, compressor efficiency	-
XCS	ARRAY*	N, turbocharger speed	rpm
XN	ARRAY***	$N/\sqrt{T_3}$, turbocharger speed parameter	$rpm/\sqrt{K}$
XNRT3	ARRAY**	$N/\sqrt{T_3}$, turbocharger speed parameter	$rpm/\sqrt{K}$
XP	ARRAY***	P_3/P_4, turbine pressure ratio	-
XPC	ARRAY**	P_2/P_1, compressor pressure ratio	-

NAME	VARIABLE TYPE	DEFINITION	UNITS
XP2	ARRAY****	P_2, compressor loading nozzle inlet pressure	bar
XP3DPO	ARRAY**	P_3/P_4, turbine pressure ratio	-
XT	ARRAY***	η_t, turbine efficiency	

*	Input data for compressor steady characteristics
**	Input data for turbine mass characteristics
***	Input data for turbine efficiency characteristics
****	Input data for nozzle mass characteristics

CHAPTER ONE

INTRODUCTION

CHAPTER ONE

INTRODUCTION

The main factors which determine the power output of an internal combustion engine are its size, speed, compression ratio, operating cycle, and charge density. In order to get maximum power output for a given engine, different methods may be applied by changing the above factors.

The first method is to increase the engine speed. Increasing the engine speed will result in increasing its power output, but the maximum power is usually attained at a certain piston speed due to breathing limitations. High speed can also cause injection problems in diesel engines.

The second method of increasing the power output is to increase the compression ratio. In diesel engines the limitations on raising the compression ratio are often imposed by structural and economic factors. In many cases the maximum compression ratio usable in practice is limited because the maximum cylinder pressure also rises, and thus the mechanical stresses may increase so that the compression ratio may have to be restricted to prevent overstressing

components or designing an excessively heavy engine. The increase in maximum cylinder pressures with greater compression ratios also causes increased friction losses, thus counteracting the improvement in power and efficiency due to the improved thermodynamic cycle.

The third method is to decrease the air-fuel ratio, as the power developed by an engine is also controlled by the fuel flow rate. In a diesel engine, to prevent emission of smoke and excessive specific fuel consumption, the amount of fuel supplied is usually less than that which could have been burnt completely in the air which is available. Excess air is essential because an even mixing of the fuel and the air in the combustion chamber space is not possible. Consequently the amount of air available limits the power output.

The most effective method of increasing the work done in the engine cylinder is to increase the charge density of the air supplied so that more fuel may be burnt. The air is compressed mechanically in a supercharger.

1.1 SUPERCHARGING

There are three methods of compressing the air entering the engine.

(1) Independently driven compressors

The compressor may be powered by an auxiliary engine, electric motor or other prime mover, Fig (1.1a). These superchargers are sometimes used in stationary plants.

(2) Engine drivencompressors

These superchargers are a further development of the superchargers in (1) above. The disadvantage of this method of supercharging is that the supercharger absorbs some of the power developed by the engine. Fig (1.1b). There is a reduction in engine power output, and the specific fuel consumption of the engine may be greater than that of the naturally aspirated engine.

(3) Turbochargers

The advent of the turbochargers before World War I was a successful substitute for the superchargers being driven mechanically by the engine. Invention of turbocharging is credited to Dr Alfred Büchi[1], who carried out experiments as early as 1911, on this system originally called "Büchi supercharging". The World War I interrupted developments, but by the mid 1920's the method began to be applied to large marine engines and later to transportation applications.

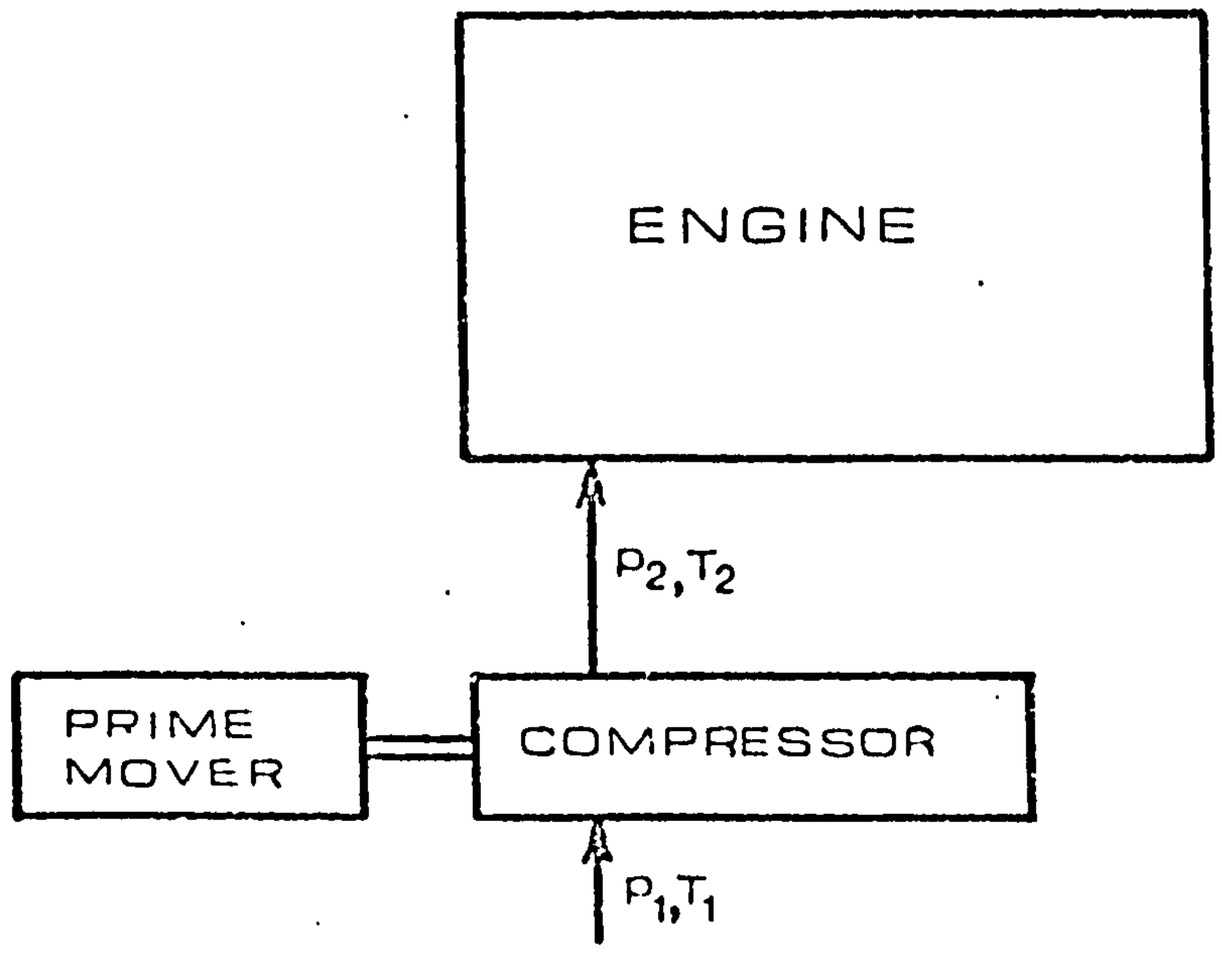

fig.(1.1a) INDEPENDENTALY DRIVEN COMPRESSORS

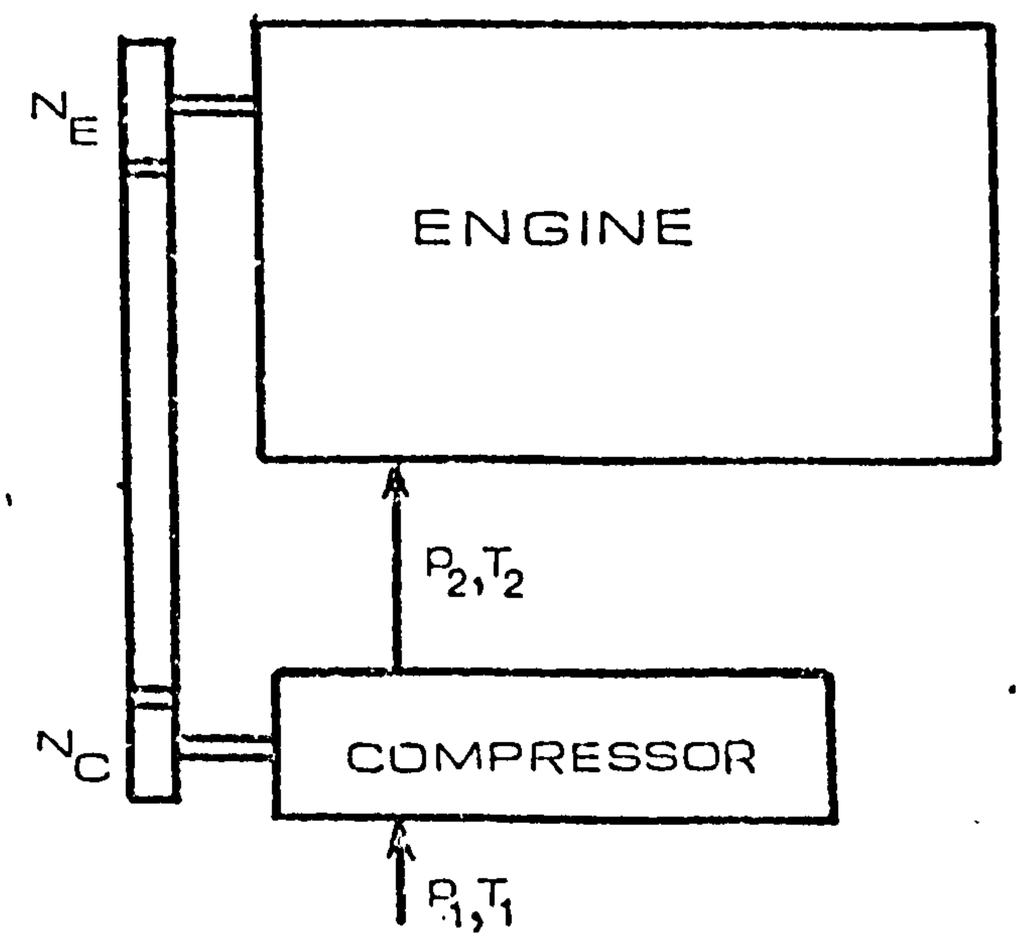

fig.(1.1b) ENGINE DRIVEN COMPRESSORS

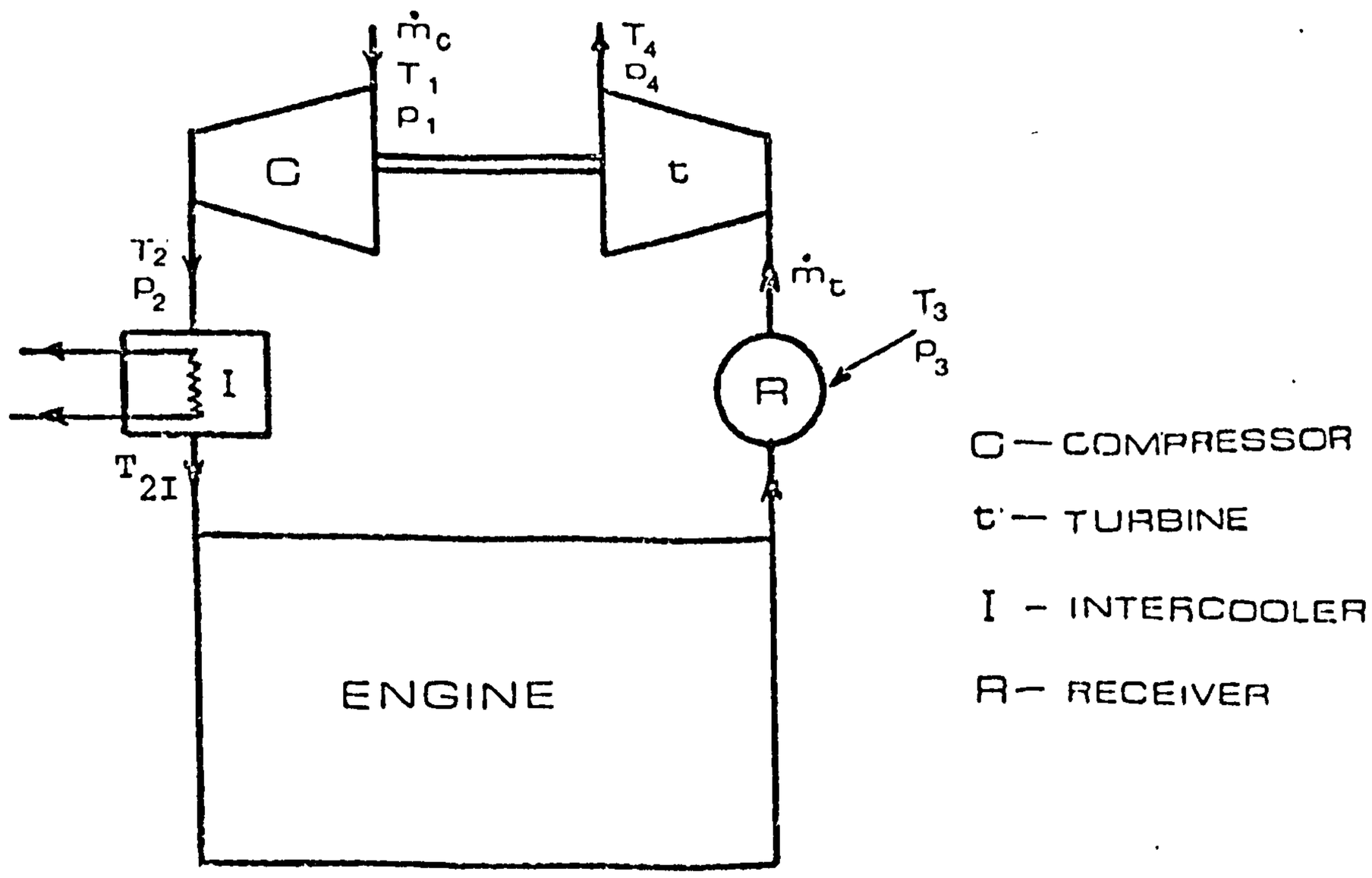

fig.(1.1c). SIMPLE TURBOCHARGER SYSTEM

fig.[1.1]. SUPERCHARGERS

1.2 TURBOCHARGING SYSTEM

A simple turbocharging system is shown in Fig (1.1c). Air from the atmosphere is compressed in compressor C from pressure P_1 to P_2 and temperature from T_1 to T_2. The air may then be cooled in the intercooler and then passed to the engine. Exhaust gas leaves the cylinders and enters a large manifold or receiver at a mean pressure P_3 and temperature T_3. It is then expanded in the turbine to the back pressure P_4. The turbine drives the compressor. The thermodynamic analysis uses the first law of thermodynamics for the control systems enclosing the turbine and the compressor separately.

When the turbine work equals the compressor work allowing for mechanical losses, the system is in equilibrium. If the turbine power is PW_t and the compressor power is PW_c then equilibrium is obtained when

$$PW_c = \eta_m PW_t \qquad \text{.. ..} \quad (1)$$

where η_m is the mechanical efficiency of the system. The mechanical losses are mainly bearing losses. Neglecting changes in air velocity the power required to drive the compressor is

$$PW_c = \dot{m}_c \Delta h = \dot{m}_c C_p \Delta T \qquad \text{.. ..} \quad (2)$$

and $\Delta T = T_2 - T_1$.

If the compressor efficiency is defined as

$$\eta_c = \frac{\text{isentropic temperature rise}}{\text{actual temperature rise}}$$

$$= \frac{T_2' - T_1}{T_2 - T_1} \qquad \ldots \ldots \quad (3)$$

where

$$T_2' = T_1 \left(\frac{P_2}{P_1}\right)^{\frac{\gamma-1}{\gamma}} . \qquad \ldots \ldots \quad (4)$$

Then the compressor power will be

$$PW_c = \frac{\dot{m}_c C_p T_1}{\eta_c} \left[\left(\frac{P_2}{P_1}\right)^{\frac{\gamma-1}{\gamma}} - 1 \right] \qquad \ldots \ldots \quad (5)$$

The turbine power, PW_t, is given by

$$PW_t = \dot{m}_t C_{pg} (T_3 - T_4) . \qquad \ldots \ldots \quad (6)$$

As the isentropic temperature T_4', due to expansion from P_3 to P_4 from temperature T_3 is given by

$$T_4' = T_3 \left(\frac{P_4}{P_3}\right)^{\frac{\gamma_g-1}{\gamma_g}} \qquad \ldots \ldots \quad (7)$$

and the isentropic efficiency of the turbine is defined as

$$\eta_t = \frac{\text{actual enthalpy drop}}{\text{isentropic enthalpy drop}}$$

$$= \frac{T_3 - T_4}{T_3 - T_4'} \qquad \ldots \ldots \quad (8)$$

then the work done by the turbine is

$$PW_t = \dot{m}_t \, \eta_t \, C_{pg} \, T_3 \left[1 - \left(\frac{P_4}{P_3}\right)^{\frac{\gamma_g - 1}{\gamma_g}} \right] . \qquad \ldots \ldots \quad (9)$$

At equilibrium, when $PW_c = \eta_m \, PW_t$,

$$\frac{\dot{m}_c C_p T_1}{\eta_c} \left[\left(\frac{P_2}{P_1}\right)^{\frac{\gamma-1}{\gamma}} - 1 \right] = \eta_t \eta_m \dot{m}_t C_{pg} T_3 \left[1 - \left(\frac{P_4}{P_3}\right)^{\frac{\gamma_g - 1}{\gamma_g}} \right]$$

or

$$\eta_m \eta_t \eta_c = \left(\frac{\dot{m}_c}{\dot{m}_t}\right) \left(\frac{C_p}{C_{pg}}\right) \left(\frac{T_1}{T_3}\right) \frac{\left[\left(\frac{P_2}{P_1}\right)^{\frac{\gamma-1}{\gamma}} - 1 \right]}{\left[1 - \left(\frac{P_4}{P_3}\right)^{\frac{\gamma_g - 1}{\gamma_g}} \right]} . \qquad \ldots \ldots \quad (10)$$

The term $\eta_m \eta_t \eta_c$ is called the overall turbocharger efficiency $\eta_{t/c}$. Assuming that $C_p = C_{pg}$ for this work, $\gamma = \gamma_g$, then

$$\eta_{t/c} = \left(\frac{\dot{m}_c}{\dot{m}_t}\right) \left(\frac{T_1}{T_3}\right) \frac{\left[\left(\frac{P_2}{P_1}\right)^{\frac{\gamma-1}{\gamma}} - 1 \right]}{\left[1 - \left(\frac{P_4}{P_3}\right)^{\frac{\gamma-1}{\gamma}} \right]} \qquad \ldots \ldots \quad (11)$$

or

$$\frac{P_2}{P_1} = \left[1 + \eta_{t/c} \left(\frac{\dot{m}_t}{\dot{m}_c}\right) \left(\frac{T_3}{T_1}\right) \left(1 - \left(\frac{P_4}{P_3}\right)^{\frac{\gamma-1}{\gamma}} \right] \right]^{\frac{\gamma}{\gamma-1}} . \qquad \ldots \ldots \quad (12)$$

If we examine this expression we can ascertain some of the more important physical aspects of turbocharging. An increase in turbocharger efficiency will increase the boost pressure ratio $\frac{P_2}{P_1}$. Similarly, the boost pressure ratio will be increased by a higher exhaust temperature T_3 or a larger expansion pressure ratio $\frac{P_3}{P_4}$ across the turbine. For a given engine the exhaust temperature T_3 is dependent on the indicated thermal efficiency, the fuel supply rate and the heat losses. The higher the indicated thermal efficiency the lower the exhaust temperature. The thermal load on the turbocharger, that is, the stress due to the engine temperature, depends on the exhaust temperature, so that it is desirable not to exceed a set value. If the expansion ratio across the turbine is increased then more work can be done and the boost pressure raised as well as high P_3 reduces engine efficiency but increases T_3. However, there is a limit to the exhaust expansion ratio $\frac{P_3}{P_4}$, this should not exceed the boost pressure by too high a margin otherwise the back pressure will cause additional pumping work in a four stroke engine or retard the scavenge process in a two stroke engine.

1.3 ADVANTAGES AND DISADVANTAGES OF TURBOCHARGING

1.3.1 Advantages

There are several advantages in the turbocharged diesel engines over naturally aspirated engines.

These advantages are ~~considerably~~ important from performance, energy utilization, pollution and economic points of view. Consequently, more engines are being turbocharged. The principal advantages of turbocharging are as follows:

(1) Turbocharging increases the power output of the engine. Consequently, there is an increase in power/wt and power/volume ratios which are very important for automotive applications.

(2) Exhaust energy which would have been wasted is utilized. This improves efficiency and leads to reduced fuel consumption.

(3) The engine cost/output ratio is reduced.

(4) The performance of the engine at high altitudes, as the reduction in air density is reduced, is improved.

A progressive increase in engine rating has resulted from the development of turbocharging. At the present time engines are marketed with bmep's of 17 bar, though engines have been operated successfully at higher bmep.

1.3.2 Disadvantages

A major disadvantage of turbocharging occurs during the transient response of a turbocharged engine to a rapid and substantial increase in load. The response of the engine is controlled by the rate at which fuel can be burnt in the cylinder. In turn this is governed by the amount of air available which is supplied by the compressor. Applying the load, the engine speed will fall, and, using a speed sensing governor, the fuel delivered to the cylinders will increase. In the case of small load changes, increasing the fuel only is sufficient to maintain the engine speed within the required limit, as there is likely to be sufficient excess air available to burn the fuel efficiently. For larger changes, the fuel rate will increase substantially, so the compressor must supply more air to enable the combustion process to remain efficient. During a transient with a large load change, the turbocharger cannot react immediately to supply the required increased amount of air. Thus a large droop in engine speed will occur and this may lead to emission of smoke due to overfuelling. However, if the turbocharger is able to accelerate fast enough to supply the extra air needed, the engine speed will recover. Unless this happens, the engine will stall.

The transients occur in particular applications where highly rated turbocharged diesel engines are being employed. One of these is in marine propulsion where unidirectional engines are coupled to fixed pitch propellers via reverse reduction gearbox. In a crash-manoeuvre from full ahead to full astern the engine speed is usually allowed to fall to a level just above idling speed before the astern gear is selected. The engine speed then continues to fall as the clutch becomes fully engaged and stalling may take place. The other case is in standby ~~the~~ electrical generation equipment where the load change could be large and invariably occurs in an ultra short time.

This large speed droop and the possibility of stalling as well as the emission of excessive smoke which is also a serious source of pollution in automotive applications are important factors ~~in~~ for obtaining the optimum transient response of turbocharged diesel engines. In order to do so, it is desirable to be able to predict the performance of the turbocharger itself under transient conditions.

This thesis reports a study of the transient response performance of the exhaust gas turbocharger when the operating conditions were changed rapidly. An

experimental programme was carried out on a test rig designed for this purpose. Computer programs were developed to predict the transient response of the turbocharger under pulsating and non-pulsating flow conditions. Under non- pulsating flow conditions a computer program used a knowledge of the conditions at the turbocharger turbine inlet during the transient to predict the response of the turbocharger. Under pulsating flow conditions, the pulse generator was used to represent the exhaust process of an engine and two programs predicted the transient response of the turbocharger. The first used a knowledge of the pulse generator characteristics and conditions of the gases entering the pulse generator and the second used the turbocharger turbine inlet conditions only. The experimental results obtained from the turbocharger test rig were used to check the validity of the theoretical predictions.

CHAPTER TWO
LITERATURE SURVEY

CHAPTER TWO

LITERATURE SURVEY

In recent years and as a result of the wide use of turbocharging the diesel engines, considerable attention has been given to turbocharger compressor and turbine performance under steady and pulsating flow conditions.

Under steady flow conditions, the turbine performance was estimated by Wallace et al[2] using the method of characteristics which takes into account the wave action through the turbine. This method was extended later[3] for a number of special cases, in particular the operation at overall pressure ratio up to 4 and partial admission.

Under pulsating flow conditions, many workers have investigated the problem of the turbine performance using either the method of characteristics or the quasi-steady method which assumes that at all times the performance of the turbine is identical with that obtained in steady flow conditions for the same pressure and temperature at the turbine inlet. Pure theoretical predictions using the method of characteristics were described in detail by Benson et al[4],[5]. This method of predicting the performance of the turbine under pulsating flow conditions was used by White[6]

for axial flow turbines and by Wallace and Adgey[7] for inward flow turbines. An experimental programme was carried out by Wallace et al[8] to measure the performance of the inward radial flow turbine under pulsating flow conditions and the results were compared with those calculated theoretically. They concluded that the pulsating flow tests show a slight dependence of turbine mass flow on pulse frequency for turbine speed up to 70 000 and mean up-stream pressure up to 26 psia. Their final conclusions were that comparisons with steady flow conditions cannot be made except on the basis of the quasi-steady flow analysis as the time consumed using the method of characteristics was too high.

Benson and Scrimshaw[9] and Wallace et al[10] used the quasi-steady approach to calculate mass flow, power and efficiency of the inward radial flow turbine. These results were then compared with the measured flow rates and power. The results reported in ref (10) and broadly confirmed in ref (9) showed that the quasi-steady treatment over-estimated the mass flow and power by an average of 10%.

Craig et al[11] used the quasi-steady theory but for axial flow turbines by predicting the turbine performance from steady flow results and comparing the prediction with the performance under pulse conditions. They found that the quasi-steady flow analysis gave an accurate prediction of mean mass flow and mean power at

pulse generator speed of 350 r.p.m., and peak pressure ratio of 1.8 . At higher pressure ratios (up to 2.6) and higher pulse generator speed of 480 rev/min, the quasi-steady flow method over-estimated the turbine power ~~by~~ up to 15% and over-estimated the mass flow ~~by~~ upto 7.5%.

They plotted the wave travel time parameter against the percentage error in quasi-steady calculations for axial turbines in order to correlate the experimental and quasi-steady results. They defined the wave travel time parameter ϕ as follows:

$$\phi = \frac{\text{single wave travel time through the blades}}{\text{periodic time of the pulse}} \quad \ldots\ldots(13)$$

$$\text{Time for the pulse to pass through the blades} = \frac{\text{length of the blade passage}}{\text{speed of propagation}} \quad \ldots(14)$$

length of the blade passage α chord of the blades

characteristic length selected = sum of nozzle guide vane chord and rotor blade chord

mean wave speed α stagnation speed of sound in the gas, which can be calculated from inlet total temperature

$$\phi \;\alpha\; \frac{cf}{12} \left(\frac{\sqrt{K\,G\,T_3}}{\frac{60}{f}} \right)$$

or using a pseudo non-dimensional parameter

$$\Phi = \frac{cf}{\sqrt{T_3}}$$

where

f	is the pulse frequency in pulses per minute
ϕ	wave travel time parameter
Φ	pseudo wave travel time parameter
c	a characteristic flow length of the turbine blades
k	$\frac{c_p}{c_v}$ ratio of specific heats
G	Gas constant
T	Total temperature

Daneshyar et al[12] carried out a similar comprehensive study to ref (11) but on three axial turbines and they found that the quasi-steady prediction over-estimated the turbine efficiency by an average of 5%.

Whitehouse et al[13] carried out a comprehensive study and presented the idea of apparent efficiency to predict the turbine performance under pulsating flow conditions from the steady state characteristics. They defined the apparent efficiency as follows:

$$\eta_{t\ app} = \frac{\text{Actual compressor work}}{\text{Available isentropic energy before turbine on an apparent constant pressure system}}$$

$$= \frac{\dot{m}_c\ C_{p_1}\ T_1 \left[\left(\frac{P_2}{P_1}\right)^{\frac{\gamma-1}{\gamma}} -1\right]/\eta_c}{\dot{m}_c\ C_{p_3}\ T_3 \left[1-\left(\frac{P_4}{P_3}\right)^{\frac{\gamma'-1}{\gamma'}}\right]} \qquad \ldots\ \ldots\ (17)$$

The apparent efficiency $\eta_{t\ app}$ was calculated from experimental results using turbine and compressor steady state characteristics. Using measured $\dot{m}_t$, T_3 and P_3 the turbine mass flow parameter $\dot{m}_t\sqrt{T3}\ /P_3$ was calculated. From $\dot{m}_t\sqrt{T_3}\ /P_3$ and turbocharger speed the turbine expansion pressure ratio was estimated from the turbine steady state characteristics. Using measured $\frac{P_2}{P_1}$ and turbocharger speed, the compressor efficiency η_c was found from compressor steady state characteristics.

The work was carried for an axial turbine and the pulse factor presented for this purpose was found to be a simple smooth curve which can be used easily to correlate the pulsating flow performance.

Wallace and Miles[14] investigated the performance of inward radial turbine under pulsating conditions with single, two and three entry casing using either the method of characteristics or a quasi-steady technique. They concluded that the quasi-steady flow treatment gave much shorter computer programs than that of the method of characteristics and gave acceptable results in terms of pulse amplitude predictions. Both treatments slightly over-estimated mass flow rate and power with that measured experimentally.

Miyashita et al[15] carried out an experimental work to investigate the effect of pulse frequency on the turbine mass flow rate and efficiency. They compared their experimental results with theoretical predictions based on the quasi-steady method to specify the degree of accuracy of the quasi-steady theory. They operated the turbine under pulsating conditions with pulse frequency of 20, 30, 40 and 50 Hz. Their results, which were shown graphically, indicate that both the mass flow rate and efficiency got lower as the pulse frequency became smaller. They concluded that the quasi-steady results were within $\pm$ 10% of the results measured experimentally.

Benson[16] carried out an experimental and theoretical work with nozzleless radial flow turbine to correlate the pulsating flow with steady flow mass flow rate and

power, using the quasi-steady approach. He established three factors for the mass flow rate, the power and the power per unit mass flow for the purpose of correlation. He plotted these factors against pulse frequency. His graphs showed that the quasi-steady method over-estimated the turbine mass flow and power with those measured experimentally.

Bhinder et al[17],[18] developed a theoretical method to predict the performance of centripetal turbines under un-steady flow conditions based on the assumption of quasi-steady flow and without the need of the experimental steady state data for the turbine. They used the geo-metrical details of the turbine in order to calculate the required turbine performance parameters. The results were within 10% of those calculated from the corresponding steady state values.

Shamsi[19],[20] introduced a method to correlate between the turbine performance parameters under pulsating conditions with those predicted from steady state conditions based on the quasi-steady approach. He gave the expression of effective turbine expansion ratio (m.e.t.e.r) for the purpose of correlation. This factor was calculated as follows:

$$PW_t = \dot{m}_t \, C_p \, T_3 \left[1 - \left(\frac{1}{K \left(\frac{P_3}{P_4}\right)^{\frac{\gamma-1}{\gamma}}} \right) \right] \eta_t \qquad \ldots\ldots (19)$$

$$= \dot{m}_t \, C_p \, T_3 \left[1 - \left(\frac{1}{m.e.t.e.r}\right)^{\frac{\gamma-1}{\gamma}} \right] \eta_t \quad \ldots \ldots (20)$$

and the turbine power PW_t is equal to compressor power (PW_C) and turbocharger bearing power loss (PW_B)

$$m.e.t.e.r = \frac{1}{\left[1 - \frac{PW_C + PW_B}{\dot{m}_t \, C_p T_3 \eta_t} \right]^{\frac{\gamma-1}{\gamma}}} \quad \ldots \ldots (21)$$

where PW_C, PW_B, $\dot{m}_t$, T_3 and η_t may be measured experimentally to calculate m.e.t.e.r. then the pulse factor K to be calculated where

$$K = \frac{m.e.t.e.r}{\frac{P_3}{P_4}}$$

He found that the pulse factor K is linear function of mass flow parameter

$$\frac{\dot{m}_t \sqrt{T_3}}{P_3}$$

for constant pulse frequency.

and

$$K = f\left(\phi, \frac{\dot{m}_t \sqrt{T_3}}{P_3}\right) \quad \ldots \ldots (23)$$

where ϕ is the pulse frequency.

And the pulse factor is a single straight line when plotted against cyclic mass flow parameter.

All the work carried out under pulsating flow conditions to demonstrate the validity of the quasi-steady method of predicting the turbine and compressor performance showed, generally, that the method over-estimated the turbine mass flow and power. The reasons why the quasi-steady approach over-estimated the turbine mass flow and power by varying amounts probably lie in the following points:

1. Neglecting the bearing power loss in power measurement, Wallace[10] and Craig et al[11].

2. Assuming turbine outlet pressure as constant, Wallace[10] and Benson[16].

3. The inaccuracy in different extra-polated data of the turbine steady state characteristics, Benson and Scrimshaw[9] and Benson[16].

The study of the turbocharger compressor performance under steady and pulsating flow conditions has received the attention of many workers.

Whitefield et al[21],[22], carried out a theroetical method to predict the performance map of the turbocharger centrifugal compressor based on one dimentional flow analysis reported by Wallace[2]. Whilst Benson and Whitefield[23] used the method of characteristics to

predict the pulsating flow performance of centrifugal compressor.

Benson and Whitfield[24] investigated experimentally the flow characteristics of a centrifugal compressor under non-steady flow conditions. They found that the operating range of the compressor as indicated by the location of the surge points is reduced, the surge point being displaced to a region of greater mass flow. The displacement of the surge point was found to be dependent upon the amplitude and frequency of the pressure pulses. Either a lower frequency or a greater pressure amplitude, and it could be both, will increase the displacement of the surge point. Outside the non-steady flow surge region the overall insentropic compressor efficiency was less than the steady flow efficiency, the difference in efficiency being dependent on frequency of the pressure pulses. They concluded that there is no simple relationship between the decrease in efficiency and the pulse frequency.

Benson and Whitfield[25] extended their work in ref (23) experimentally and theoretically to study the effect of pulse frequency on the compressor performance. They extended the method of characteristics to include non-steady flow in the suction and delivery system. They also indicated a method of evaluating the equivalent length of the compressor using the measured steady flow

surge frequency. The shift in the surge line and the reverse flow conditions were examined. Their experimental work has shown that the reverse flow developed gradually as the frequency was reduced, and that the strongest reverse flow pulses occurred at higher mass flow rates than steady flow surge. The experimental results were compared with the theoretical results obtained by the method of characteristics and the quasi-steady method. They concluded that the quasi-steady method gave more acceptable results than the methods of characteristics.

As mentioned in Chapter 1, the inability of the turbocharger to respond sufficiently rapidly to give enough air for combustion, is a reason for the sluggish transient performance of the turbocharged diesel engine. Any increase in the acceleration of the turbocharger while the load increases rapidly will improve the response of the engine. Injection of compressed air onto the compressor rotor has been suggested as a means of obtaining this increase in turbocharger acceleration. It has the advantage of increasing the air flow rate. This was investigated by Furukawa et al[26],[27] who studied the effect on compressor performance of injecting air into the compressor rotor. They found that the compressor delivery pressure ratio was slightly increased for the same speed and mass flow parameter, and the torque required from the turbine was greatly reduced enabling the turbine to accelerate. The engine response, therefore, was improved and stalling

was avoided when large loads were applied.

In the current investigation the compressor discharges into a loading nozzle. The flow through the nozzle changes slowly with time and is, therefore, comparatively steady. In an engine the flow through the compressor will be unsteady because air is admitted to the engine through inlet valves.

Very little work had been done concerning the turbocharger performance under transient operation.

Aburwin[28] studied experimentally the transient response performance of the turbocharger by changing the turbine inlet conditioncs rapidly from one steady state condition to another steady state condition. His calculation, carried out by hand, required a complete knowledge of turbine inlet conditions.

Stockton[29] was involved in measuring turbocharger turbine and compressor characteristics under steady state conditions, the development of a turbine dynamometer and unsuccessful developments on temperature measurements. He did some work on steady transients similar to that carried out by Aburwin[28].

CHAPTER THREE

EXPERIMENTAL EQUIPMENT

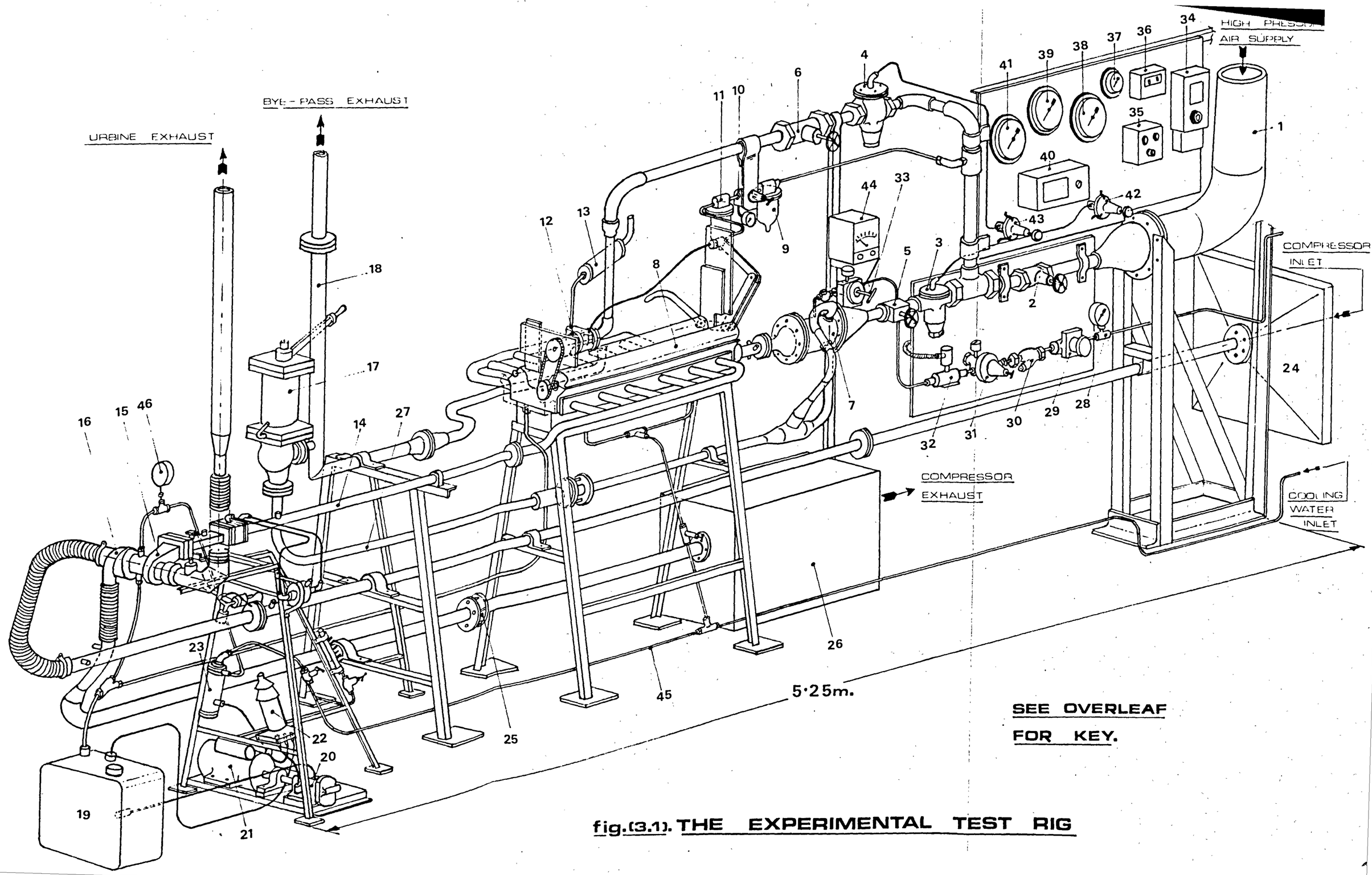

fig.(3.1). THE EXPERIMENTAL TEST RIG

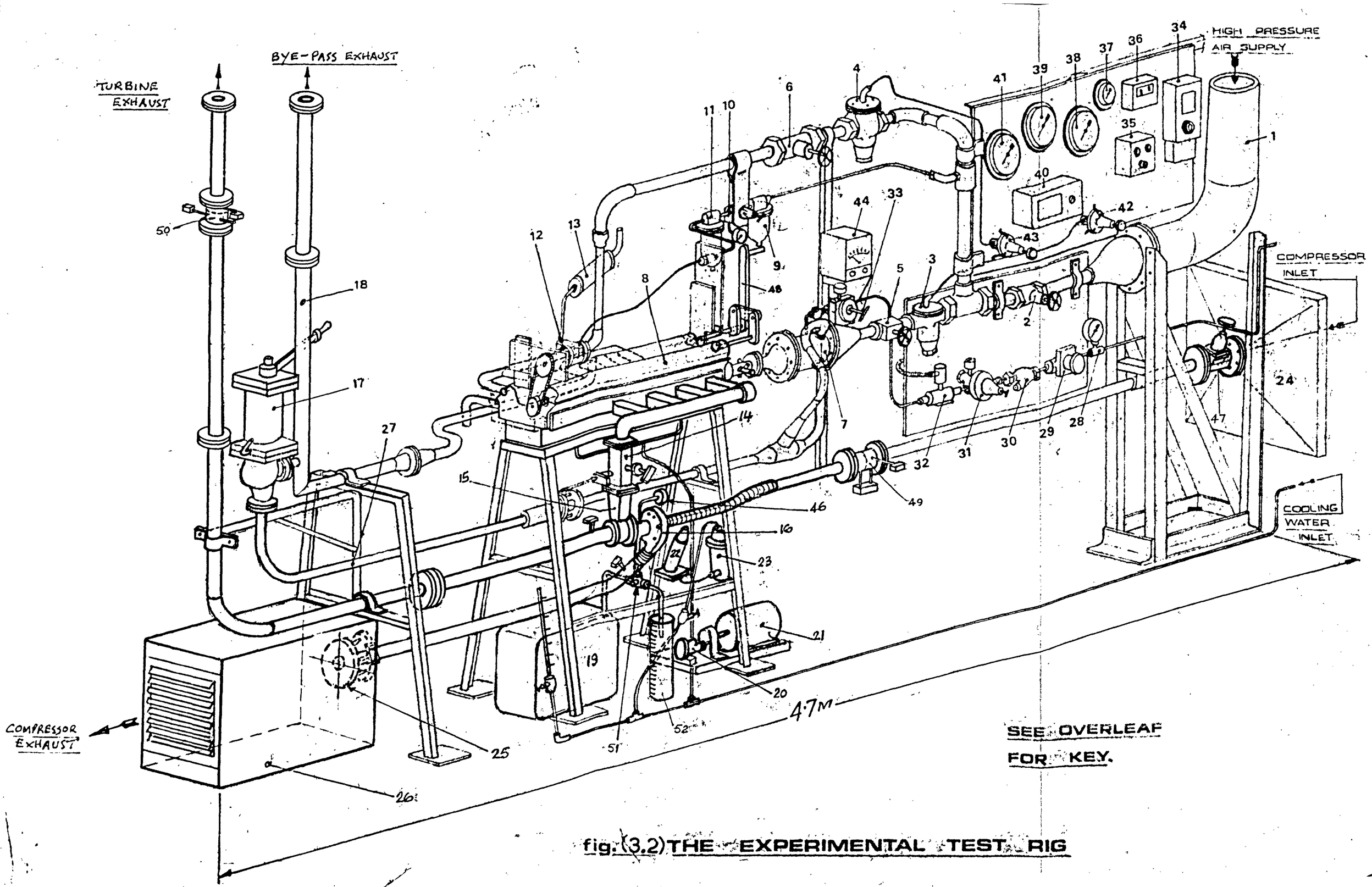

fig. (3.2) THE EXPERIMENTAL TEST RIG

KEY FOR FIGURES (3.1) AND (3.2)

1. Main air inlet
2. Main stop valve
3. Pilot operated pressure regulator HP line
4. Pilot operated pressure regulator LP line
5. Stop valve for the HP line
6. Stop valve for the LP line
7. Combustion chamber
8. Pulse generator and flow changeover valve
9. Filter
10. Pressure regulator
11. Oil fog lubricator
12. Air motor
13. Exhaust silencer for air motor
14. Turbine inlet
15. Turbine
16. Compressor
17. Pressure relief valve for combustion chamber
18. Bye-pass pipe for hot combustion gases
19. Oil tank
20. Oil pump
21. Oil pump electric motor
22. Oil filter
23. Oil cooler
24. Compressor inlet air filter
25. Compressor loading nozzle
26. Compressor exhaust

27. Pipe from the combustion chamber to pressure relief valve
28. Propane pressure gauge
29. Propane stop valve
30. Propane filter
31. Propane pressure regulator
32. Solenoid operated stop valve
33. Final propane control regulator
34. Spark ignition unit
35. Propane ignition control
36. Oil pump starter
37. Oil pressure gauge
38. Regulated LP line pressure
39. Main supply pressure gauge
40. Turbocharger speed indicator
41. Regulated HP line pressure
42. Pressure regulator for LP line regulator valve
43. Pressure regulator for HP line regulator valve
44. Combustion chamber outlet temperature indicator: fitted with over and under temperature trips
45. Cooling water supply for pulse generator and turbo-charger oil cooler
46. Oil pressure gauge
47. Gate valve
48. Pulse Generator change-over lever
49. Orifice plate at the compressor inlet
50. Orifice plate at the turbine outlet
51. Three way valve
52. Measuring cylinder

CHAPTER THREE

EXPERIMENTAL EQUIPMENT

3.1 THE EXPERIMENTAL TEST RIG

The test rig has been designed to enable the performance of a turbocharger to be studied when the condition of the fluid entering the turbine changes rapidly from a steady flow of low pressure air at ambient temperature to either a pulsating or a steady flow of higher pressure air at ambient temperature, or a pulsating or a steady flow of higher pressure products of combustion at an elevated temperature.

The rig was initially built by Aburwin[28] to study the transient performance of the turbocharger when the inlet conditions to the turbine were changed rapidly from one steady state to another steady state condition. Another modification was carried out by Stockton.[29]

For the purpose of this research the rig has been reconstructed twice with further developments. Fig. (3.1) shows the arrangement of the rig for tests results reported in chapter seven, Figs (7.1) to (7.30). In the next chapters these tests will be called as "Test Series I.". Fig. (3.2) shows the arrangement used for the tests presented in Figs. (7.31) to (7.59) and this will be

called "Test Series II".

The current rig layout is shown in Fig. (3.2) (see also Plates (1) and (2)). Compressed air from a Broom and Wade V750 compressor was supplied at 120 lb/in^2 to two large receivers of approximately 1100ft^3 capacity which then supplied air to the turbine. In order to be able to vary the turbocharger turbine operating conditions rapidly, the compressed air supply was divided into HP and LP branches, Figs (3.1) and (3.2). A stop valve was installed at the inlet to the rig to stop the flow in an emergency and isolate the system for maintenance. An isolating stop valve and a pressure regulator valve were mounted in each of the LP air and HP air branches in order to control the pressure and the rate of flow. The combustion chamber was fixed in the HP branch downstream of the regulator valve and the two branches were connected to the pulse generator in such a way that this pulse generator could be used for both hot and cold running. The air was filtered before entering the turbocharger compressor and discharged through a nozzle and then to a sound reducing box, Figs. (3.1) and (3.2). The nozzle was designed and mounted between pipe flanges according to BS1042[30], Fig. (3.3). Propane was passed through a filter and regulator before flowing to the combustion chamber. A closed lubrication circuit was installed for lubricating the turbocharger and the pulse generator. Cooling water was passed through the pulse generator, the oil cooler and pressure transducers adaptors. Stainless

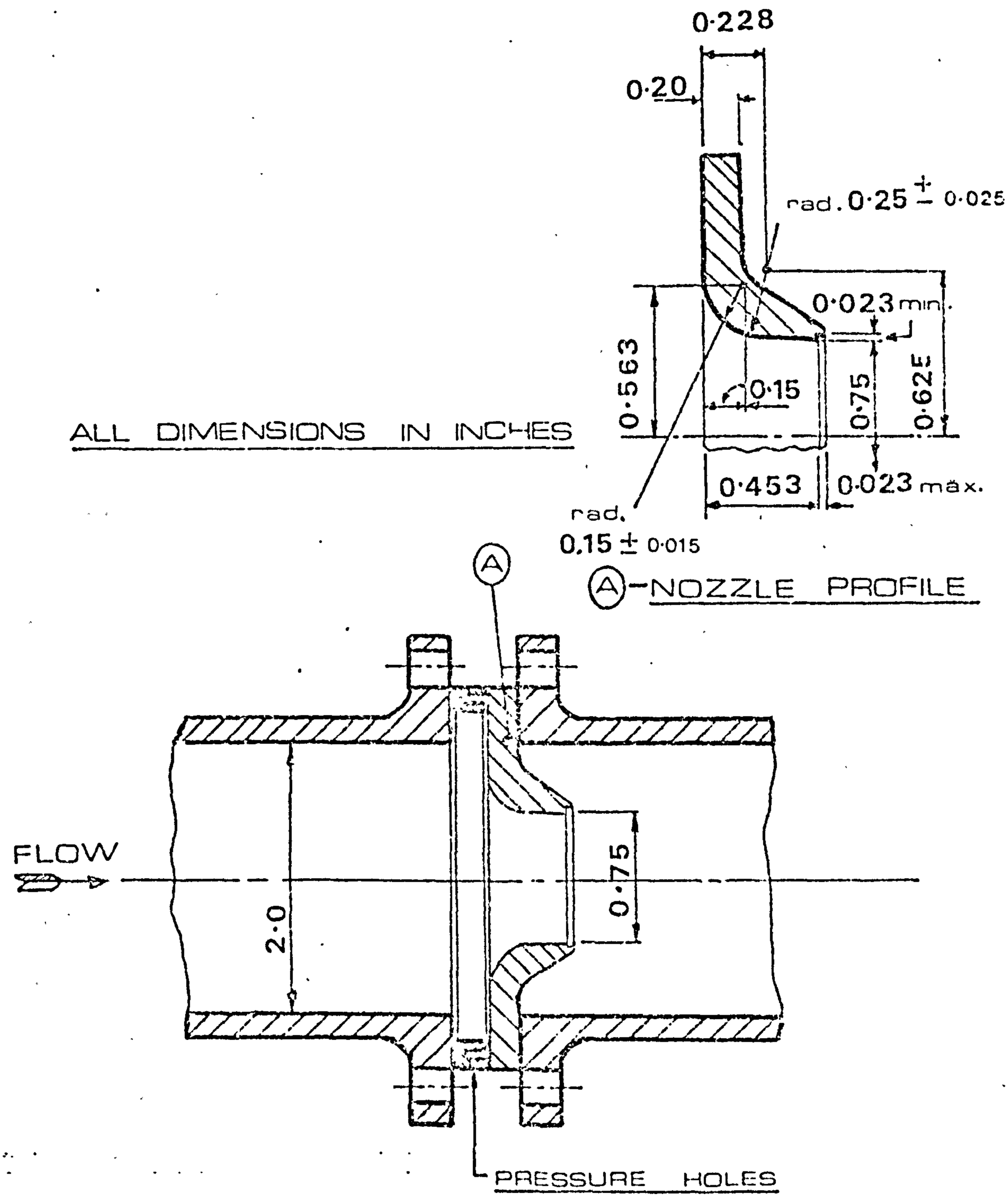

ALL DIMENSIONS IN INCHES

fig.(3.3) CONSTRUCTIONAL ARRANGEMENT OF THE COMPRESSOR LOADING NOZZLE.

steel pipes and fittings which could withstand the high temperature were used for the hot air sections. Thermocouples and resistance wire thermometers, pressure transducers and a photo-electric device were used to measure temperature, pressure and turbocharger speed respectively while orifice plates were used for mass flow measurements.

3.2 TURBOCHARGER

Holset 3LD/.68 Serial Number 144362 turbocharger was used during the tests. See Plate (3). This turbocharger, Fig. (3.4), consists of a single stage centrifugal compressor and a single stage radial turbine mounted on the bearing shaft. The turbocharger was mounted on the turbine inlet flange as recommended by the manufacturer; the rest of the connections were flexible and heavy pipework was separately supported. As there was no information about the turbocharger moment of inertia, the latter was measured as explained in Section (5.3).

3.3 TURBOCHARGER LUBRICATION SYSTEM

The lubrication system, Fig (3.5), provided the turbocharger bearings with oil at a regulated pressure using an automatic gear pump type GP ¼/4/AS/V driven by a single phase motor running at a speed of 960 rpm. Following the manufacturer's recommendation when running the turbocharger on load, the oil was filtered to better

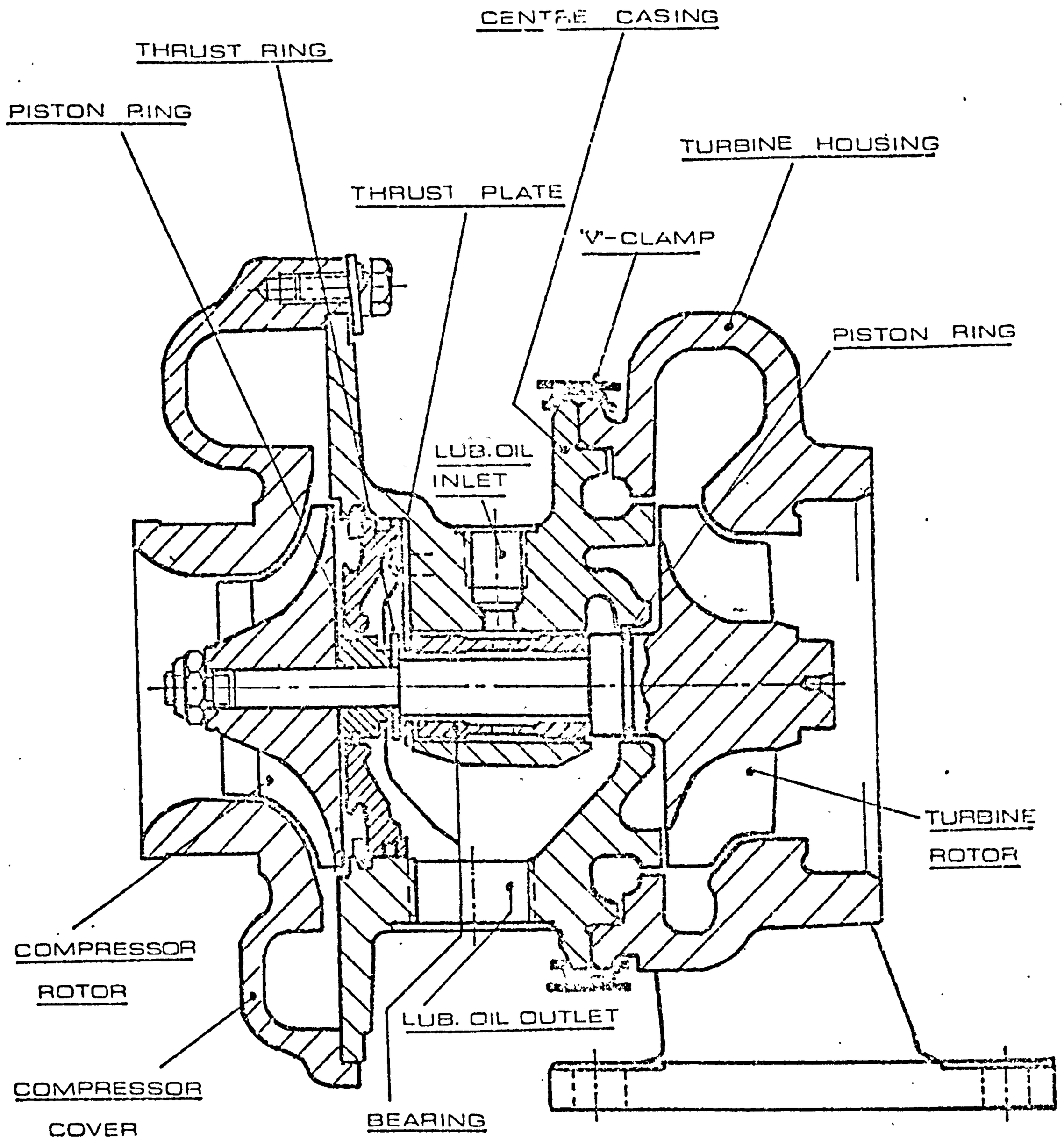

fig.(3.4) CROSS-SECTION OF HOLSET 3LD TURBOCHARGER

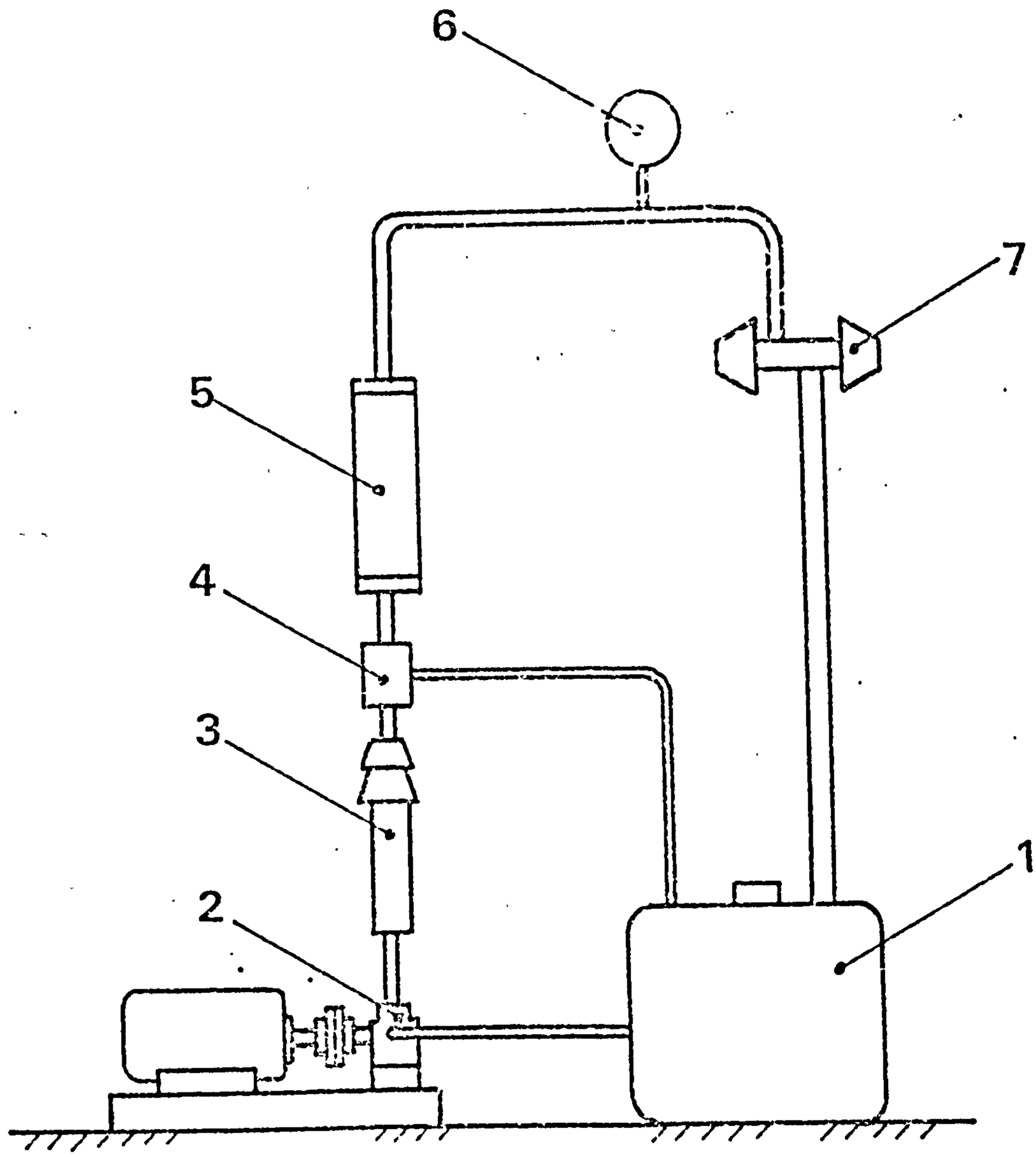

1 — OIL TANK

2 — OIL PUMP AND MOTOR

3 — OIL FILTER

4 — RELIEF VALVE

5 — OIL COOLER

6 — PRESSURE GAUGE

7 — TURBOCHARGER

fig.(3.5). LUBRICATION CIRCUIT

than 15 microns using an automobile type filter and the turbocharger was operated with an oil pressure above 2 bar. An oil pressure relief valve in series with the pump restricted the maximum oil pressure to 5 bar.

Standard 20 - 50 W multigrade lubricating oil of a type normally used in an engine was used for lubricating the turbocharger.

In order to reduce the oil temperature, the cooling water was passed through an oil cooler before it was supplied to the turbocharger. Cooling water was not required during transient operation.

For safety two oil pressure gauges were used: one was mounted at the turbocharger and the other was fixed to the control panel.

3.4 COMBUSTION CHAMBER

In order to make it possible to heat the high pressure air supply a gas turbine combustion chamber was incorporated in the high pressure branch. The combustion chamber used was made by Joseph Lucas Limited. Originally this combustion chamber was designed to burn aviation fuel, but in order to keep the hot air supply clean and thereby reduce the effect of contaminations on the turbocharger and instrumentation, it was decided to burn propane gas instead of the aviation fuel. The propane was passed

through a filter before injection into the combustion chamber. A pressure gauge, a pressure regulator, and a stop valve as well as a solenoid operated stop valve were installed on the propane line, Fig. (3.2). The solenoid operated valve was fitted to cut the propane supply if the temperature of the gases leaving the combustion chamber was too low (due to ignition failure) or too high (due to excess fuel). As the maximum designed operated pressure of the combustion chamber was 50 lbf/ in^2, a connection to a relief valve was fitted to the combustion chamber, Fig. (3.2). The relief valve was set to open if the pressure exceeded the designed limit.

3.5 PULSE GENERATOR

Many workers have designed pulse generators to simulate the gas flow in an actual engine and provide an analogue of the engine exhaust. Jenney[31] was one of the first researchers to use the pulse generator in order to simulate the exhaust flow processes of a four stroke engine, while Wallace and Nassif[32] designed a pulse generator to simulate the flow processes of a two stroke engine. The pulse generator used in this test rig, which used compressed air to provide exhaust pulses, was designed to simulate the exhaust from a multicylinder diesel engine (see Plates (4) and (5)). The general arrangement and the sectional view of the apparatus is shown in Figs. (3.6) and (3.7). The pulse generator was manufactured from the cylinder head of a 6 cylinder twin overhead

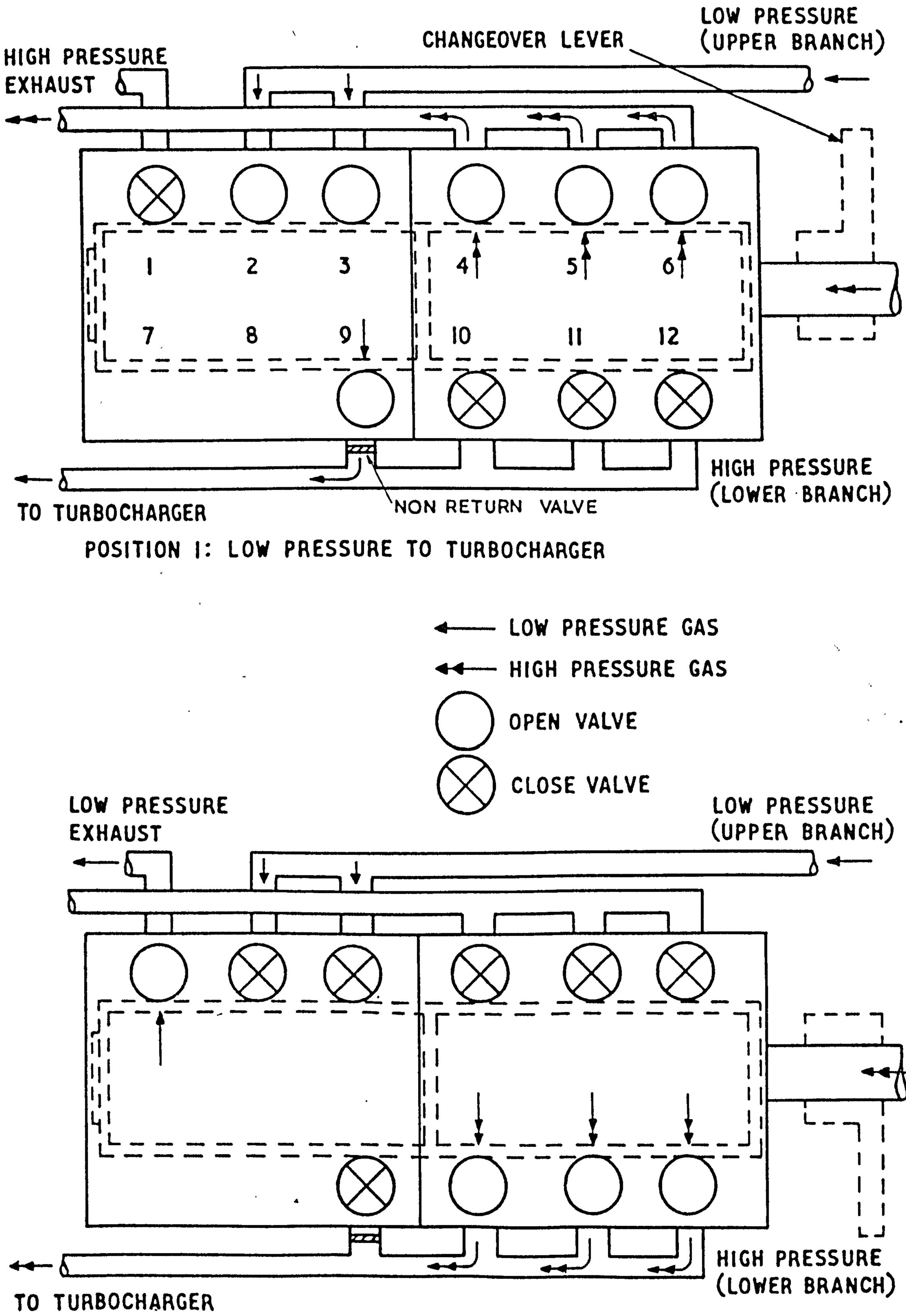

FIG. (3.6) DIAGRAMMATIC PLAN VIEW OF PULSE GENERATOR

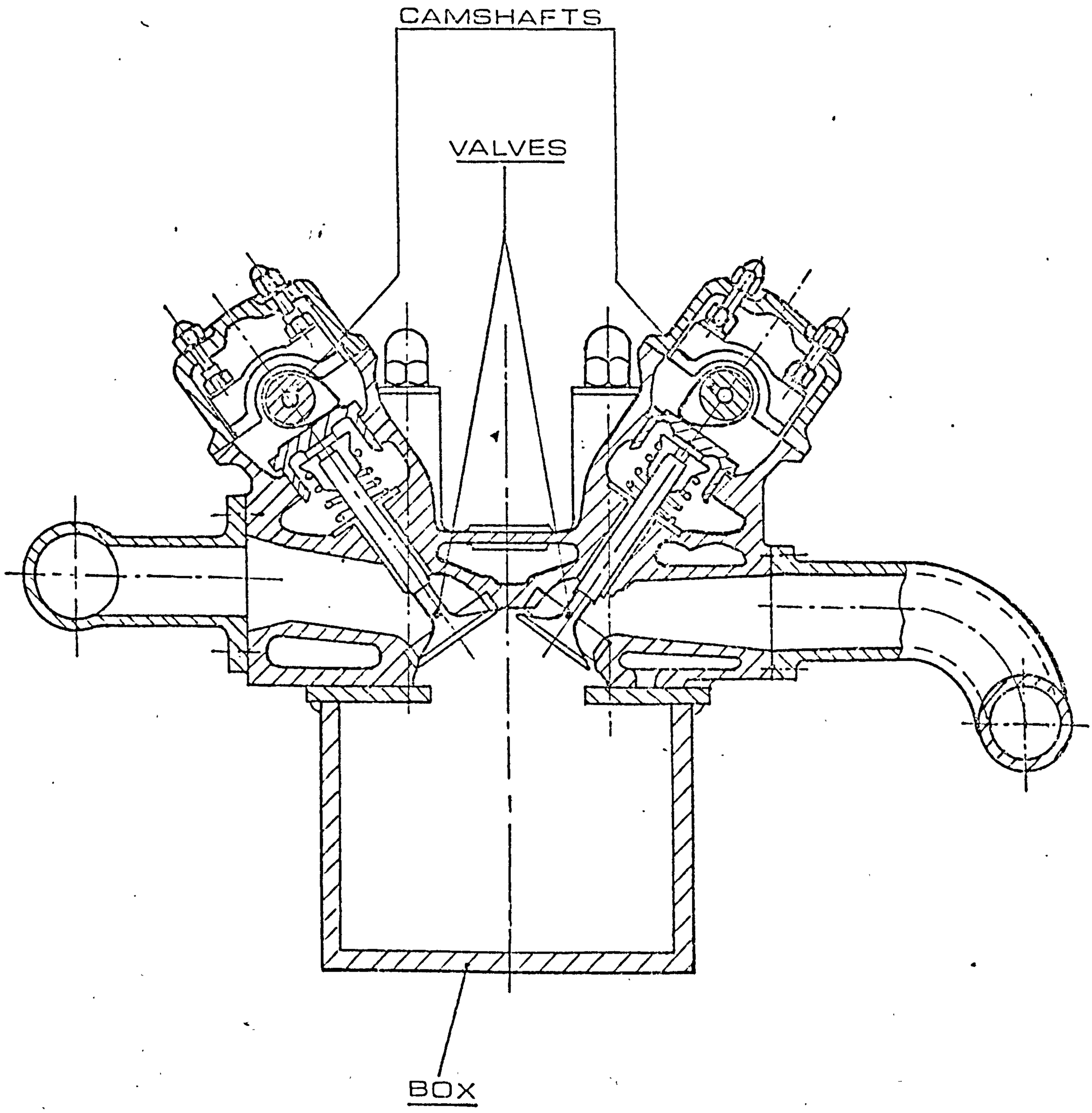

CROSS SECTION THROUGH

PULSE GENERATOR

FIG. (3.7)

camshaft engine, which was mounted on a water cooled box divided into two sections. The pulse generator was used to provide HP pulsating flow or pass HP steady flow to the turbine as well as passing LP steady flow to the turbine.

A non-return valve was designed, Fig. (3.8), and fitted in the low pressure port as shown in Fig. (3.6) to prevent the high pressure air passing into the low pressure plenum chamber and to atmosphere through valve 9 while the high pressure was supplied to the turbine.

Two camshafts were used for each mode of operation. One of the camshafts controlled valves 1 to 6 and the other camshaft controlled valves 9 to 12, Fig. (3.6). The valve guides for valves 7,8 and 9 were blanked off. The camshaft controlling valves 1 to 6 was operated manually and linked to the other camshaft (for transients using non-pulsating high pressure air) or to the air motor stop valve (for transients using pulsating high pressure air). Before the beginning of the transient valves 4, 5 and 6 were open and dumped high pressure air to waste, vavles 2 and 3, passed low pressure air to the turbine and valve 1 was closed to seal the LP plenum chamber, position 1, Fig (3.6). During the transient, valves 2, 3, 4, 5 and 6 were closed and valve 1 was opened to atmosphere, and high pressure air passed to the turbine through valves 10, 11 and 12, position 2, Fig. (3.6). Two camshafts were used to control valves 10, 11 and 12.

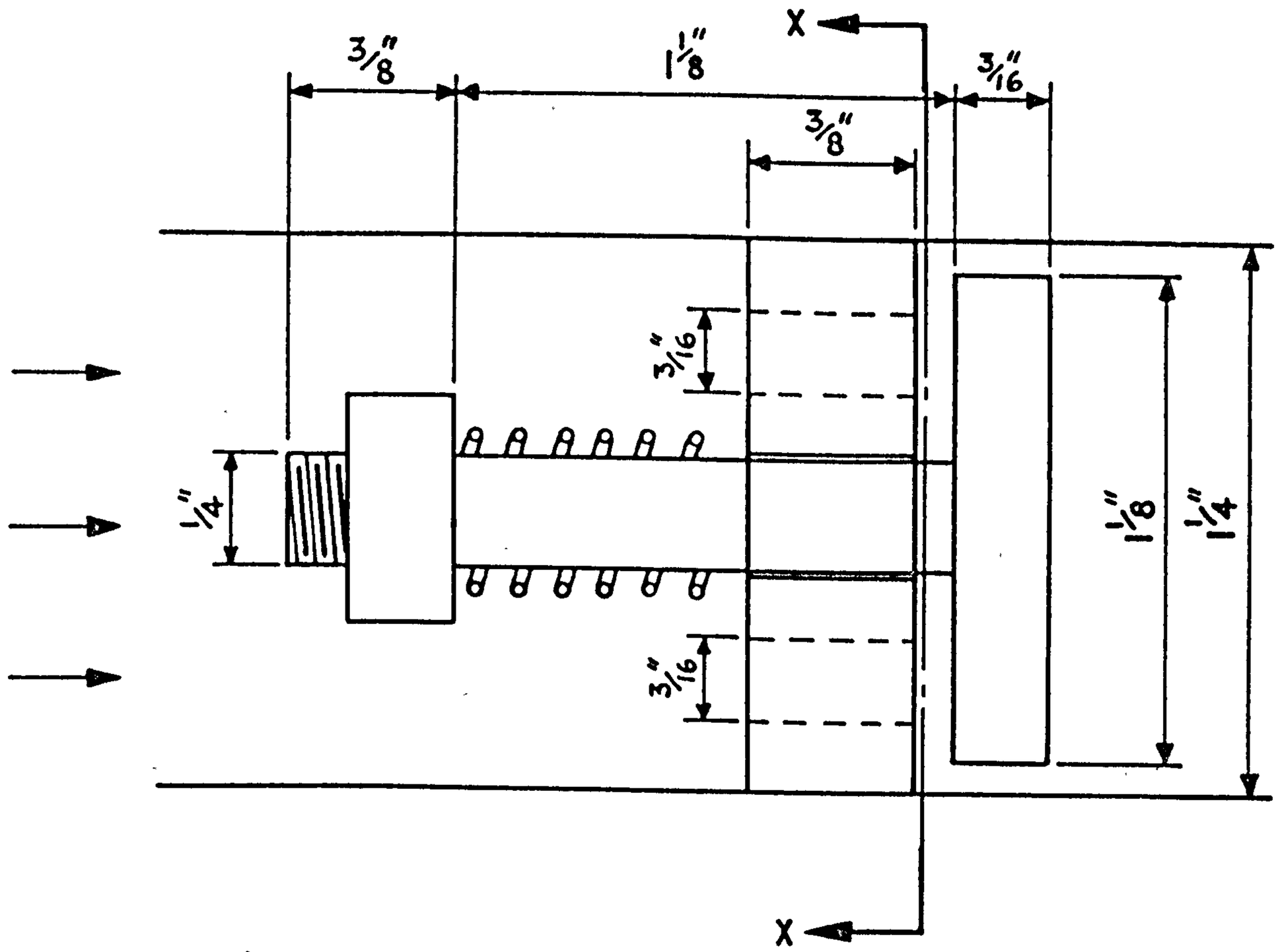

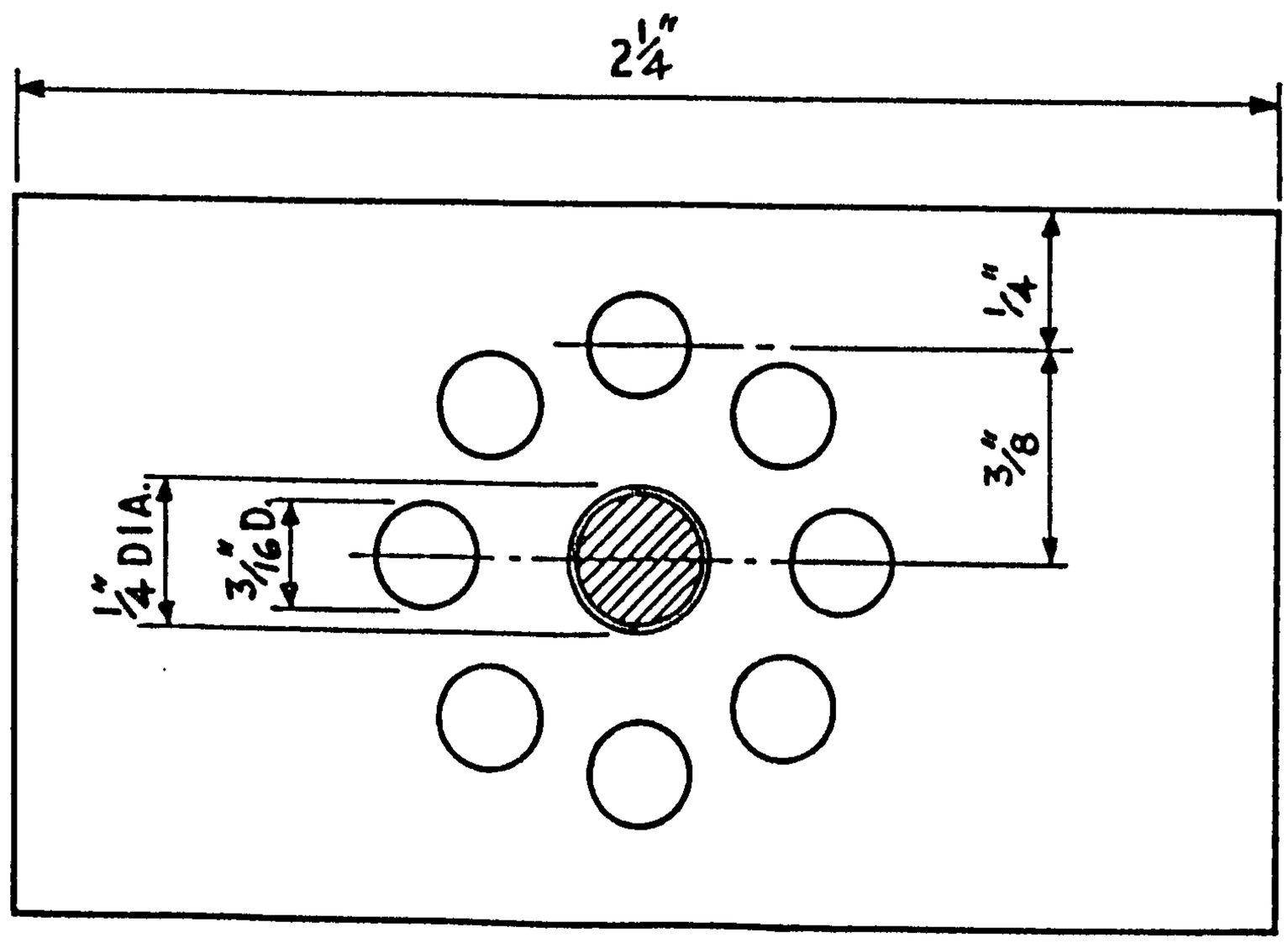

SECTION X-X

FIG. (3.8) NON-RETURN VALVE

To obtain a pulsating flow of high pressure air the camshaft controlling valves 10, 11 and 12 was driven by an air motor, with the valves opening 120° out of phase to each other to obtain 3 pulses per camshaft revolution. During Test Series II, in order to simulate engine exhaust pulse conditions more effectively, it was decided to obtain 1 pulse revolution instead of 3. That was done by blanking off valves 11 and 12 and by reducing the pulse generator exhaust system volume by inserting an iron bar of 1½" diameter in the exhaust pipe.

To obtain a steady flow of high pressure air a simple camshaft was used with staggered cam profiles so that the opening of valves 10, 11 and 12 was progressive.

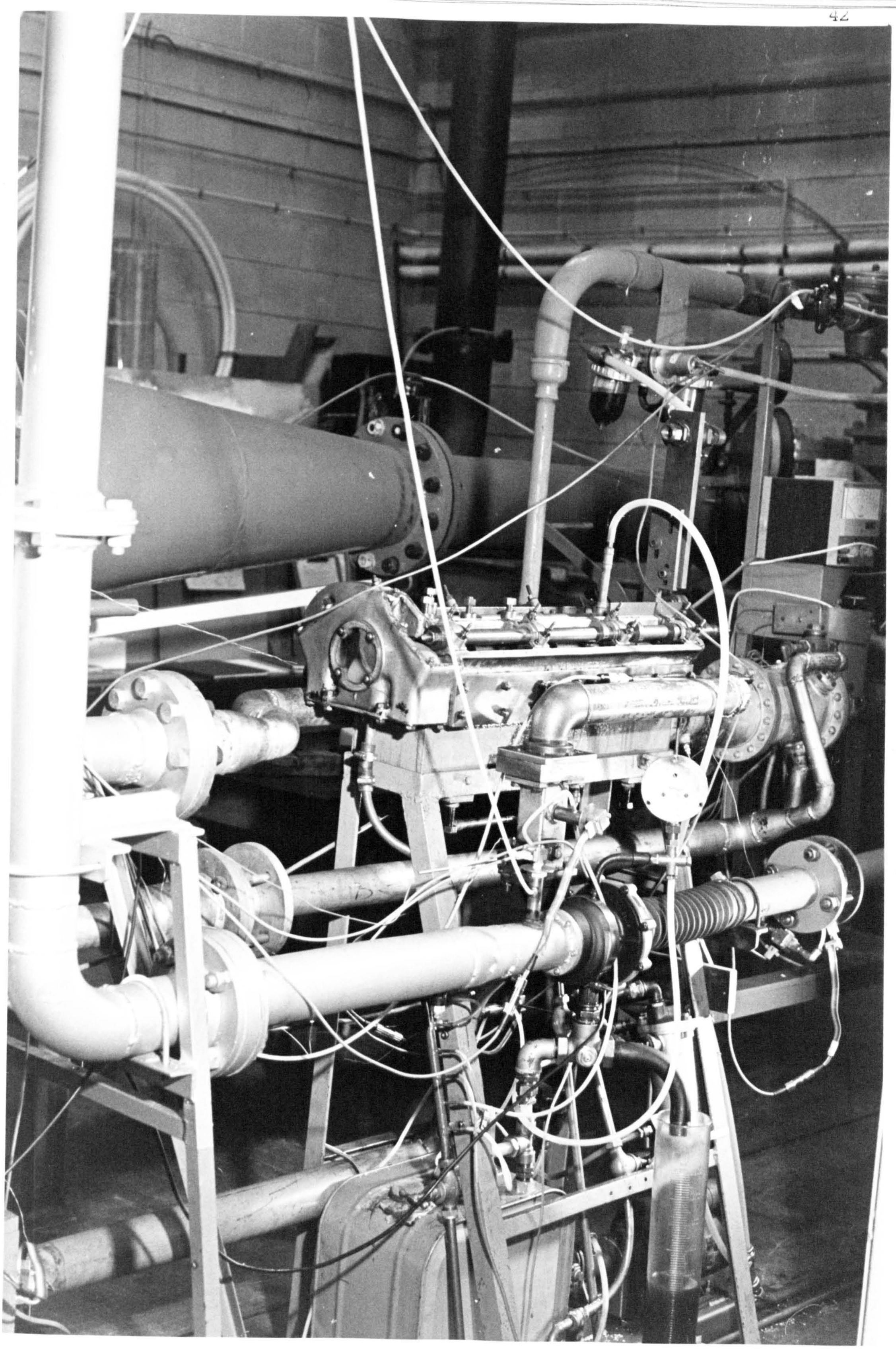

PLATE (1) THE EXPERIMENTAL TEST RIG

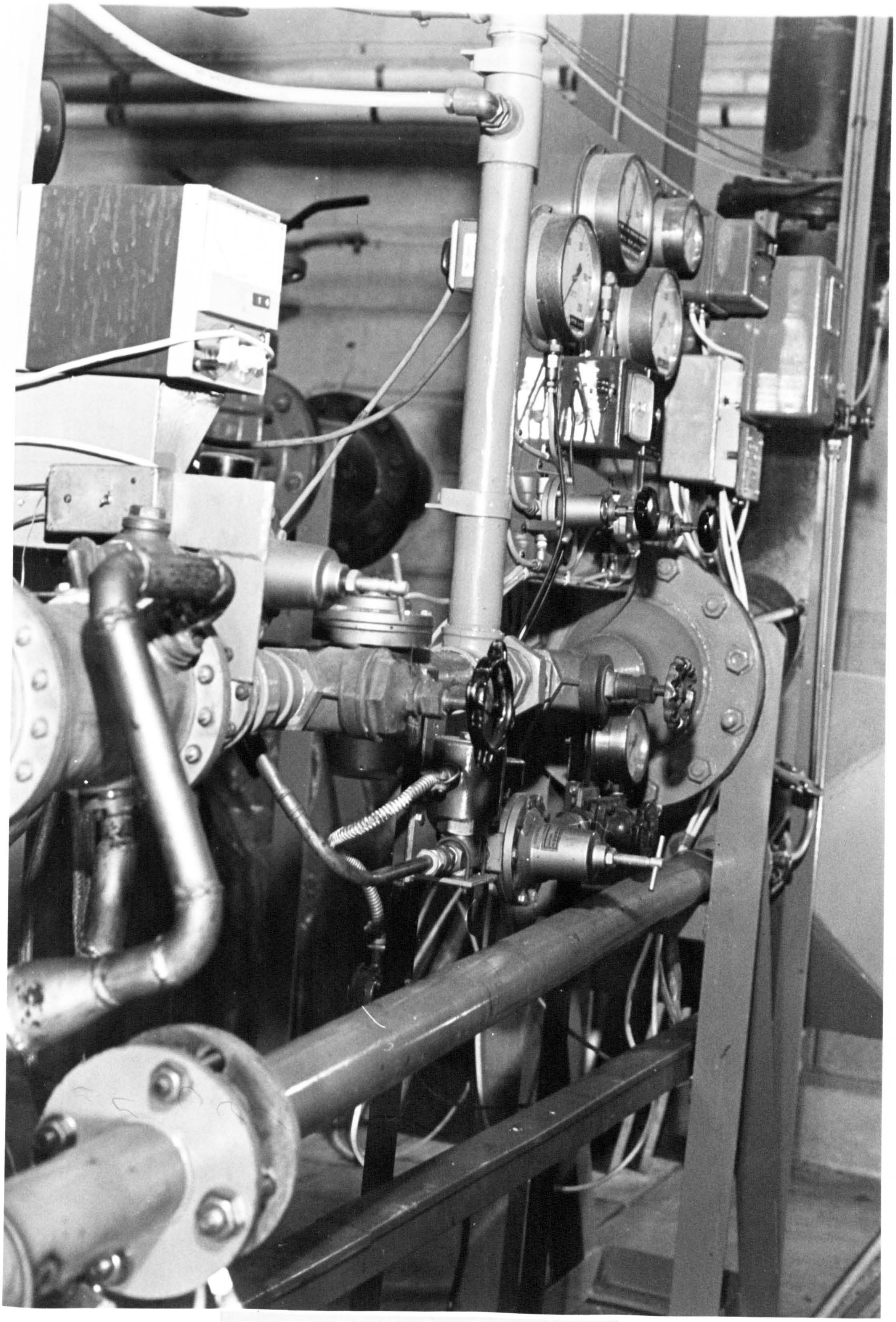

PLATE (2) THE EXPERIMENTAL TEST RIG

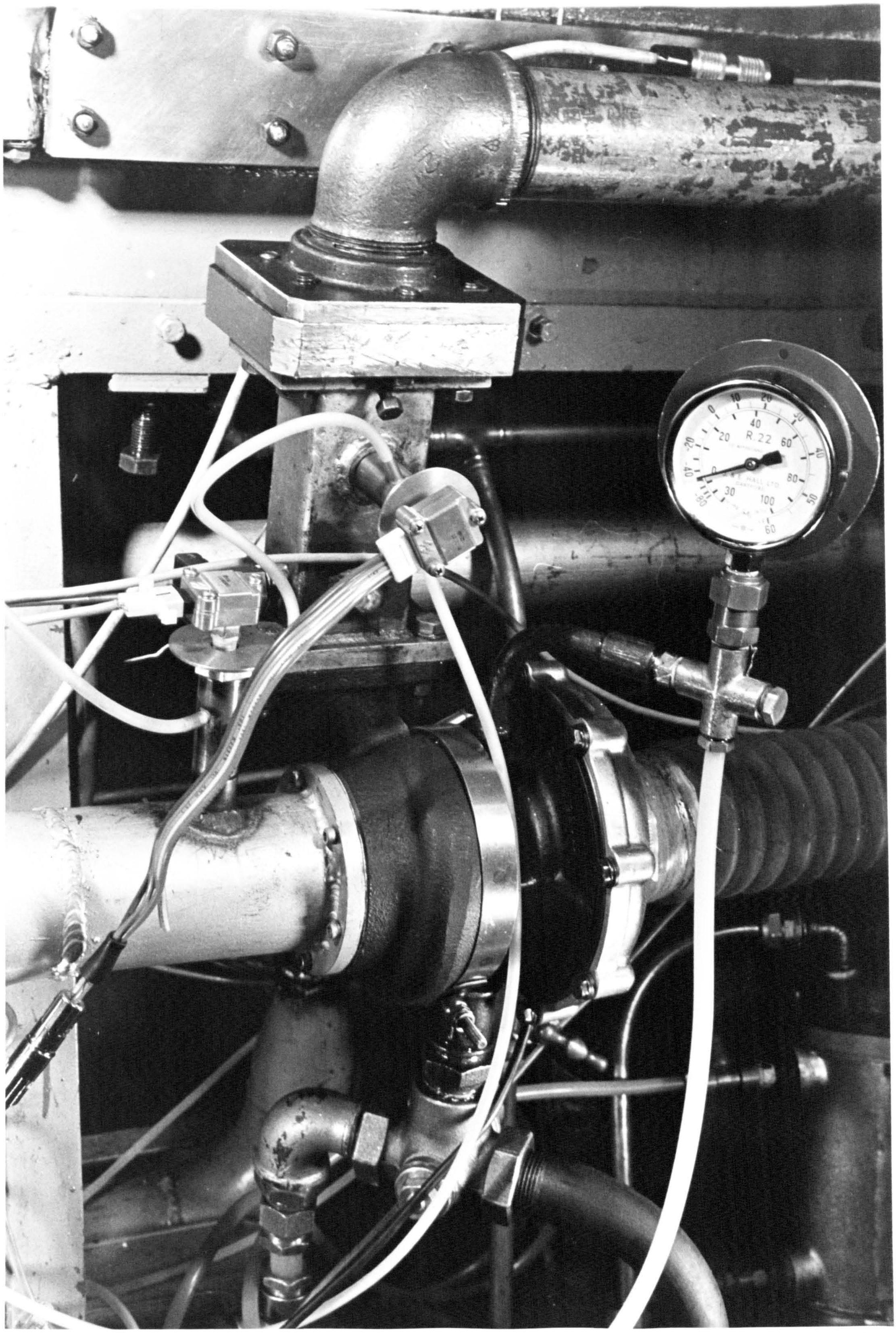

PLATE (3) THE TURBOCHARGER

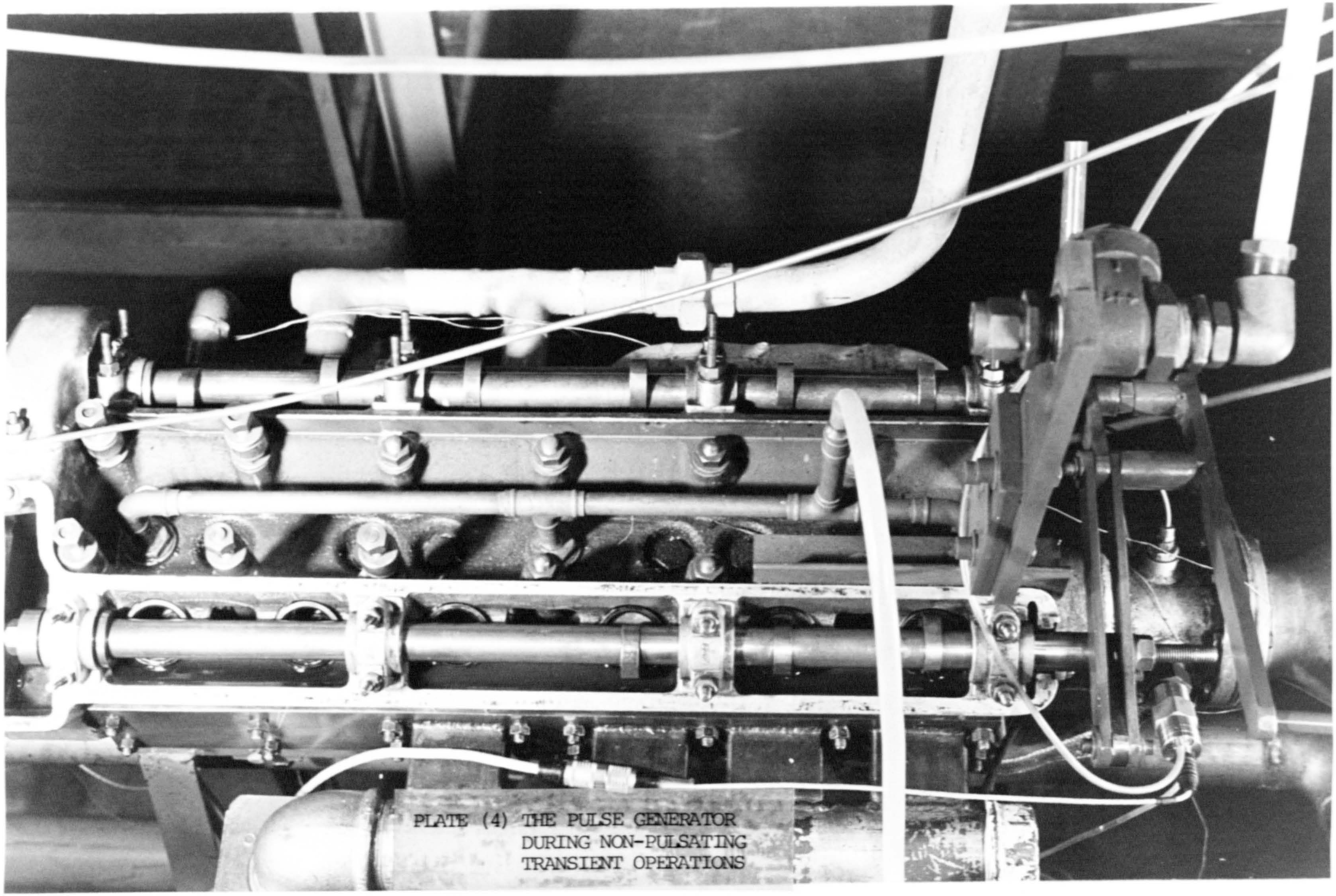

PLATE (4) THE PULSE GENERATOR
DURING NON-PULSATING
TRANSIENT OPERATIONS

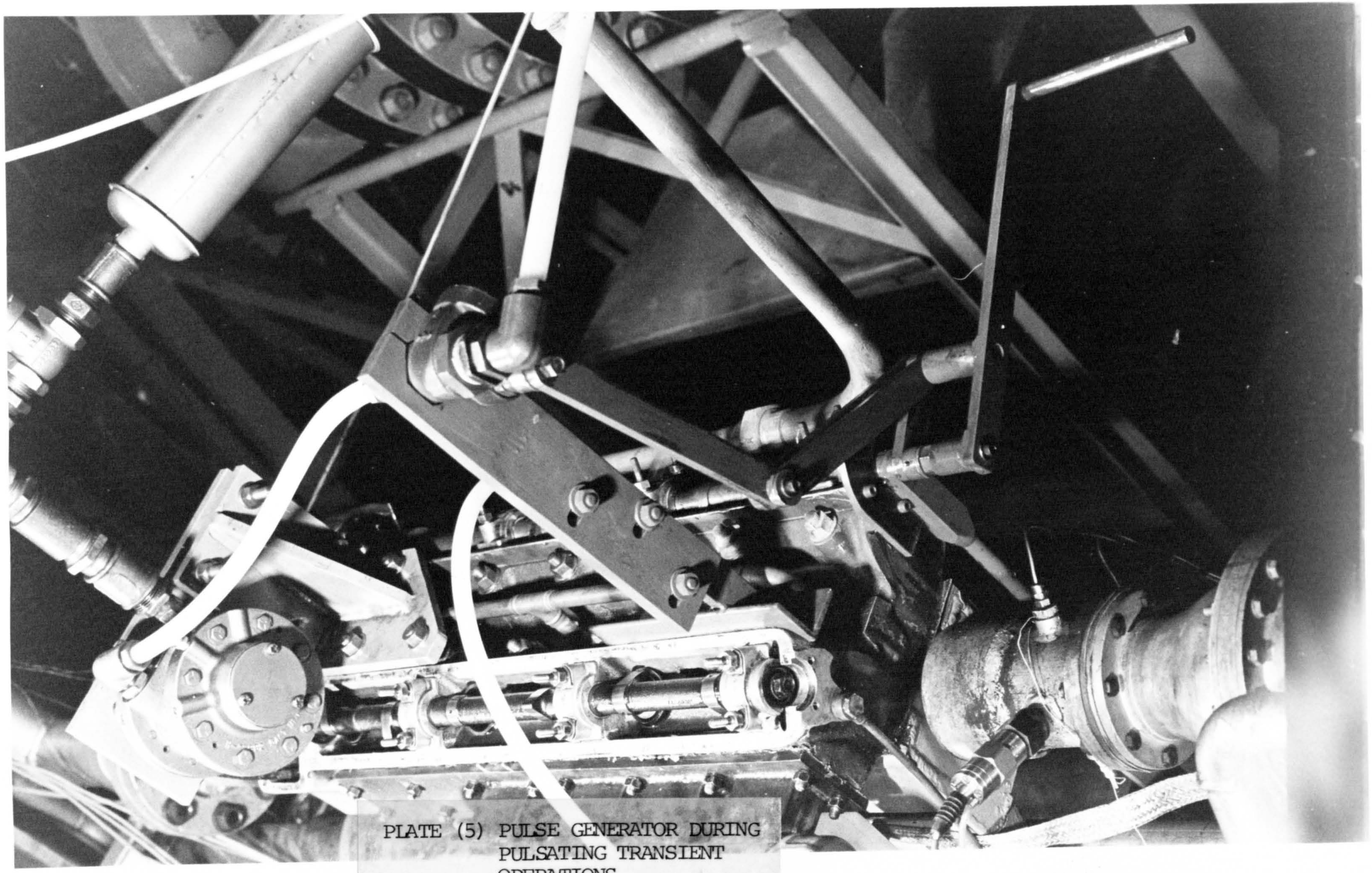

PLATE (5) PULSE GENERATOR DURING PULSATING TRANSIENT OPERATIONS

CHAPTER FOUR

INSTRUMENTATION

CHAPTER FOUR

INSTRUMENTATION

Appropriate instrumentation was selected and fitted to the rig to enable the turbocharger speed and the temperature and pressure of the working fluid to be recorded at salient points during steady and transient operations, see Figs (4.1) and (4.2).

4.1 PRESSURE MEASUREMENTS

Test Series I:

Inductive type transducers, which were used gave reasonable response to pressure variations, and according to Considine[33], temperature had slight effect on the measurements. From the manufacturer specification the linearity should be within ± 1%. The pressure transducers, which were used, were Southern Instruments type G301 and type G255 and Vibrometer inductive transducers type PK/10 as follows.

Turbine inlet	:	G301 transducer (0-100 lbf/in^2)
Turbine outlet	:	G301 transducer (0- 50 lbf/in^2)
Compressor inlet	:	G255 differential transducer (-10-0-10 lbf/in^2) (Measuring the difference between the compressor inlet pressure and atmospheric pressure)

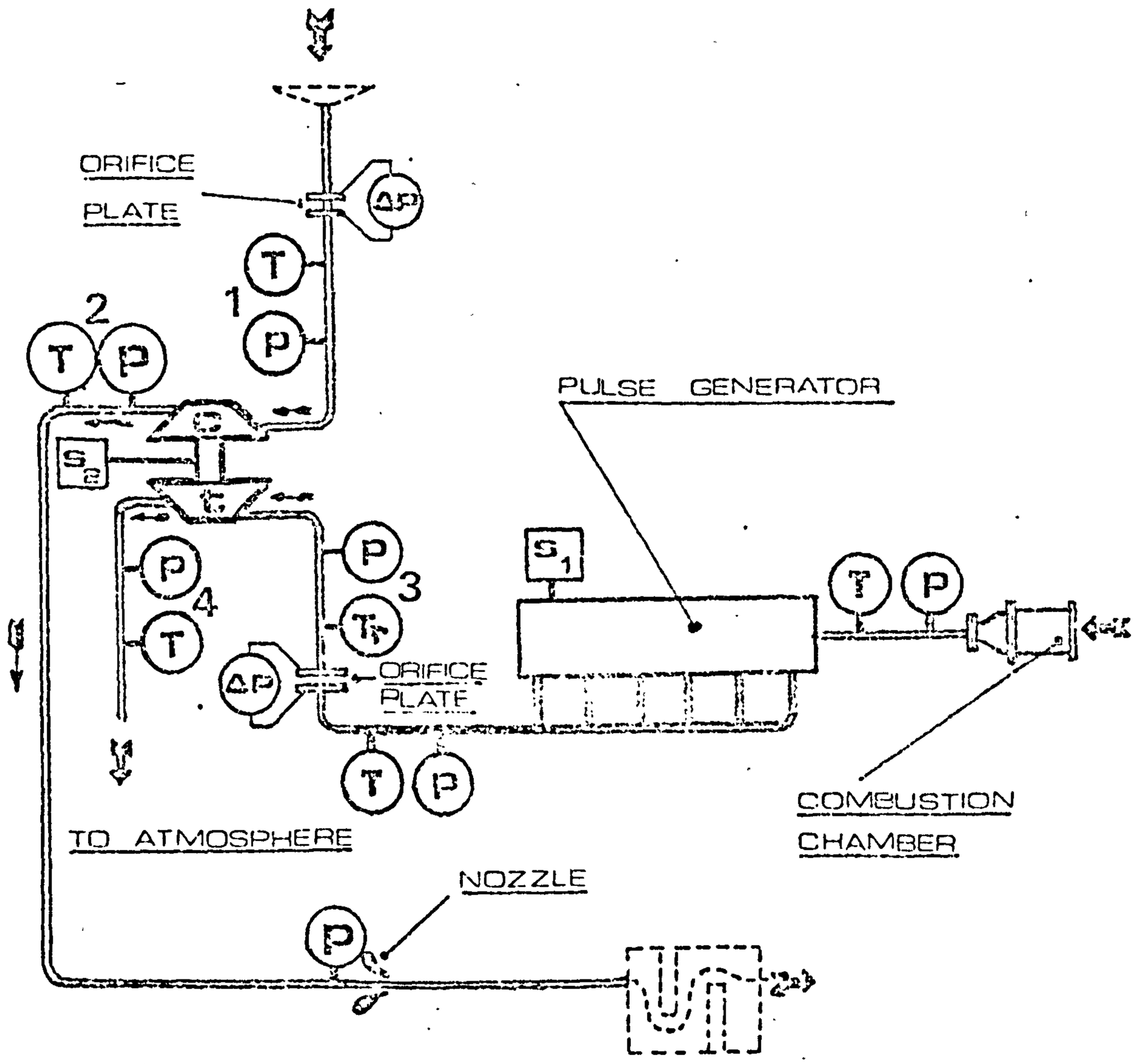

P — PRESSURE TRANSDUCER

T — THERMOCOUPLE

ΔP — PRESSURE TRANSDUCER — DIFFERENTIAL

Tr — RESISTANCE WIRE PROBE FOR TEMPERATURE MEASUREMENT

S_1 — TACHOMETER

S_2 — PHOTO-ELECTRIC SPEED MEASURING DEVICE

c — COMPRESSOR t — TURBINE

fig.(4.1) DIAGRAMATIC LAYOUT OF MEASURING INSTRUMENTS (TEST SERIES I)

Compressor outlet	:	G301 transducer (0-100 lbf/in^2)
Orifice plate at the turbine inlet	:	G255 differential transducer (-10-0-10 lbf/in^2) (Measuring the difference across the orifice plate)
Orifice plate at compressor inlet	:	G255 differential transducer (-10-0-10 lbf/in^2) (Measuring the difference across the orifice plate)
Pulse generator inlet	:	Vibrometer PK/10 transducer (0-142 lbf/in^2)
Nozzle inlet	:	Vibrometer PK/10 transducer (0-142 lbf/in^2)

See Fig. (4.1)

The Southern Instruments transducers were each coupled to a Southern Instruments type 1860 frequency modulated unit through an oscillator type 1822. See Plate (6). The method of operation of the Southern transducers was as follows:

(i) the pressure applied to the diaphragm of the transducer deflected the diaphragm causing a variation in the inductance of the transducer,

(ii) the variation in inductance in turn modified the natural frequency of the oscillator circuit. Consequently a change in the pressure applied to the transducer was converted into a proportional change in the frequency of 2 MHz carrier wave,

(iii) the carrier wave was then passed to the frequency modulated unit. In the frequency modulated unit

the signal was amplified and then applied to a frequency-discriminator circuit, and the output produced by this circuit was a direct voltage proportional to the change in the input frequency. The output from the frequency discriminator circuit was passed through a filter to give a low value of output-noise level. The output voltage was thus directly proportional to the pressure applied to the transducer, and could be either used to operate an oscilloscope or used to drive a galvanometer in a galvanometer recorder.

The Vibrometer equipment consisted of an inductive full bridge pressure transducer type PK/10 using 8 kHz carrier system with conditioning unit type 8ICF-24/AG. The output from the unit could be used to operate an oscilloscope or used to drive a galvanometer in a galvanometer recorder.

All the pressure variations were recorded using an Ultra-Violet recorder type SE 2100 with 24 channels.

The transducers were calibrated within the ranges previously specified. The high pressure calibrations were carried out using a dead-weight tester. Each low pressure transducer was calibrated by installing it in its operating position on the rig and connecting a manometer across the transducer; the rig was then

operated under a range of steady conditions and the corresponding galvanometer deflections and manometer readings were recorded. From these values a graph of deflection against pressure was obtained for each pressure transducer.

Test Series II

For this series all the Southern Inductive transducers were replaced by National Semiconductor Transducers because they were found unsuitable. The replacement transducers were supplied to the following specifications:

TRANSDUCER POSITION	TYPE	OPERATING RANGE	SENSITIVITY CALIBRATION mv/psi
Comp.Orif.Plate inlet	LX 1701 G	-5 to 5 psig	1000 ± 20
Comp.Orif.diff.	LX 1801 DZ	-5 to 5 psid	1000 ± 20
Comp.Outlet	LX 1702 G	0 to 15 psig	670 ± 13
Nozzle inlet	LX 1802 GBZ	0 to 15 psig	670 ± 13
Turbine inlet	LX 1703 GB	0 to 30 psig	333 ± 6
Turbine outlet	LX 1802 GBZ	0 to 15 psig	670 ± 13
Turbine Orif.inlet	LX 1802 GBZ	0 to 15 psig	670 ± 13
Turbine Orif.diff.	LX 1801 DZ	-5 to 5 psid	1000 ± 20

The transducers were calibrated within the ranges previously specified. The calibrations were carried out using power source and two digital voltmeters as well as calibrating each transducer with a manometer across it as described earlier.

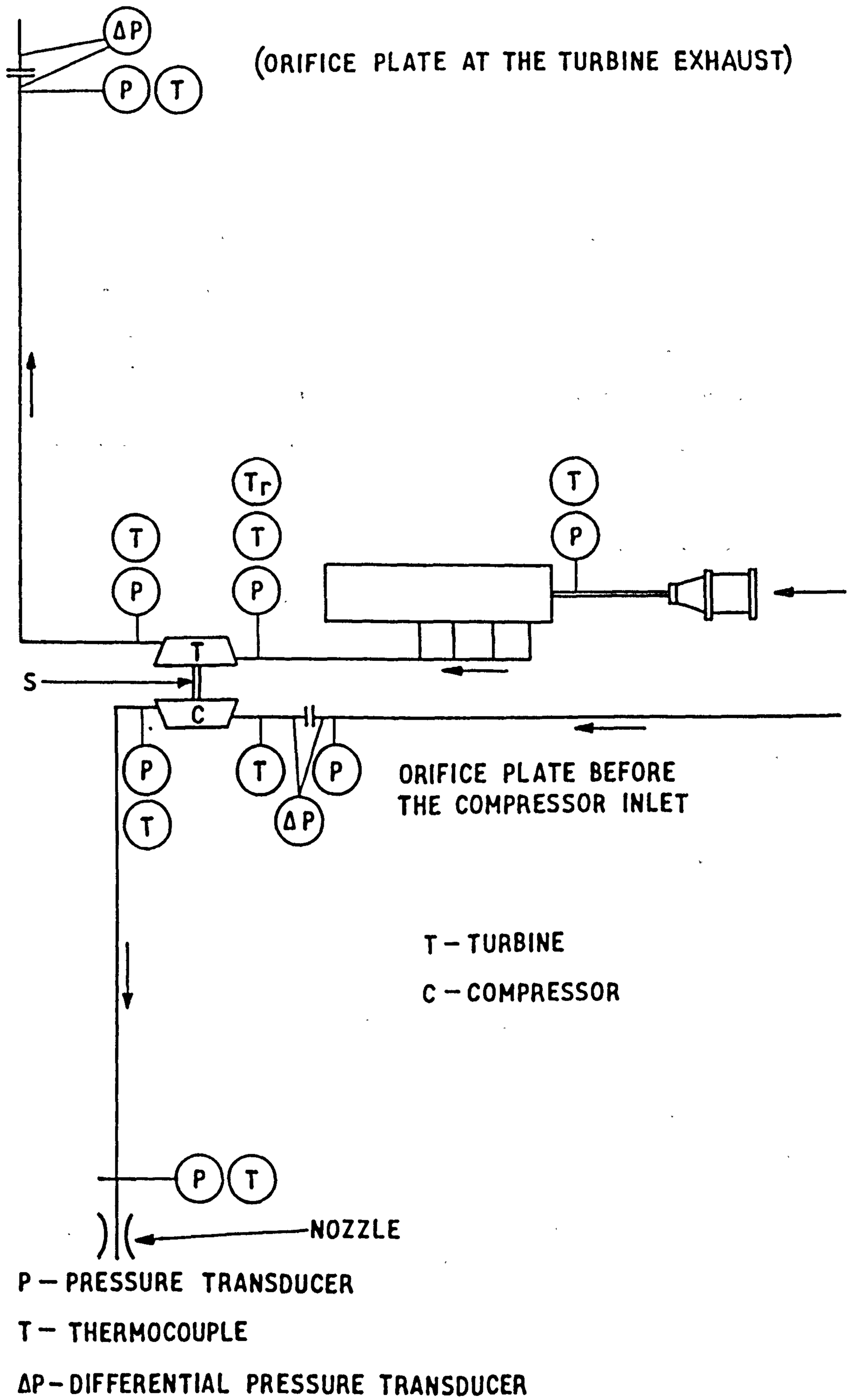

FIG. (4.2) DIAGRAMMATIC LAYOUT OF MEASURING INSTRUMENTS
(TEST SERIES II)

4.2 MASS FLOW RATE MEASUREMENTS

Orifice plates with corner tappings to measure the turbine and compressor mass flow rate were designed and fitted in the test rig according to BS1042[30]. In "Test Series I" the turbine orifice plate was fitted at the turbine inlet, Fig (3.1), and in "Test Series II" it was fitted in the turbine exhaust, see Fig (3.2) and plate (8). The compressor orifice plate in both series was fitted at the compressor inlet, see Figs (3.1), (3.2) and plate (9).

A record of the variations of the upstream pressure and temperature as well as the pressure drop across the orifice plate was obtained from the U.V. recorder. Using these recorded values, the mass flow rates under the transient operation through the turbine and compressor were calculated using BS1042.

The details of the orifice plates, were as follows:

(i) Turbine Orifice plate - Test Series I

Orifice diameter $d = 1\frac{13}{16}$"

Pipe diameter $D = 1\frac{5}{8}$"

Diameter ratio $\frac{d}{D} = 0.740$

Area ratio $(\frac{d}{D})^2 = 0.548$

Material - Stainless Steel

(ii) Turbine Orifice plate - Test Series II

Orifice diameter d = 2¼"

Pipe diameter D = $3\frac{3}{16}$"

Diameter ratio $\frac{d}{D}$ = 0.7059

Area ratio $(\frac{d}{D})^2$ = 0.4983

Material - Stainless Steel

(iii) Compressor Orifice plate -
Test Series I and Test Series II

Orifice diameter d = 1⅞"

Pipe diameter D = 2½"

Diameter ratio $\frac{d}{D}$ = 0.75

Area ratio $(\frac{d}{D})^2$ = 0.5625

Material - Brass

4.3 TEMPERATURE MEASUREMENTS

30 swg nickel chromium-nickel aluminium thermocouples were used for all the temperature measurements except at the turbine inlet where tungsten resistance wire probe with balanced Wheatstone bridge was used. See Plate (10).

Tungsten Wire Resistance Probe

The electrical resistance of tungsten, as that of most metals, increases with temperature, and this effect was used to measure the transient temperature at the turbine inlet[34][35]. As the highest accuracy and sensitivity was required the balanced form of Wheatstone's bridge was used. In this method, the resistance of one arm of the bridge is adjusted until the bridge is balanced, Fig. (4.3). When the probe temperature changes, the probe resistance will vary and the bridge will be unbalanced. The output of this circuit was used to drive a galvanometer of the UV recorder. As the wire was very fine (5 microns) and soild particles, which cause wire fracture,might be present in the air, the probe was inserted in the pipe only as required.

The fine wire probe was calibrated as follows:
A thermocouple was connected very near to the probe in the experimental rig. The turbocharger was run in steps of 5,000 rpm and the thermocouple temperature was recorded from a Comark electronic temperature indicator as well as

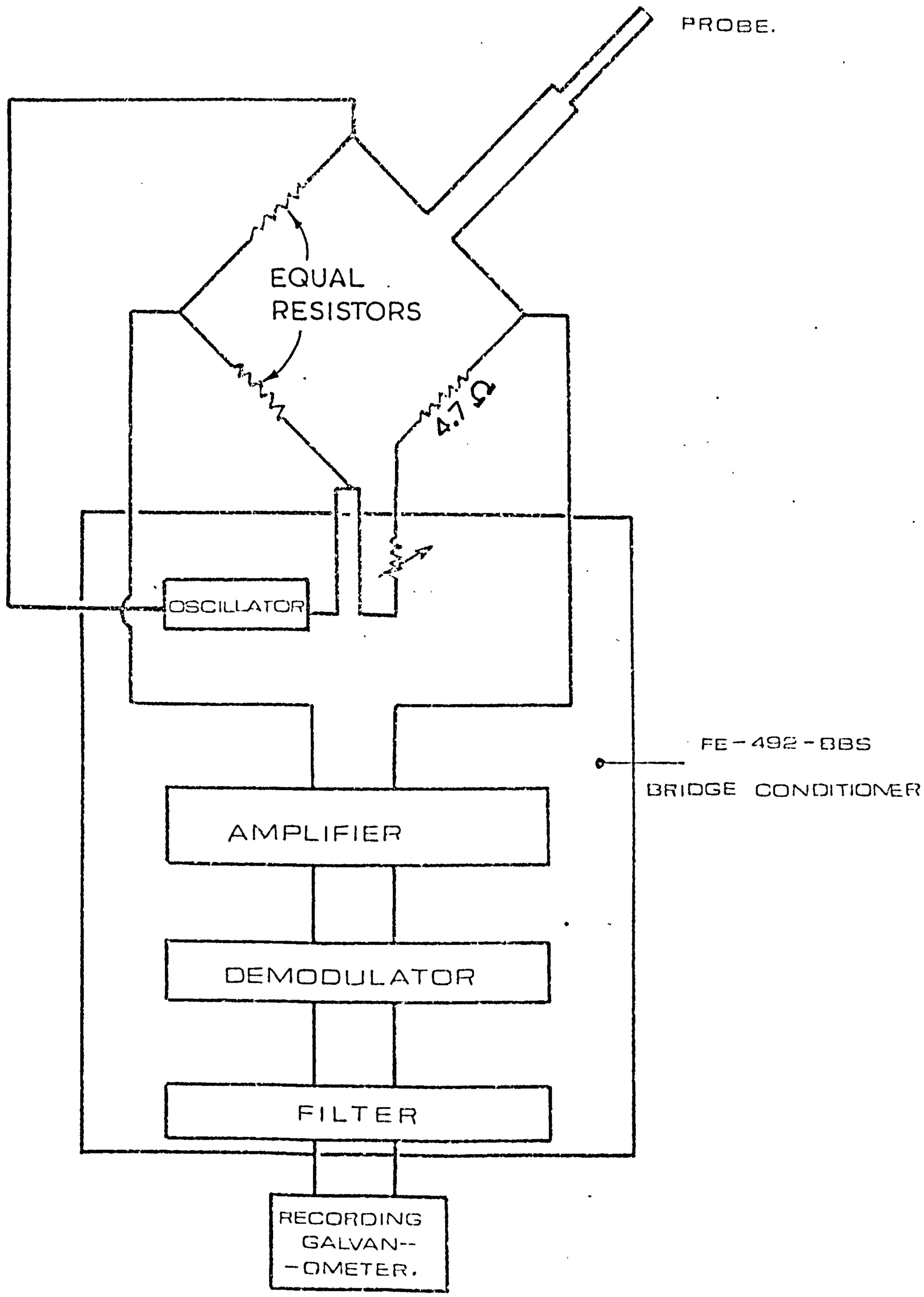

fig.(4.3) WHEATSTONE BRIDGE CIRCUIT FOR MEASURING TURBINE INLET TEMPERATURE

the galvonometer deflection of the probe. The temperature was plotted against the galvanometer deflection as shown in Fig. (4.4).

4.4 SPEED MEASUREMENTS

A photo-electric pulse pick up was used to measure the turbocharger speed. It consisted of an admitter and receiver and was mounted on the turbocharger casing above the compressor rotor, Fig. (4.5). As there are six large blades and six small blades on the rotor, the device was mounted in such a way that it received reflected signals from the six large blades only. A beam of light was projected through the admitter and the reflected beam of light fell on the receiver. The electrical impulses generated by the receiver were passed through an integrating and filter circuit. The output of this circuit was proportional to the turbocharger speed and the signal was recorded using the Ultra Violet galvanometer recorder. The gain of the amplifier was adjusted to obtain a suitable deflection and the ratio between the galvanometer deflection and turbocharger speed was attained using a pulse counter.

4.5 INTERFACE UNIT

An interface unit was manufactured to connect the various items of electronic instrumentation to the Ultra Violet Recorder (Test Series II). It consisted of:

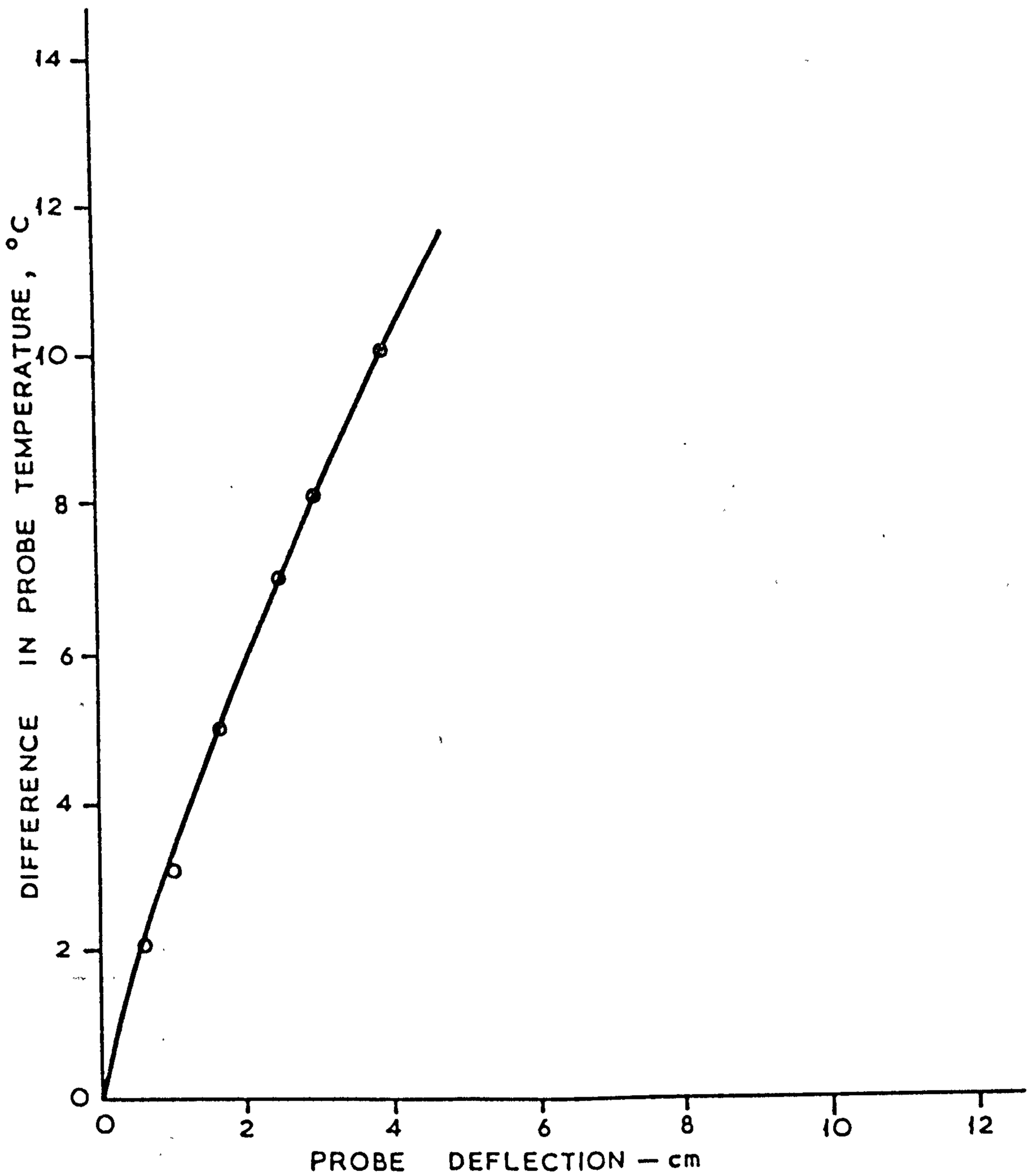

Fig. (4.4) DIFFERENCE IN PROBE TEMPERATURE vs GALVANOMETER DEFLECTION.

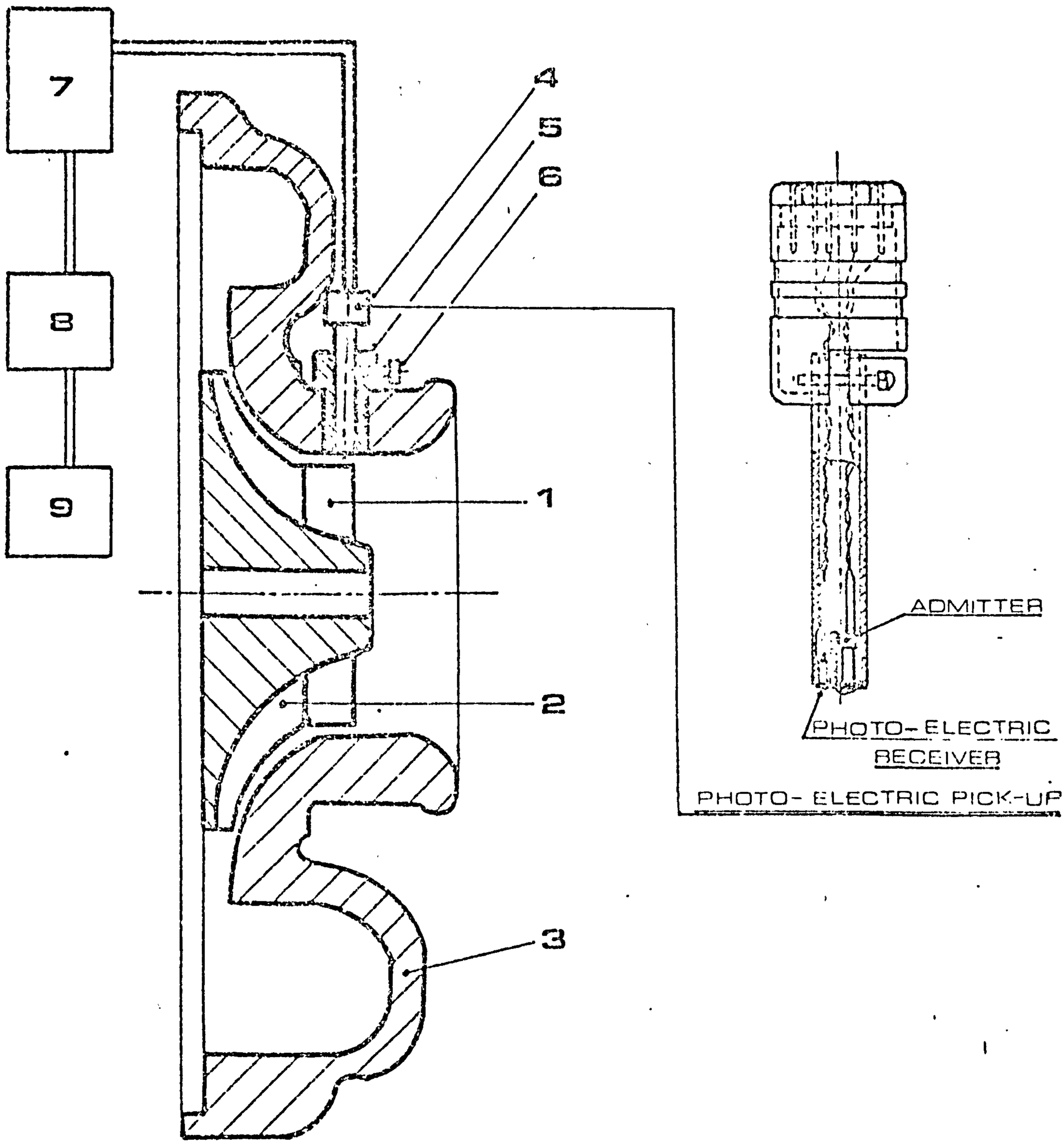

1 LARGE BLADES
2 SMALL BLADES
3 COMPRESSOR CASING
4 PHOTO-ELEC. PICK-UP
5 BOSS
6 TIGHTENING SCREW
7 INTEGRATING CIRCUIT
8 FILTER CIRCUIT
9 ULTRA-VIOLET RECORDER

fig.(4.5) TURBOCHARGER PHOTO-ELECTRIC SPEED MEASUREMENT SYSTEM

(i) 8 thermocouple amplifiers with attenuation and balancing circuits, (Fig. 4.6) ,

(ii) attenuation, offset, and filter networks for the pressure transducers, Fig. (4.7) ,

(iii) straight "through" connections for the vibrometer pressure transducer and the resistance wire temperature measuring system ,

(iv) turbocharger speed measuring system,

(v) power unit for (i), (ii), (iv) above and the pressure transducers.

The interface outputs were used to drive the galvanometer of a 24 channel UV recorder. The recorded measurements with their channels are shown in Table (1).

TABLE (1)

UV recorder channel	Measurement	Galvonometer frequency Hz
1	Comp.Orif.Inlet P.	160
2	Comp.Orif.diff P.	420
3	Comp.Outlet P.	160
4	Nozzle Inlet P.	160
5	Turbine Inlet P.	160
6	Turbine Outlet P.	160
7	Turbine Orif.Inlet P.	160
8	Turbine Orif.diff P.	420
9	P.G.Inlet P.	1000
10	Turbine Inlet Temp. (Res.Wire)	160
12	Turbocharger speed	1000
13	Comp.Inlet Temp.	160
14	Comp.Outlet Temp.	160
15	Nozzle Inlet Temp.	160
16	Turbine Outlet Temp.	160
20	Turbine Orif.Inlet Temp	160

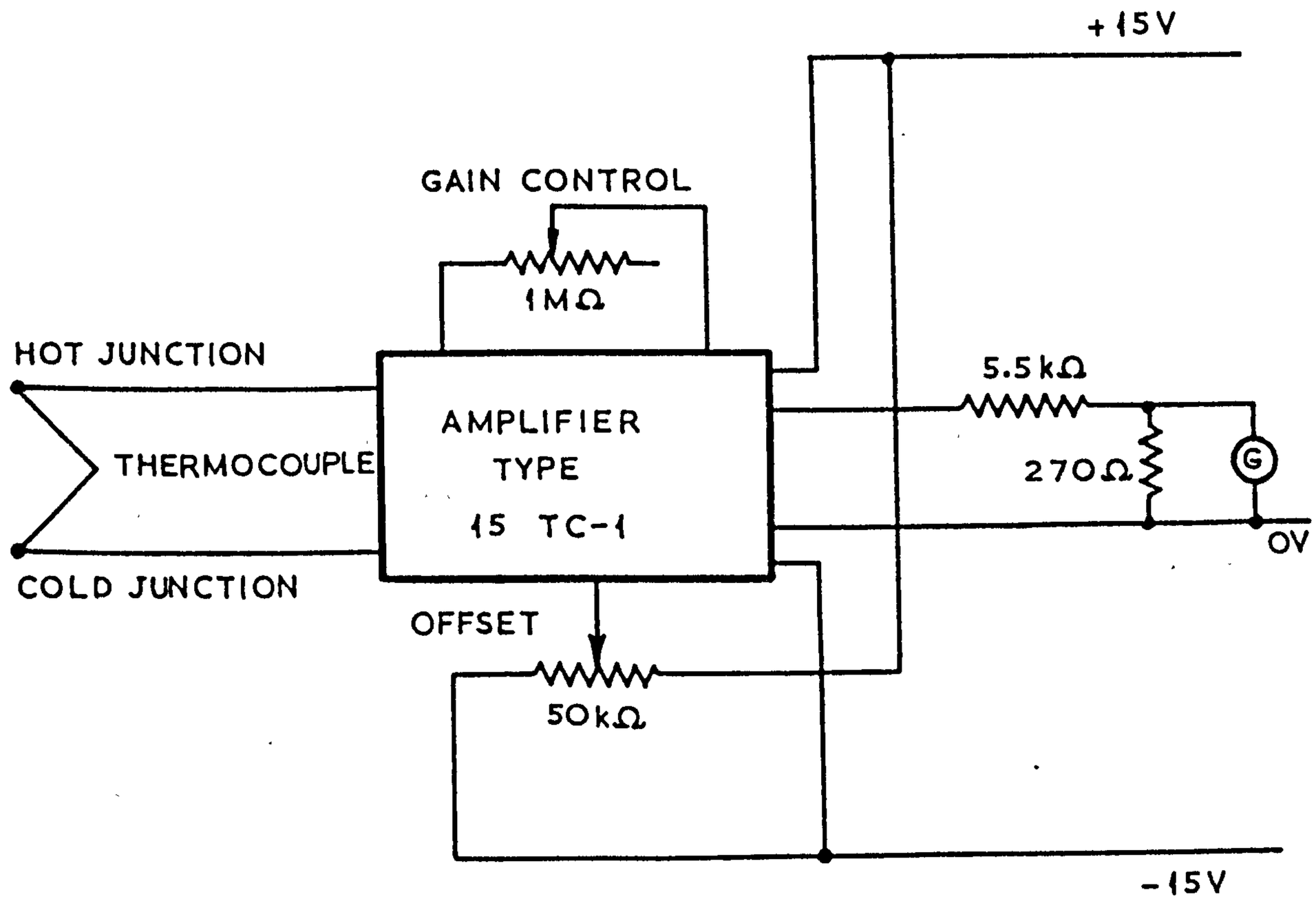

FIG. (4.6) THERMOCOUPLE AMPLIFIER CIRCUIT

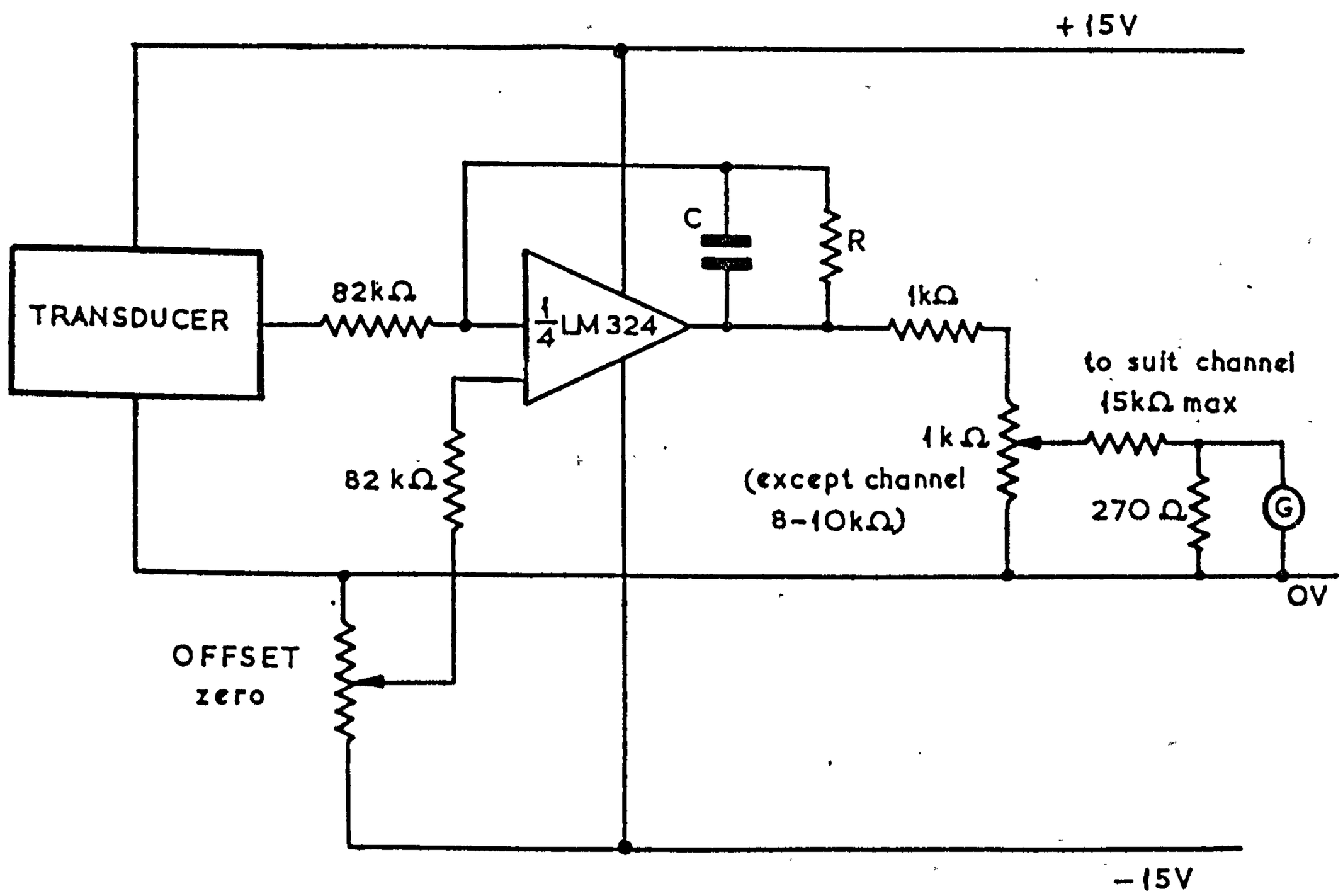

FIG.(4.7)PRESSURE TRANSDUCER AMPLIFIER CIRCUIT

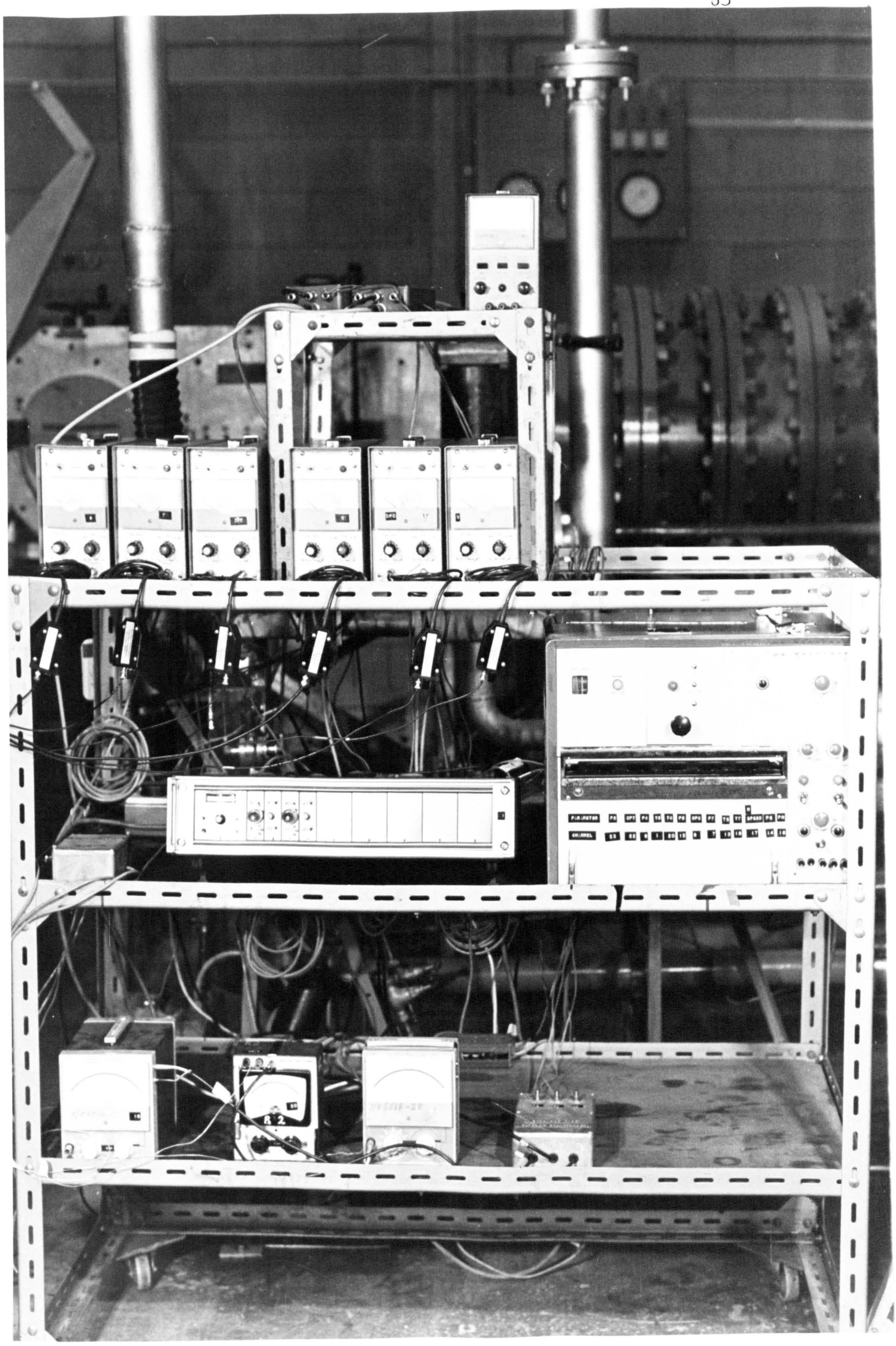

PLATE (6) INSTRUMENTATION
TEST SERIES I

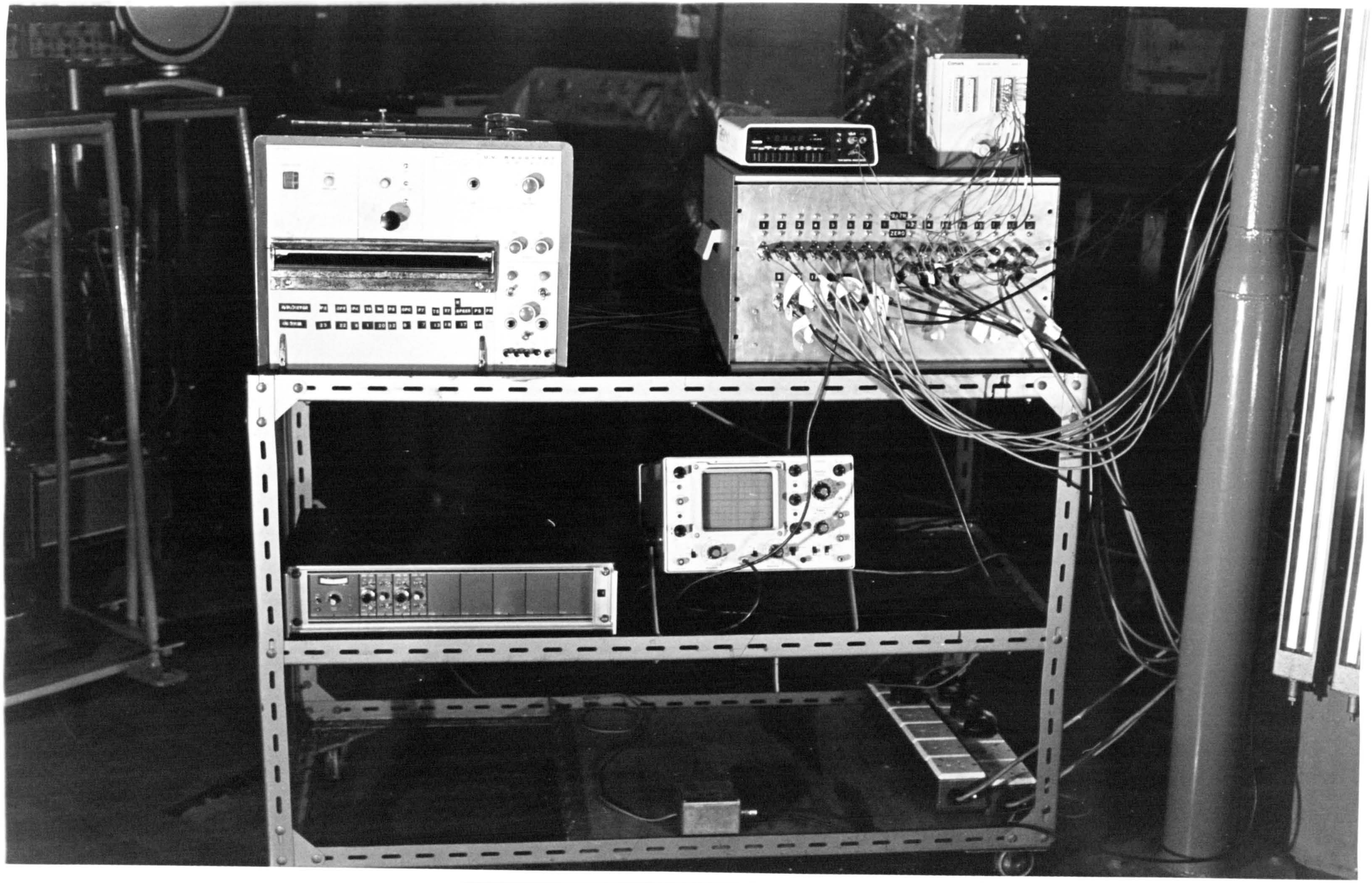

PLATE(7) INSTRUMENTATION
- TEST SERIES II

PLATE (8) ORIFICE PLATE AT
TURBINE EXHAUST

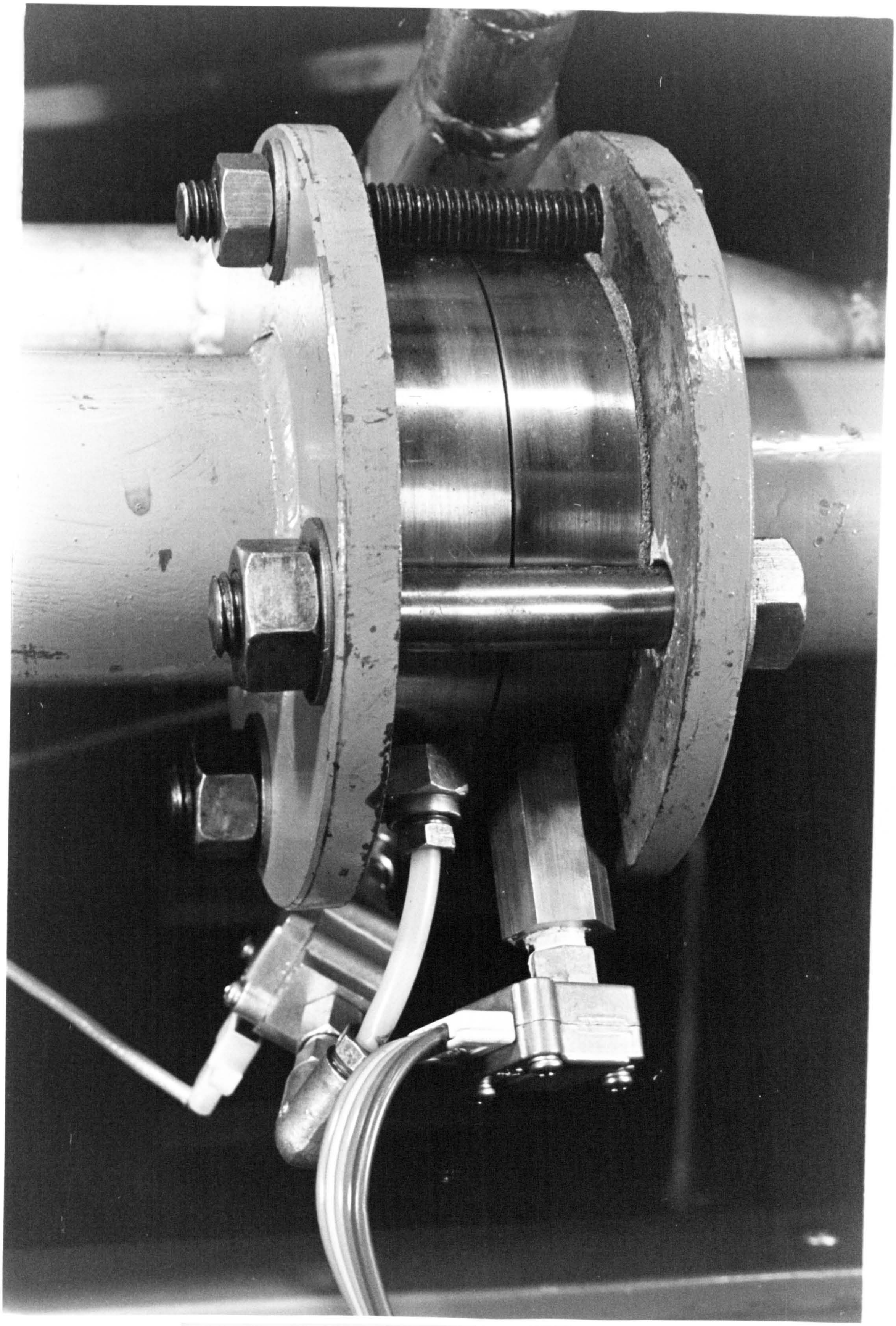

PLATE (9) ORIFICE PLATE AT COMPRESSOR INLET

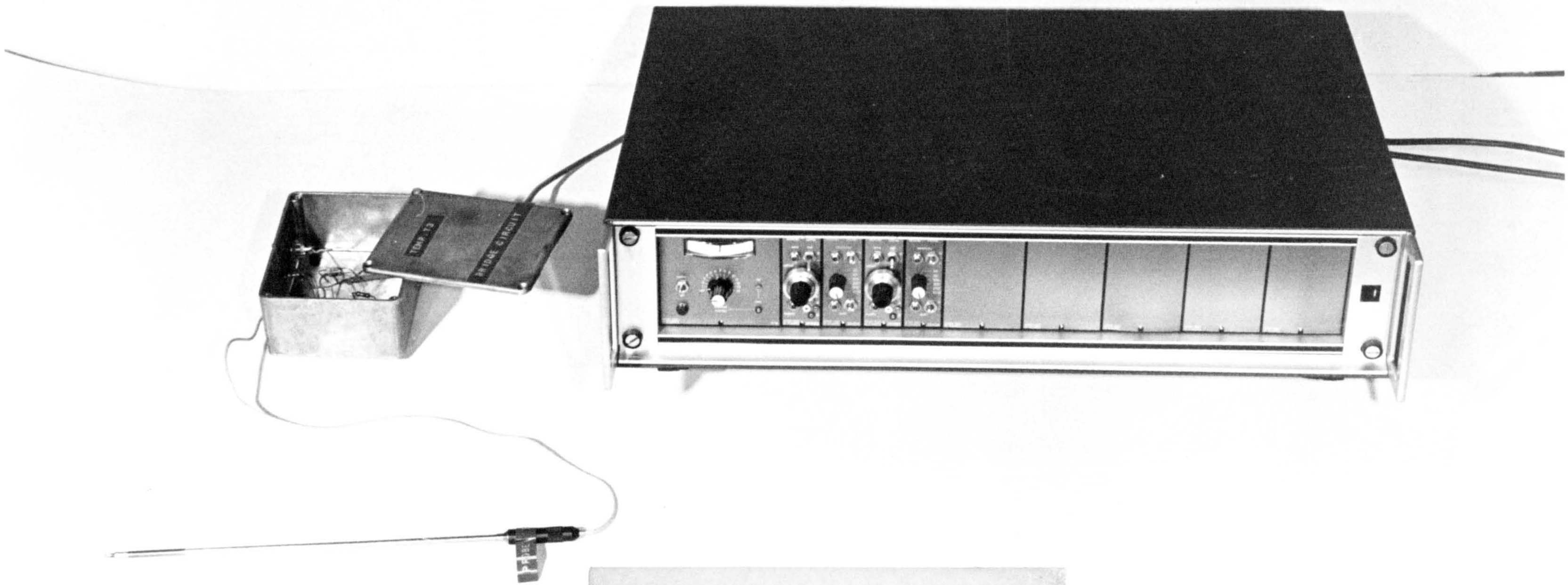

PLATE (10) THE RESISTANCE WIRE PROBE WITH BALANCED WHEATSTONE BRIDGE

CHAPTER FIVE

EXPERIMENTAL PROCEDURE

CHAPTER FIVE

EXPERIMENTAL PROCEDURE

5.1 PULSE GENERATOR VALVE OPENING AREA

The pulse generator cam profile was first measured accurately by "Ferranti Conquest Three-Coordinate Measure Machine". The camshaft was rotated every 10° angle and the displacement of the follower was recorded using a digital gauge. The method of measuring the follower displacement can be seen in Fig (5.1).

Once the valve geometry is known the valve opening area can be calculated as follows:

(1) When the slant height between the valve faces is perpendicular, Fig (5.2a), the valve area is equal to the frustrum of a cone, and the following equations were used:

Area of a frustrum of a cone = $\pi(2B-X)S$.. .. (26)

where

$S = L \cos \alpha$ .. .. (27)

$X = S \sin \alpha$ .. .. (28)

$B = X + r$ .. .. (29)

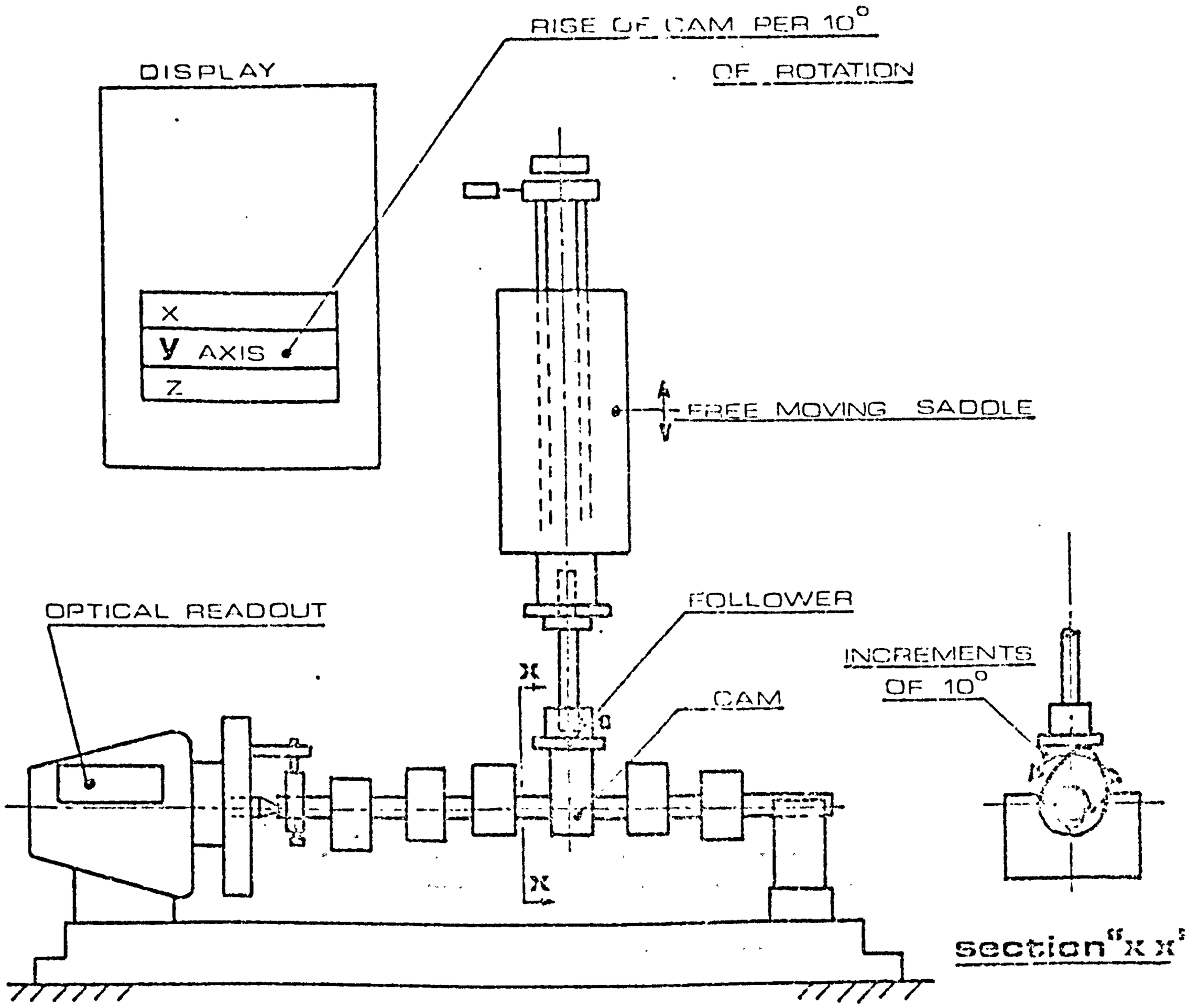

fig. (5.1) DIAGRAMATIC LAYOUT OF CAM

TESTING APPARATUS

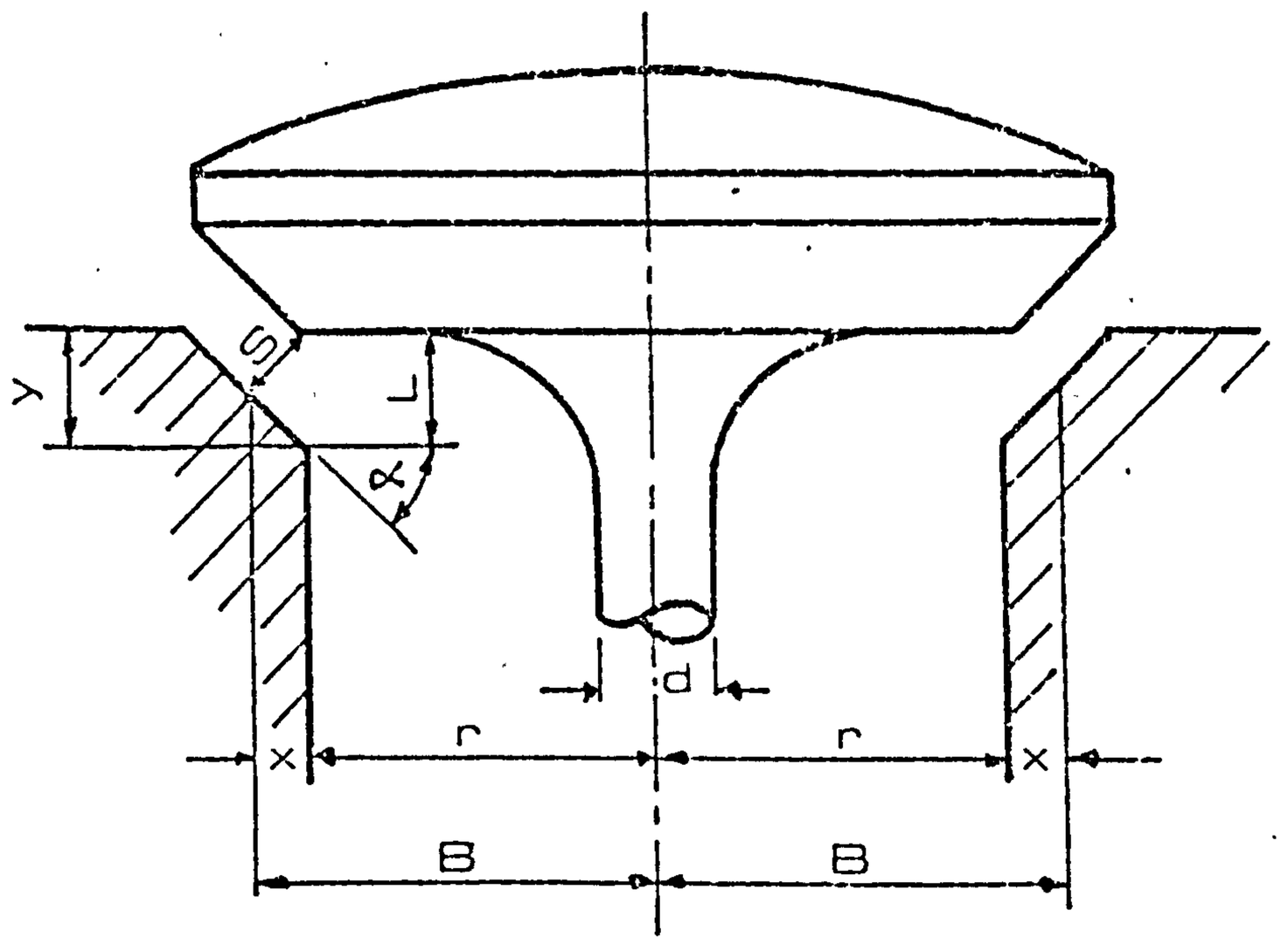

(a) SLANT HEIGHT PERPENDICULAR

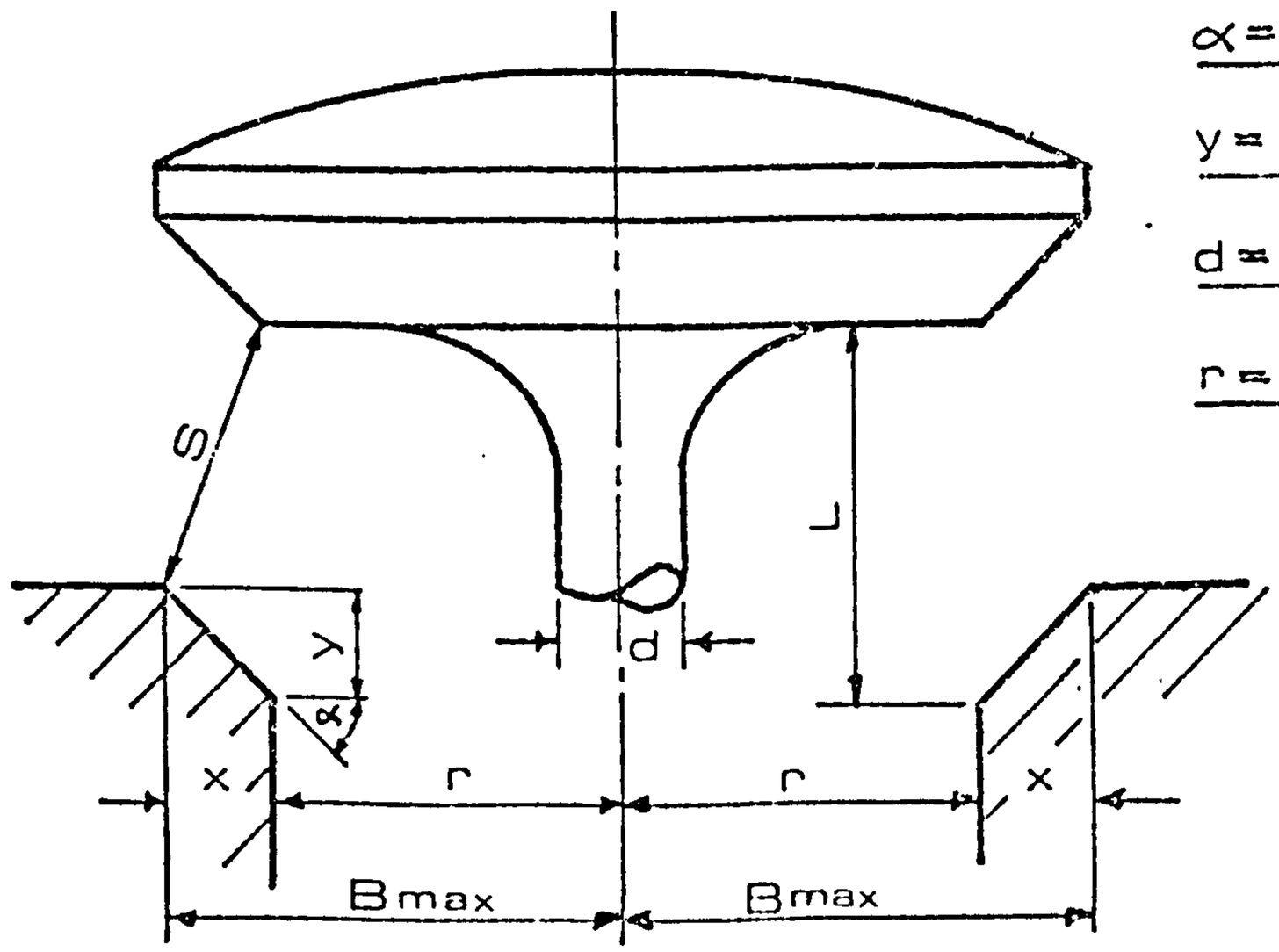

$\alpha = 45^0$

$y = 3 \cdot 175 mm$

$d = 7 \cdot 938 mm$

$r = 17 \cdot 463 mm$

(b) SLANT HEIGHT NOT PERPENDICULAR

fig.(5.2) PULSE GENERATOR VALVE POSITIONS.

Substituting equations (27),(28),(29) into equation (26):

Area through the valve=$\pi L \cos\alpha(2r+L\cos\alpha\sin\alpha)$.(30)

Equation (30) is valid only for a perpendicular slant height and the limiting criterion for its use is

$$L_{limit} = \frac{B\ max - r}{\cos\alpha \sin\alpha} \qquad \ldots\ldots(31)$$

(2) When the valve lift is greater than L_{limit}, the slant height is no longer perpendicular, Fig (5.2b) and the following equations were used:

$$S = \left[X^2 + (L - y)^2\right]^{\frac{1}{2}} \qquad \ldots\ldots(32)$$

$$X = B - r \qquad \ldots\ldots(33)$$

$$Y = (B - r) \tan\alpha \ . \qquad \ldots\ldots(34)$$

Substituting equations (32),(33), and (34) into equation (26):

$$\text{Area through the valve} = \pi(B+r)\left[x^2+(L-y)^2\right]^{\frac{1}{2}}$$

$$= \pi(B+r)\left[(B-r)^2(1+\tan^2\alpha)+L^2-2L(B-r)\tan\alpha\right]^{\frac{1}{2}} \qquad \ldots(35)$$

The valve geometry was checked and it was found that the maximum valve lift was greater than L_{limit}, as follows.

valve seat angle with reference to the horizontal plane (α) = 45°

vertical dimension of valve seat chamber (y) = 3.175 mm

diameter of the valve stem (d) = 7.938 mm

minimum radius of valve seat (r) = 17.463 mm.

Substituting into equation (31):

$$L_{limit} = \frac{B_{max} - r}{\cos\alpha \sin\alpha} \qquad \ldots\ldots(31)$$

$$= \frac{y \tan\alpha}{\cos\alpha \sin\alpha}$$

$$= 6.35 \text{ mm} .$$

As the maximum measured valve lift was 9.765 mm, Table (2), which was greater than L_{limit}, both equations (30) and (35) were used as appropriate to calculate the valve opening area for the whole cycle. Fig (5.3) shows the valve opening area plotted against camshaft angles, 360° representing one complete cycle. It will be noted that there is some valve overlap. The effect of the valve clearances on the calculated area has been neglected.

TABLE 2

PULSE GENERATOR VALVE LIFTS

camshaft angle degree	first valve lifts mm	second valve lifts mm	third valve lifts mm
0	0.010	0.234	.442
10	0.011	.119	2.674
20	.011	.037	5.160
30	.011	.010	7.161
40	.011	.008	8.619
50	.011	.009	9.493
60	.010	.008	9.765
70	.009	.009	9.417
80	.013	.011	8.459
90	.053	.012	6.945
100	.134	.012	4.887
110	.273	.010	2.358
120	.442	.010	.343
130	2.674	.011	.234
140	5.160	.011	.119
150	7.161	.011	.037
160	8.619	.011	.010
170	9.493	.011	.008
180	9.765	.010	.009
190	9.417	.009	.008
200	8.459	.013	.009
210	6.945	.053	.011
220	4.887	.134	.012
280	2.358	.273	.012
240	.343	.442	.010
250	.234	2.674	.010
260	.119	5.160	.011
270	.037	7.161	.011

/Cont'd ...

camshaft angle degree	first valve lifts mm	second valve lifts mm	third valve lifts mm
280	.010	8.619	.011
290	.008	9.493	.011
300	.009	9.765	.011
310	.008	9.417	.010
320	.009	8.459	.009
330	.011	6.945	.013
340	.012	4.887	.053
350	.012	2.358	.134
360	.010	.343	.273

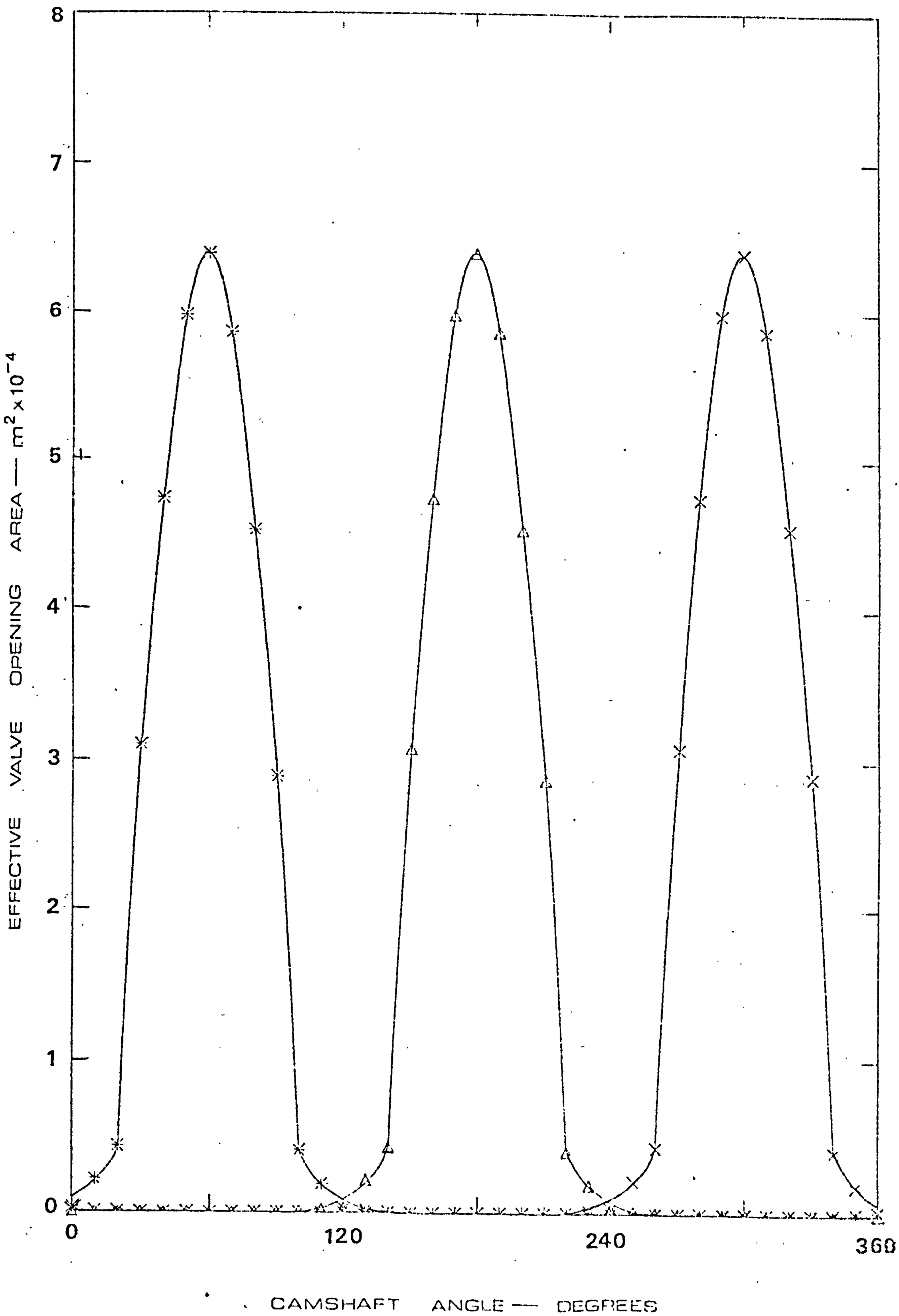

fig.(5.3) PULSE GENERATOR VALVE OPENING AREA

(PULSE GENERATOR SPEED = 2000 R.P.M.)

5.2 PULSE GENERATOR VALVE DISCHARGE COEFFICIENTS

(a) Under cold running

The actual air flow rate through the inlet valve is expected to be less than the air flow rate which could be calculated assuming isentropic flow through the valve with its area fully effective. The steady flow coefficient of discharge is specified as being the ratio of actual mass flow to the theoretical mass flow, under a given set of steady flow conditions, that is, it is a flow loss factor. Applying elementary nozzle theory, the following assumptions are made:

(i) the valve is analogous to a convergent nozzle

(ii) the inlet velocity of the air is very much smaller than the outlet velocity and may be neglected without incurring undue error.

Using the above assumptions, the isentropic mass flow through the pulse generator valve can be calculated as follows:

Continuity equation

$$\dot{m} = \rho_v c_v F_v \quad . \qquad \ldots \ldots (36)$$

For isentropic flow

$$\frac{T_v}{T_u} = \left(\frac{P_v}{P_u}\right)^{\frac{\gamma-1}{\gamma}} \qquad \ldots\ldots (37)$$

$$\frac{\rho_v}{\rho_u} = \left(\frac{P_v}{P_u}\right)^{\frac{1}{\gamma}} \qquad \ldots\ldots (38)$$

but

$$\rho = \frac{P}{RT} \qquad \ldots\ldots (39)$$

energy equation

$$h_u + \frac{c_u^2}{2} = h_v + \frac{c_v^2}{2} \qquad \ldots\ldots (40)$$

$$C_v = \left[2(h_u - h_v)\right]^{\frac{1}{2}} \quad C_u \simeq o$$

$$= \left[2C_p(T_u - T_v)\right]^{\frac{1}{2}} \qquad \ldots\ldots (41)$$

for ideal gas

$$C_p = \frac{\gamma}{\gamma-1} R \ . \qquad \ldots\ldots (42)$$

Substituting equations (37) and (38) into equation (41)

$$C_v = \left[2\ T_u\ \left(\frac{\gamma}{\gamma-1}R\right)\left(1-\left(\frac{p_v}{p_u}\right)^{\frac{\gamma-1}{\gamma}}\right)\right]^{\frac{1}{2}} \qquad \ldots\ldots (43)$$

Substituting equations (38), (39), and (43) into (36)

$$\dot{m} = \frac{P_u F_v}{\sqrt{T_u}} \left(\frac{2\gamma}{R(\gamma-1)}\right)^{\frac{1}{2}} \left[\left(\frac{P_v}{P_u}\right)^{\frac{2}{\gamma}} - \left(\frac{P_v}{P_u}\right)^{\frac{\gamma+1}{\gamma}} \right]^{\frac{1}{2}} \qquad \ldots\ldots (44)$$

Equation (44) may only be used to calculate the mass flow rate when the initial velocity of the fluid is negligible, as when the air flows from the pulse generator plenum chamber through the valves into the pipe which leads to the turbine.

The mass flow rate through the valve, for different valve lifts, was measured using the rig shown in Fig (5.4). A plate was mounted on the pulse generator cylinder head with an adjustable screw passing through the plate and on the axis of the valve stem. The action of turning the screw 360° moves the valve a distance equal to the screw pitch. An orifice plate with the corner tappings was fixed in the pipe downstream to the valve. Air at a specified pressure was supplied to the valve, and the screw was turned 360° at a time to vary the valve opening. For each position the following readings were recorded, Fig (5.4):

pulse generator valve inlet pressure (P_u)
pulse generator valve outlet pressure (P_v)
orifice plate inlet pressure (P_e)
pressure across the orifice plate (ΔP)
inlet temperature to the pulse generator and orifice plate (T_u,T_e).

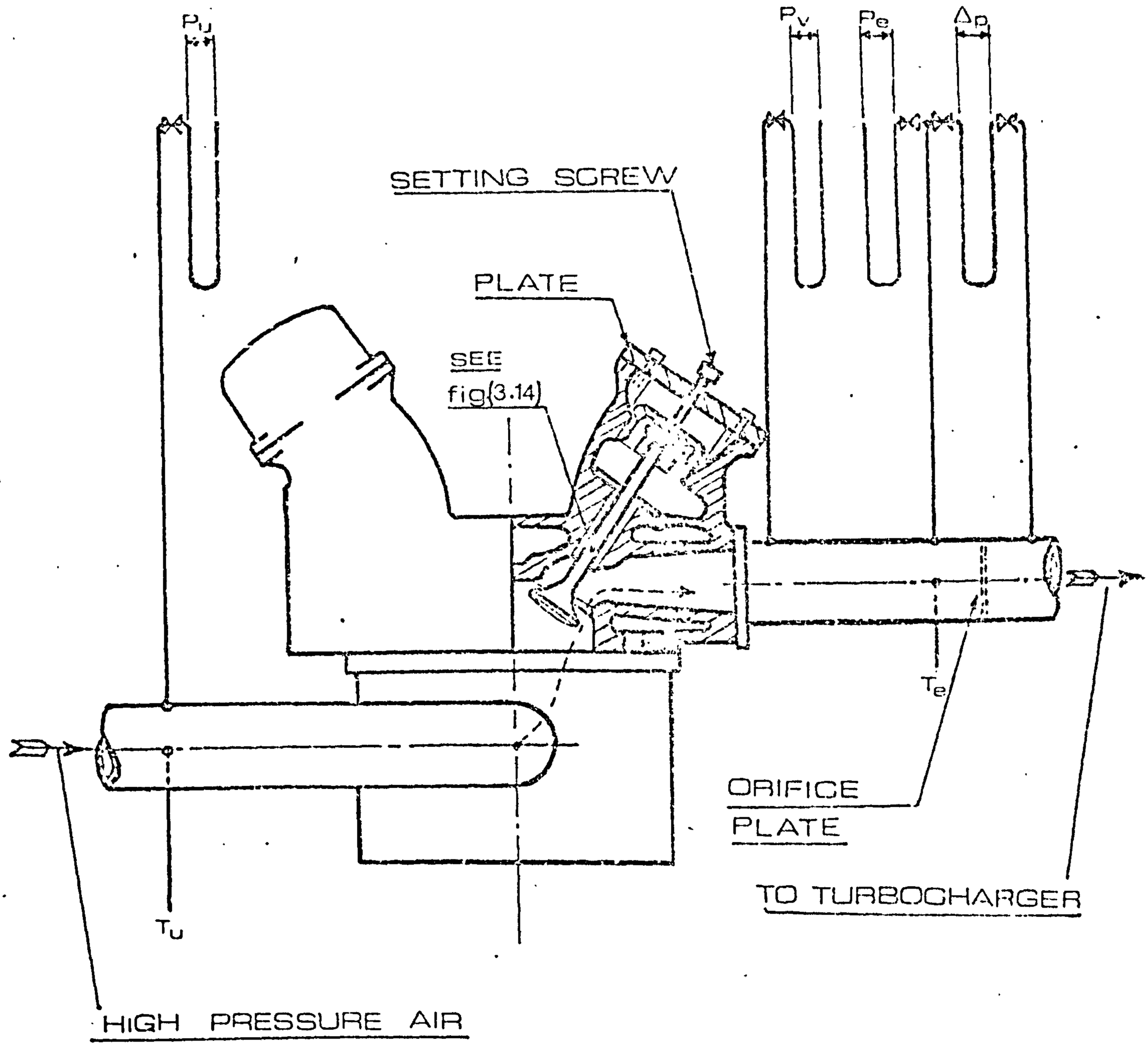

fig.(5.4) STEADY FLOW RIG FOR PULSE GENERATOR VALVE COEFFICIENT OF DISCHARGE

The pulse generator valve coefficient of discharge was evaluated by dividing the actual mass flow rate through the orifice plate which was obtained by using BS 1042, See Appendix (2), by the isentropic mass flow rate through the valve which was calculated by equation (44). The coefficient of discharge was evaluated for a range of 10, 20, 30, 40 and 50 lbf/in^2 pressure (P_u) applied to the pulse generator valve, Table (3), and was plotted against the valve lift as shown in Fig (5.5). The valve coefficient of discharge increased as the valve lift was increased. This agreed with results obtained by Williams and Cox[36].

(b) Under hot running

In the steady flow tests to calculate the valve coefficient of discharge, the temperature of the air passing through the experimental rig was not much higher than normal ambient values. However, in running the rig with hot air (to simulate engine exhaust conditions), the values of temperature attained at the valves would in fact be much higher. It would, therefore, be incorrect to use the experimental values of the coefficient of discharge directly in the computer program, unless a temperature correction was included. The temperature correction can be introduced by relating the

TABLE 3

PULSE GENERATOR VALVE COEFFICIENT OF DISCHARGE

valve lift mm	10 lbf/in^2	20 lbf/in^2	30 lbf/in^2	40 lbf/in^2	50 lbf/in^2	average
0.907	.77	.65	.66	.68	.71	.69
1.814	.55	.57	.60	.60	.61	.59
2.721	.47	.51	.52	.53	.52	.51
3.629	.41	.42	.43	.44	.43	.43
4.536	.33	.35	.36	.37	.37	.36
5.443	.28	.29	.30	.31	.31	.30
6.350	.25	.25	.26	.27	-	.26
7.257	.21	.22	.23	.23	-	.22
8.164	.19	.20	.20	.21	-	.20
9.070	.17	-	.18	.19	-	.18

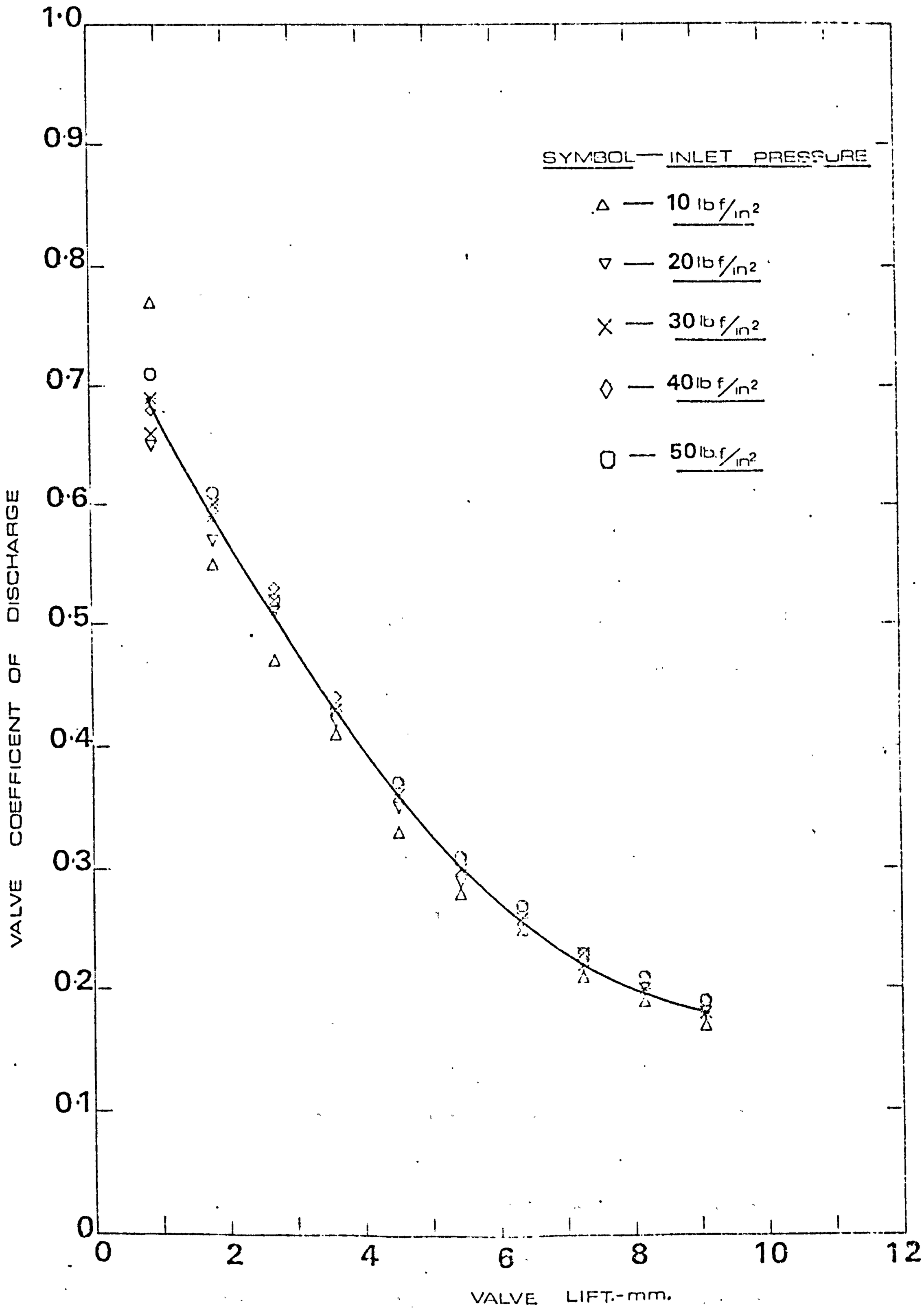

fig. 5.5 VARIATION OF PULSE GENERATOR VALVE COEFICIENT OF DISCHARGE WITH VALVE LIFT.

coefficient of discharge to the Reynolds Number at the throat, ie,

$$Re = \frac{\rho_v c_v d_v}{\mu_v} \qquad \text{.. .. (45)}$$

where

ρ_v density $\frac{kg}{m^3}$

c_v the gas velocity $\frac{m}{s}$

d_v diameter of the throat m

μ_v gas viscosity $\frac{kg}{m.s}$.

From which the viscosity μ is related directly to the temperature by the use of Sutherland's Law[37]

$$\frac{\mu}{\mu_o} = \left(\frac{T}{T_o}\right)^{\frac{3}{2}} \left(\frac{T_o+K}{T+K}\right) \qquad \text{.. .. (46)}$$

where

$$\mu_o = 1.52 \times 10^{-5} \frac{lbm}{ft.s}$$

$$T_o = 492^oR \ .$$

K is a constant which for air assumes a value of 198^oR. The density and velocity at the throat are known from equations (35) and (40). As a result the Reynolds Number at the throat may be calculated at the new temperature to adjust the Reynolds Number correction factor Z_R,

equation (128), Appendix (2), in the calculations using BS 1042, thus the coefficient of discharge could be corrected for temperature difference.

5.3 TURBOCHARGER MOMENT OF INERTIA

The moment of inertia of the turbocharger rotor was measured by suspending the rotor by means of a length of wire as shown in the diagram below:

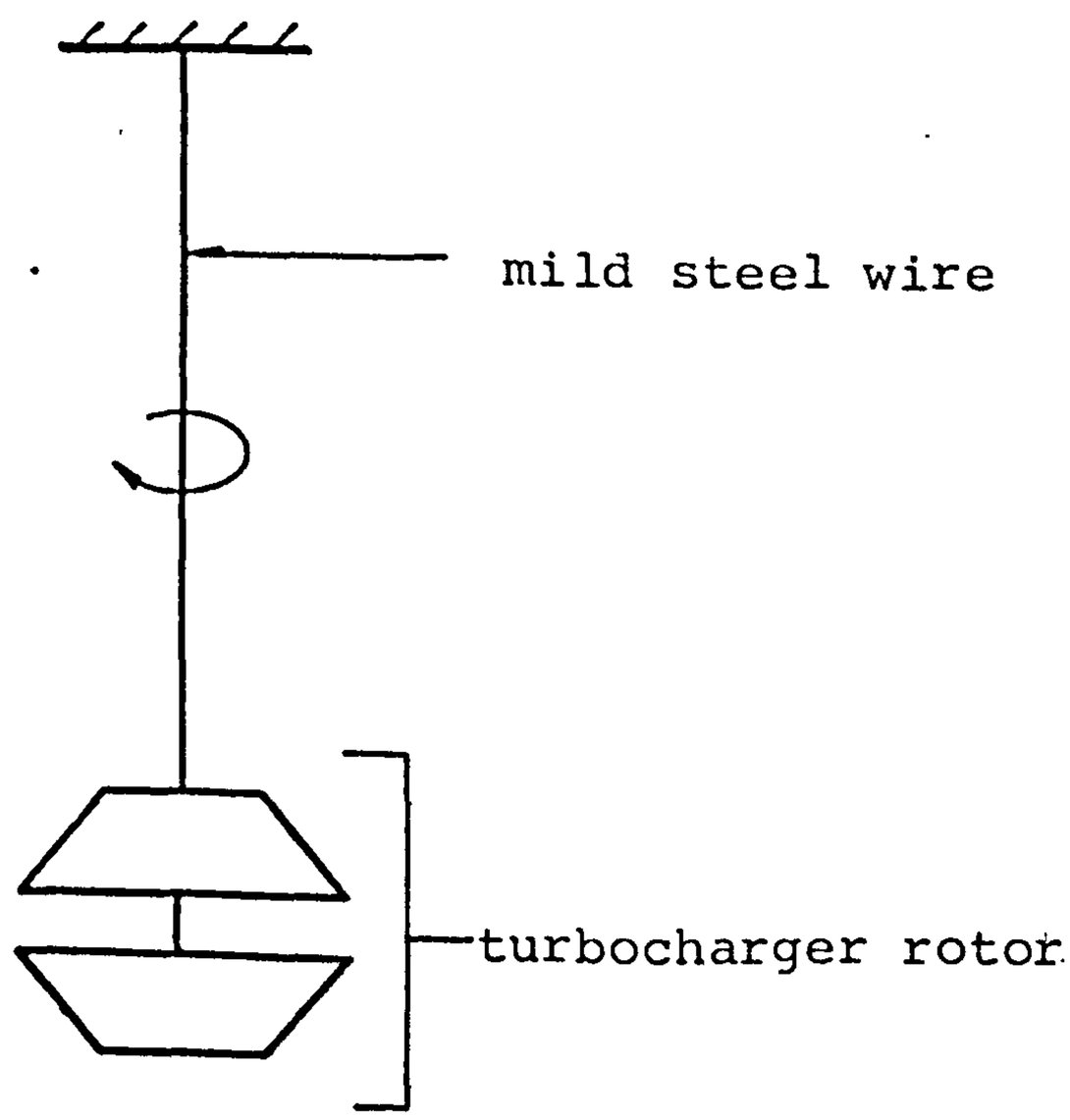

The rotor was rotated through a small angle, and the frequency of oscillation was measured. The moment of inertia was then calculated from the frequency equation:-

$$f = \frac{1}{2\pi} \sqrt{\frac{GJ}{I\ell}} \qquad \ldots \ldots (47)$$

where

f frequency

G modulus of rigidity for the steel wire

ℓ wire length

I rotor moment of inertia

J polar second moment of area of wire cross section $= \frac{\pi d^4}{32}$ where d is wire diameter.

5.4 TURBOCHARGER BEARING POWER LOSS

Due to the friction, a fraction of the turbine power was lost in the bearings. The frictional heat generated within the bearing clearance was partly carried away in oil flowing out from the ends of the bearing and partly transmitted by conduction through the body of the bearing and along the shaft.

Although fairly accurate analytical means are available for determining the rate of oil flow out and, hence, the heat lost to the escaping oil, the two other paths of heat transfer present difficult problems for analysis since they depend to a large extent upon special features of the bearing and other structural details. However, as far as forced-feed bearings are concerned, it is claimed that experimental evidence shows that almost all the frictional heat is removed by the oil flow[38].

Freeman[39] asserts that the amount of heat conducted away via the shaft or pedestal is only a small proportion of the total heat generated and can usually be neglected.

The Oil Temperature

The oil film temperature should not exceed about 180°F. A higher temperature than this would promote

rapid deterioration of the lubricant and change in the oil viscosity due to oxidation and a possible softening and distortion of the bearing metals themselves. If, due to reasons beyond the control, a temperature in excess of 180°F is continually reached, then some means of auxiliary cooling to the oil must be adopted[40]. According to this, cooling water is used to cool the oil flowing to the turbocharger bearing.

Bearing Power Loss Measurements

To measure the bearing power loss the test rig was modified by fitting a three-way valve in the oil flow return to the tank from the turbocharger bearing, see Plate (11). Two thermocouples were fitted in the inlet and outlet pipes as near as possible to the turbocharger, see Fig (5.6). The following procedure was used at specified turbocharger speeds from 10 000 rpm to 75 000 rpm increasing 5 000 rpm each time.

1. The oil temperature at the bearing inlet was kept constant (about 13±0.5°C) throughout the experiment by passing the oil through a water cooled heat exchange to eliminate any change in oil viscosity.

2. The turbocharger oil inlet and outlet temperatures were measured.

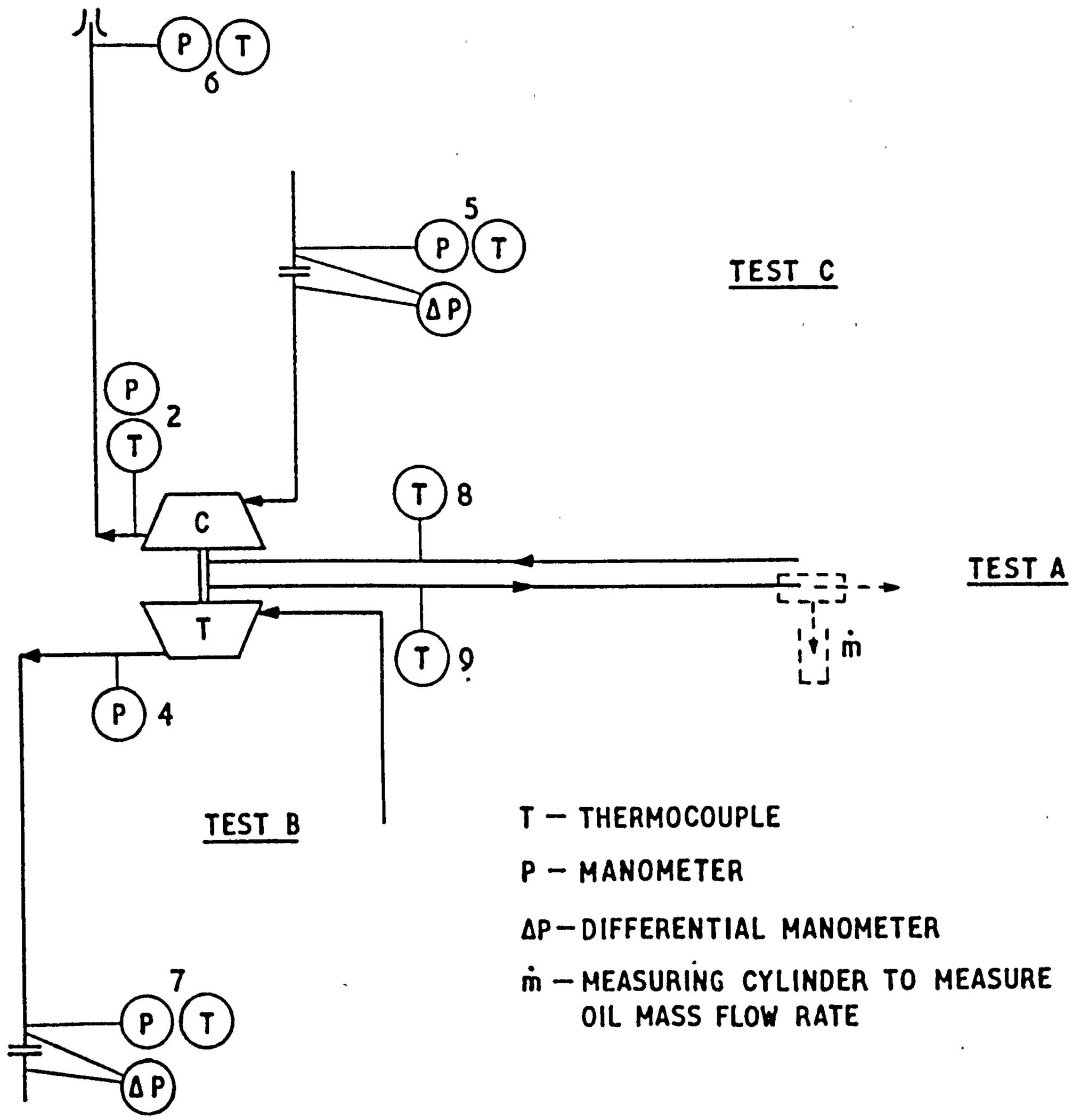

FIG. (5.6) MEASURING INSTRUMENTS TO MEASURE:
TEST A TURBOCHARGER BEARING POWER LOSS
TEST B TURBINE EXHAUST SYSTEM FLOW LOSSES
TEST C COMPRESSOR LOADING NOZZLE MASS FLOW CHARACTERISTIC

3. The oil flow rate from the bearing was measured over a specified time limit (30 sec), by diverting the oil from the tank to a measuring cylinder before the oil was driven back to the tank. As a result, the turbocharger bearing power loss was calculated

$$PW_B = \dot{m}\ S\ \ \Delta T \qquad \ldots\ \ldots\ (48)$$

$\dot{m}$ oil mass flow rate kg/s

S specific heat of the oil $\frac{kJ}{kg.K}$

$\Delta T = T_{out} - T_{in}$ K

The specific heat of the oil S was calculated from the following empirical formula supplied by the manufacturer[41]

$$S = (0.388 + 0.00045\ T)/\sqrt{D} \qquad \ldots\ \ldots\ (49)$$

S specific heat of the oil BTU/lb.^{o}F

T oil temperature in deg.^{o}F

D specific gravity of the oil

The turbocharger bearing power loss was plotted against turbocharger speed, as shown in Fig (5.7).

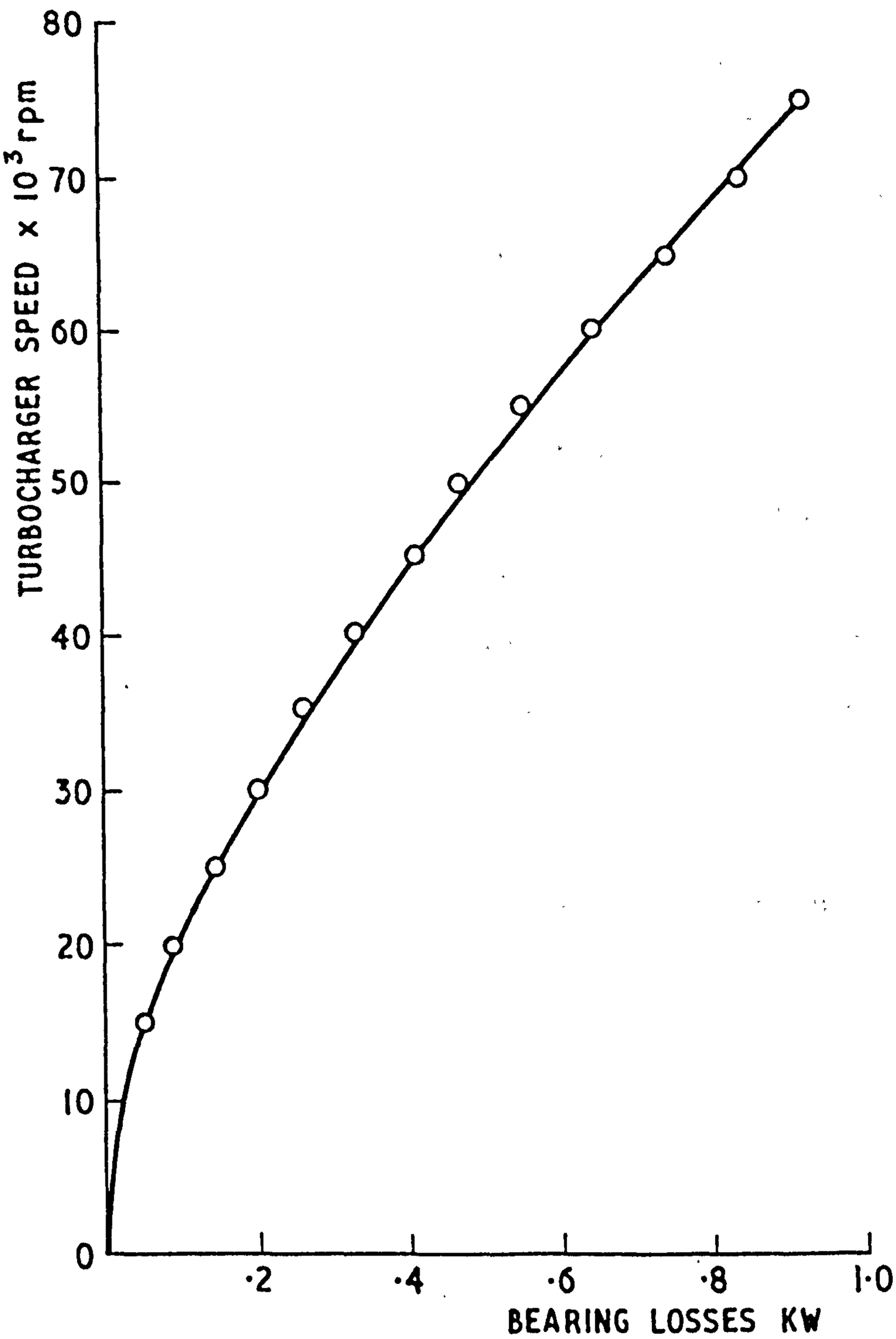

FIG. (5.7) TURBOCHARGER BEARING POWER LOSS vs TURBOCHARGER SPEED

(OIL INLET TEMP 13 ± 0.5°C)

5.5 TURBINE EXHAUST SYSTEM FLOW LOSSES

The flow losses of the turbine exhaust system were measured by connecting three manometers at the turbine outlet, the orifice plate inlet and across the orifice plate, Fig (5.6). A thermocouple was used to measure the temperature at the orifice plate inlet. The turbine was operated over a wide range of speed, measuring the turbine outlet pressure, orifice plate inlet pressure, differential pressure and the atmospheric pressure. For each turbocharger speed, the mass flow rate through the orifice plate was calculated using BS1042 and plotted against the pressure drop in the exhaust system (from the turbine outlet to orifice plate inlet). The turbine exhaust flow losses were plotted against air volume flow rates as shown in Fig.(5.8).

5.6 COMPRESSOR LOADING NOZZLE MASS FLOW CHARACTERISTICS

In order to produce a back pressure for the compressor, a nozzle was designed, Fig (3.3), and fitted at the compressor outlet to represent the engine, as explained in section (3.1).

Manometers were connected to the compressor orifice plate, inlet and differential, compressor exhaust and nozzle inlet. Thermocouples were installed at the orifice plate inlet, compressor exhaust and nozzle

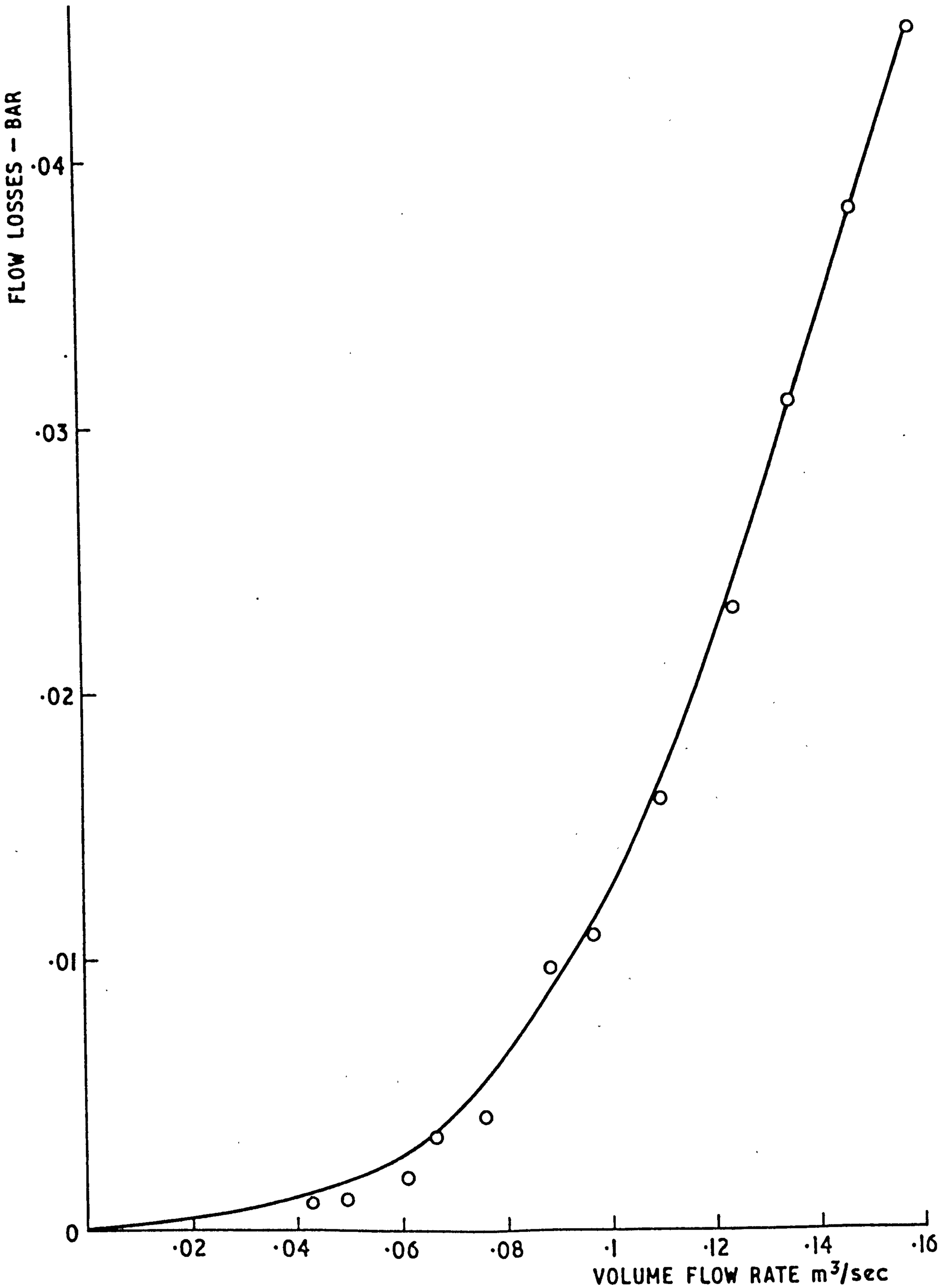

FIG. (5.8) TURBINE EXHAUST SYSTEM FLOW LOSSES vs VOLUME FLOW RATE

pressure drop due to

inlet, Fig (5.6). The compressor was operated over a very wide range of flow rates by increasing the turbocharger speed in steps of 5000 rpm so as to measure the above pressures and temperatures. The pressure loss between the compressor outlet and the nozzle inlet was found to be negligible.Using the orifice plate at the compressor inlet, the mass flow rate through the nozzle for each turbocharger speed was calculated by BS1042[30] and plotted against nozzle inlet pressure, as shown in Fig (5.9).

5.7 TRANSIENT TESTS

After studying the air supply and the turbocharger characteristics it was decided that the experimental work should take into account that the turbine expansion ratio must not exceed 3; consequently, the turbocharger speed would not exceed 80,000 rpm. Before the rig was operated the following checks were carried out:

(1) Pressure transducers, resistance wire circuit, thermocouples, speed measuring circuit and UV recorder were checked to ensure that they were operational.

(2) Minimum oil pressure was attained.

(3) Cooling water to the following pressure transducers, which required cooling, was turned on to reduce the temperature drift,

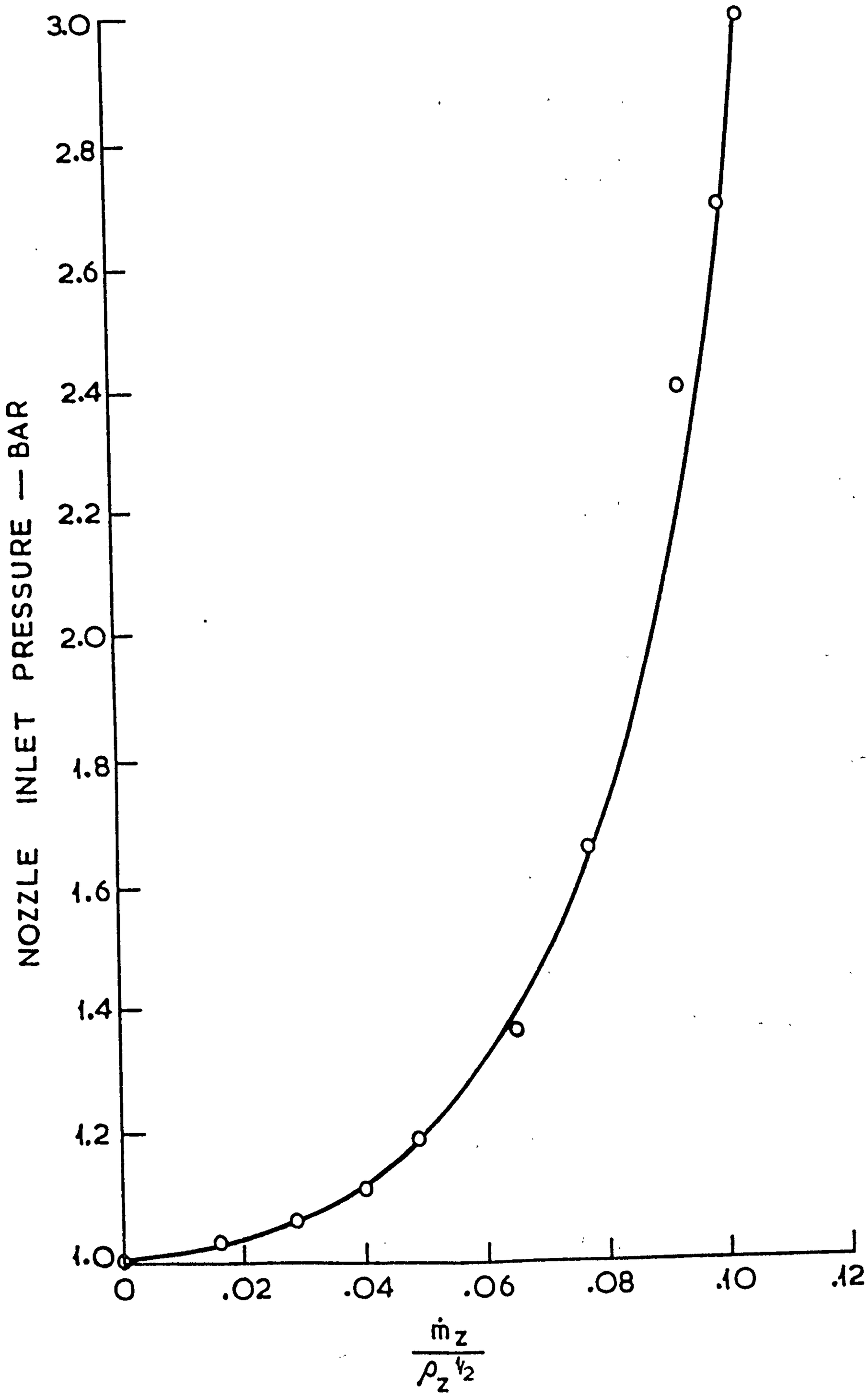

FIG.(5.9)NOZZLE MASS CHARACTERISTICS

compressor outlet transducer
turbine inlet transducer
turbine outlet transducer
turbine orifice plate inlet transducer
nozzle inlet transducer
turbine orifice plate differential transducer.

See Fig (4.2).

(4) The UV recorder was switched on and the galvanometers set to pre-determined positions.

To enable the transient performance of the turbocharger to be measured, a series of experimental tests under pulsating and steady conditions were carried out. These transients were compared with the computer predicted results under the same conditions. The procedure of each of the series of tests of the pulsating transients was:

(i) the initial temperature at each thermocouple was determined using a digital voltmeter to record the voltage across every set of thermocouple terminals on the interface units;

(ii) the UV recorder paper speed was set at low speed (either 0.15 in/sec or 0.30 in/sec) and the paper advance started;

(iii) the LP branch air flow was adjusted to obtain the initial turbocharger speed condition and the HP branch flow was adjusted to give the final pressure required in the HP line at the end of the transient;

(iv) the air supply pressure was adjusted so that the air motor could be operational;

(v) the UV recorder paper feed was switched off and the paper speed changed to 10 times the initial speed. The paper feed was switched on again and simultaneously the flow of air to the turbine was changed from a steady flow of low pressure air to a pulsating flow of high pressure air. The paper feed was switched off 1½ to 2 seconds later;

(vi) at the end of the transient the turbocharger speed was recorded.

A sample of the UV recorder trace for a typical transient test under pulsating flow conditions is shown in Plate (12).

The procedure of the non-pulsating transient was the same as the pulsating transient procedure except the pulse generator was not in use in (iv) and for the changeover in part (v) which was from a steady flow of LP air to steady flow of HP air using the steady flow changeover lever.

A specimen of UV recorder trace for a typical transient test under non-pulsating flow conditions is shown in Plate (13).

The actual test conditions for non-pulsating and pulsating flow conditions is shown in Table 4.

The following information was recorded using the galvonometers on the recorder:

PRESSURE

Compressor inlet and outlet pressure (P_1,P_2)

Turbine inlet and outlet pressure (P_3,P_4)

Pulse generator inlet pressure (P_e)

Compressor loading nozzle inlet pressure (P_z)

Pressure difference across the orifice plate in compressor entry (ΔP_c)

Compressor orifice plate inlet pressure

Pressure difference across the orifice plate in turbine entry (ΔP_t)

Turbine orifice plate inlet pressure

TEMPERATURE

Compressor inlet and outlet temperature (T_1,T_2)

Turbine inlet and outlet temperature (T_3,T_4)

Turbine orifice plate inlet temperature

Pulse generator inlet temperature (T_u)

Compressor loading nozzle inlet temperature

SPEED

Turbocharger speed

The positions of measuring points can be seen in Figs (4.1) and (4.2).

TABLE 4

Non-Pulsating Transient Tests Setting Conditions

Test No.	Initial turbo-charger speed	Final HP branch pressure
1	20 000	20
2	20 000	25
3	20 000	30
4	20 000	35
5	20 000	40
6	25 000	25
7	25 000	30
8	25 000	35
9	25 000	40
10	30 000	25
11	30 000	30
12	30 000	35
13	30 000	40
14	35 000	25
15	35 000	30
16	35 000	35
17	35 000	40
18	40 000	30
19	40 000	40
20	40 000	40

Pulsating Transient Tests Setting Conditions
nominal pulses/sec = 25

Test No.	Initial turbo-charger speed rpm	Final HP branch pressure psi
1	20 000	40
2	20 000	50
3	20 000	60
4	25 000	50
5	25 000	60
6	25 000	70
7	30 000	40
8	30 000	50
9	30 000	60
10	30 000	70

Pulsating Transient Tests Setting Conditions
nominal pulses/sec = 38

Test No.	Initial turbo-charger speed rpm	Final HP branch pressure psi
1	20 000	40
2	20 000	50
3	20 000	60
4	25 000	50
5	25 000	60
6	25 000	70
7	30 000	40
8	30 000	50
9	30 000	60
10	30 000	70

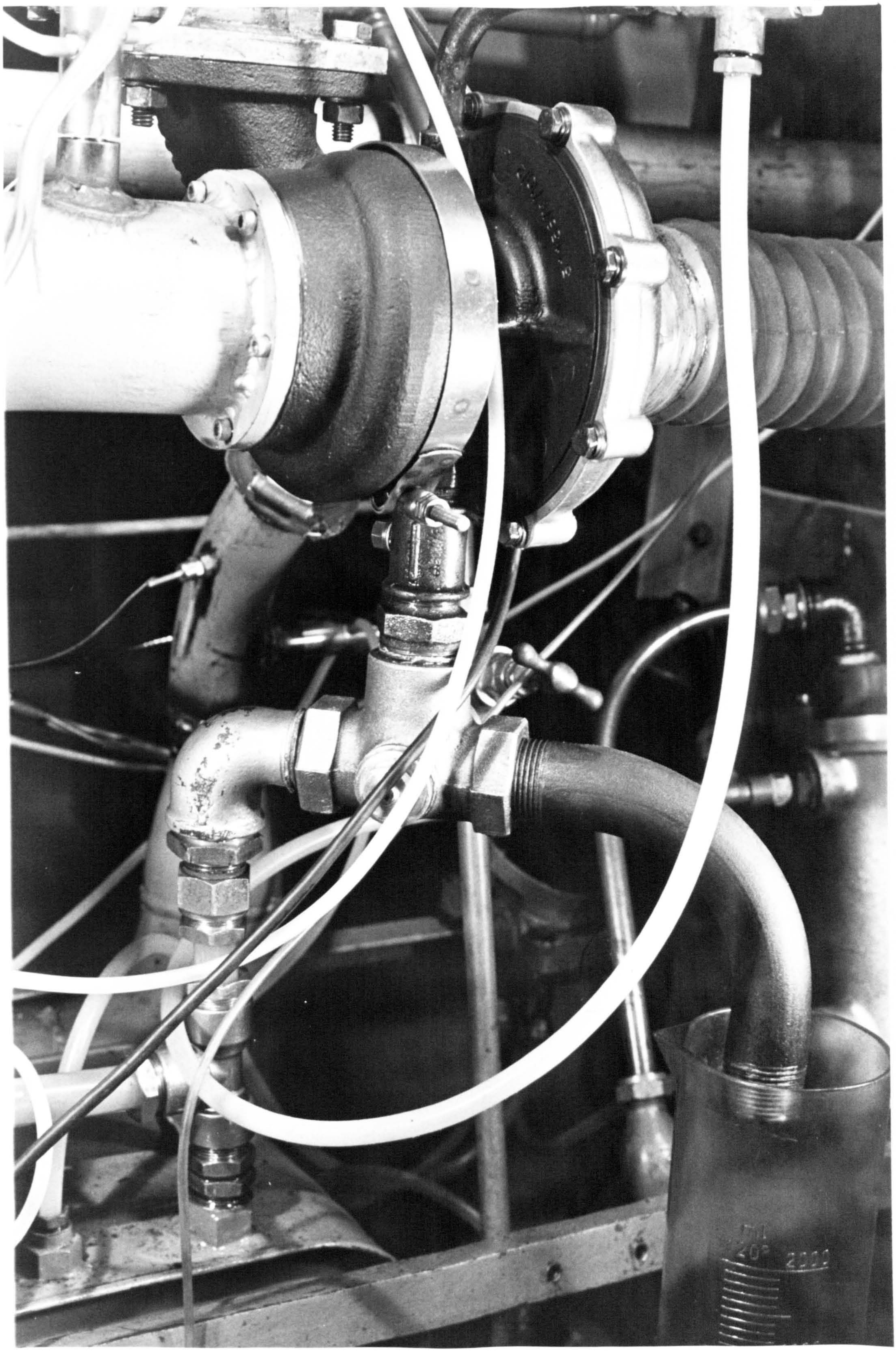

PLATE (11) THREE WAY VALVE

Channel No.	Measurements	Calibration on U.V. paper
1	Comp.Orif.Inlet P.	1 psi = 16 cm
2	Comp.Orif.diff. P.	1 psi = 16 cm
3	Comp.Outlet P.	1 psi = 1 cm
4	Nozzle Inlet P.	1 psi = 1 cm
5	Turbine Inlet P.	1 psi = 5 mm
6	Turbine Outlet P.	1 psi = 4 cm
7	Turbine Orif.Inlet P.	1 psi = 4 cm
8	Turbine Orif.diff. P.	1 psi = 7 cm
9	Pulse Generator Inlet P.	1 psi = 2 mm
10	Turbine Inlet Temp.	see Fig (4.4)
12	Turbocharger Speed	6950 rpm = 1 cm
13	Comp.Inlet Temp.	1°C = 1 cm
14	Comp.Outlet Temp.	1°C = 2 mm
15	Nozzle Inlet Temp.	1°C = 2 mm
16	Turbine Outlet Temp.	1°C = 2 mm
20	Turbine Orif.Inlet Temp.	1°C = 2 mm

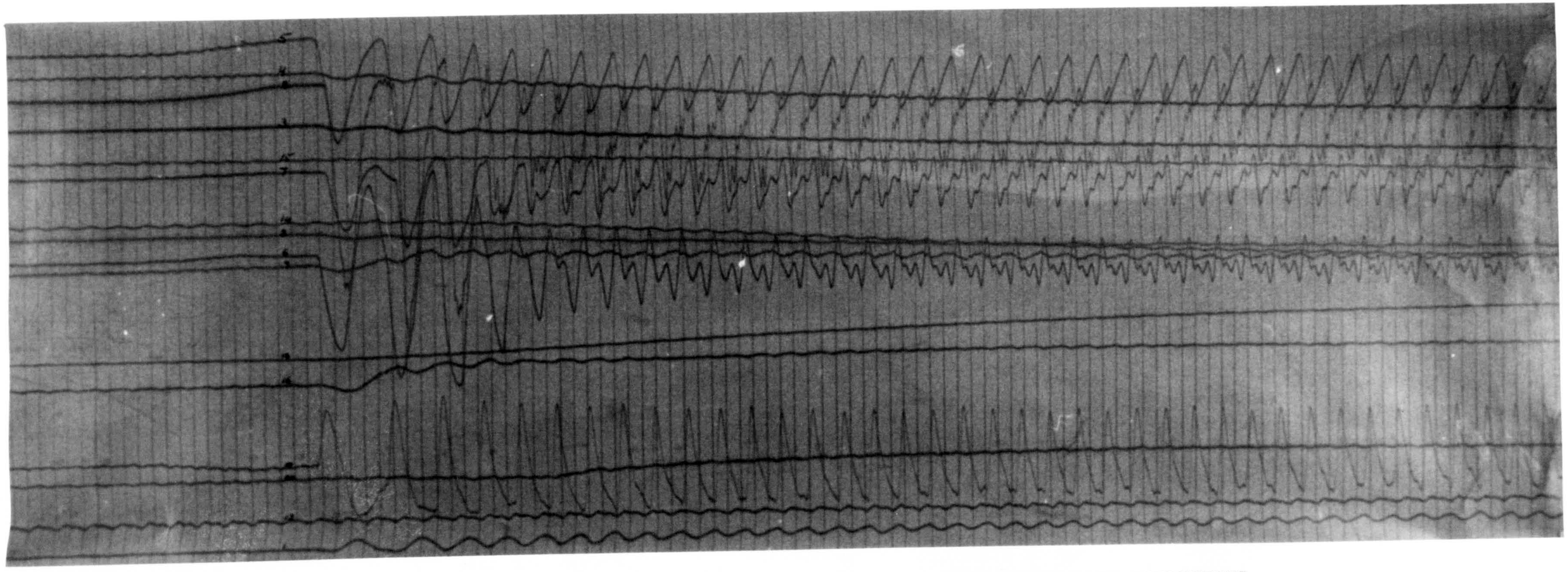

PLATE (12) SAMPLE OF THE UV RECORDER TRACE UNDER PULSATING TRANSIENT TEST CONDITIONS

Channel No.	Measurements	Calibration on U.V. paper
1	Comp.Orif.Inlet P.	1 psi = 16 cm
2	Comp.Orif.diff. P.	1 psi = 16 cm
3	Comp.Outlet P.	1 psi = 1 cm
4	Nozzle Inlet P.	1 psi = 1 cm
5	Turbine Inlet P.	1 psi = 5 mm
6	Turbine Outlet P.	1 psi = 4 cm
7	Turbine Orif.Inlet P.	1 psi = 4 cm
8	Turbine Orif.diff. P.	1 psi = 7 cm
9	Pulse Generator Inlet P.	1 psi = 2 mm
10	Turbine Inlet Temp.	see Fig (4.4)
12	Turbocharger Speed	6950 rpm = 1 cm
13	Comp.Inlet Temp.	1°C = 1 cm
14	Comp.Outlet Temp.	1°C = 2 mm
15	Nozzle Inlet Temp.	1°C = 2 mm
16	Turbine Outlet Temp.	1°C = 2 mm
20	Turbine Orif.Inlet Temp.	1°C = 2 mm

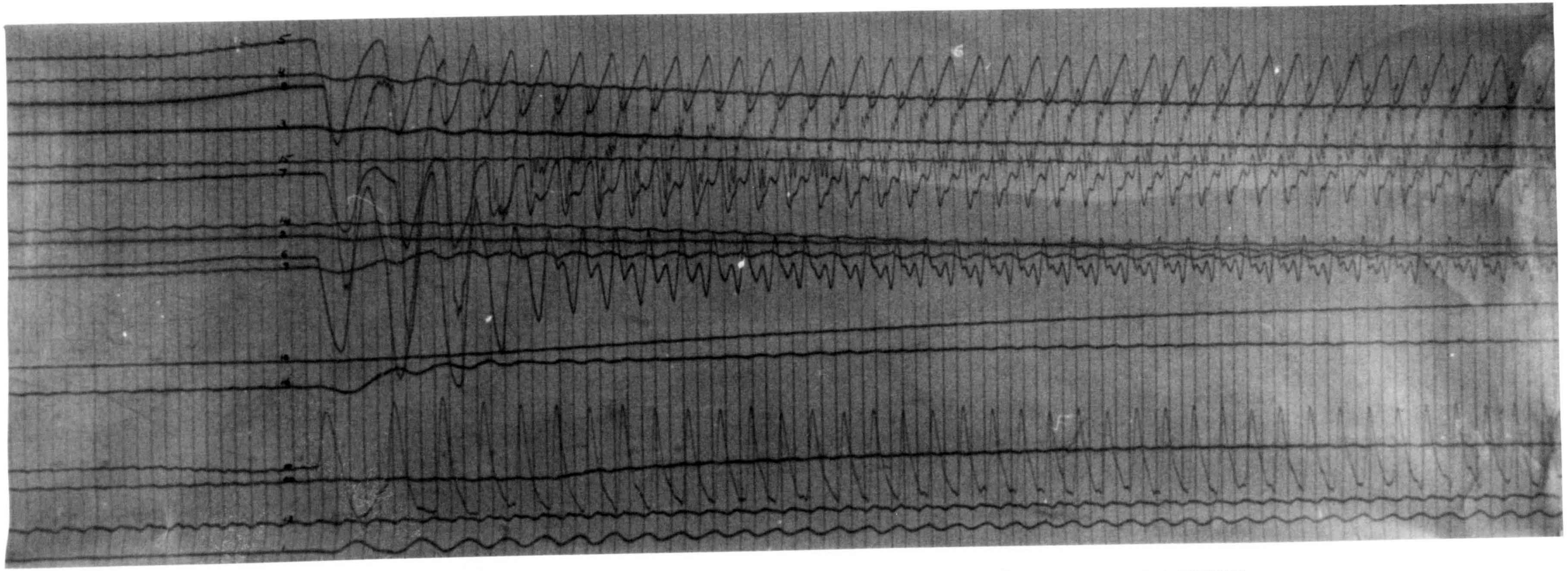

PLATE (12) SAMPLE OF THE UV RECORDER TRACE UNDER PULSATING TRANSIENT TEST CONDITIONS

Channel No.	Measurements	Calibration on U.V. paper
1	Comp.Orif.Inlet P.	1 psi = 16 cm
2	Comp.Orif.diff. P.	1 psi = 16 cm
3	Comp.Outlet P.	1 psi = 1 cm
4	Nozzle Inlet P.	1 psi = 1 cm
5	Turbine Inlet P.	1 psi = 5 mm
6	Turbine Outlet P.	1 psi = 4 cm
7	Turbine Orif.Inlet P.	1 psi = 4 cm
8	Turbine Orif.diff. P.	1 psi = 7 cm
9	Pulse Generator Inlet P.	1 psi = 2 mm
10	Turbine Inlet Temp.	see Fig (4.4)
12	Turbocharger Speed	6950 rpm = 1 cm
13	Comp.Inlet Temp.	1°C = 1 cm
14	Comp.Outlet Temp.	1°C = 2 mm
15	Nozzle Inlet Temp.	1°C = 2 mm
16	Turbine Outlet Temp.	1°C = 2 mm
20	Turbine Orif.Inlet Temp.	1°C = 2 mm

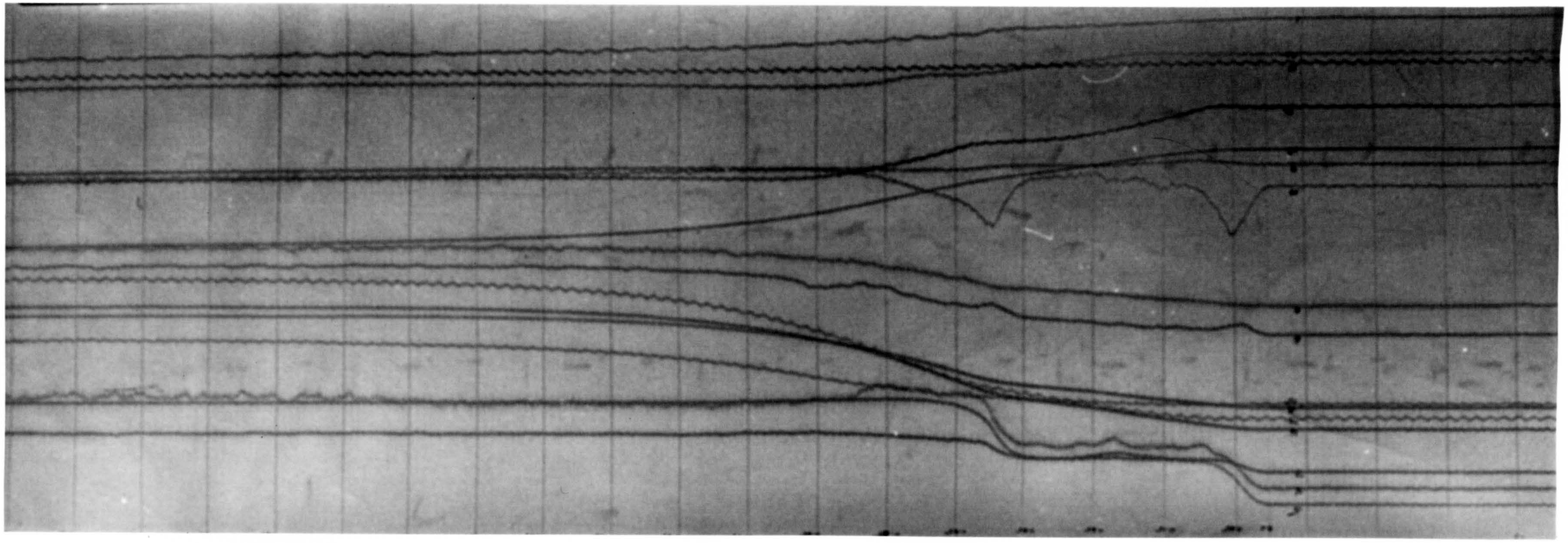

PLATE (13) SAMPLE OF THE UV RECORDER TRACE UNDER NON-PULSATING TRANSIENT TEST CONDITIONS

CHAPTER SIX

THEORY AND COMPUTATION

CHAPTER SIX

THEORY AND COMPUTATION

6.1 OBJECTIVE

The objective of the theoretical work is to establish a theory which can be used to predict the transient response performance of a turbocharger under pulsating and non-pulsating flow conditions and to compare the results with that obtained experimentally under the same conditions.

Under non-pulsating flow conditions, the method used only the variations of turbine pressure ratio and turbine inlet temperature as input data. The steps followed will be explained in section (6.3).

Under pulsating flow conditions, two methods were used. The first method, section (6.4.1), used the complete system (pulse generator, exhaust system and the turbocharger) to predict the transient response performance of the turbocharger where the calculations started from the pulse generator inlet, and the flow in the exhaust system was considered, section (6.5). The second method started the calculations from the turbocharger turbine inlet to predict the transient response performance of the turbocharger.

The methods used the information obtained from the steady state turbine and compressor characteristics assuming these to be valid instantaneously during the transient operations. Predicting the turbocharger parameters from turbine and compressor steady state characteristics were explained in section (6.7).

6.2 ASSUMPTIONS

Throughout this analysis the fluid was assumed to be a perfect gas with a constant ratio of specific heats, and that the fluid flow was hometropic, that is, neither frictional effects nor heat transfer occurred and that temperature discontinuities were absent. A quasi-steady flow analysis was adopted (see Chapter 2) in predicting the transient response performance of the turbocharger under pulsating and non-pulsating transient operations. In the quasi-steady flow analysis it was assumed that under pulsating and non-pulsating transient operations, the turbine and compressor always operate instantaneously as they would under steady flow conditions, and that transients could be considered as a series of successive steady states.

6.3 PREDICTING THE TRANSIENT RESPONSE PERFORMANCE OF THE TURBOCHARGER UNDER NON-PULSATING FLOW CONDITIONS

The transient response performance of the turbocharger

under non-pulsating flow conditions was predicted from the steady state condition at the beginning of the transient to another steady state condition at the end of the transient.

The principal feature of the developed method is that only the pressure and temperature variations at the turbine inlet during the transient are required, see Fig (6.1).

As the transient response performance of the turbocharger cannot be predicted without knowing (or being able to calculate) either the mass flow rate through the turbine or through the compressor, the compressor mass flow rate was calculated indirectly by discharging the compressed air through a nozzle fitted in the pipe from the compressor outlet, see Figs (3.3), (5.9) and Appendix (4). The procedure for predicting the turbocharger performance during a transient can be divided into two sections: Part A: to predict the turbocharger operating points at the end of the steady state condition which precedes the transient, Part B: to predict the performance of the turbocharger during the transient operation.

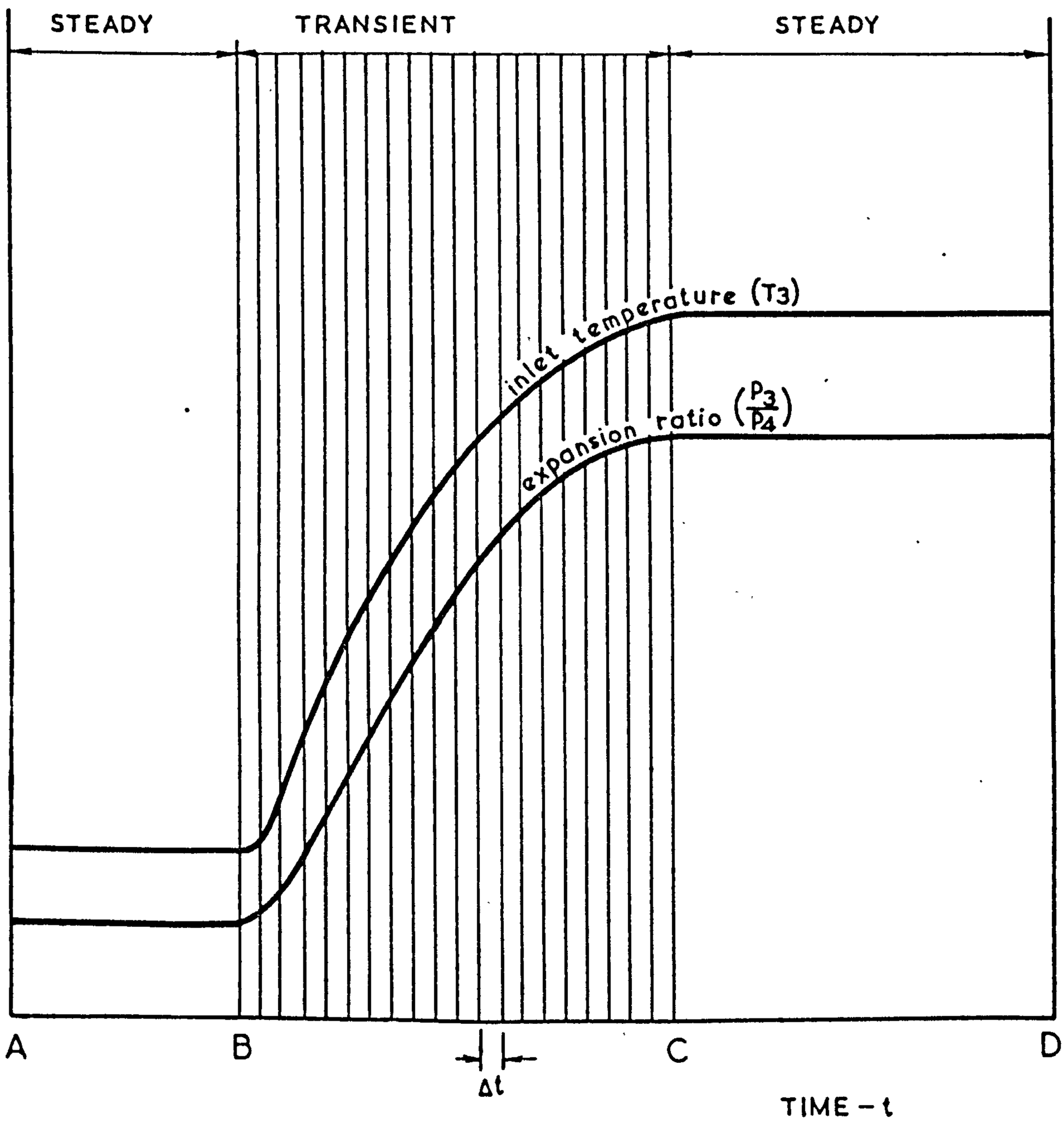

Fig.(6.1) TRANSIENT VARIATIONS AT THE TURBINE INLET

PART A

The operating conditions of the turbocharger at the end of the steady state phase before the beginning of the transient (position B, Fig (6.1)) were determined using the method illustrated in Fig (6.6) and as explained below:

A.I

The turbine expansion pressure ratio $\frac{P_3}{P_4}$ at the beginning of the transient was known. If the transient operation is superimposed on turbine mass flow characteristics, Fig (6.2), then the beginning of the transient, position B, Fig (6.2) must lie on line KL where the height of this line represents $\frac{P_3}{P_4}$.

A.II

The turbine mass flow rate is initially assumed to be the lowest value in the turbine mass characteristics. Therefore, the mass flow parameter $\dot{m}_t\sqrt{T_3}/P_3$ was estimated initially, and as the turbine pressure ratio $\frac{P_3}{P_4}$ was known, the turbine speed parameter $N/\sqrt{T_3}$ was determined using the turbine mass characteristics, Fig (6.3).

A.III

The turbine efficiency was determined from the turbine

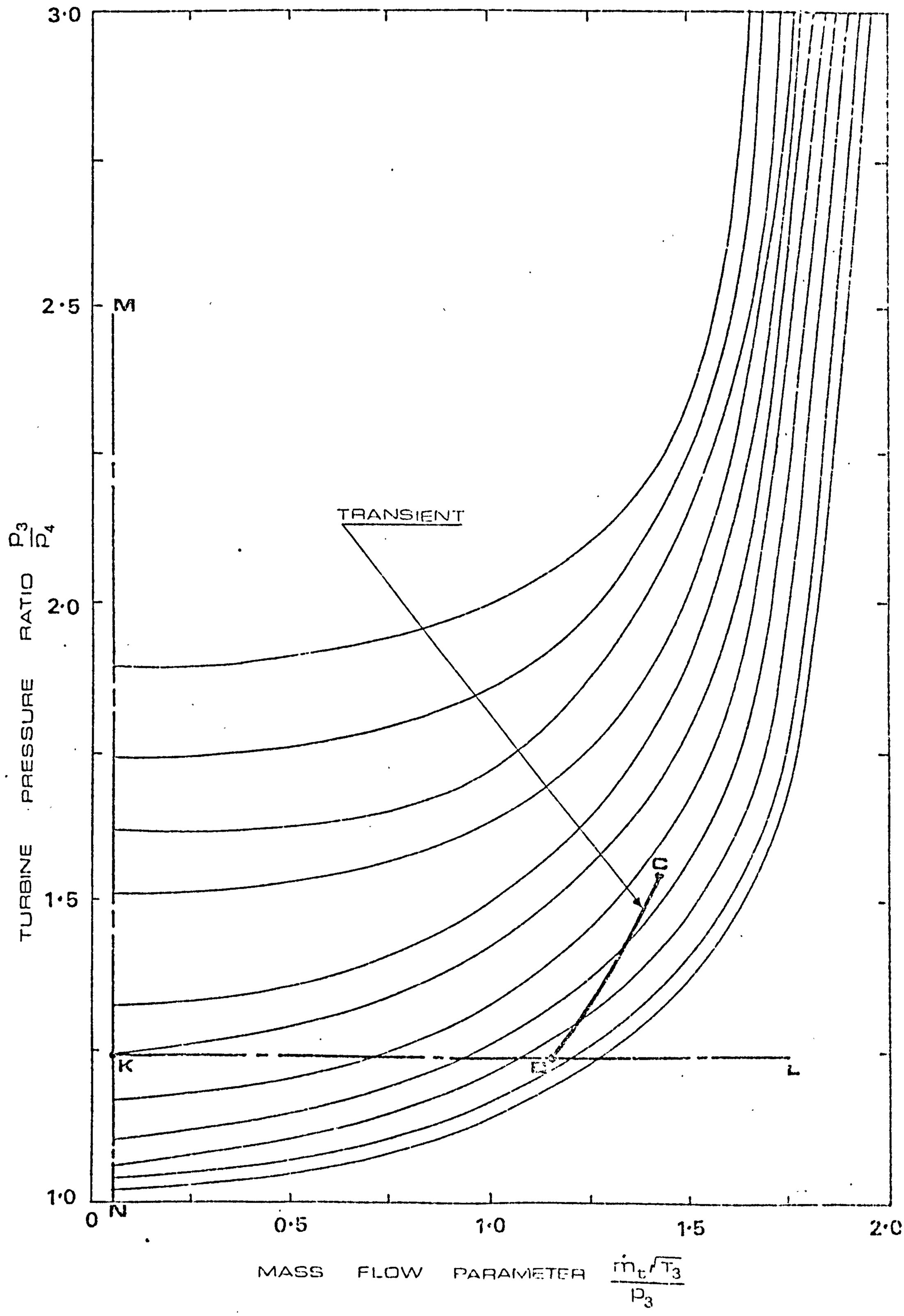

fig.(6.2) SUPERIMPOSITION OF A TRANSIENT ON THE TURBINE MASS CHARACTERISTIC

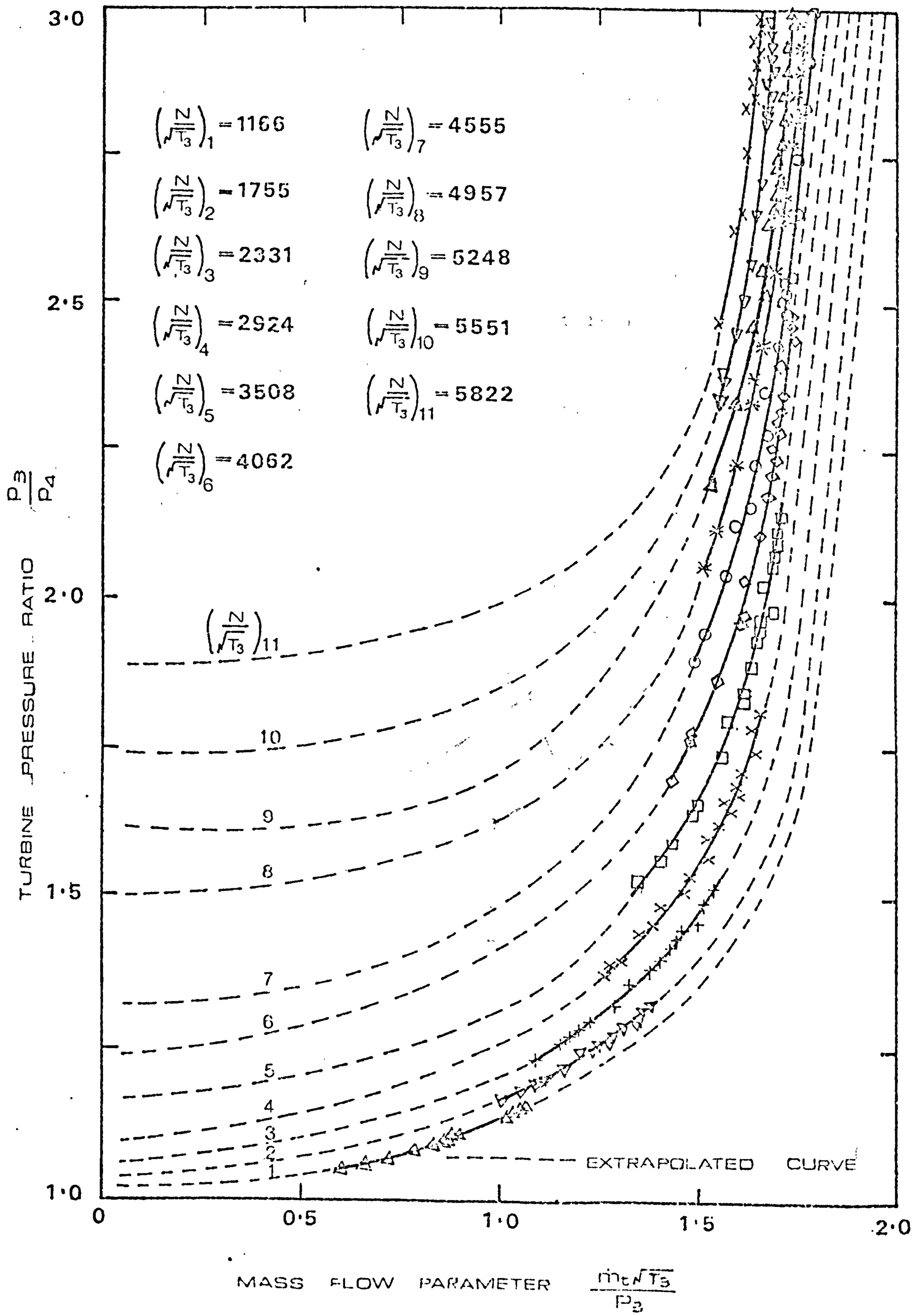

fig.(6.3) TURBINE MASS CHARACTERISTIC

pressure ratio and the turbine speed parameter, using the turbine efficiency characteristics, Fig (6.4).

A.IV

From the speed parameter $N/\sqrt{T_3}$ evaluated in step A.II, the turbocharger speed N was determined. Using Fig (5.7) the bearing power loss PW_B was evaluated, and thus the mechanical efficiency η_m could be calculated.

A.V

The gas density leaving the turbine was calculated

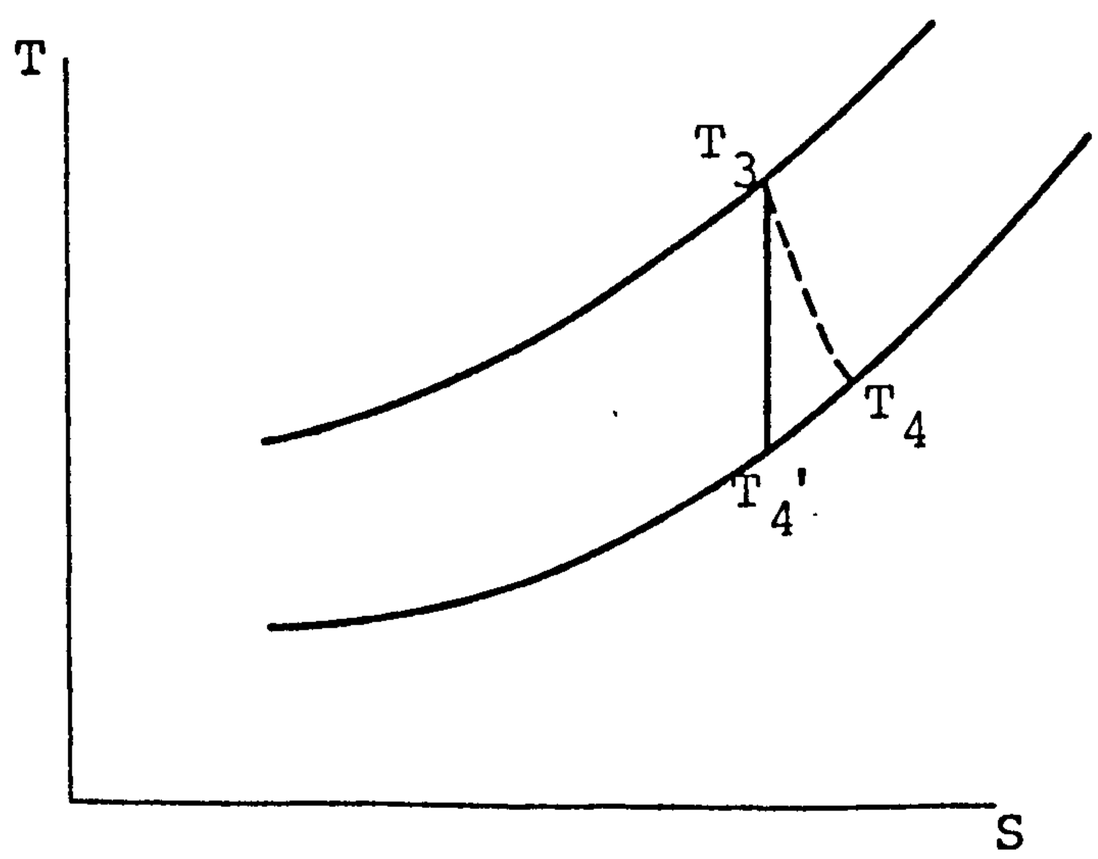

$$\frac{T_3}{T_4'} = \left(\frac{P_3}{P_4}\right)^{\frac{\gamma-1}{\gamma}} \qquad \ldots\ldots (50)$$

$$\eta_t = \frac{T_3-T_4}{T_3-T_4'} \qquad \ldots\ldots (51)$$

$$T_4 = T_3-T_4' \quad \eta_t \left[\left(\frac{P_3}{P_4}\right)^{\frac{\gamma-1}{\gamma}} -1\right] \qquad \ldots\ldots (52)$$

$$\rho_4 = \frac{P_4}{RT_4} \qquad \ldots\ldots (53)$$

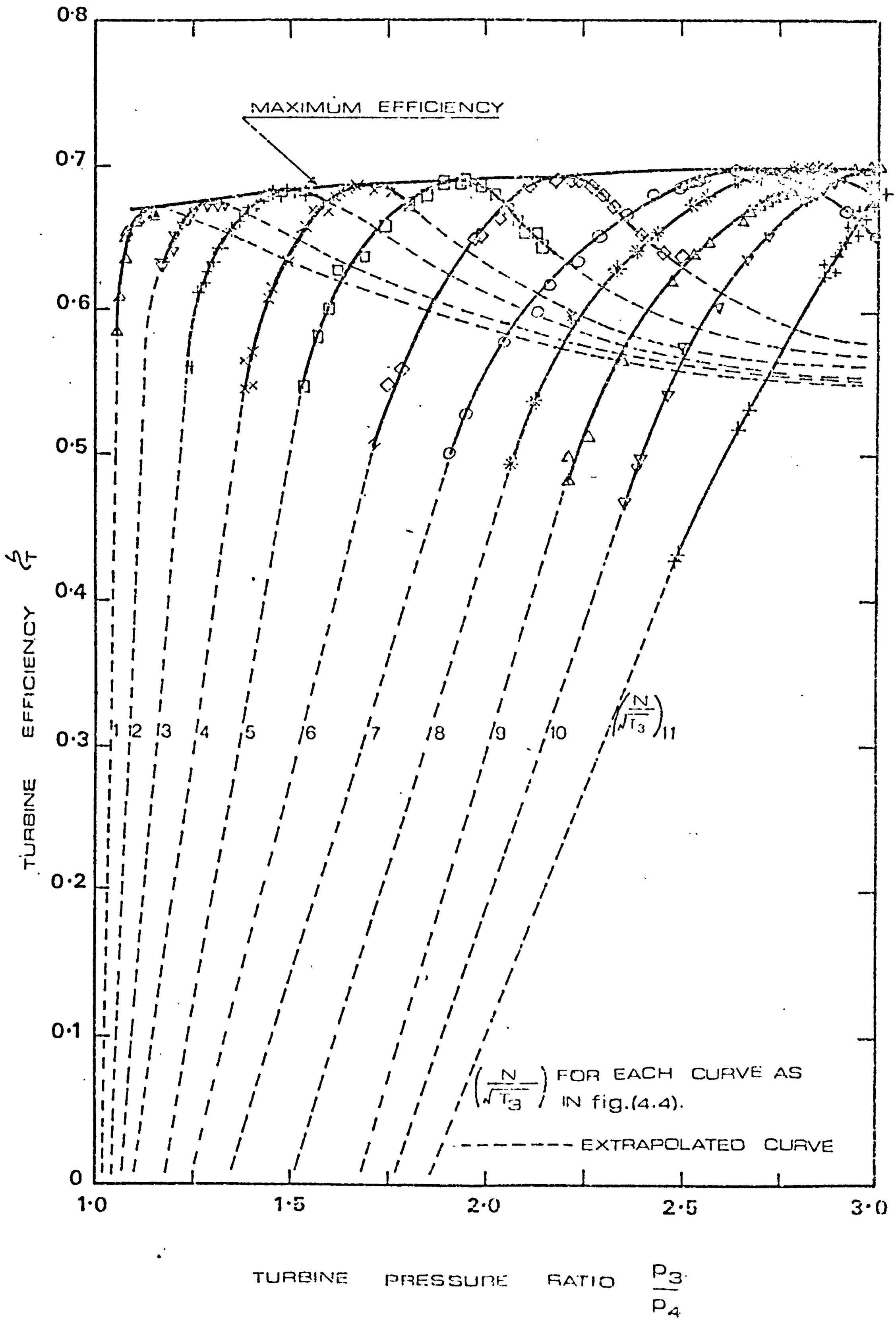

fig.(6.4) TURBINE EFFICIENCY CHARACTERISTIC

A.VI

The gas volume flow rate leaving the turbine was calculated in order to find the pressure drop (ΔPL) across the turbine exhaust system, Fig (5.8) and thus the turbine outlet pressure.

A.VII

The turbine power was calculated using the steady flow energy equation,

$$PW_t = \dot{m}_t \, C_p \, T_3 \, \eta_t \eta_m \left[1 - \left(\frac{P_4}{P_3}\right)^{\frac{\gamma-1}{\gamma}} \right] \qquad \ldots \ldots (54)$$

A.VIII

Using the compressor steady state characteristics, Fig (6.5), an arbitrary point was determined on this turbocharger speed to start the calculation with its compressor mass flow rate $\dot{m}_c$, and from its pressure ratio $\frac{P_2}{P_1}$, the compressor outlet pressure P_2 was calculated assuming the compressor inlet pressure P_1 was almost atmospheric. From this compressor outlet pressure P_2, a mass flow parameter $\frac{\dot{m}_z}{\rho_2^{\frac{1}{2}}}$ through the compressor loading nozzle was evaluated using the nozzle mass characteristics, Fig (5.9). As the nozzle mass flow parameter $\frac{\dot{m}_z}{\rho_2^{\frac{1}{2}}}$ was expressed in terms of the density of the air entering the nozzle, this density had to be calculated as follows:

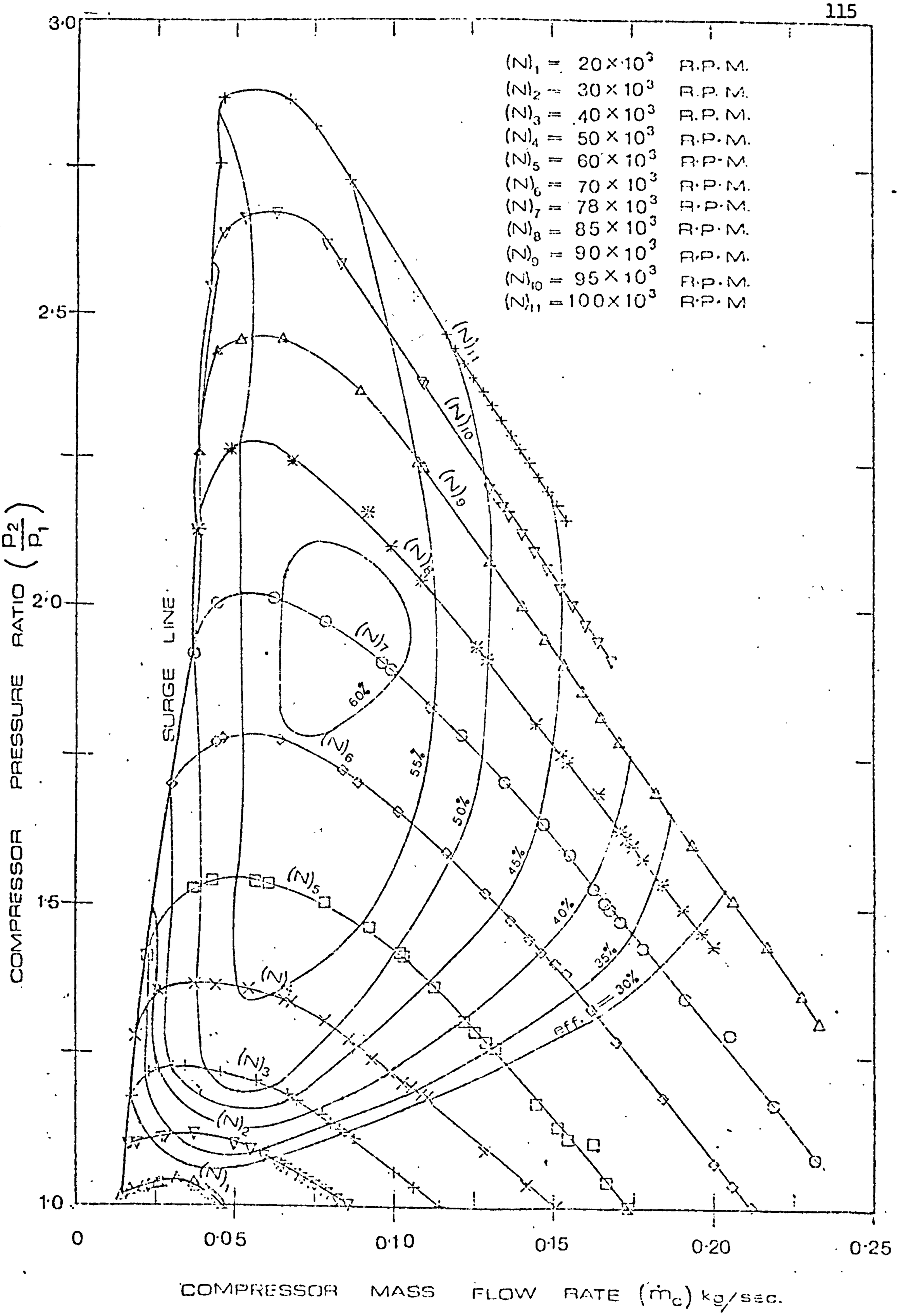

fig.(6.5) COMPRESSOR STEADY CHARACTERISTICS

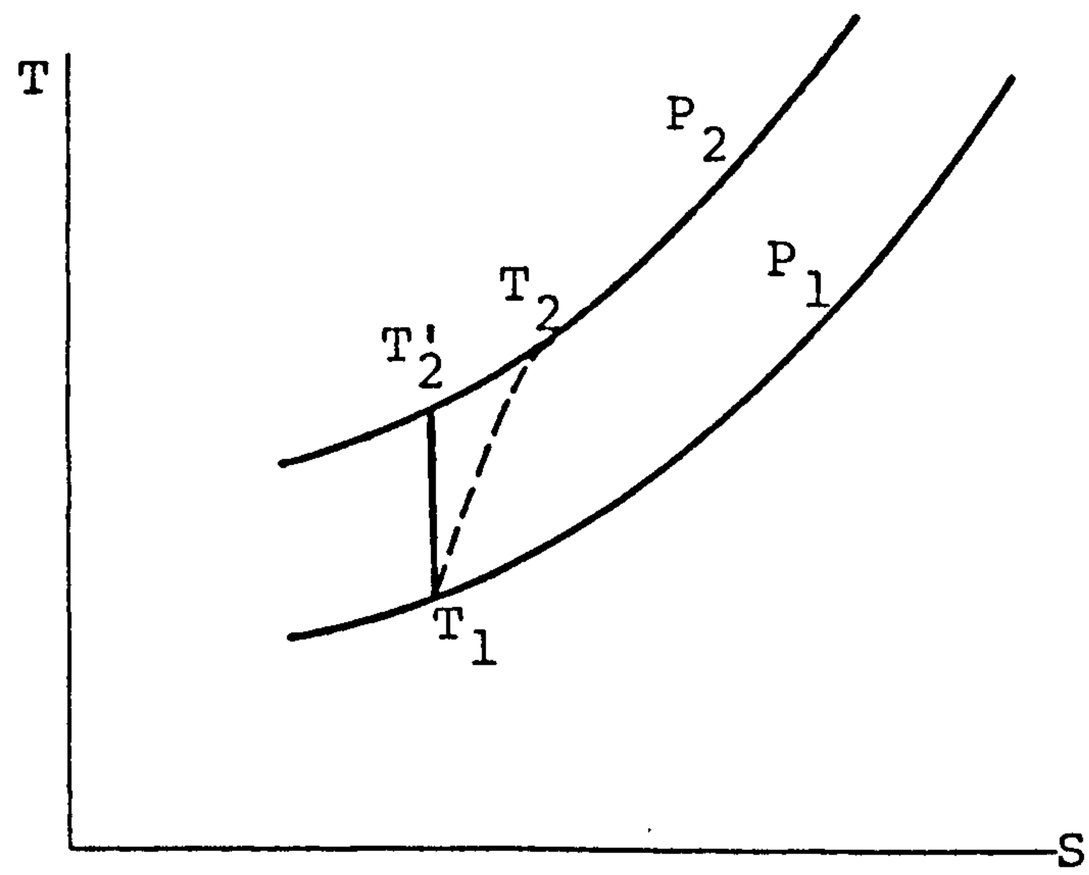

$$\frac{T_2'}{T_1} = \left(\frac{P_2}{P_1}\right)^{\frac{\gamma-1}{\gamma}} \qquad \ldots\ldots (55)$$

$$\eta_c = \frac{T_2' - T_1}{T_2 - T_1} \; . \qquad \ldots\ldots (56)$$

Substituting equation (55) into equation (56),

$$T_2 = \frac{T_1 \left(\frac{P_2}{P_1}\right)^{\frac{\gamma-1}{\gamma}} - T_1}{\eta_c} + T_1 \qquad \ldots\ldots (57)$$

and

$$\rho_2 = \frac{P_2}{R\,T_2} \; . \qquad \ldots\ldots (58)$$

Equation (57) was substituted into equation (58) to calculate ρ_2, the air density at the compressor outlet. Substituting ρ_2 into the term $\frac{\dot{m}_z}{\rho_2^{\frac{1}{2}}}$ predicted earlier from the nozzle mass characteristics, the mass flow rate through the nozzle $\dot{m}_z$ was obtained. This must be equal

to the mass flow rate through the compressor $\dot{m}_c$ which was calculated earlier in this step. If this was not so, this step, AVIII, was repeated using the new estimate of $\dot{m}_c$ until successive values of $\dot{m}_c$ were sufficiently close (within 1%).

AIX

As the compressor mass flow rate had been determined, the compressor efficiency was evaluated using compressor steady characteristics at the known speed, Fig (6.5).

AX

Meanwhile, knowing the compressor mass flow rate, efficiency and pressure ratio, the compressor power was calculated,

$$PW_c = \frac{\dot{m}_c C_p T_1}{\eta_c} \left[\left(\frac{P_2}{P_1}\right)^{\frac{\gamma-1}{\gamma}} - 1 \right] \qquad \ldots\ldots (59)$$

AXI

The turbine power calculated from equation (54) and the compressor power calculated from equation (59) must satisfy the compatibility equation (60),

$$PW_c = PW_t \quad . \qquad \ldots\ldots (60)$$

If this was not satisfied, steps (A.II) to (A.XI) were repeated and a new value of $\dot{m}_t$ used to obtain better

estimates of PW_c and PW_t until successive values of PW_c and PW_t satisfied equation (60).

The operating point of the turbocharger at the end of the steady flow conditions (the beginning of the transient) was thus predicted, position B, Fig (6.1) and position B, Fig (6.2).

PART B

The second part of the procedure was to predict the performance of the turbocharger during transient operation at the end of each step. The transient B to C, Fig (6.1) or B to C, Fig (6.2) was divided into small intervals and during each of these intervals a procedure similar to that discussed in part A was used except when applying the compatibility equation in step A.XI. As the turbocharger speed was not constant the work required to accelerate the turbocharger had to be included in that equation. Therefore, the following compatibility equation was used for the turbocharger during the transient operation

$$\int_n^{n+1} PW_t \, dt = \int_n^{n+1} PW_c \, dt + \int_n^{n+1} I \, \omega \frac{d\omega}{dt} \, dt \, . \qquad \ldots \ldots (61)$$

Assuming the variation in turbine power and compressor power during the time interval were linear, equation (61) could be written in the following numerical form

$$\left[\frac{(PW_t)_n + (PW_t)_{n+1}}{2}\right] \Delta t = \left[\frac{(PW_c)_n + (PW_c)_{n+1}}{2}\right] \Delta t + \frac{I}{2}\left[\omega^2_{n+1} - \omega^2_n\right] \quad \ldots\ldots (62)$$

This method, described in this section, is shown superimposed on turbine, compressor and compressor loading nozzle characteristics Fig (6.6).

6.4 PREDICTING THE TRANSIENT RESPONSE PERFORMANCE OF THE TURBOCHARGER UNDER PULSATING FLOW CONDITIONS

6.4.1 METHOD 1

In real turbocharging operation the engine discharges into an exhaust system where it delivers the exhaust gases to the turbocharger turbine. The first method developed to simulate the turbocharging operation in the test rig started the calculation from the pulse generator inlet valve which represented the engine inlet valve. This calculation included the pulse generator exhaust system which in fact represented the turbocharger turbine inlet system. The filling and emptying method described in section (6.5) was used to calculate the pressure and temperature at the turbine inlet at the end of each step in the transient.

Initially, the condition of the turbocharger was predicted at the end of the steady state phase before starting the transient, see position B, Figs (6.2), and that was done exactly as section (6.3) part A.

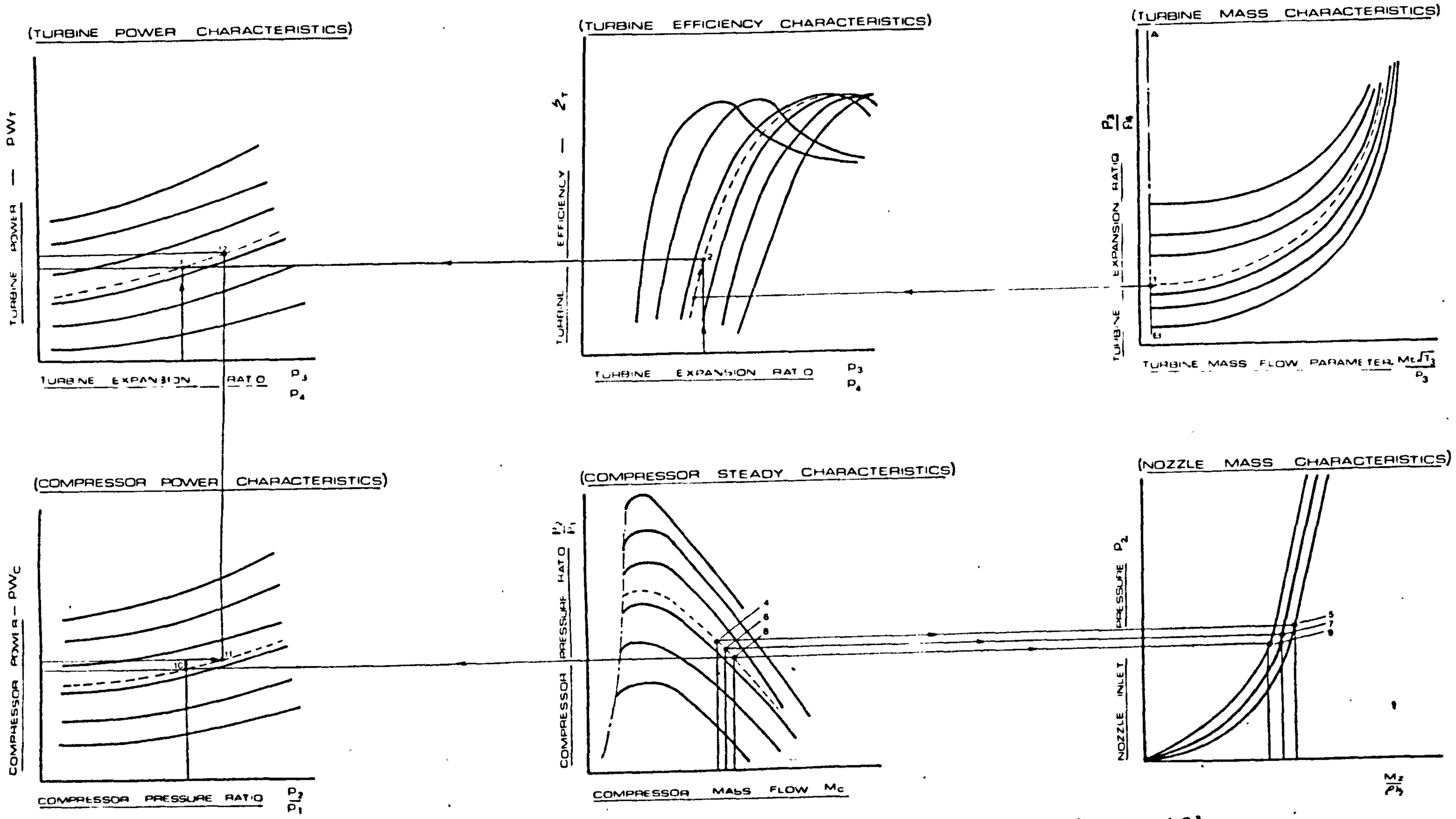

fig. 6.6 SEQUENCE OF PREDICTING TURBINE AND COMPRESSOR OPERATING POINTS [section 6.3]

After the turbocharger steady state condition was determined, the transient response performance of the turbocharger during the transient operation was predicted. The transient, from B to C, Fig (6.2), was divided into small time intervals. Then, for the next step:

(1) The turbocharger speed was increased by a small amount of 500 rpm, therefore, new turbine speed parameter = $\frac{N + 500}{\sqrt{T_3}}$

(2) The turbine pressure ratio $\frac{P_3}{P_4}$ at the step was evaluated at this new turbine speed parameter, using the original mass flow parameter and turbine mass characteristics, Fig (6.3).

(3) Using the turbine efficiency characteristics, Fig (6.4), the turbine efficiency at the end of this step was determined for the new turbine speed parameter and turbine pressure ratio.

(4) From the turbocharger speed estimated in step (1), the bearing power loss PW_B was evaluated, Fig (5.7), and thus the mechanical efficiency η_m could be calculated ignoring the change in power during this step.

(5) The gas density leaving the turbine was calculated, see equations (50) to (53).

$$\rho_4 = \frac{P_4}{RT_4} \qquad \ldots\ldots (53)$$

(6) The gas volume flow rate leaving the turbine was calculated in order to find the pressure drop ΔPL across the turbine exhaust system, Fig (5.8) and thus the turbine outlet pressure.

(7) The turbine power at the end of this step was calculated at the new turbine speed,

$$PW_t = \dot{m}_t \; C_p \; T_3 \; \eta_t \eta_m \left[1 - \left(\frac{P_4}{P_3}\right)^{\frac{\gamma-1}{\gamma}} \right] \qquad \ldots\ldots (54)$$

(8) Assuming that during this small increase in the turbocharger speed, the shape of the compressor inlet and outlet velocity triangle did not change and therefore the new compressor mass flow rate was proportional to the new speed,

$$\dot{m}_c = \dot{m}_c \times \frac{N + 500}{N} \qquad \ldots\ldots (63)$$

(9) Knowing the compressor mass flow rate from the previous step and using the compressor steady state characteristics, Fig (6.5), the corresponding compressor pressure ratio $\frac{P_2}{P_1}$ and compressor efficiency were evaluated at the new speed.

(10) The compressor power was calculated at the new speed,

$$PW_c = \frac{\dot{m}_c \; C_p \; T_1}{\eta_c} \left[\left(\frac{P_2}{P_1}\right)^{\frac{\gamma-1}{\gamma}} - 1 \right] \qquad \ldots \ldots (59)$$

(11) The turbine power calculated in step (7) and the compressor power calculated in step (10) must satisfy the turbocharger compatibility equation during the transient operation. As the turbocharger speed was not constant, the work required to accelerate the turbocharger had to be included in that equation. Therefore, the compatibility equation for the turbocharger during the transient operation was used, equation (61),

$$\int_n^{n+1} PW_t \, dt = \int_n^{n+1} PW_c \, dt + \int_n^{n+1} I\omega \frac{d\omega}{dt} \, dt \qquad \ldots \ldots (61)$$

Assuming the variation in turbine power and compressor power during the time interval were linear, equation (61) could be written in the following numerical form,

$$\omega_{n+1} = \sqrt{\omega_n^2 + \frac{\Delta t}{I} \left[(PW_t)_{n+1} + (PW_t)_n - (PW_c)_{n+1} - (PW_c)_n \right]}. \qquad \ldots \ldots (64)$$

This new value of turbocharger speed was used in

steps (2) to (11) and a further value of speed obtained until successive values of turbocharger speeds were sufficiently close (within 1%) and satisfying equation (64).

6.4.2 METHOD 2

Alternatively, the transient performance of the turbocharger under pulsating conditions could be calculated using step by step data at the turbine inlet. By doing so, any inaccuracy in the calculations of pressure, temperature and mass flow rate in the pulse generator and pulse generator exhaust system could be eliminated.

The method requires a knowledge of the measured variations of pressure and temperature at the turbine inlet, and the turbocharger speed variations with time during the transient. The procedure for predicting the transient performance of the turbocharger was as follows:

(i) Initially, from the turbocharger speed N and turbine inlet temp T_3, the speed parameter $\frac{N}{\sqrt{T_3}}$ was found.

(ii) Knowing the speed parameter $\frac{N}{\sqrt{T_3}}$ and turbine

expansion pressure ratio $\frac{P_3}{P_4}$, the turbine mass flow parameter $\dot{m}_t \sqrt{T_3}/P_3$ was predicted from turbine mass characteristics, Fig (6.3).

(iii) The turbine mass flow rate $\dot{m}_t$ was calculated from turbine mass parameter $\dot{m}_t \sqrt{T_3}/P_3$.

(iv) From turbine expansion pressure ratio $\frac{P_3}{P_4}$ and speed parameter $N/\sqrt{T_3}$, the turbine efficiency was evaluated from turbine efficiency characteristics, Fig (6.4).

(v) Using Fig (5.7) the bearing power loss PW_B was evaluated, and thus the mechanical efficiency η_m could be calculated.

(vi) The gas density leaving the turbine was calculated

$$\frac{T_3}{T_4'} = \left(\frac{P_3}{P_4}\right)^{\frac{\gamma-1}{\gamma}} \qquad \ldots\ldots (50)$$

$$\eta_t = \frac{T_3 - T_4}{T_3 - T_4'} \qquad \ldots\ldots (51)$$

$$T_4 = T_3 - T_4' \quad \eta_t \quad \left[\left(\frac{P_3}{P_4}\right)^{\frac{\gamma-1}{\gamma}} - 1\right] \qquad \ldots\ldots (52)$$

$$\rho_4 = \frac{P_4}{RT_4} \qquad \ldots\ldots (53)$$

(vii) The gas volume flow rate leaving the turbine was

calculated in order to find the pressure drop (ΔPL) across the turbine exhaust system, Fig (5.8) and thus the turbine outlet pressure.

(viii) The turbine power was calculated using the steady flow energy equation,

$$PW_t = \dot{m}_t \, C_p \, T_3 \, \eta_t \eta_m \left[1 - \left(\frac{P_4}{P_3}\right)^{\frac{\gamma-1}{\gamma}} \right] \qquad \ldots \ldots (54)$$

(ix) Using the compressor steady state characteristics, Fig (6.5), an arbitrary point was determined on this turbocharger speed to start the calculation with its compressor mass flow rate $\dot{m}_c$, and from its pressure ratio $\frac{P_2}{P_1}$, the compressor outlet pressure P_2 was calculated assuming the compressor inlet pressure P_1 was almost atmospheric. From this compressor outlet pressure P_2, a mass flow parameter $\dot{m}_z/\rho_2^{\frac{1}{2}}$ through the compressor loading nozzle was evaluated using the nozzle mass characteristics, Fig (5.9). As the nozzle mass flow parameter $\dot{m}_z/\rho_2^{\frac{1}{2}}$ was expressed in terms of the density of the air entering the nozzle, this density had to be calculated as follows:

$$\frac{T_2'}{T_1} = \left(\frac{P_2}{P_1}\right)^{\frac{\gamma-1}{\gamma}} \qquad \ldots \ldots (55)$$

$$\eta_c = \frac{T_2' - T_1}{T_2 - T_1} \qquad \ldots \ldots (56)$$

Substituting equation (55) into equation (56),

$$T_2 = \frac{T_1 \left(\frac{P_2}{P_1}\right)^{\frac{\gamma-1}{\gamma}} - T_1}{\eta_c} + T_1 \qquad \ldots\ldots (57)$$

and

$$\rho_2 = \frac{P_2}{R\ T_2} \qquad \ldots\ldots (58)$$

Equation (57) was substituted into equation (58) to calculate ρ_2, the air density at the compressor outlet. Substituting ρ_2 into the term $\dot{m}_z/\rho_2^{\frac{1}{2}}$ predicted earlier from the nozzle mass characteristics, the mass flow rate through the nozzle $\dot{m}_z$ was obtained. This must be equal to the mass flow rate through the compressor $\dot{m}_c$ which was calculated earlier. If this was not so, step (IX) was repeated using the new estimate of $\dot{m}_c$ until successive values of $\dot{m}_c$ were sufficiently close (within 1%).

(x) As the compressor mass flow rate had been determined, the compressor efficiency was evaluated using compressor steady characteristics at the known speed, Fig (6.5).

(xi) Meanwhile, knowing the compressor mass flow rate, efficiency and pressure ratio, the compressor power was calculated

$$PW_c = \frac{\dot{m}_c \; C_p \; T_1}{\eta_c} \left[\left(\frac{P_2}{P_1}\right)^{\frac{\gamma-1}{\gamma}} - 1 \right]$$

This method is shown superimposed on turbine, compressor and compressor loading nozzle characteristics, Fig (6.7).

6.5 THE FLOW IN THE PIPES

The disturbance of one end of a stationary column of gas in a pipe will result in transmission of this disturbance to the other gas particles by a pressure wave that is propagated along the pipe. Therefore, when this pressure dominates every element of gas, the particles acquire a velocity. Then the pressure wave will be reflected and returned up the pipe after it reaches the end of the pipe in a form depending on the pipe boundary conditions. If more pressure waves are still being

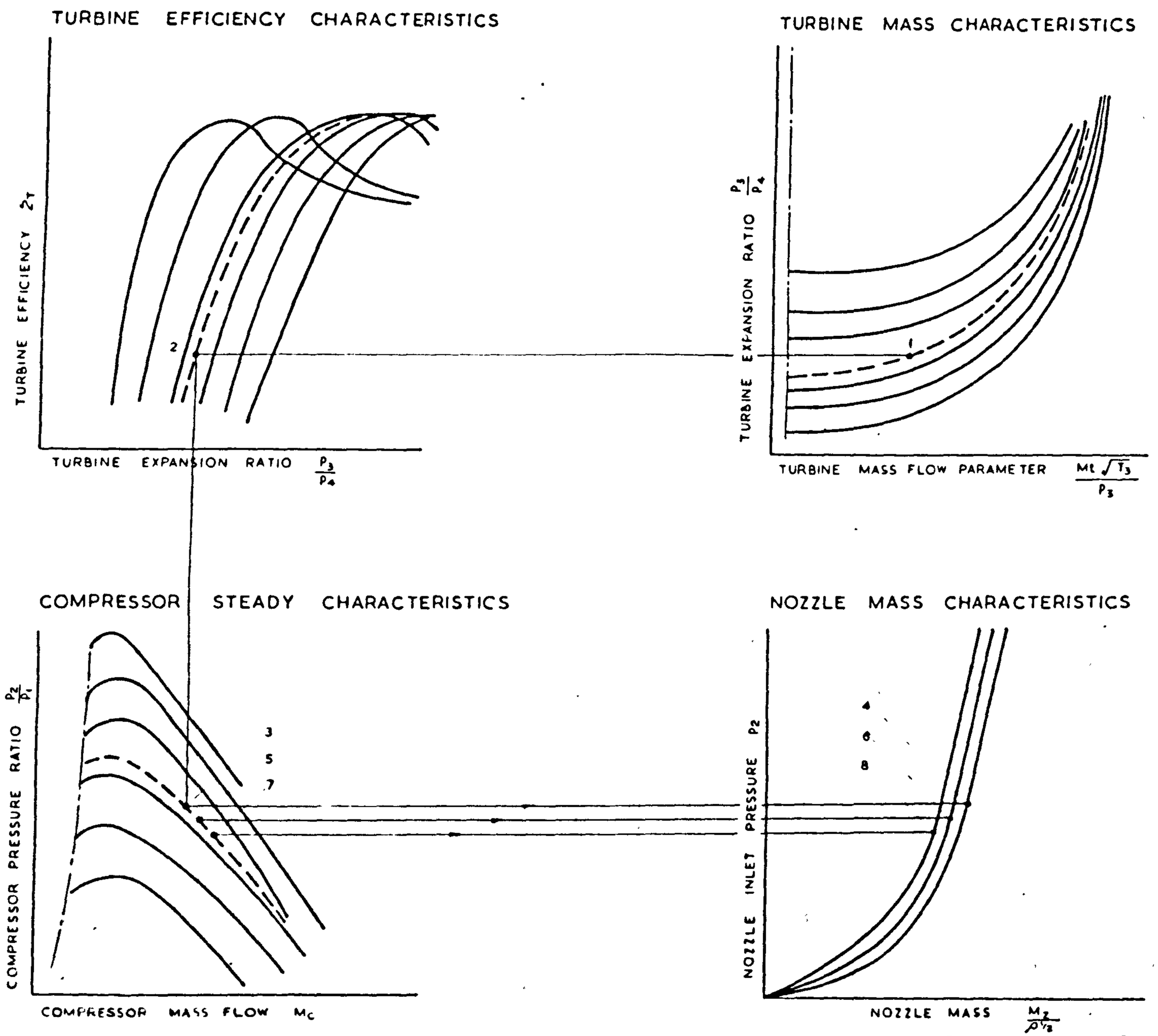

Fig (6.7) Sequence of Predicting Turbine and Compressor Operating Points [section 6.4.2]

generated by the original source, the gas in the pipe will be influenced by pressure waves moving in opposite directions and these will constitute a compound wave system. An acoustic or sound wave is the simplest form of pressure disturbance and it is one of very small amplitude whose propagation speed is constant for all parts of the wave and is solely a function of the ambient temperature. The disturbed particle velocity is a function of the pressure ratio. The wave profile is not affected as the disturbance travels along the pipe. The first worker who used this theory with regard to the charging process of engines was List[42]. This was found to be unsuitable for pulses of any significant amplitude. In a finite wave the pressure ratio changes the local temperature and the particle velocity is taken into account. The disturbance propagation speed of any wave point is then the algebraic sum of the local acoustic velocity and the local particle velocity. The particle velocity varies with the density changes as well as pressure. The finite wave equations were derived by Earnshaw[43]. The general flow pattern describing the interaction of finite waves cannot be determined directly but two simultaneous differential equations may be obtained for the lines on which the derivatives of the flow properties can be discontinuous. These lines are referred to as characteristics, and the flow pattern can be expressed as a net of position characteristics and a net of corresponding state characteristics. The two

differential equations can be solved graphically or numerically by a step-by-step process from the initial gas properties and boundary conditions. The graphical approach is extensively described by Shapiro[44] and the numerical solution by Benson et al[45].

In this investigation two methods were used for the flow analysis in the pipes, first the method of characteristics and then the "filling and emptying" method. Due to the excessive computing time for a small increase in accuracy by using the method of characteristics, the filling and emptying method was adopted to predict the flow in the pipes under pulsating conditions. The latter method takes no account whatsoever of the wave nature of the unsteady flow in the system. This method was first successfully used by Ryti[46] and Eberle[47].

FILLING AND EMPTYING METHOD

Fig (6.8) shows the exhaust system which transmits exhaust gas from the pulse generator to the turbocharger turbine.

The calculation of pulsating flow in the exhaust system requires a knowledge of the initial pressure and temperature of the fluid in the pipes. These initial values of pressure and temperature were assumed to be equal to those during the period of steady flow immediately before the transient started. In the real engine

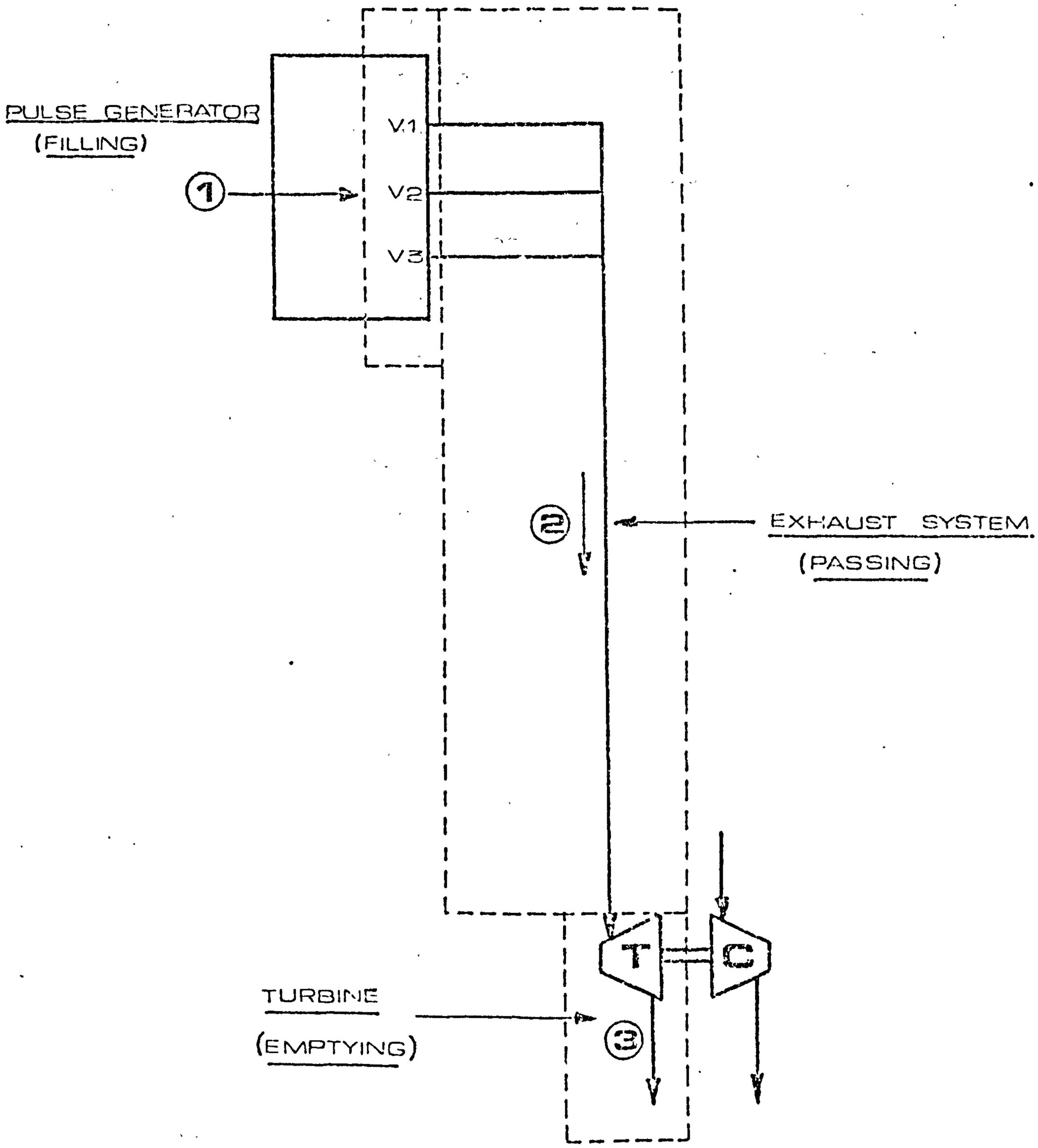

fig.(6.8) FILLING AND EMPTYING OPERATIONS

this pressure and corresponding temperature depend on the engine operating conditions. The calculation of the pulsating flow commenced with the pulse generator valve opening, Fig (5.3). Downstream the pulse generator the continuity equation becomes

$$\dot{m}_v = \rho_v c_v F_v \quad . \qquad \ldots\ldots (65)$$

Applying the energy equation between upstream and downstream the pulse generator valve

$$h_u + \frac{c_u^2}{2} = h_v + \frac{c_v^2}{2} \qquad \ldots\ldots (66)$$

Assuming that the gas velocity upstream the pulse generator valve is very much less than the downstream gas velocity and can, therefore, be neglected without incurring undue inaccuracy

$$c_v = \left[2C_p(T_u - T_v)\right]^{\frac{1}{2}} \quad . \qquad \ldots\ldots (67)$$

For isentropic flow

$$\rho_v = \rho_u \left(\frac{P_v}{P_u}\right)^{\frac{1}{\gamma}} \qquad \ldots\ldots (68)$$

$$T_v = T_u \left(\frac{P_v}{P_u}\right)^{\frac{\gamma-1}{\gamma}} \qquad \ldots\ldots (69)$$

Substituting equations (67), (68) and (69) in equation (65) gives the isentropic mass flow rate leaving the pulse generator value, $(\dot{m}_v)_{isen}$

$$(\dot{m}_v)_{isen} = \frac{P_u R\, F_v}{\sqrt{T_u}} \left[\frac{2\gamma}{R(\gamma-1)}\right]^{\frac{1}{2}} \left(\frac{P_v}{P_u}\right)^{\frac{1}{\gamma}} \left[1 - \left(\frac{P_v}{P_u}\right)^{\frac{\gamma-1}{\gamma}}\right]^{\frac{1}{2}} \quad \ldots\ldots (70)$$

Since there are three valves in the pulse generator, the mass flow rate leaving each of the three valves is as follows:

$$(\dot{m}_{v1})_{isen} = \frac{P_u R\, F_{v1}}{\sqrt{T_u}} \left[\frac{2\gamma}{R(\gamma-1)}\right]^{\frac{1}{2}} \left(\frac{P_v}{P_u}\right)^{\frac{1}{\gamma}} \left[1 - \left(\frac{P_v}{P_u}\right)^{\frac{\gamma-1}{\gamma}}\right]^{\frac{1}{2}}$$

$$(\dot{m}_{v2})_{isen} = \frac{P_u R\, F_{v2}}{\sqrt{T_u}} \left[\frac{2\gamma}{R(\gamma-1)}\right]^{\frac{1}{2}} \left(\frac{P_v}{P_u}\right)^{\frac{1}{\gamma}} \left[1 - \left(\frac{P_v}{P_u}\right)^{\frac{\gamma-1}{\gamma}}\right]^{\frac{1}{2}}$$

$$(\dot{m}_{v3})_{isen} = \frac{P_u R\, F_{v3}}{\sqrt{T_u}} \left[\frac{2\gamma}{R(\ -1)}\right]^{\frac{1}{2}} \left(\frac{P_v}{P_u}\right)^{\frac{1}{\gamma}} \left[1 - \left(\frac{P_v}{P_u}\right)^{\frac{\gamma-1}{\gamma}}\right]^{\frac{1}{2}} .$$

By definition the coefficient of discharge is the ratio of the actual mass flow to the isentropic mass flow

$$Cd = \frac{\dot{m}_v}{(\dot{m}_v)_{isen}}$$

$$\dot{m}_v = C_d (\dot{m}_v)_{isen} \quad \ldots\ldots (71)$$

The actual mass flow rate leaving each of the three values is

$$\dot{m}_{v1} = C_{d1}(\dot{m}_{v1})_{isen}$$

$$\dot{m}_{v2} = C_{d2}(\dot{m}_{v2})_{isen}$$

$$\dot{m}_{v3} = C_{d3}(\dot{m}_{v3})_{isen}$$

and the actual mass flow rate entering the exhaust system is the algebraic sum of the actual mass flow rate of the three values

$$\dot{m}_{v} = \dot{m}_{v1} + \dot{m}_{v2} + \dot{m}_{v3}$$

$$\dot{m}_{v} = C_{d1}(\dot{m}_{v1})_{isen} + C_{d2}(\dot{m}_{v2})_{isen} + C_{d3}(\dot{m}_{v3})_{isen} \qquad \text{.. .. (72)}$$

where C_{d1}, C_{d2} and C_{d3} are the coefficients of discharge of the pulse generator values measured experimentally under a range of supply pressure and different valve lift, Fig (5.5).

The initial mass of gas in the exhaust system is

$$(m_s)_n = \frac{(P_s)_n \, V_s}{(T_s)_n \, R} \quad . \qquad \text{.. .. (73)}$$

that the change in

Assuming the mass flow rate through the valve and the turbine is small, the mass of gas in the exhaust system after a time step (Δt) is:

$$(m_s)_{n+1} = (m_s)_n + \left[(\dot{m}_v)_{n+1} - (\dot{m}_t)_n\right] \Delta t \qquad \ldots\ldots (74)$$

where $\dot{m}_t$ is the mass flow rate leaving the exhaust system to enter the turbine.

And also assuming the change in temperature of the air in the pipes during the step is small, then by applying the first law of thermodynamics

$$(\dot{Q}-\dot{W})_{n+1} \Delta t = (m_s)_{n+1} (u)_{n+1} - (m_s)_n (u)_n - \left[(\dot{m}_v)_{n+1} (h_v)_{n+1} - (\dot{m}_t)_n (h_s)_n\right] \Delta t \qquad \ldots\ldots (75)$$

Equation (73) is substituted into equation (75) and assuming that there is no heat transfer or work done, the pressure after a time step is,

$$(P_s)_{n+1} = (P_s)_n + \left[(\dot{m}_v)_{n+1} (T_\mu)_{n+1} - (\dot{m}_t)_n (T_s)_n\right] \frac{\gamma R \Delta t}{V_s} \qquad \ldots\ldots (76)$$

Thus, the temperature after a time step is:

$$(T_s)_{n+1} = \frac{(P_s)_{n+1} V_s}{(m_s)_{n+1} R} \qquad \text{.. .. (77)}$$

From this pressure $(P_s)_{n+1}$ and temperature $(T_s)_{n+1}$, the mass flow rate through the turbine $\dot{m}_t$ was calculated using the method described in section (6.4.1) in conjunction with turbine and compressor characteristics and the same procedure was applied repeatedly to find the pressure and temperature after each time step to cover the whole required period.

6.6 TURBOCHARGER BEARING POWER LOSS

Some of the turbine power is lost in the bearings due to friction. This power loss was measured experimentally as explained in section (5.5). It may also be calculated by Petroff's method, as follows:

Due to Newton's equation of viscous flow where the viscosity is defined as the ratio of shearing stress to the rate of shear

$$\mu = \frac{F/A}{U/h} \qquad \text{.. .. (78)}$$

where

μ	dynamic viscosity
F	friction force
A	surface area
U	surface velocity
h	film thickness

Petroff published the following equation for friction losses in journal bearing[48]

$$F = \pi \mu UDL/C \qquad \text{.. .. (79)}$$

$$PW_B = F.U$$
$$= \pi^3 \mu D^3LN^2/C \qquad \text{.. .. (80)}$$

where

D diameter of the bearing

L axial length of the bearing

C radial clearance

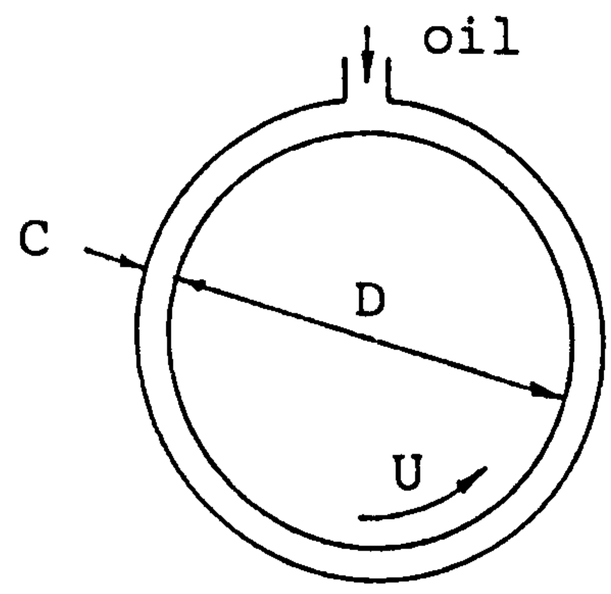

Journal surrounded by oil film of uniform thickness C
(Petroff bearing)

The turbocharger bearing power loss which was measured experimentally and shown in Fig (5.7), was used in the computer programs.

6.7 EVALUATION OF TURBINE AND COMPRESSOR PARAMETERS FROM STEADY STATE CHARACTERISTICS

Each point within the range of turbine mass characteristics Fig (6.3), turbine efficiency characteristics Fig (6.4) or compressor steady characteristics Fig (6.5) has three parameters - the speed parameter Z and the X and Y axis parameters, see Fig (6.9). If point P was a state condition located within any of the turbine or compressor characteristics with two parameters known, then the third parameter had to be evaluated. Two methods were used to evaluate the third parameter from the known parameters.

6.7.1 Method A

If parameters Xp and Zp were known, Yp could be evaluated, Fig (6.9). This method was used within the turbine and compressor characteristics as follows:

After finding the two successive speed curves $(Z)_j$ and $(Z)_{j+1}$ on either side of the given speed $(Z)_p$, the two points 1 and 2 on either side of P on the speed curve $(Z)_j$, in addition to the other two points 3 and 4 on either side of P but on the speed curve $(Z)_{j+1}$ were determined. By this, the four points 1, 2, 3 and 4 surrounding points P were specified. As X, Y and Z parameters for

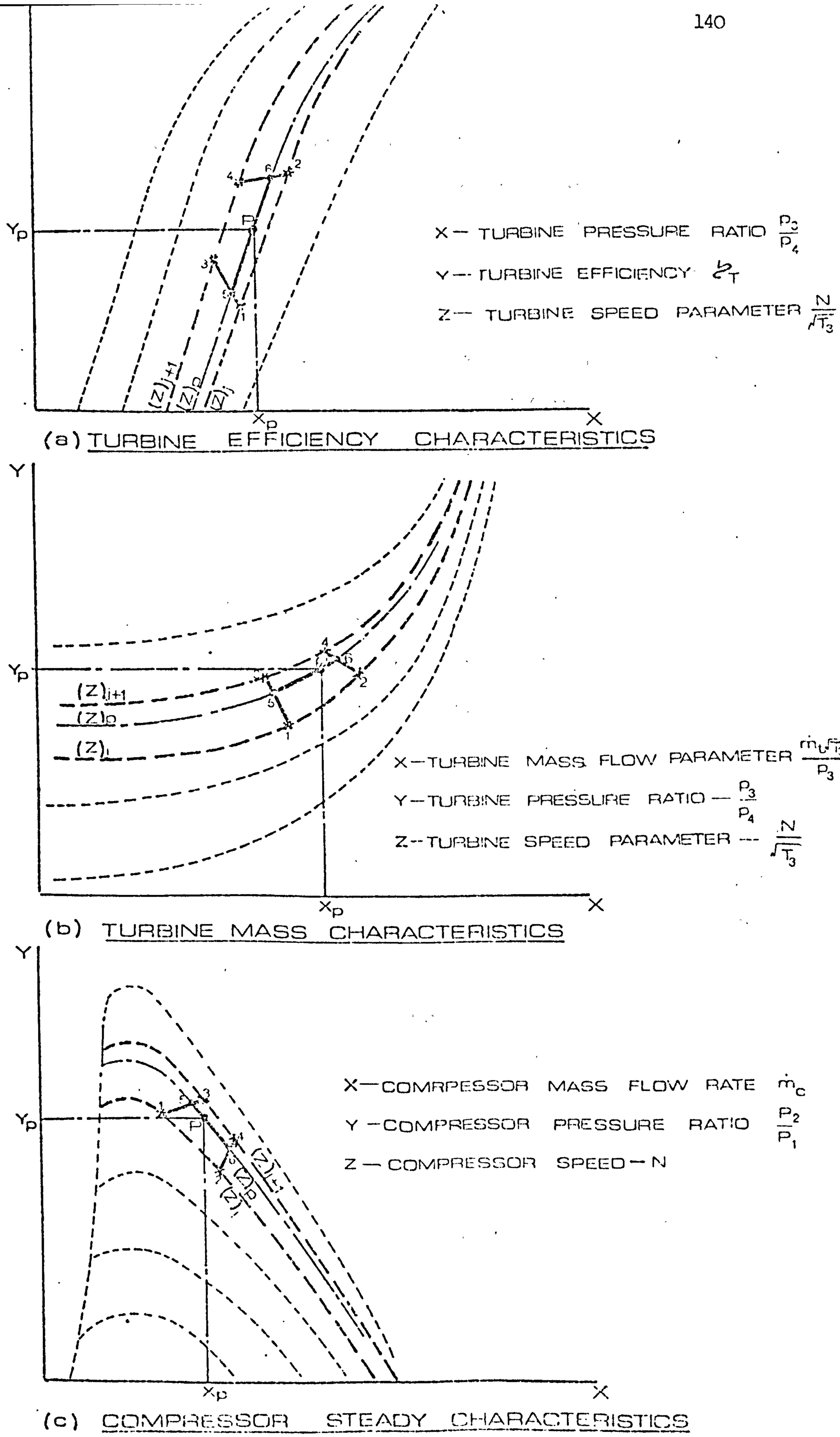

fig.(6.9) INTERPOLATION METHOD — A.

these points were known, a linear interpolation was carried out between points 1 and 3 to find X_5 and Y_5 for point 5, see Fig (6.9) and another linear interpolation was carried out between points 2 and 4 to find X_6 and Y_6 for point 6. As X_5, Y_5, X_6 and Y_6 were obtained, a linear interpolation between points 5 and 6 was carried out to find Yp for the given Xp.

6.7.2 Method B

Xp and Yp were known and Zp was to be evaluated, Fig (6.10). This method was used in turbine mass characteristics as follows:

After finding the two successive speed curves $(Z)_j$ and $(Z)_{j+1}$ where point P was located between them, the two points 2 and 3, which were on either side of P on the speed curve $(Z)_j$, in addition to the other two points 5 and 6 on either side of P but on the speed curve $(Z)_{j+1}$ were determined. A quadratic curve through points 1,2 and 3 was fitted where point 1 was the data point preceding point 2. Lagrange inter-polation was used, (see Appendix 5) to find Y_8 for the given Xp. Similarly a quadratic curve was fitted through points 4, 5 and 6 where point 4 was the data point preceding point 5 and a Lagrange inter-

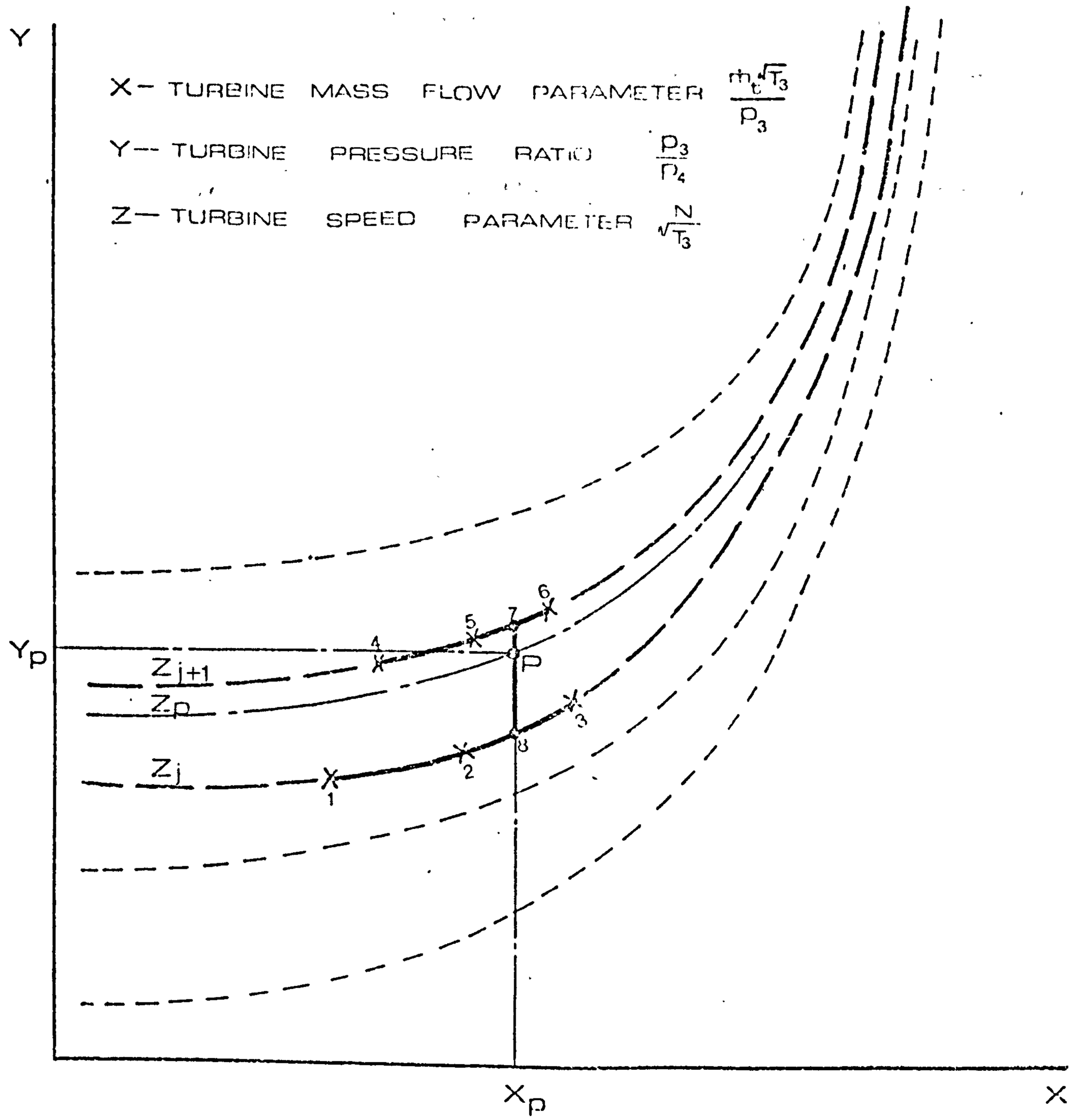

TURBINE MASS CHARACTERISTICS

fig.(6.10) INTERPOLATION METHOD – B

polation was used to find Y_7 for the given Xp. As the speed parameter $(Z)_j$ and Y_8 for point 8 had been determined as well as the speed parameter $(Z)_{j+1}$ and Y_7 for point 7, a linear interpolation was carried out between points 7 and 8 to find the speed parameter $(Z)_p$ passing through point P corresponding to the given Yp.

6.8 COMPUTER PROGRAMS

Three computer programs and seven subroutines were written to predict the transient response performance of the turbocharger. They were as follows:

(1) Program NON-PULSATING used the method described in section (6.3) to predict the transient response performance of the turbocharger under non-pulsating flow conditions.

(2) Program PULSATING1 used the method described in section (6.4.1) to predict the transient response performance of the turbocharger under pulsating flow conditions (complete system).

(3) Program PULSATING2 used the method described in section (6.4.2) to predict the transient response performance of the turbocharger under pulsating flow conditions (turbocharger only).

When organizing the calculations it was decided to keep the common calculations in the three programs, such as predicting turbine and compressor parameters from their steady state characteristics and program independent calculations in form of subroutines which were called in the program as required. This flexibility enabled a range of different types of calculations to be performed. The subroutines, see Appendix (6), were as follows:

(1) Subroutine TSCHAR (turbine mass characteristics),

Fig (6.3), which used methods A and B described in section (6.7.1) and (6.7.2).

(2) Subroutine TEFFCH (turbine efficiency characteristics),

Fig (6.4), which used method A, section (6.7.1).

(3) Subroutine CCHAR (compressor steady characteristics),

Fig (6.5), which used method A, section (6.7.1).

(4) Subroutine PIPES which used the Filling and Emptying Method described in section (6.5) for the flow in the exhaust pipes.

(5) Subroutine VAREA which was used to calculate the pulse generator valve opening area, Fig (5.3),

at the time of operation.

(6) Subroutine CFTINT (curve fit interpolation) which was used to fit a curve through a set of data points using Lagrange interpolation, Appendix (5), to find the interpolated value of the required point.

(7) Subroutine TSCHARM (turbine mass characteristics) which used method 4, section (6.7.1).

The symbols used in each subroutine are described in their related subroutine section, Appendix (6), but if that symbol is common with the main programs, its description was included in the nomenclature of the main programs, page (xi).

The flow charts and the listings of the programs are included in Appendix (7) and Appendix (8) respectively.

CHAPTER SEVEN

DISCUSSION OF RESULTS

CHAPTER SEVEN

DISCUSSION OF RESULTS

In order to compare the predicted and actual transient response performance of the turbocharger under pulsating and non-pulsating flow conditions, an experimental programme was carried out. In each of these tests the transient limits were determined by presetting the LP and HP pressures and the test was carried out as explained in section (5.7). Meanwhile, in order to obtain a comparison between the experimental and the computed results the computer programs, which had been written to use the theoretical methods of predicting the transient were run under the same boundary conditions as each of the experimental test.

All the experimental tests were carried out at room temperature because propane fuel storage facilities were not available at the Aeronautical and Mechanical Engineering Building. The experimental rig and the computer programs can be run within any likely range of engine exhaust pressure and temperature. In each figure of the transient, Figs (7.1) to (7.59) the X-axis represents the time from the beginning of the transient and the Y-axis used for the turbocharger parameter. The experimental results were plotted in full curves while the computed results were plotted in dotted curves. The same limits and scales were used for each

parameter to facilitate comparison of the results during the various transients.

As mentioned in section (3.1), the experimental work was divided into two series: Test Series I and Test Series II, which will be considered successively with their theoretical comparisons.

7.1 TEST SERIES I

The test rig was constructed as shown in Fig (3.1) and the instrumentation used was described in sections (4.1) to (4.4).

Sixteen experimental transient tests were carried out under non-pulsating flow conditions. The theoretical method (Section 6.3) required only the variations of turbine inlet pressure and turbine inlet temperature as data for the computer program (program "NON-PULSATING"). Three sets of results for non-pulsating transients under different conditions are presented. The results obtained by experiments and by computation are compared in Figs (7.1) to (7.12).

Another sixteen transient tests were carried out under pulsating flow conditions. As in the non-pulsating transients the limits of each transient were determined by pre-setting the LP and HP pressures. The computer

program, which had been written to apply the theoretical method outlined in Section (6.4.1) to predict the transient response performance of the turbocharger under pulsating flow conditions, was used under the same boundary conditions as each of the experimental tests to compare the experimental and the computed results. The results from three typical transients are presented graphically in Figs (7.13) to (7.30).

7.1.1 TURBINE MASS FLOW RATE AND PRESSURE RATIO

It was observed that the measured air mass flow rate through the turbine, using the unsteady coefficients of discharge for the orifice plate was greater than the predicted mass flow rate which in turn was usually greater than the measured mass flow rate calculated using the BS1042 coefficients for the orifice plate. The mass flow rate calculated using BS1042 was much closer to the predicted mass flow rate than that calculated using the unsteady coefficients (for an example see Fig 7.21). The overestimate using the unsteady coefficients of discharge is thought to arise because they were derived under shock wave conditions (see Appendix 1) with increasing pressure gradients whilst during the

transients in this work the pressure before the orifice plate was oscillating about a rising mean pressure during the transient. The results using the BS1042 coefficients and the predicted mass flow rates through the turbine are compared in Figs (7.4), (7.6) and (7.7) for the non-pulsating transients and Figs (7.19), (7.20) and (7.21) for the pulsating transients. A comparison between the experimental and the computer predicted mass flow rates then showed that there was variable agreement between the measured and the computer predicted mass flow rates. In general, the predicted mass flow rates overestimated the experimental mass flow rate. In the computer programs the turbine outlet pressure was assumed to be atmospheric. In fact, it was always greater than atmospheric pressure (and fluctuating). In the worst case this reduced the turbine pressure ratio from 2.407 to 2.119 at the end of the transient. Consequently, the predicted pressure ratio is likely to be too high and this is confirmed by most of the results, Figs (7.16) to (7.18). These overestimates of pressure ratio caused the turbine mass flow parameters $\dot{m}_t\sqrt{T_3}/P_3$ evaluated from turbine mass characteristics, Fig (6.3), at a specific speed, to be overestimated causing an overestimate in turbine mass flow rate $\dot{m}_t$ to be predicted by the computer program.

7.1.2 TURBINE INLET TEMPERATURE

It was noticed that the turbine inlet temperature

increased at the beginning of the transient and decreased almost to the initial value by the end of the transient. The extent of the temperature variation depended upon initial and final supply pressure. These results are shown in Figs (7.22), (7.23) and (7.24) for the pulsating transients. From the Joule-Thompson effect the temperature of the HP air will be slightly greater than the temperature of the LP air. At the beginning of the pulsating transient the air mass flow rate into the pipework connecting the pulse generator to the turbine is greater than the air mass flow rate through the turbine, so an increase in turbine inlet temperature is anticipated from the non-steady flow energy equation. As the flow rate into the pipework reduces to that entering the turbine the temperature of the air entering the turbine will fall to the supply temperature.

The turbine inlet temperature was measured by probe wires, see Section (4.3) and no correction had been made for the heat transfer from the wire to its support. Therefore, it would be expected that the observed temperature would be lower than the predicted temperature. The results showed that there is a good agreement between the two temperatures, see Figs (7.22), (7.23) and (7.24) for pulsating transients.

7.1.3 TURBOCHARGER SPEED

It was found that the measured turbocharger speed and

that predicted by the computer program are in fairly good agreement in both the non-pulsating transients, Figs (7.1), (7.2) and (7.3) and in the pulsating transients, Figs (7.13), (7.14) and (7.15).

7.1.4 COMPRESSOR MASS FLOW RATE AND PRESSURE RATIO

A comparison between compressor measured mass flow rate and that predicted by the computer program is given in Figs (7.10), (7.11) and (7.12) for non-pulsating transients and Figs (7.28), (7.29) and (7.30) for the pulsating transients. These showed that there were discrepancies in the measured and predicted mass flow rates particularly at the beginning of the transients. The same happened to the compressor pressure ratio at the beginning of the transient, too, see Figs (7.7), (7.8) and (7.9) for the non-pulsating transients and Figs (7.25), (7.26) and (7.27) for the pulsating transients. The resolution of the pressure transducers was not specified by the manufacturer, but the hysteresis is claimed to be not more than 2% of full scale deflection. As full scale deflection corresponds to 10 lbf/in^2, this implies a hysteresis error equivalent to up to 0.2 lbf/in^2. As the maximum pressure reached was only 0.5 lbf/in^2, this could lead to a large error in the pressure differential and consequently in the measured mass flow rate.

7.2 TEST SERIES II

In Test Series I, considerable discrepancies were found between the experimental and the computed results. Therefore, it was decided to improve the experimental equipment and the method of predicting the results.

7.2.1 EXPERIMENTALLY

The test rig was reconstructed as shown in Fig (3.2) and partially re-equipped as follows:

1. New pressure transducers with their offset amplifiers were used, see sections (4.1) and (4.5).

2. The pulse generator exhaust system was re-designed to give a smaller volume, consequently,

3. The turbine orifice plate was relocated in the turbine outlet instead of the turbine inlet.

4. Variable pulse generator camshaft speed was attained.

5. A three way valve was fitted in the oil flow from the turbocharger bearing outlet in order to facilitate measuring the turbocharger

bearing power loss.

6. Compressor loading nozzle mass characteristics were measured experimentally.

7.2.2 THEORETICALLY

1. The computer program for the pulsating flow conditions was modified to start the calculations from the turbocharger turbine inlet, see section (6.4.2).

2. The speed dependent measured turbocharger bearing power loss was taken into account instead of assuming the mechanical efficiency was constant throughout the calculations, see section (6.6).

3. Compressor loading nozzle mass flow characteristics which were measured experimentally, see section (5.6), were used instead of the theoretical characteristics calculated by BS1042, Appendix (2).

4. The turbine outlet pressure was calculated for each time step, using the measured pressure drop across the turbine exhaust system, while in Test Series I it was assumed atmospheric throughout the calculations.

For this series of tests, twenty experimental transient tests were carried out under non-pulsating flow conditions. Another twenty transient tests were made under pulsating flow conditions, ten with the pulse frequency about 25 pulses/sec and another ten with pulse frequency around 38 pulses/sec. That was done by changing the ratio between the air motor speed and the pulse generator camshaft speed.

7.2.3 Form of the transient

A. Non-pulsating flow conditions

During non-pulsating transients the pressure changed from low to high pressure in not more than 0.5 sec. The actual form and duration of the pressure ramp depended on the operator. (For an example see plate (13)). There was a small temperature excursion at the turbine inlet during this time. The turbine mass flow rate followed the turbine inlet pressure pattern. The turbocharger speed, compressor mass flow rate and pressure ratio increased gradually over 0.5 to 1.0 sec.

B. Pulsating Flow conditions

Under pulsating transient operation, the turbine inlet pressure was changed rapidly from a steady low

pressure to a pulsating one in which the amplitude varied from a little above atmospheric to about 1.7 to 1.8 bar. The turbine inlet temperature varied with the pulsating pressure. Due to the characteristics of the changeover mechanism, the low supply pressure dropped significantly before the pulsating flow was established. (See plate (12)). The turbocharger speed, compressor mass flow rate and pressure ratio increased gradually and the overall duration of the transient was about 1.0 sec.

7.2.4 Criteria for Assessing the Results

Although great care was taken in calibrating the equipment, instrumentation errors are unavoidable. Instrumentation errors depend on the hysteresis and repeatability of the instrument, accuracy of calibration, and the precision of the reading equipment.

For example, errors in measuring the mass flow rate through the compressor arise from:

Calibration error	up to ± 2%
Zero error	1%
Reading error	1%
Hysteresis and repeatability	5% low pressure
(Manufacturers specification)	1% high pressure

This gives a predicted error band from ± 5.5% for

low pressure readings to ± 2.5% for high pressure one. To these the errors inherent in the method of flow measurement should be added. Consequently, there is some uncertainty when comparing calculated with experimental results. At low flow rate differences of up to 5% may, in part, be due to measurment; this band of uncertainty drops to about 2% as the pressure increases to the maximum range of the pressure transducer. It is also well established that the quasi-steady method of predicting turbine performance is not entirely accurate (see the literature survey pages 13-21).

In the discussion which follows, agreement of calculated and experimental results, within 5%, will therefore be regarded as very satisfactory.

7.2.5 Factors Affecting the Accuracy of the Results

(1) As the turbine and compressor experimental characteristics were limited in ranges, Figs (6.3), (6.4) and (6.5), they were extended as described in Appendix (3) to cover the greater range of operation anticipated during the transient flow tests. This might cause inaccuracy in predicting the transient performance of the turbocharger at the higher pressure ratios. Whilst the extended characteristics were necessary to find the initial operating points, they were actually not used during the transient (see specimen transient plotted on Fig. (7.31A).

(2) The permitted error of iterative procedures used for the computer programs was 1%. When this permitted error was decreased from 1% to 0.1%, it was found that the results were not affected significantly as shown in Figs (7.58) and (7.59) but computer running time increased from 5 to 25%.

(3) As the quasi-steady method of computing parameters in predicting flow gives increasing errors as the pulse rate increases, a poorer match between computed and observed results is expected at the pulse rate of 38 pulses/sec.

(4) As the turbine mass flow parameter changes subsequently for small changes in low pressure ratios, errors in measuring the initial pressure can have a substantial effect on the predicted initial state of the turbocharger and therefore throughout the transient.

7.2.6 Comparison between Experimental and Predicted Results

From Fig (7.31) to (7.59) which gives typical results obtained for a large range of non-pulsating and pulsating transients. It can be seen that the theoretical and the experimental results are generally very close. The greatest error occurs in

Fig (7.49) under the amount of 4% at the end of the transient conditions. This compares well with the error band anticipated in section (7.2.4).

The two important turbocharger parameters during the transient operation are the compressor air mass flow rate and pressure ratio, where they increased gradually from the initial condition to the final one and the computer predicted results were within 5% with the results measured experimentally, see Figs (7.31) to (7.36) for non-pulsating and Figs (7.43) to (7.48) for pulsating transients. Generally, the theoretical results overestimated the experimental ones and under pulsating conditions the overestimate increased as the pulse frequency was increased. The most critical parameter is the compressor air mass flow rate as this controls the amount of fuel which can be burnt in the engine. The maximum difference between the experimental and the computed compressor air mass flow rate was 0.0015 kg/s at the end of the transient as shown in Fig (7.49). An error in compressor mass flow rate is more important at the beginning of the transient than at the end, because early in the transient the air flow rate is critical for combustion and at the end of the transient the air supply will be adequate for a well matched turbocharger engine.

It should also be noted that the theoretical air flow

rate anticipates the actual air flow rate by up to .025 sec. This is not likely to be very significant in engine cycle synthesis calculations.

Under pulsating flow conditions, the measured turbine mass flow rate which followed the turbine inlet pressure pattern was out of phase with that predicted theoretically by around 0.005 sec. This is to be expected because the flow rate is calculated at the turbine inlet and measured at the orifice plate which is 2½ metres downstream from the turbine. Figs (7.55) to (7.57) showed the variation of the transient turbine mass flow rate under different conditions, at the beginning, at the middle and at the end of the transient operation.

7.3 GENERAL DISCUSSION

The first series of results, Test Series I, were not satisfactory, but in Test Series II:

(a) the errors observed are within those anticipated in section (7.2.4) and are well within those generally expected when the quasi-steady method is used to predict pulsating flow parameters from steady flow data. Therefore, the methods of calculation used can be regarded as satisfactory.

(b) As there is a tendency for the compressor air flow rate to be overestimated the computed air flow rate should be reduced by (say) 5% when carrying out transient engine performance calculations.

BEST COPY

AVAILABLE

Variable print quality

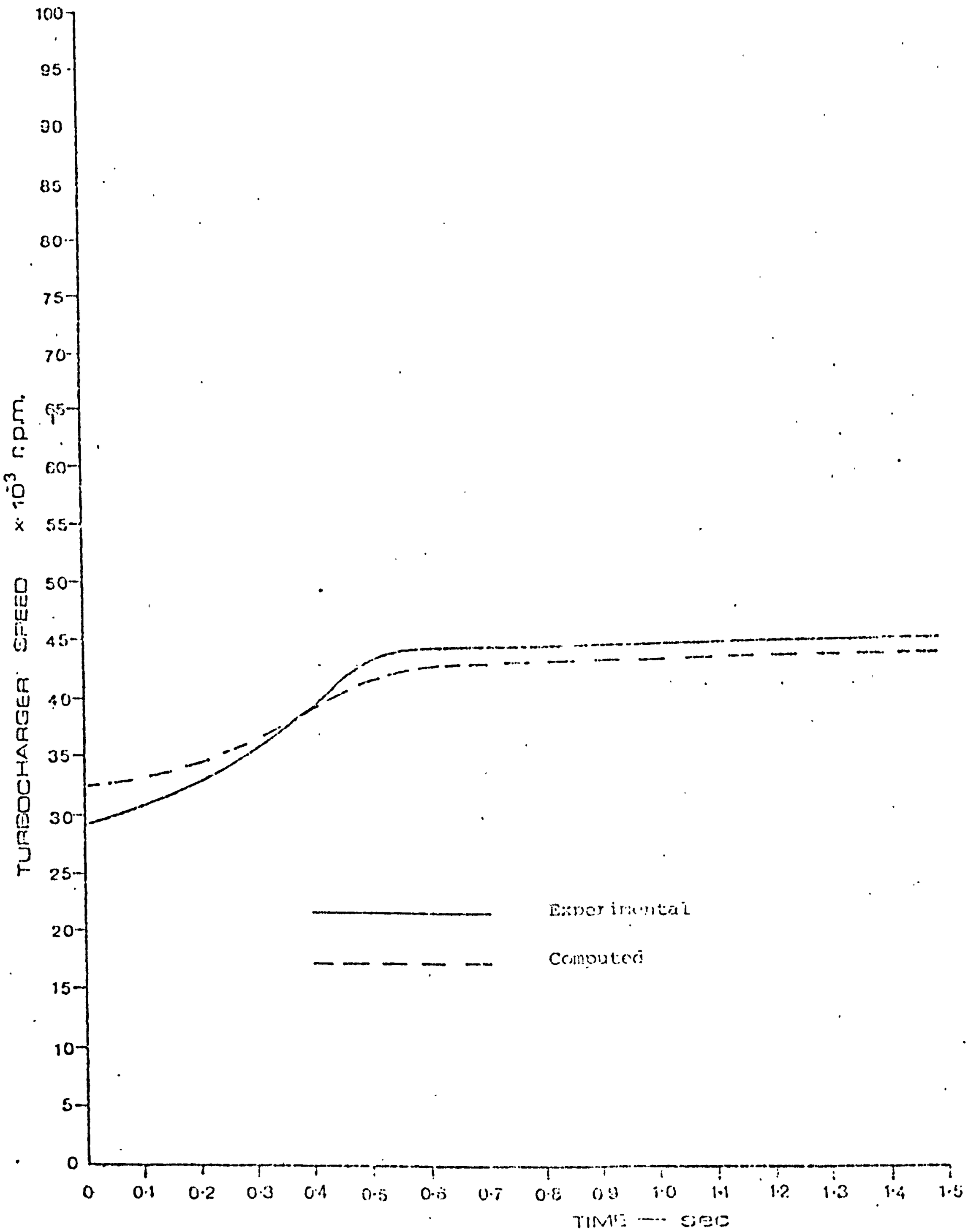

fig.(7.1). TURBOCHARGER SPEED DURING NON-PULSATING TRANSIENT

INITIAL SUPPLY PRESSURE = 1.350 bar

FINAL SUPPLY PRESSURE = 1.889 bar

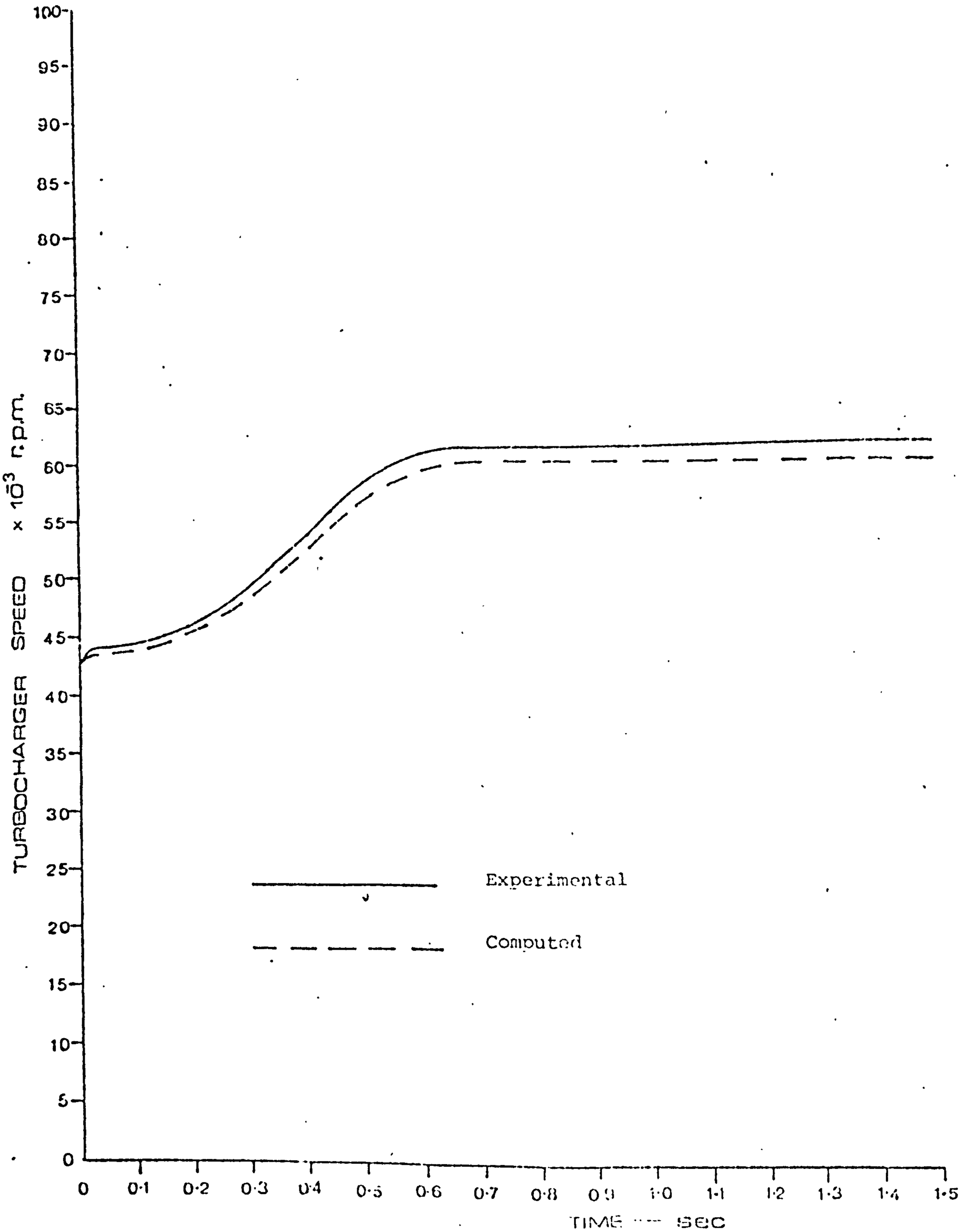

fig.(7.2) TURBOCHARGER SPEED DURING NON-PULSATING TRANSIENT

INITIAL SUPPLY PRESSURE = 1.669 bar

FINAL SUPPLY PRESSURE = 2.286 bar

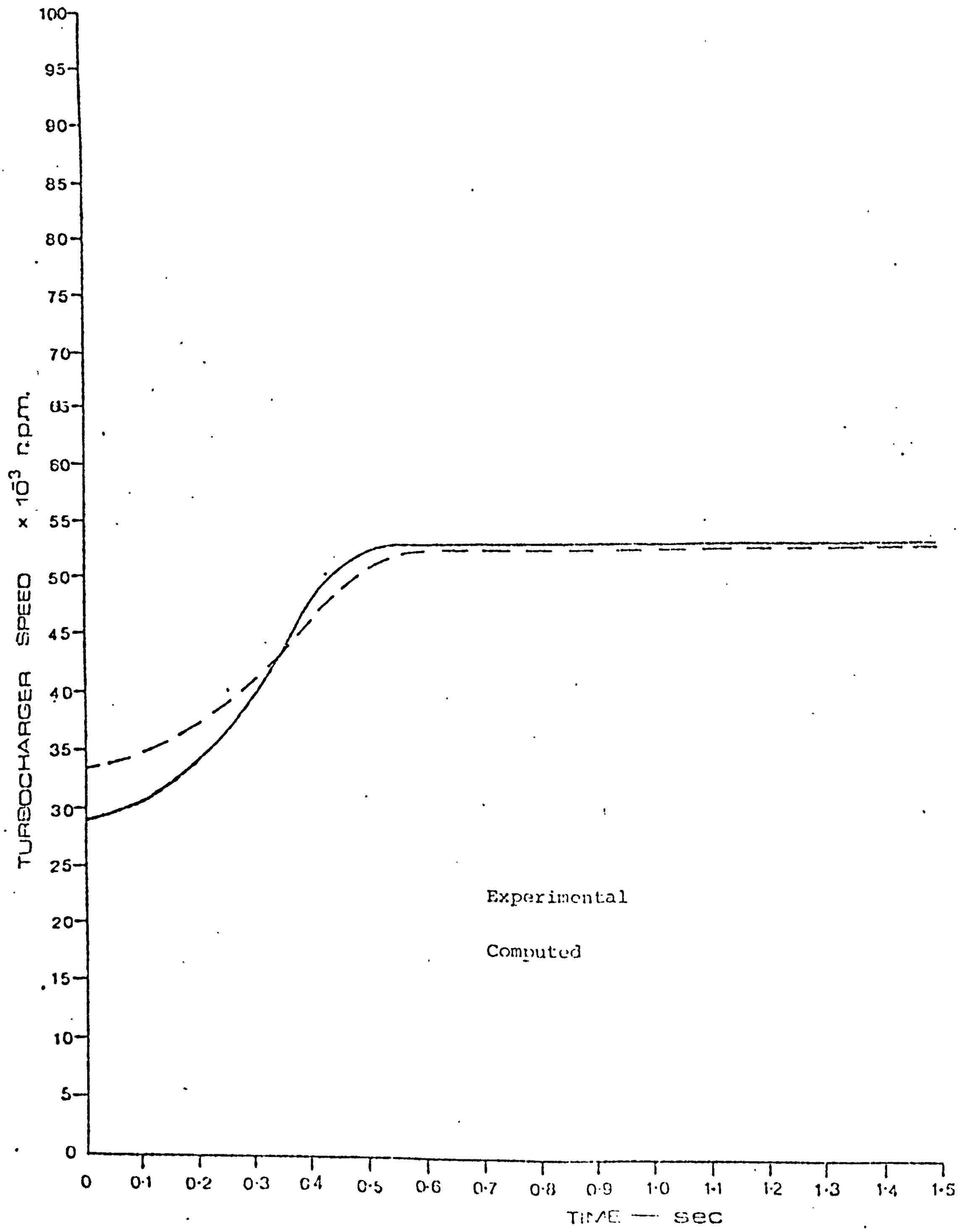

fig.(7.3). TURBOCHARGER SPEED DURING NON-PULSATING TRANSIENT

INITIAL SUPPLY PRESSURE = 1.352 bar

FINAL SUPPLY PRESSURE = 2.696 bar

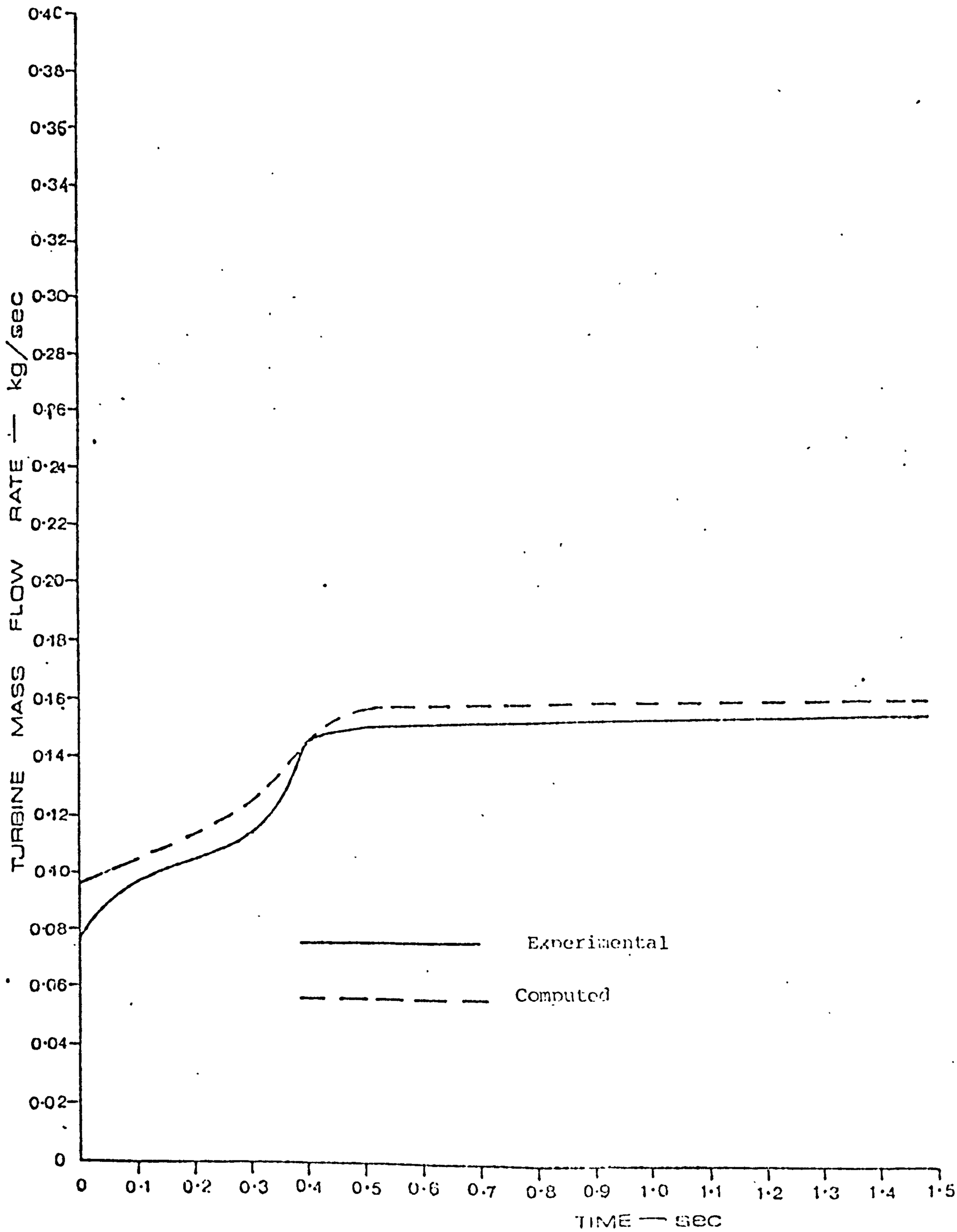

fig.(7.4). TURBINE MASS FLOW RATE

DURING NON - PULSATING TRANSIENT

INITIAL SUPPLY PRESSURE = 1.359 bar

FINAL SUPPLY PRESSURE = 1.889 bar

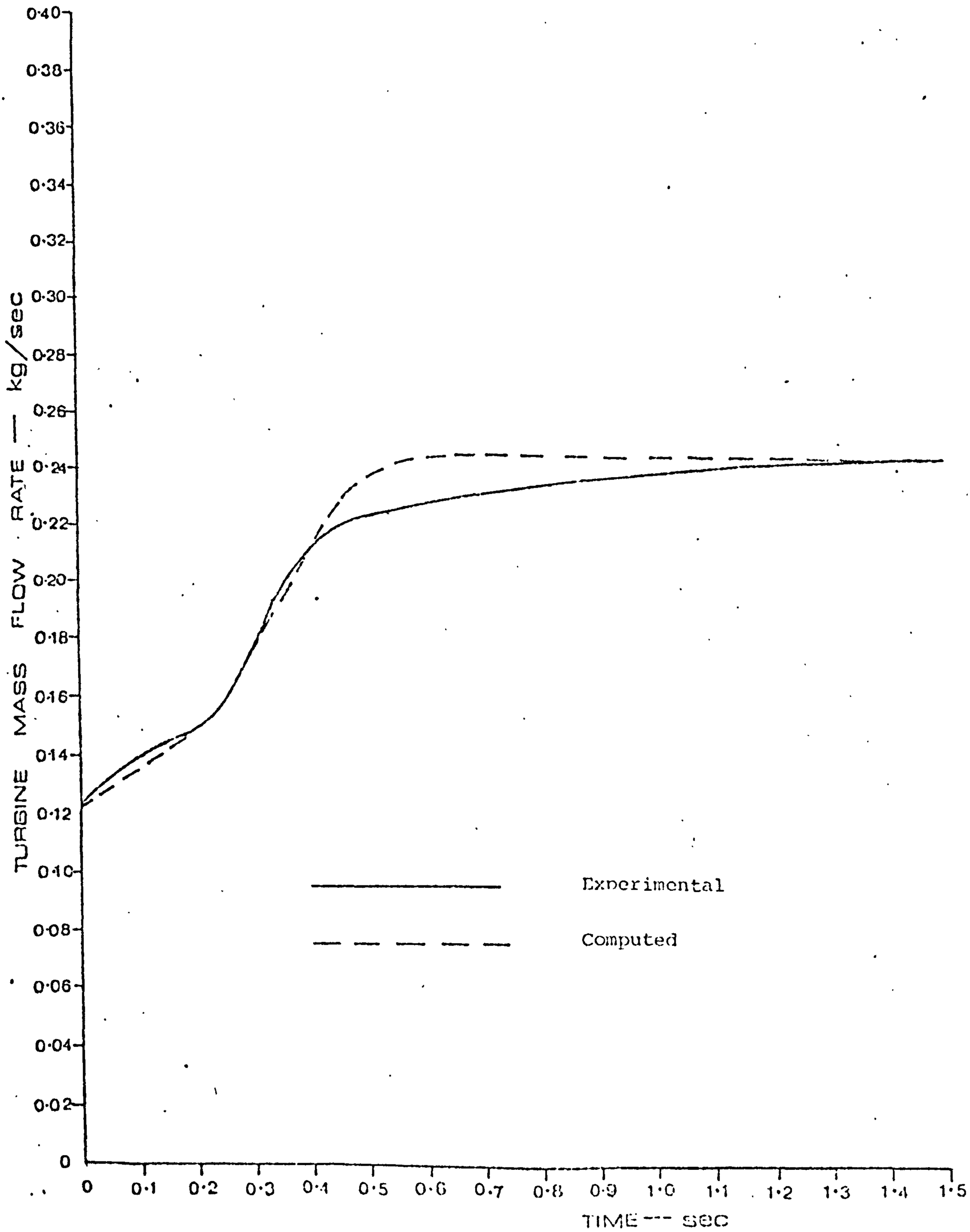

fig.(7.5). TURBINE MASS FLOW RATE

DURING NON - PULSATING TRANSIENT

INITIAL SUPPLY PRESSURE == 1.669 bar

FINAL SUPPLY PRESSURE == 2.862 bar

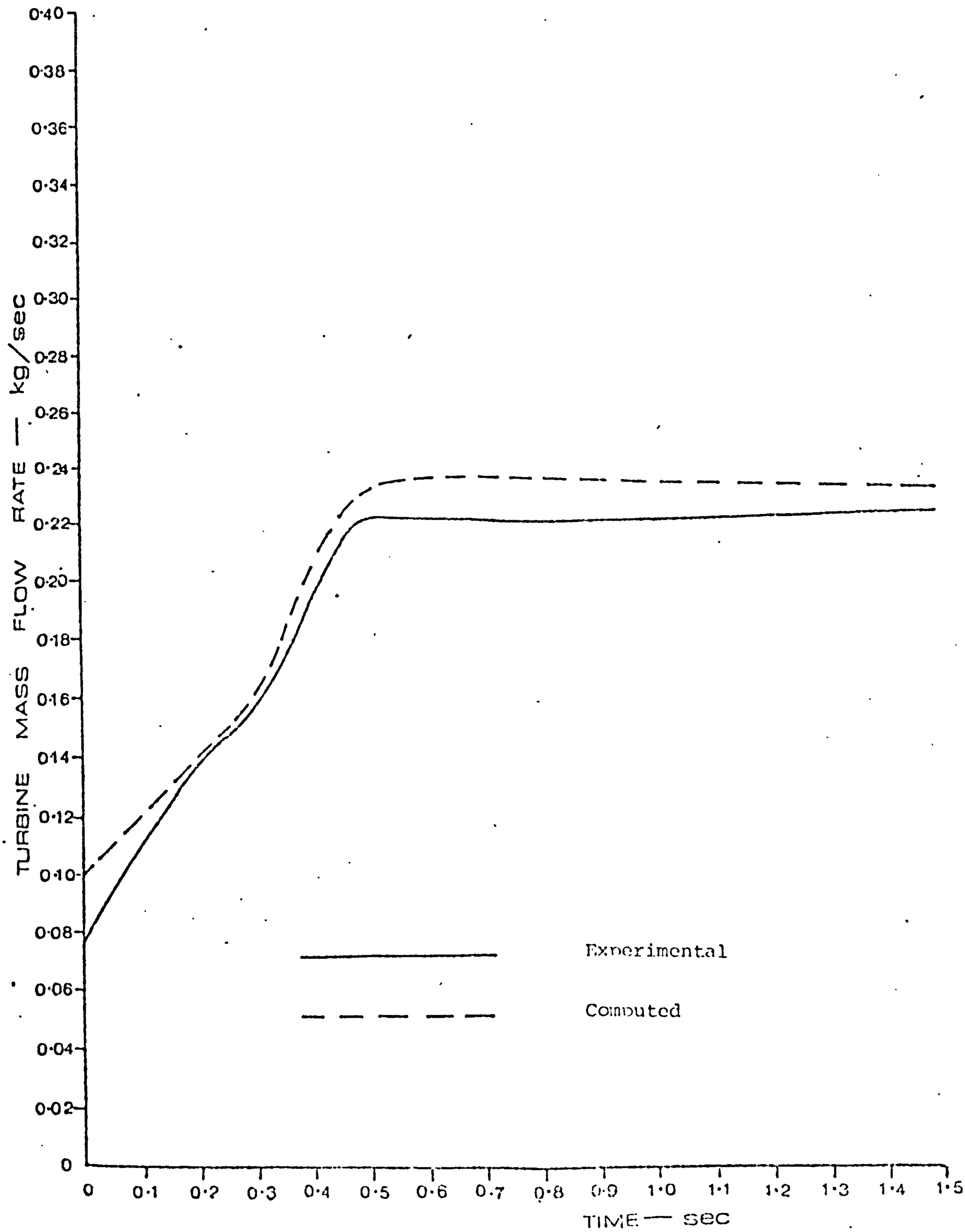

fig.(7.6). TURBINE MASS FLOW RATE

DURING NON - PULSATING TRANSIENT

INITIAL SUPPLY PRESSURE = 1.352 bar

FINAL SUPPLY PRESSURE = 2.696 bar

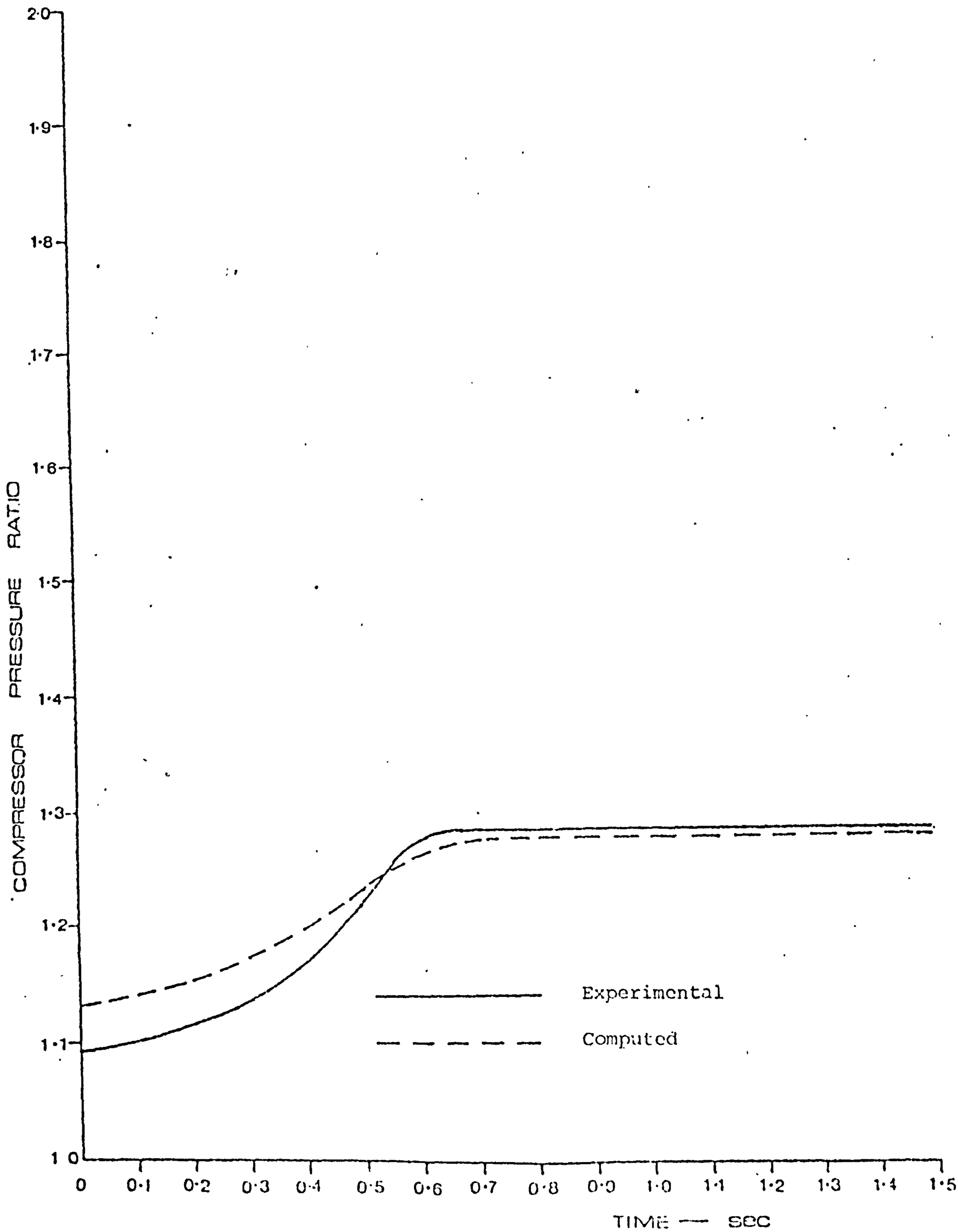

fig.(7.7).. COMPRESSOR PRESSURE RATIO

DURING NON-PULSATING TRANSIENT

INITIAL SUPPLY PRESSURE = 1.359 bar

FINAL SUPPLY PRESSURE = 1.089 bar

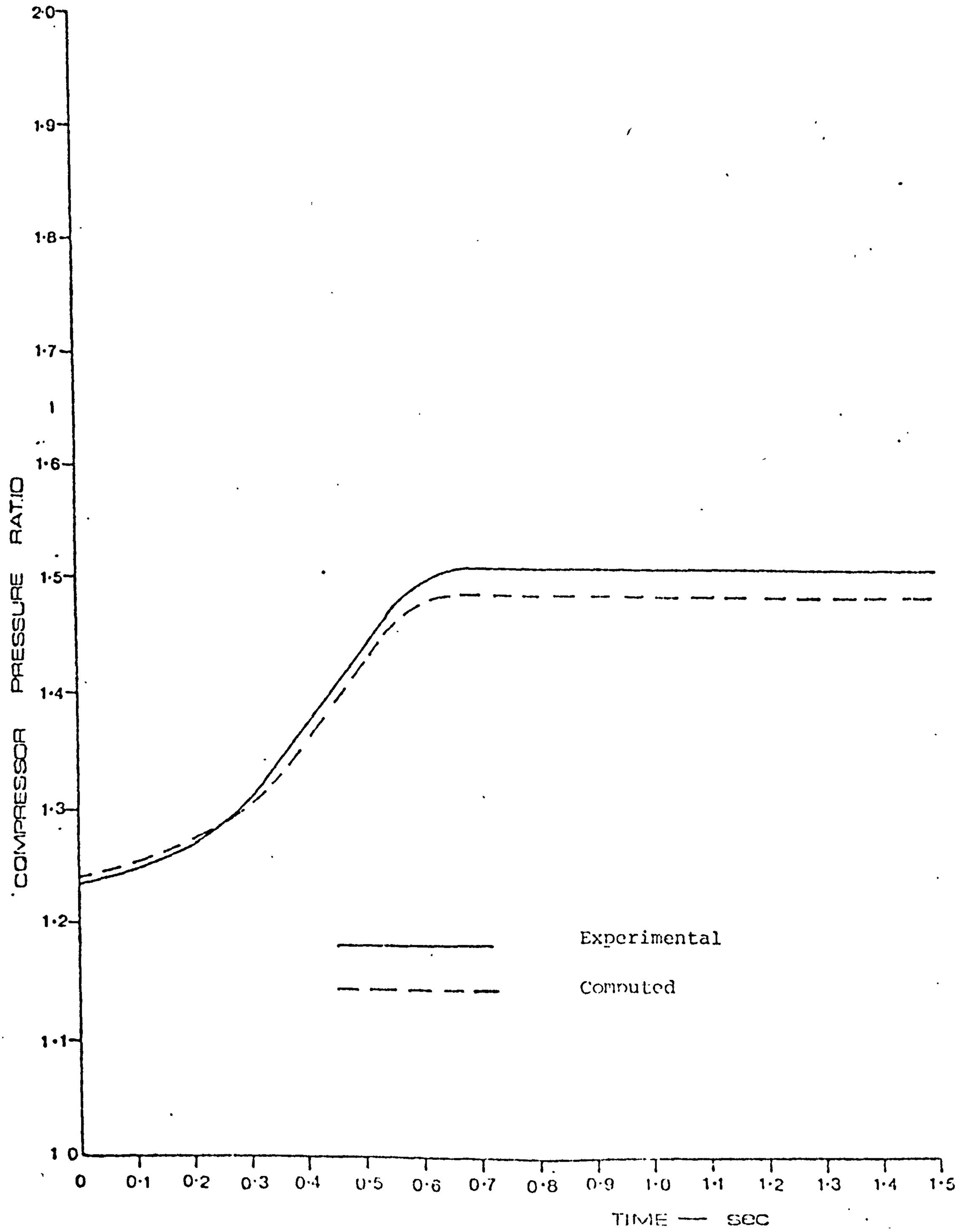

fig.(7.8). COMPRESSOR PRESSURE RATIO

DURING NON-PULSATING TRANSIENT

INITIAL SUPPLY PRESSURE = 1.669 bar

FINAL SUPPLY PRESSURE = 2.862 bar

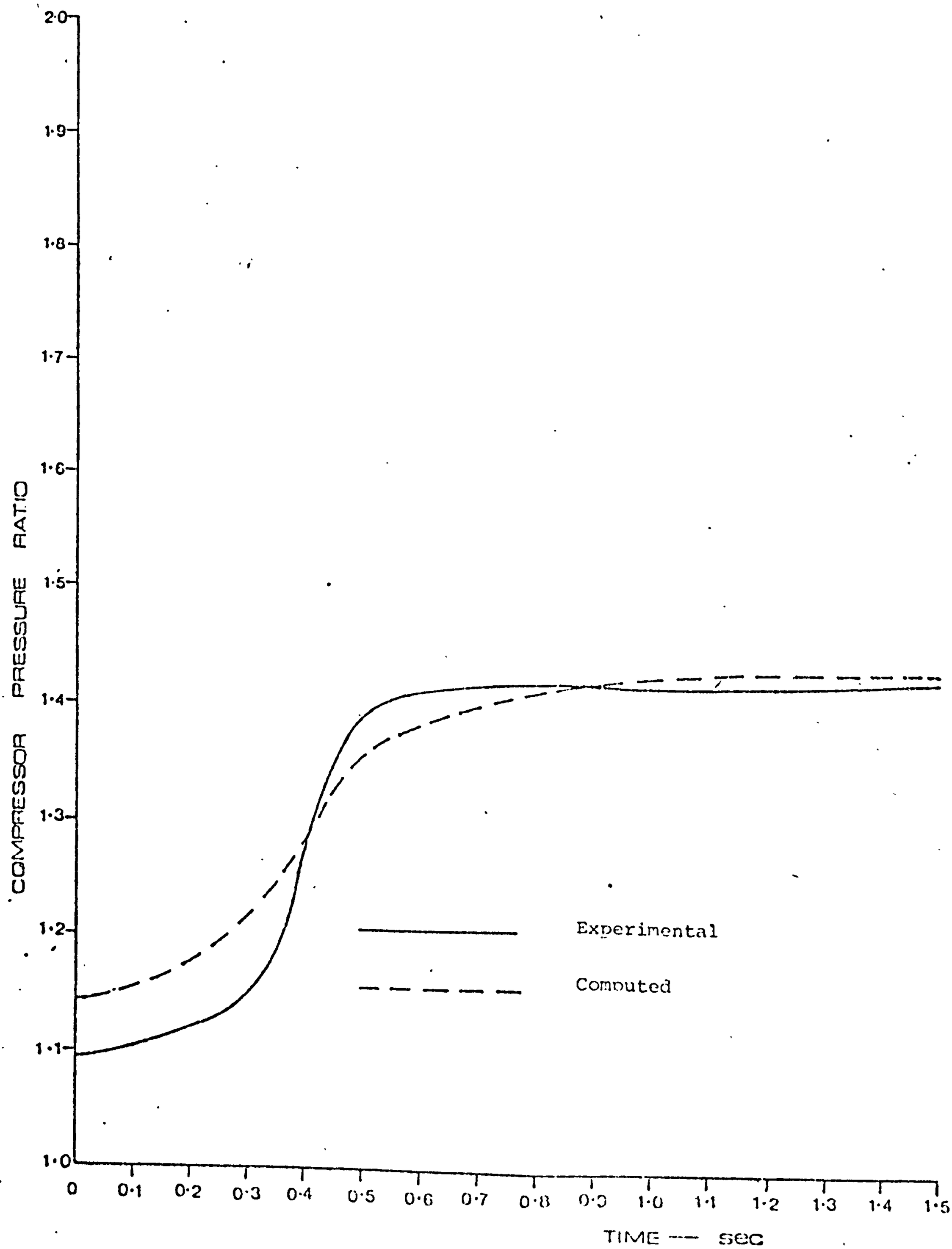

fig.(7.9). COMPRESSOR PRESSURE RATIO

DURING NON-PULSATING TRANSIENT

INITIAL SUPPLY PRESSURE = 1.352 bar

FINAL SUPPLY PRESSURE = 2.696 bar

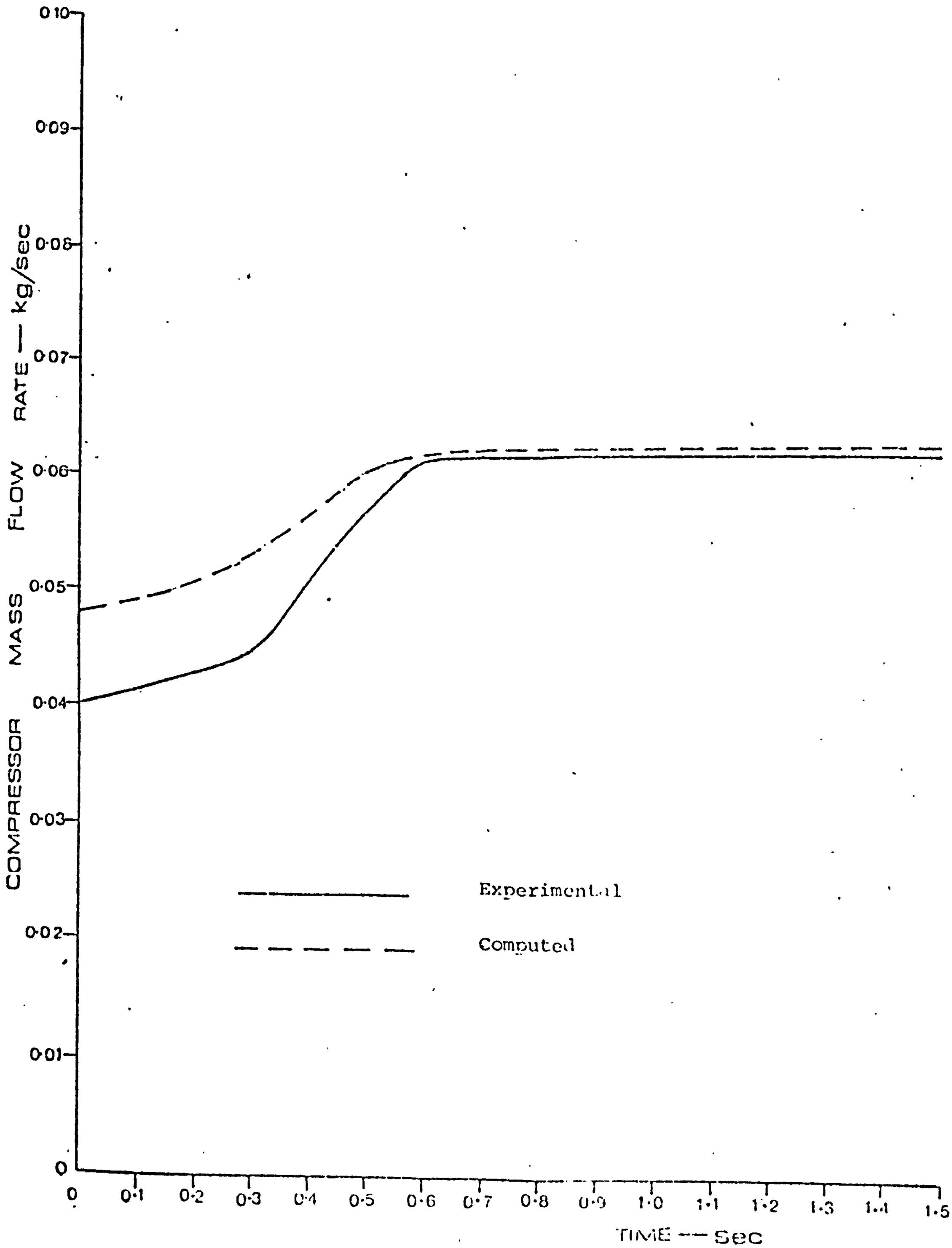

fig.(7.10) COMPRESSOR MASS FLOW RATE DURING NON-PULSATING TRANSIENT

INITIAL SUPPLY PRESSURE = 1.359 bar

FINAL SUPPLY PRESSURE = 1.889 bar

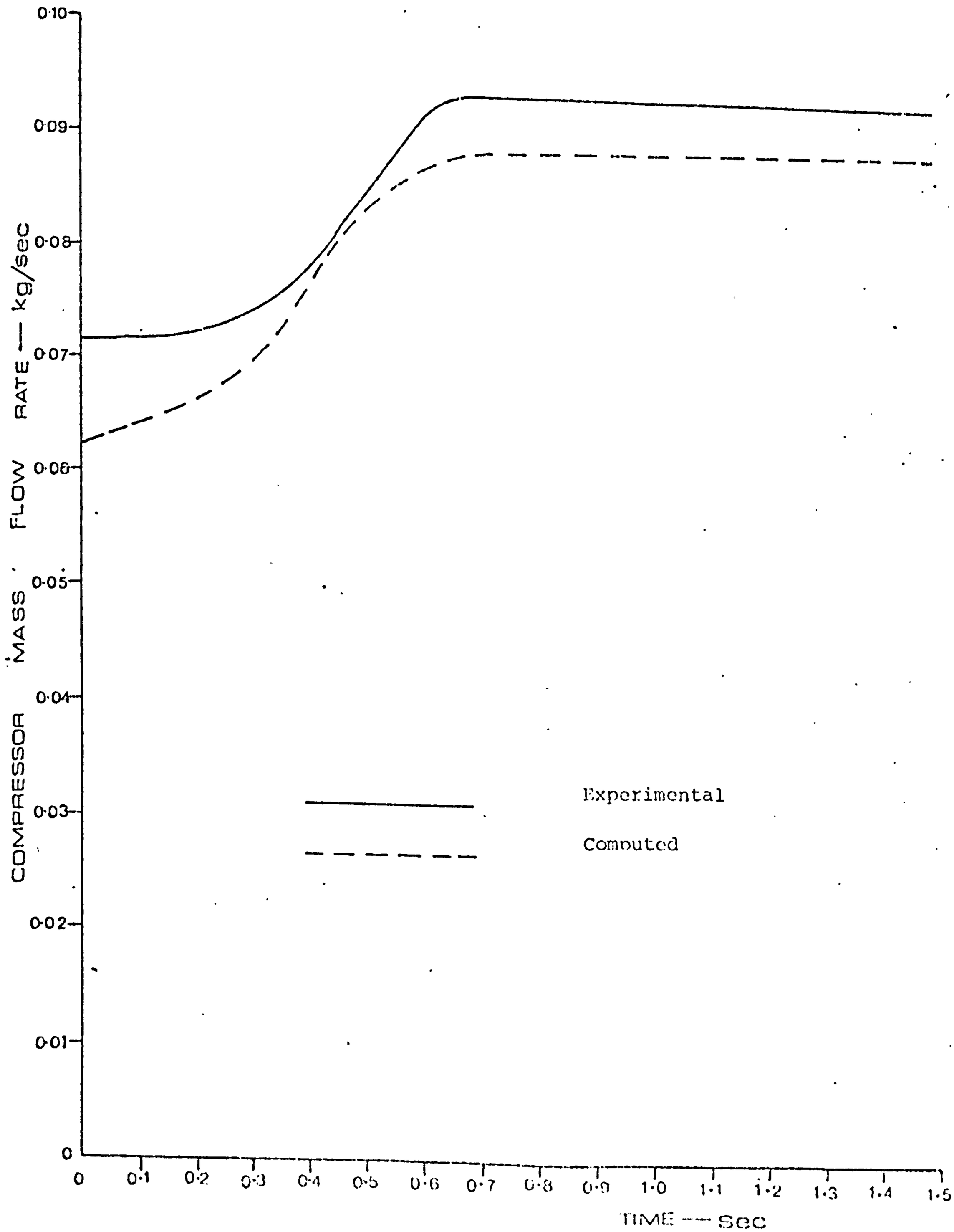

fig.(7.11) COMPRESSOR MASS FLOW RATE DURING NON-PULSATING TRANSIENT

INITIAL SUPPLY PRESSURE = 1.669 bar

FINAL SUPPLY PRESSURE = 2.862 bar

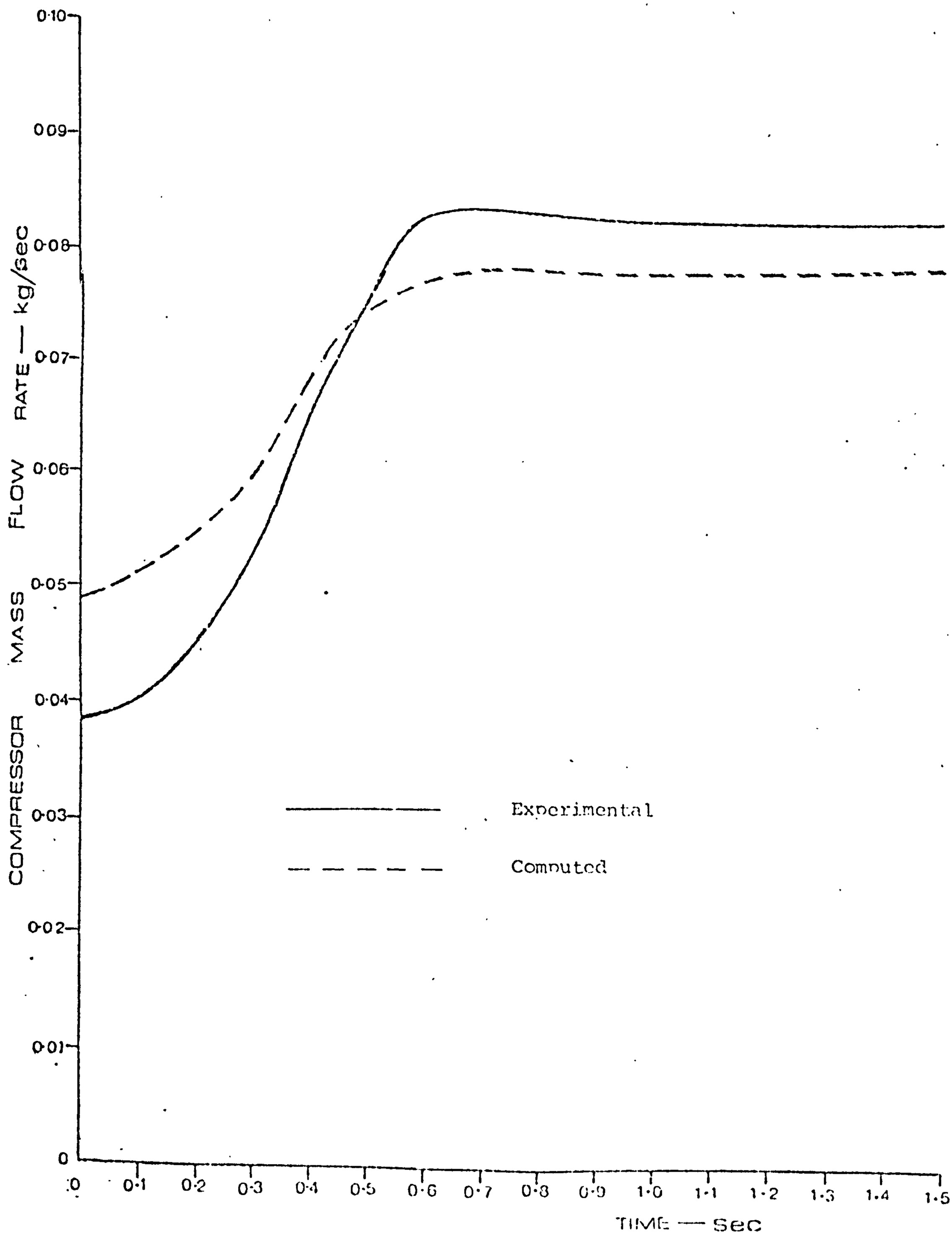

fig.(7.12) COMPRESSOR MASS FLOW RATE DURING NON-PULSATING TRANSIENT

INITIAL SUPPLY PRESSURE = 1.352 bar

FINAL SUPPLY PRESSURE = 2.696 bar

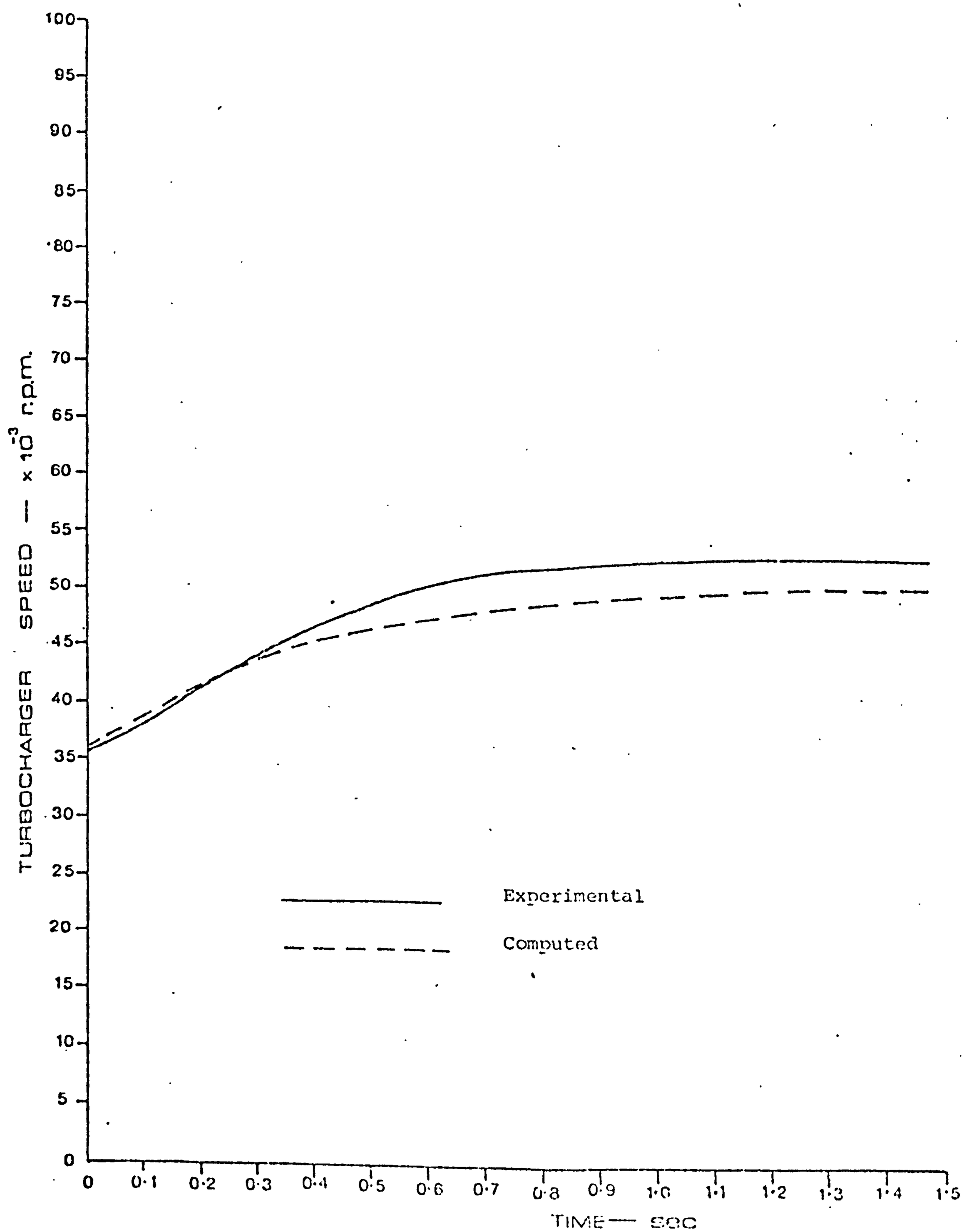

fig.(7.13) TURBOCHARGER SPEED DURING PULSATING TRANSIENT

INITIAL SUPPLY PRESSURE = 1.472 bar

FINAL SUPPLY PRESSURE = 1.699 bar

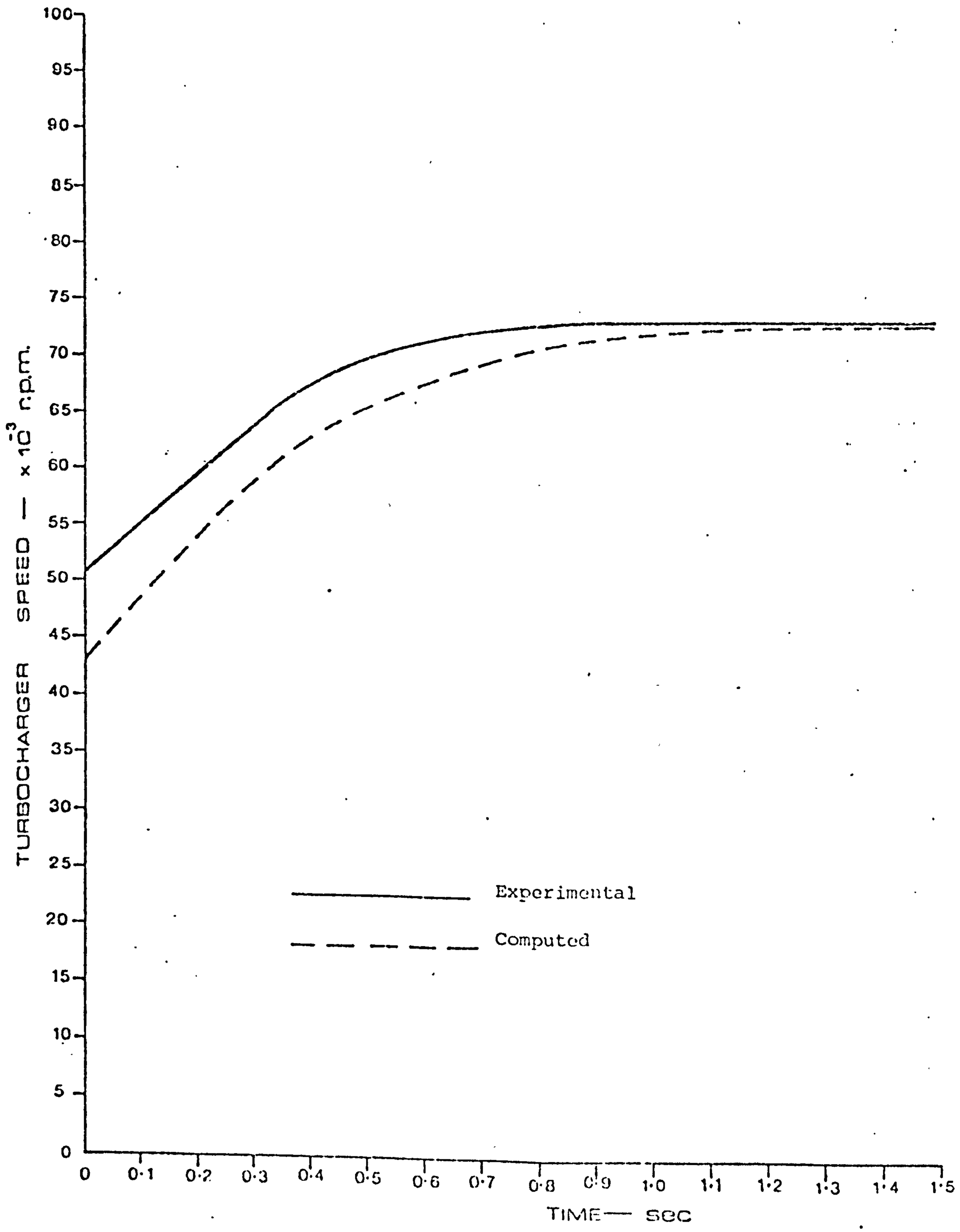

fig.(7.14) TURBOCHARGER SPEED DURING PULSATING TRANSIENT

INITIAL SUPPLY PRESSURE = 1.676 bar

FINAL SUPPLY PRESSURE = 2.575 bar

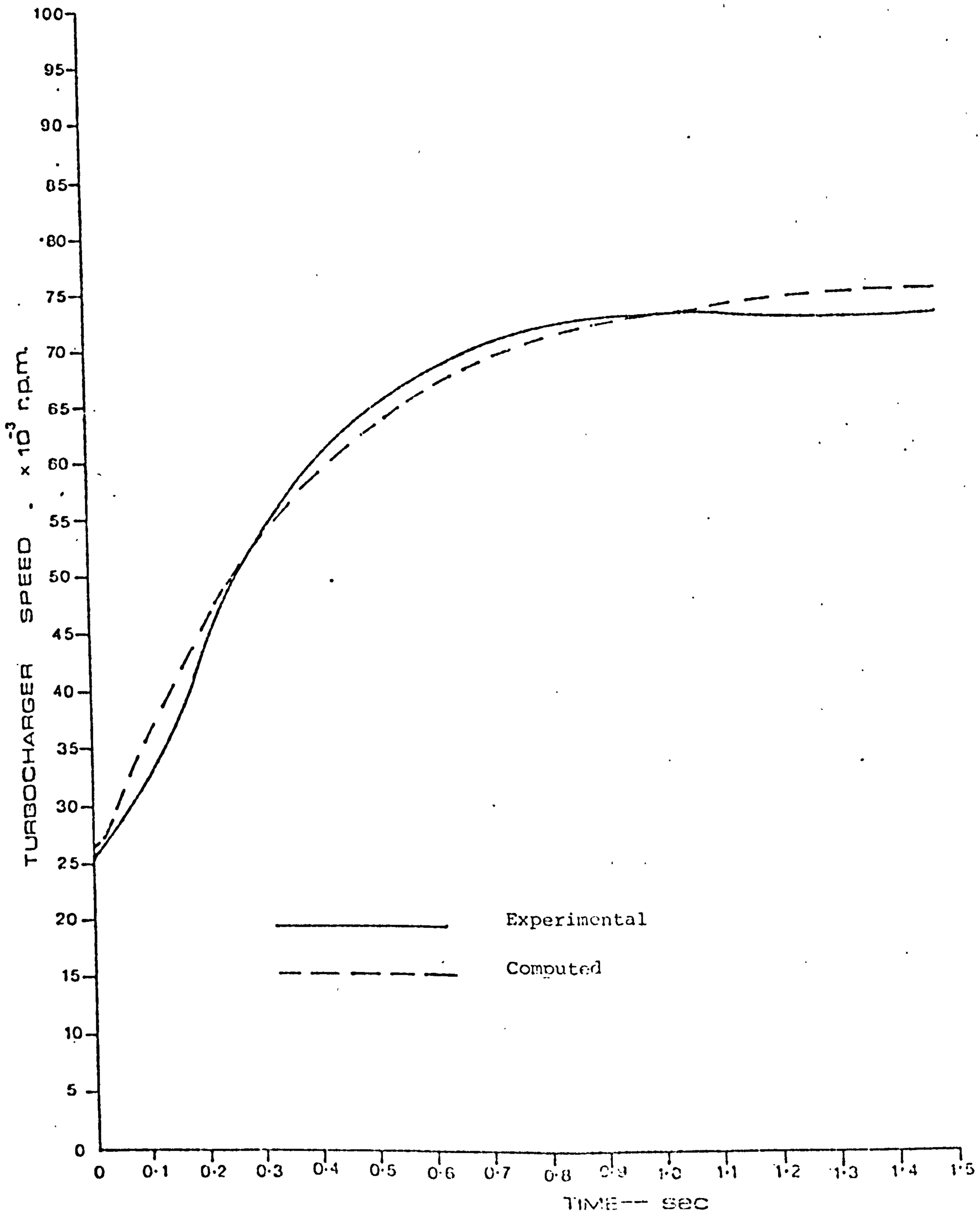

fig.(7.15) TURBOCHARGER SPEED DURING PULSATING TRANSIENT

INITIAL SUPPLY PRESSURE = 1.241 bar

FINAL SUPPLY PRESSURE = 2.689 bar

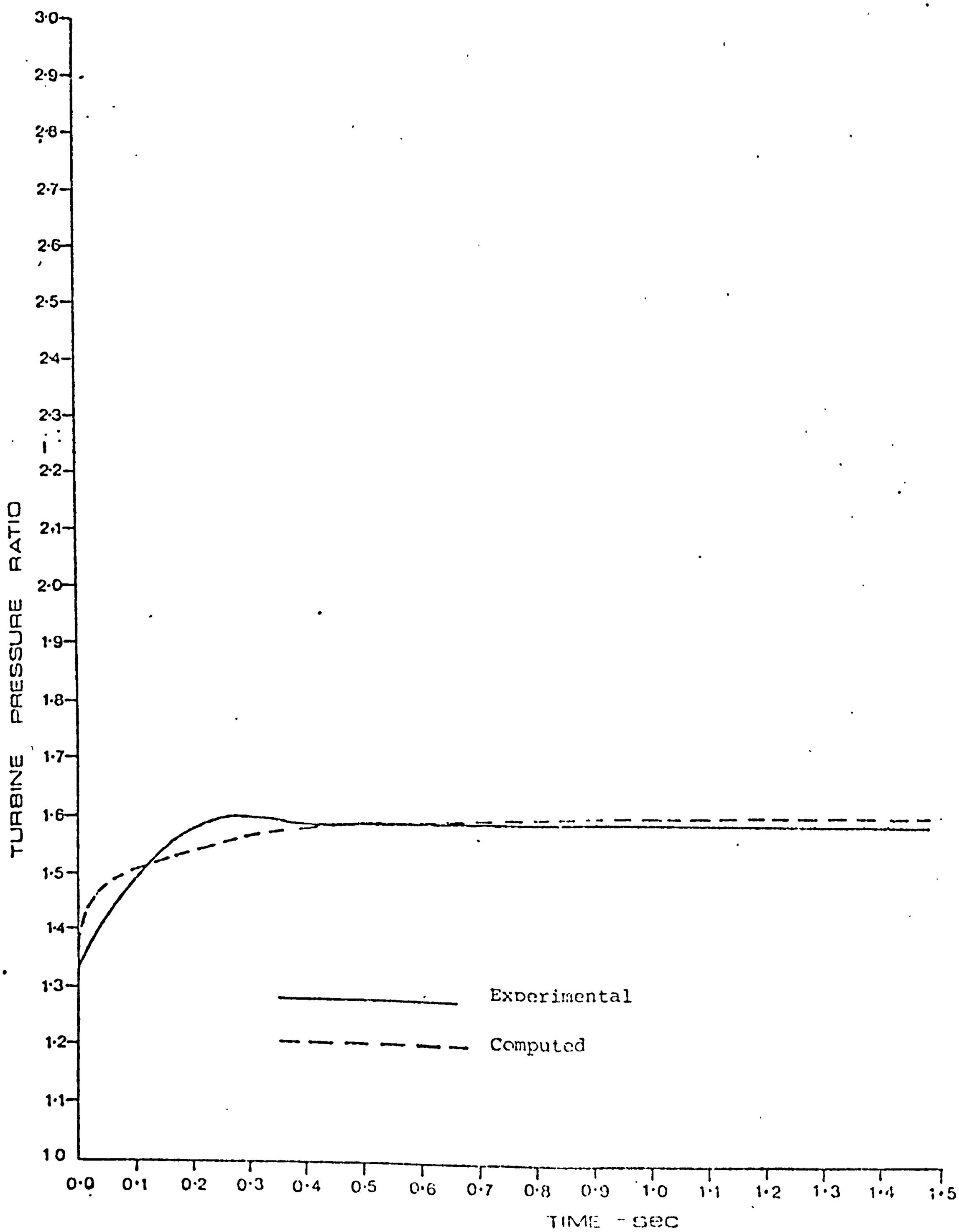

fig.(7.16) TURBINE PRESSURE RATIO DURING PULSATING TRANSIENT

INITIAL SUPPLY PRESSURE = 1.472 bar

FINAL SUPPLY PRESSURE = 1.699 bar

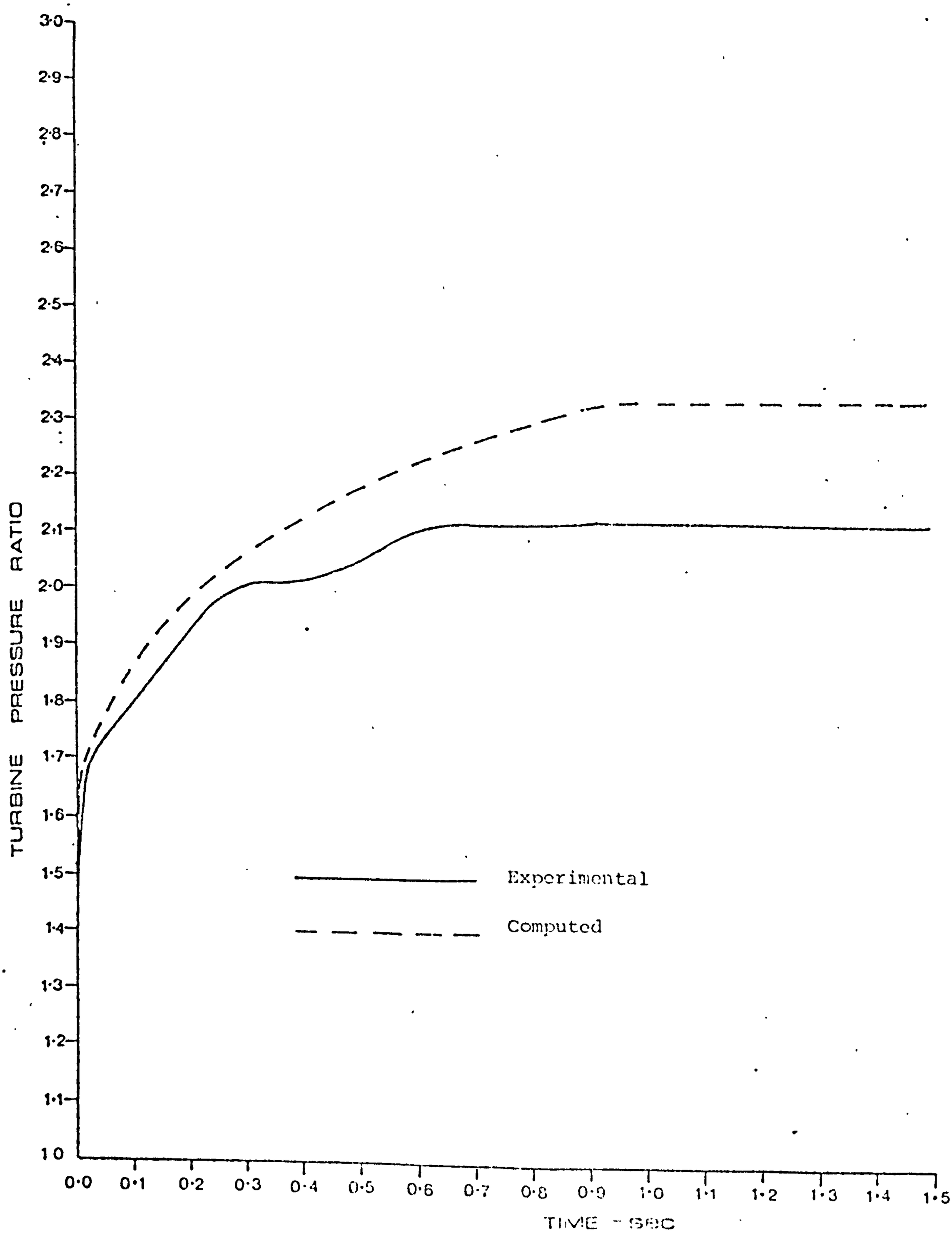

fig.(7.17) TURBINE PRESSURE RATIO DURING PULSATING TRANSIENT

INITIAL SUPPLY PRESSURE = 1.676 bar

FINAL SUPPLY PRESSURE = 2.575 bar

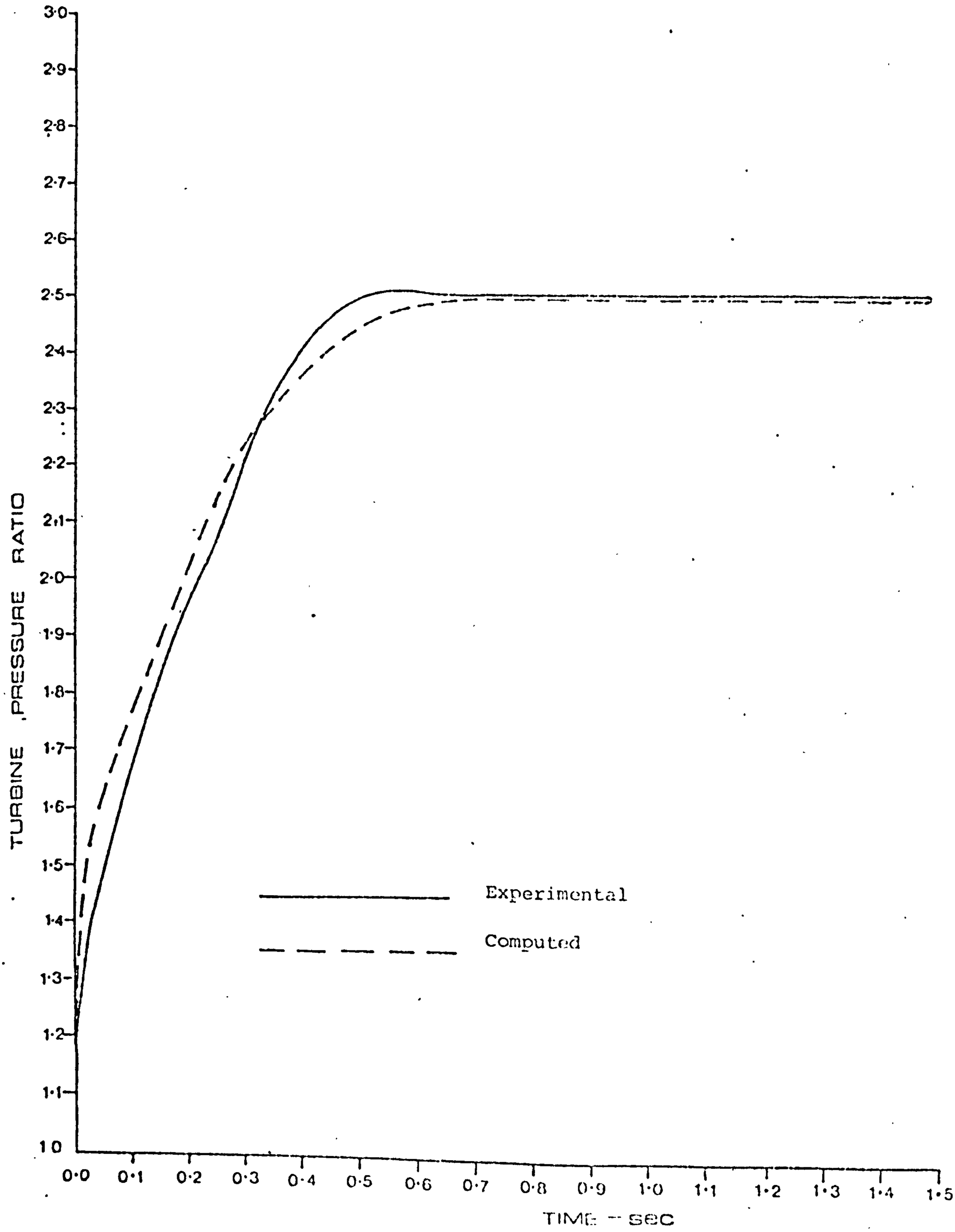

fig.(7.18) TURBINE PRESSURE RATIO DURING PULSATING TRANSIENT

INITIAL SUPPLY PRESSURE = 1.241 bar

FINAL SUPPLY PRESSURE = 2.689 bar

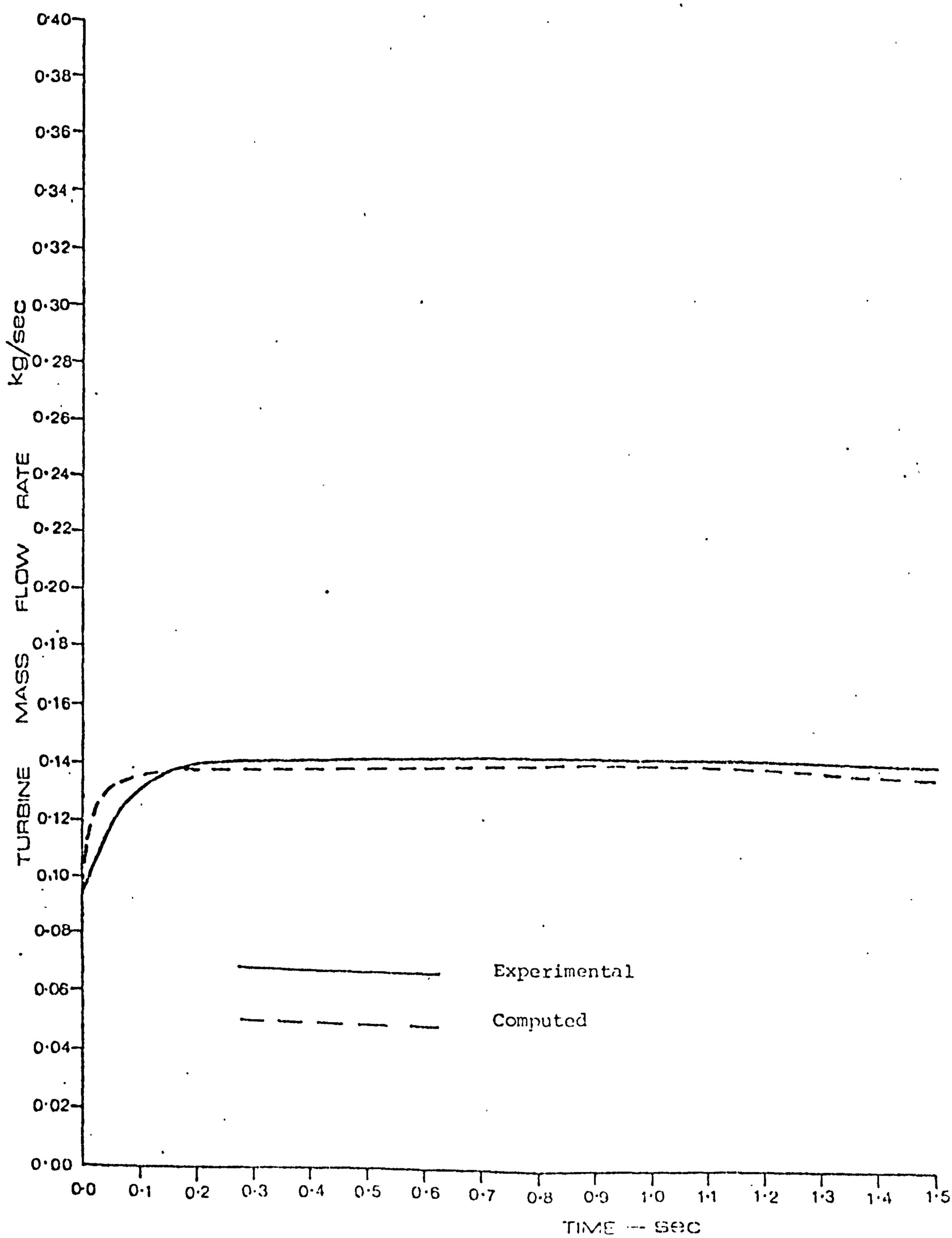

fig.(7.19) TURBINE MASS FLOW RATE DURING PULSATING TRANSIENT

INITIAL SUPPLY PRESSURE == 1.472 bar

FINAL SUPPLY PRESSURE == 1.699 bar

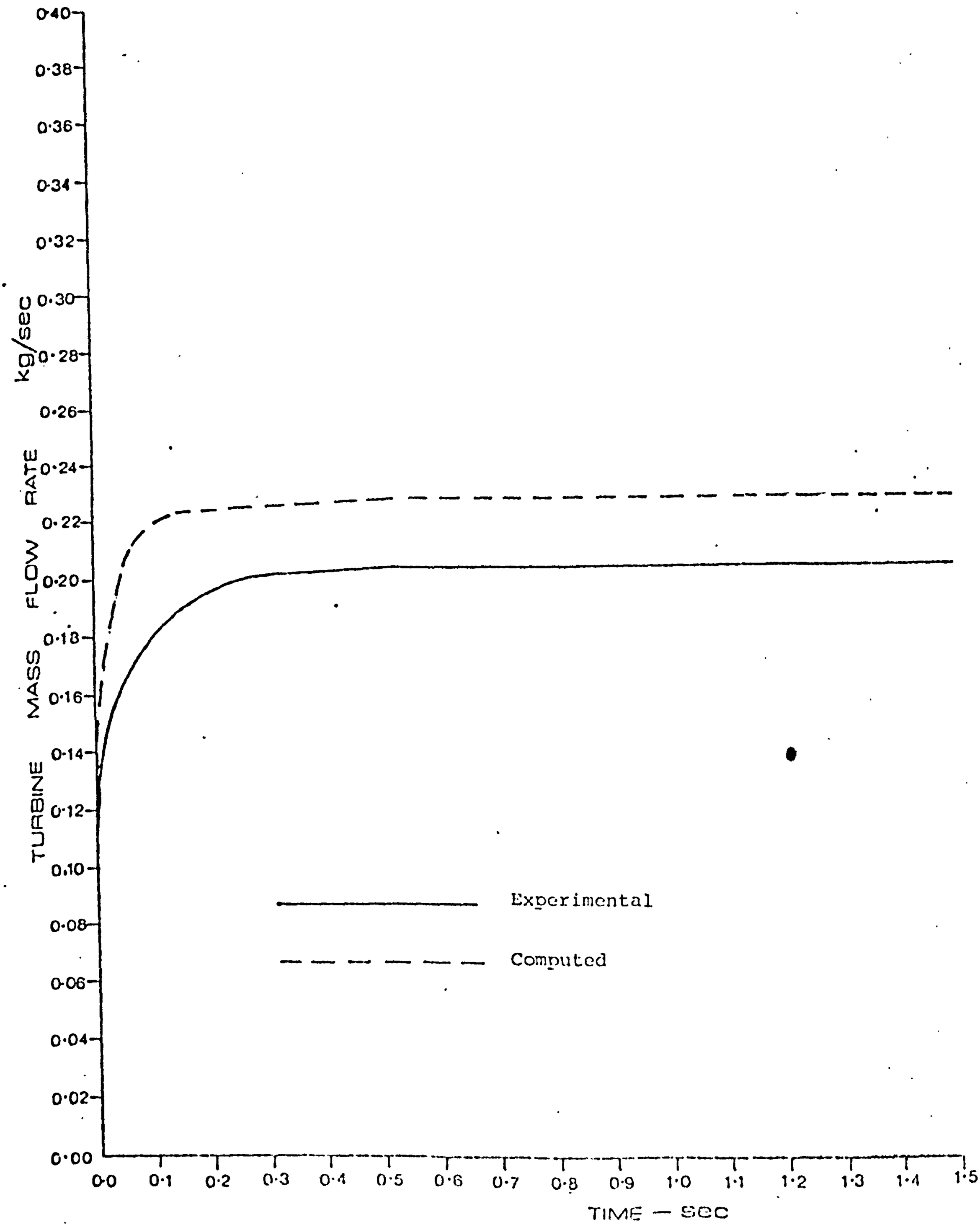

fig.(7.20) TURBINE MASS FLOW RATE DURING PULSATING TRANSIENT

INITIAL SUPPLY PRESSURE == 1.676 bar

FINAL SUPPLY PRESSURE == 2.575 bar

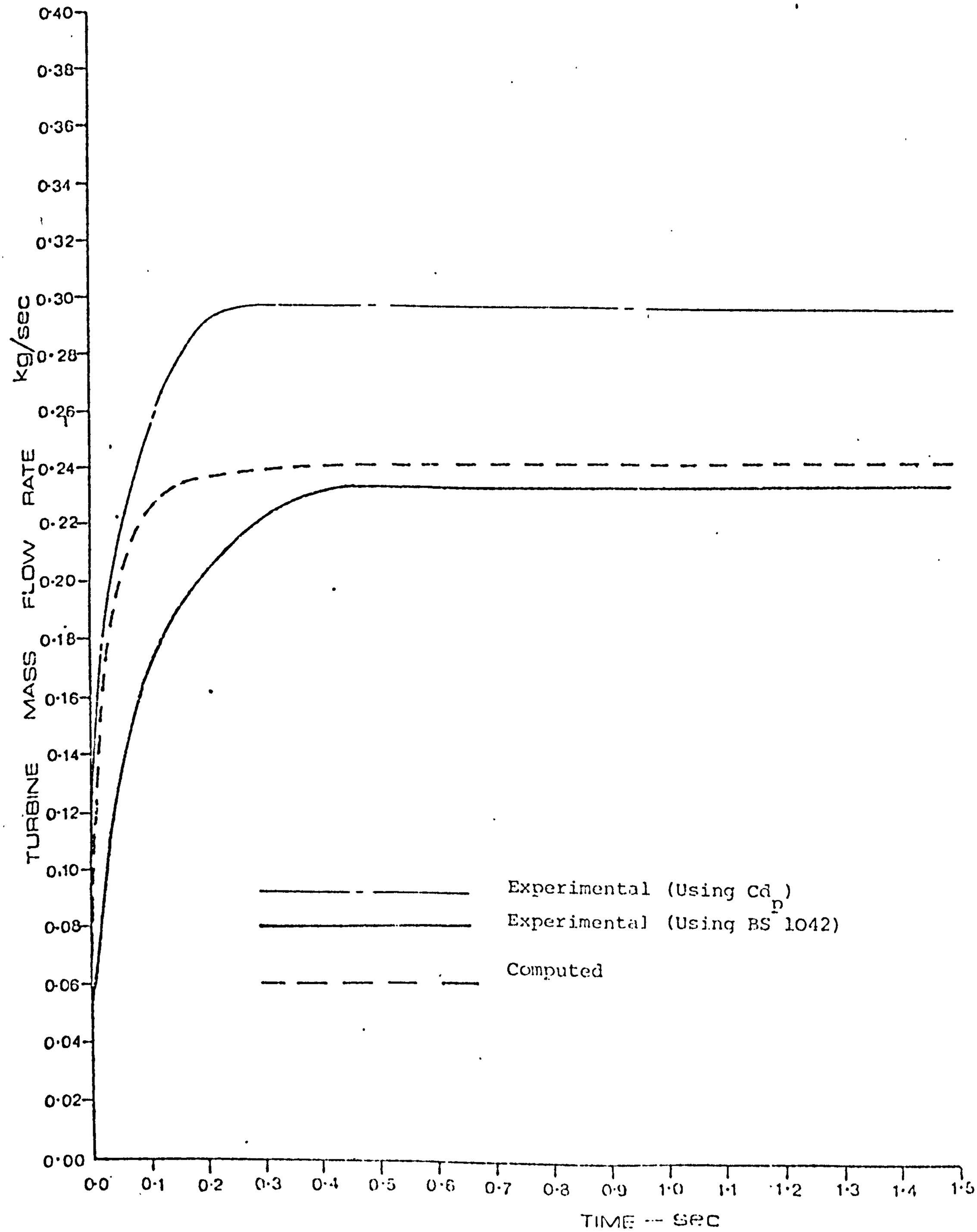

fig.(7.21). TURBINE MASS FLOW RATE DURING PULSATING TRANSIENT

INITIAL SUPPLY PRESSURE = 1.241 bar

FINAL SUPPLY PRESSURE = 2.689 bar

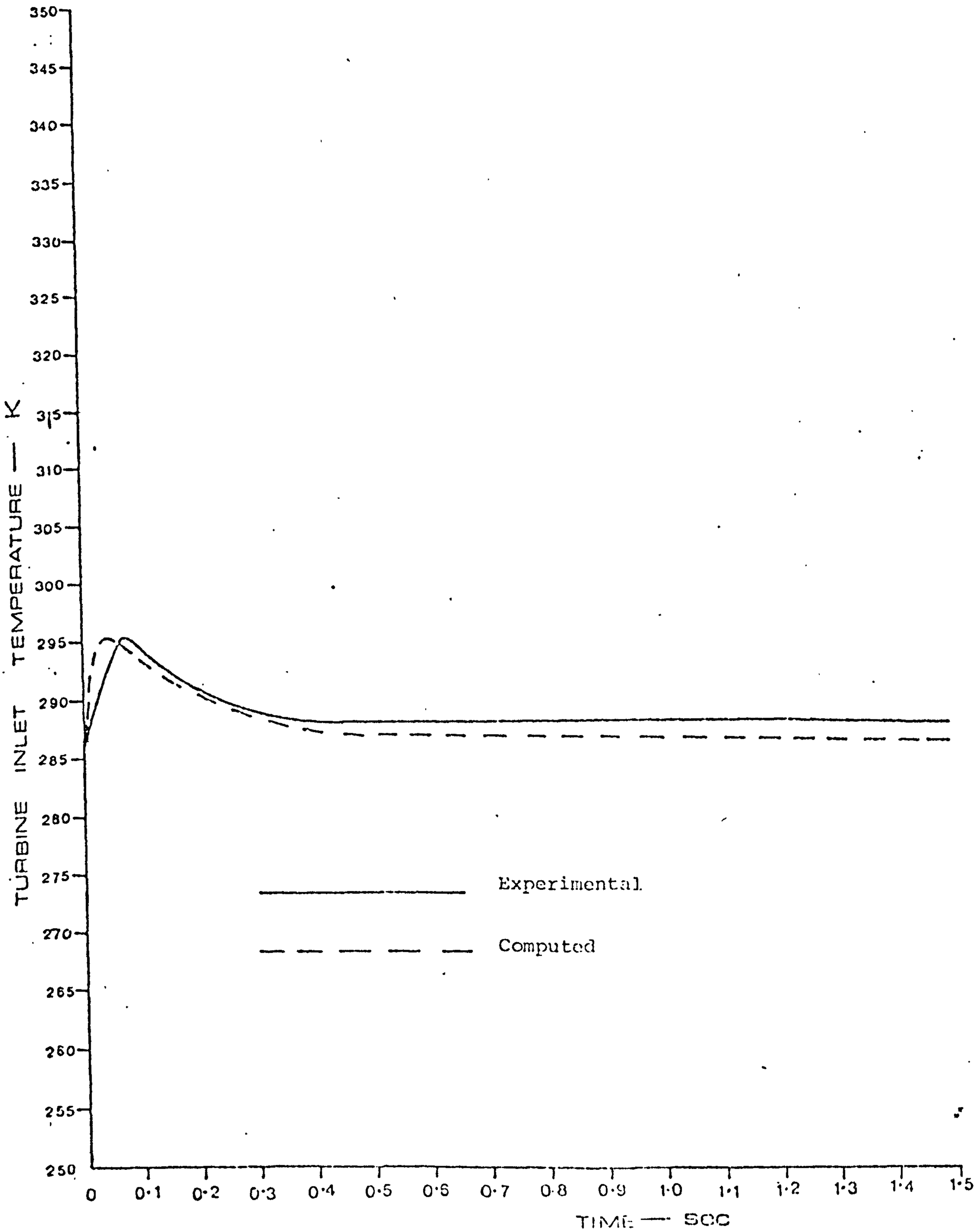

fig.(7.22) TURBINE INLET TEMPERATURE DURING PULSATING TRANSIENT

INITIAL SUPPLY PRESSURE = 1.472 bar

FINAL SUPPLY PRESSURE = 1.699 bar

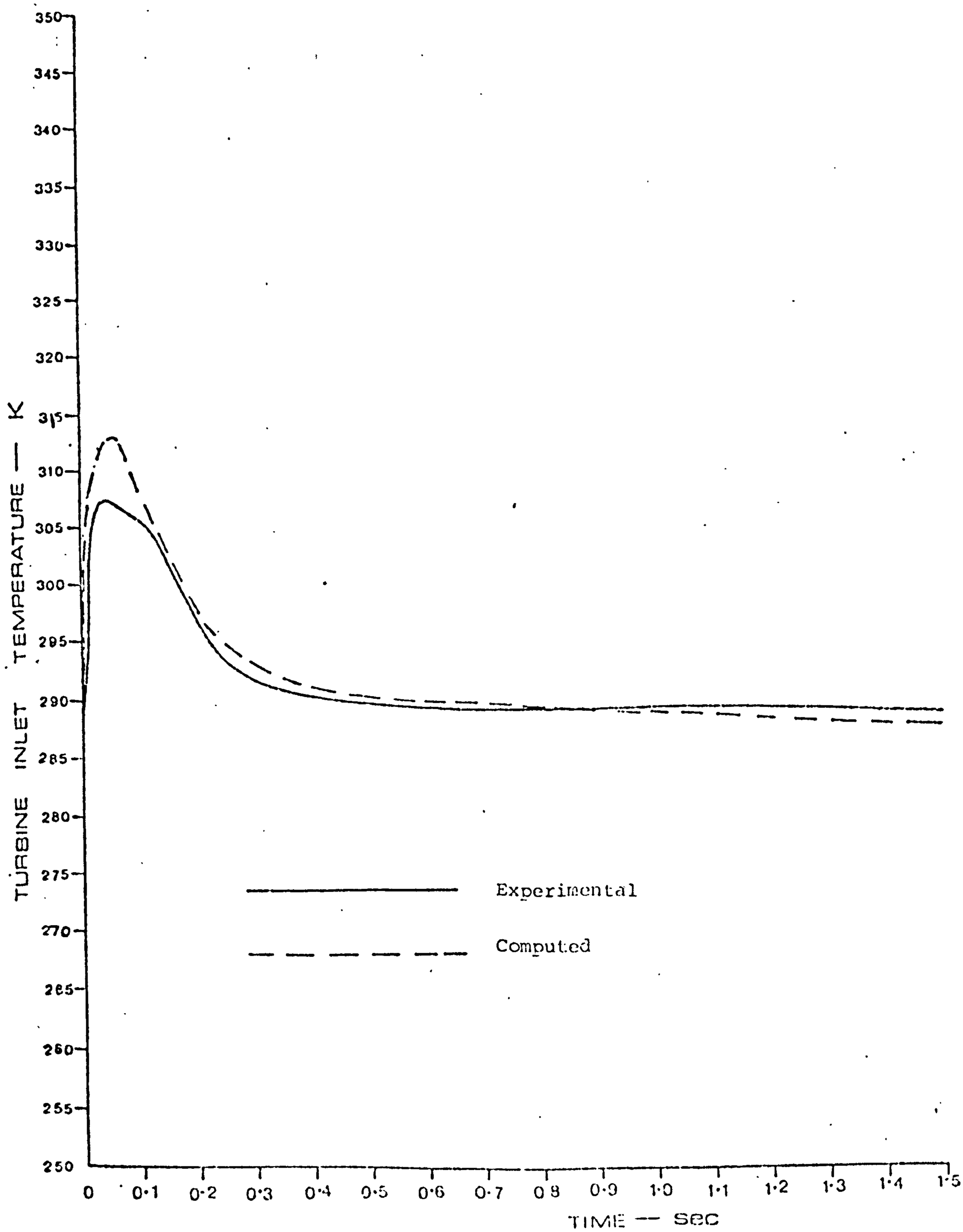

fig.(7.23) TURBINE INLET TEMPERATURE DURING PULSATING TRANSIENT

INITIAL SUPPLY PRESSURE = 1.676 bar

FINAL SUPPLY PRESSURE = 2.575 bar

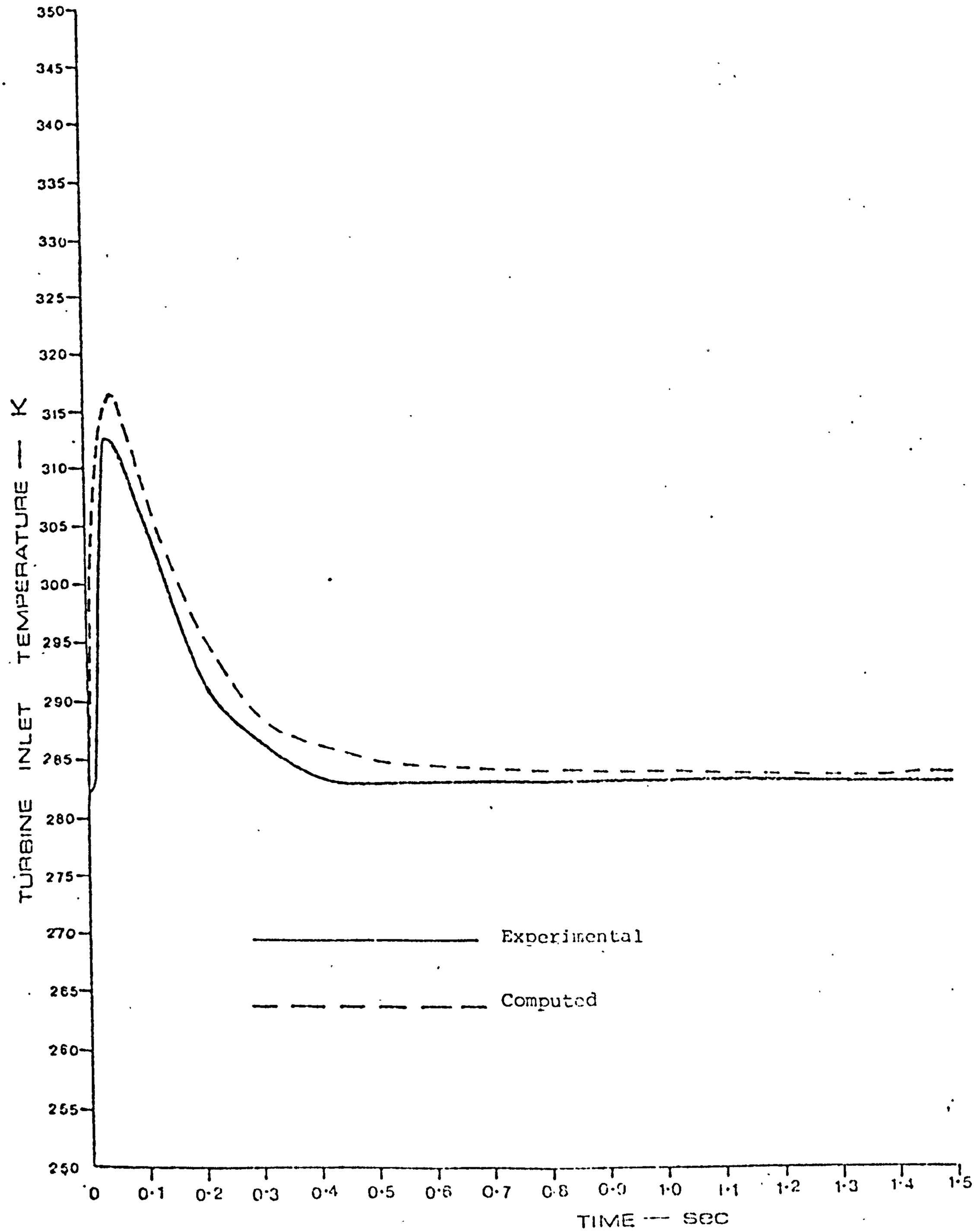

fig.(7.24) TURBINE INLET TEMPERATURE DURING PULSATING TRANSIENT

INITIAL SUPPLY PRESSURE = 1.241 bar

FINAL SUPPLY PRESSURE = 2.689 bar

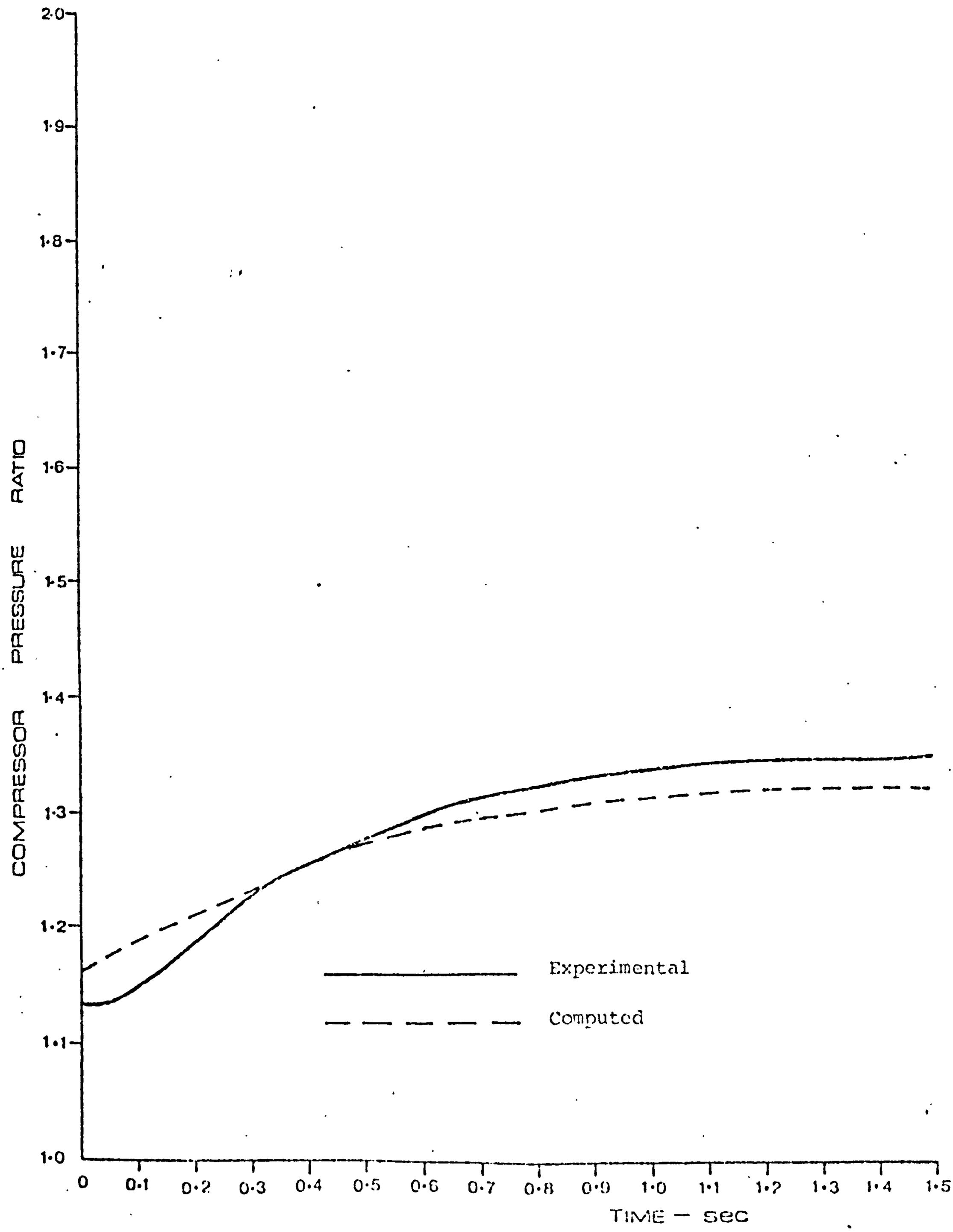

fig.(7.25) COMPRESSOR PRESSURE RATIO DURING PULSATING TRANSIENT

INITIAL SUPPLY PRESSURE = 1.472 bar

FINAL SUPPLY PRESSURE = 1.699 bar

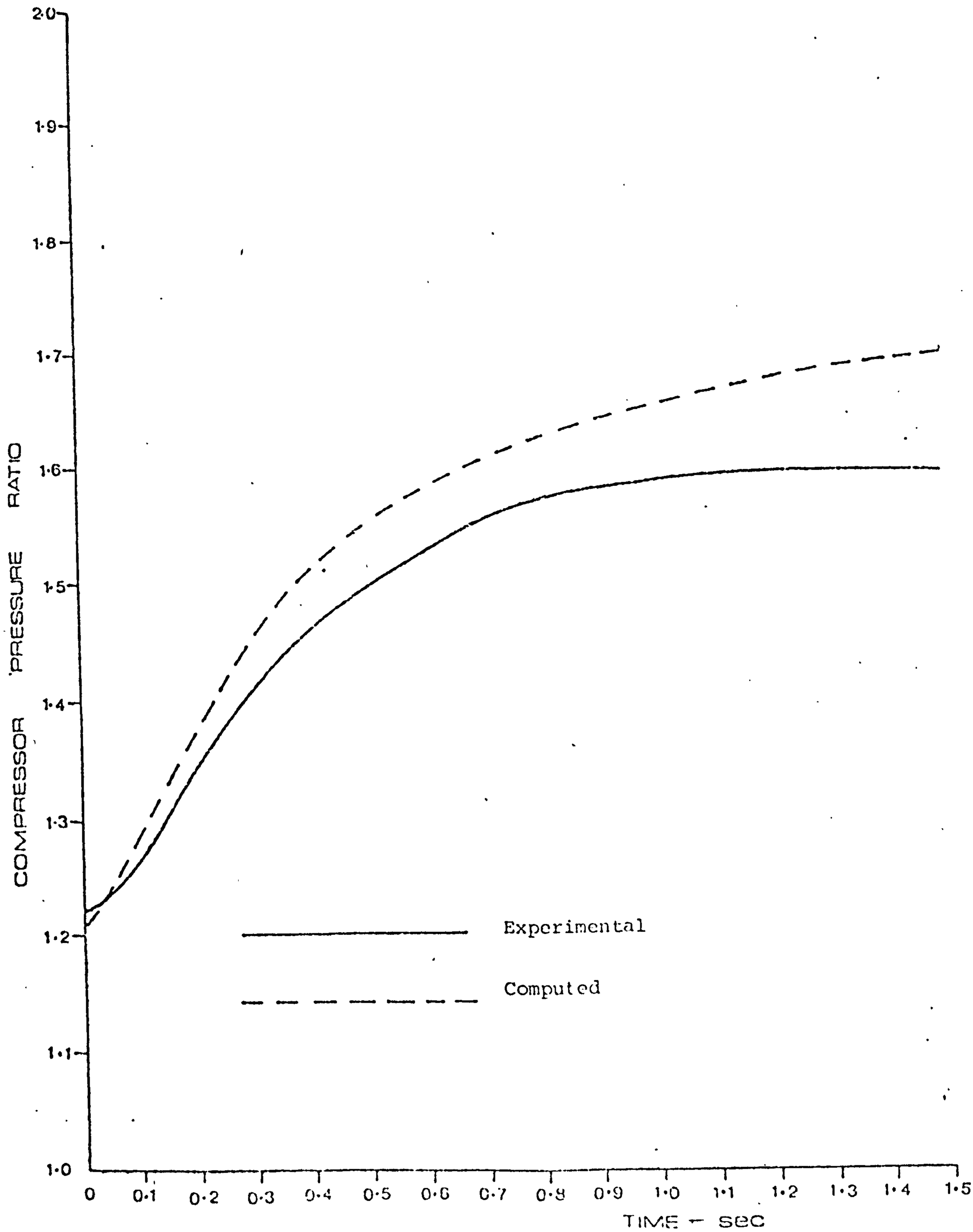

fig.(7.26) COMPRESSOR PRESSURE RATIO DURING PULSATING TRANSIENT

INITIAL SUPPLY PRESSURE = 1.676 bar

FINAL SUPPLY PRESSURE = 2.575 bar

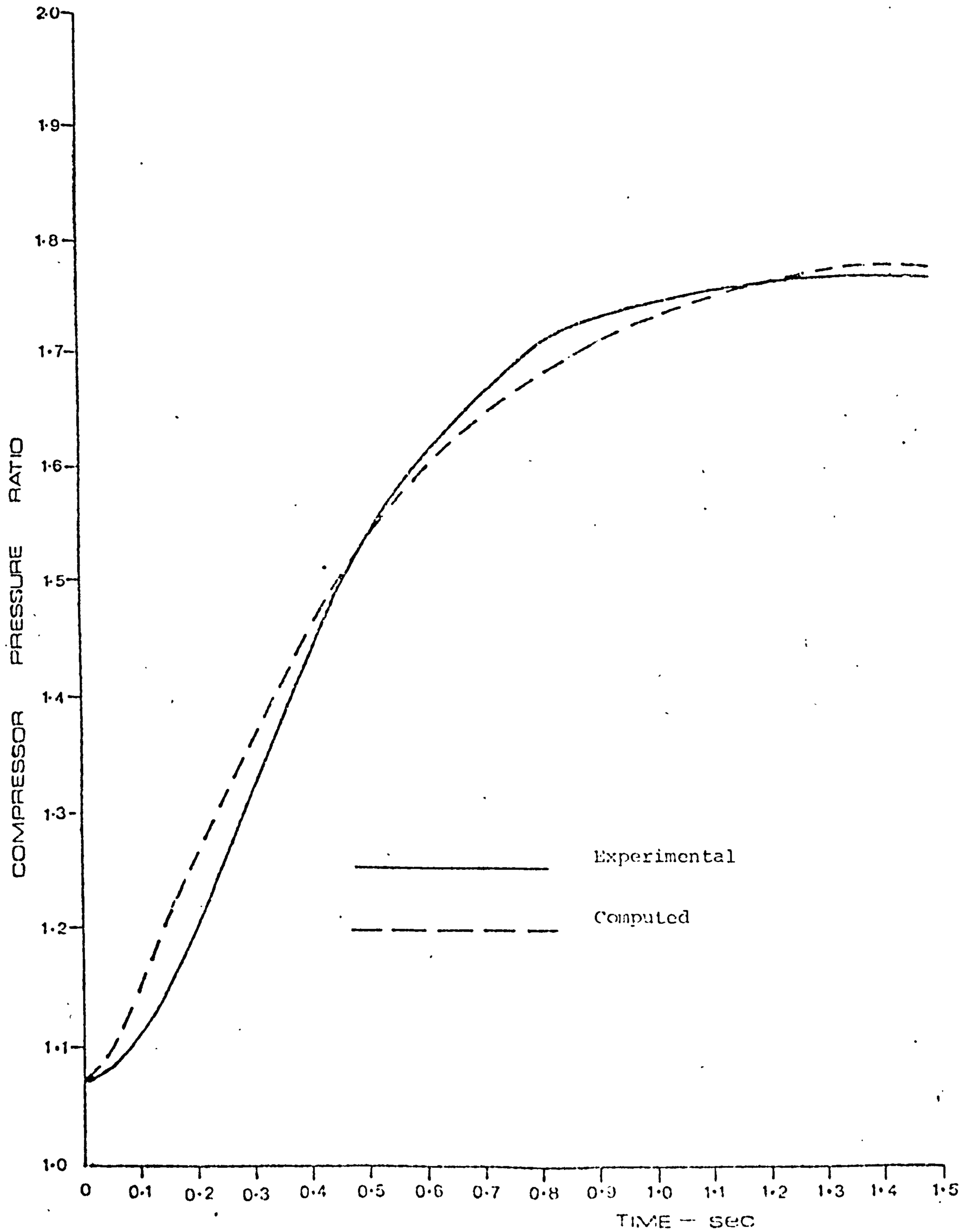

fig.(7.27) COMPRESSOR PRESSURE RATIO CURVE

PULSATING TRANSIENT

INITIAL SUPPLY PRESSURE = 1.241 bar

FINAL SUPPLY PRESSURE = 2.689 bar

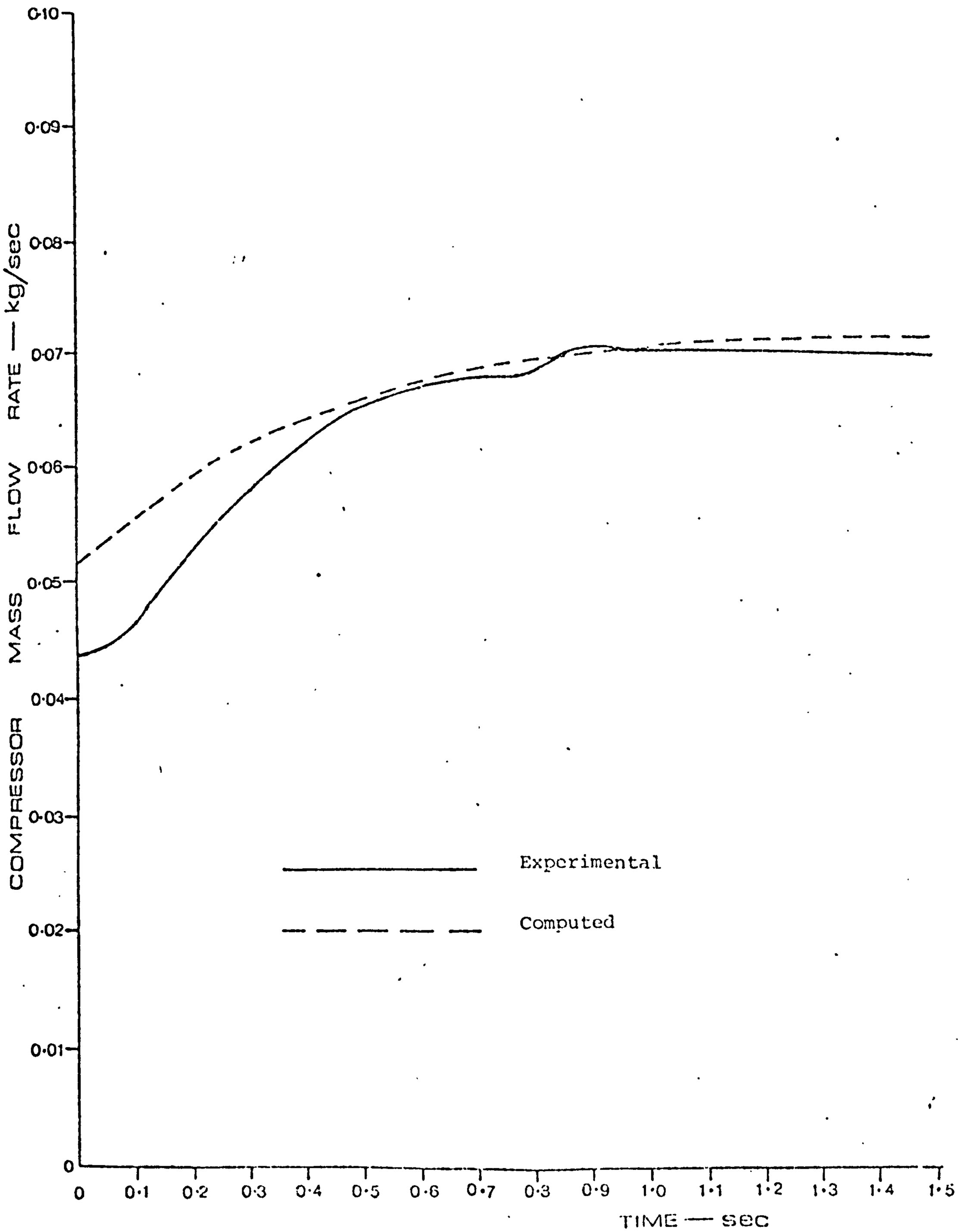

fig.(7.28) COMPRESSOR MASS FLOW RATE DURING PULSATING TRANSIENT

INITIAL SUPPLY PRESSURE == 1.472 bar

FINAL SUPPLY PRESSURE == 1.699 bar

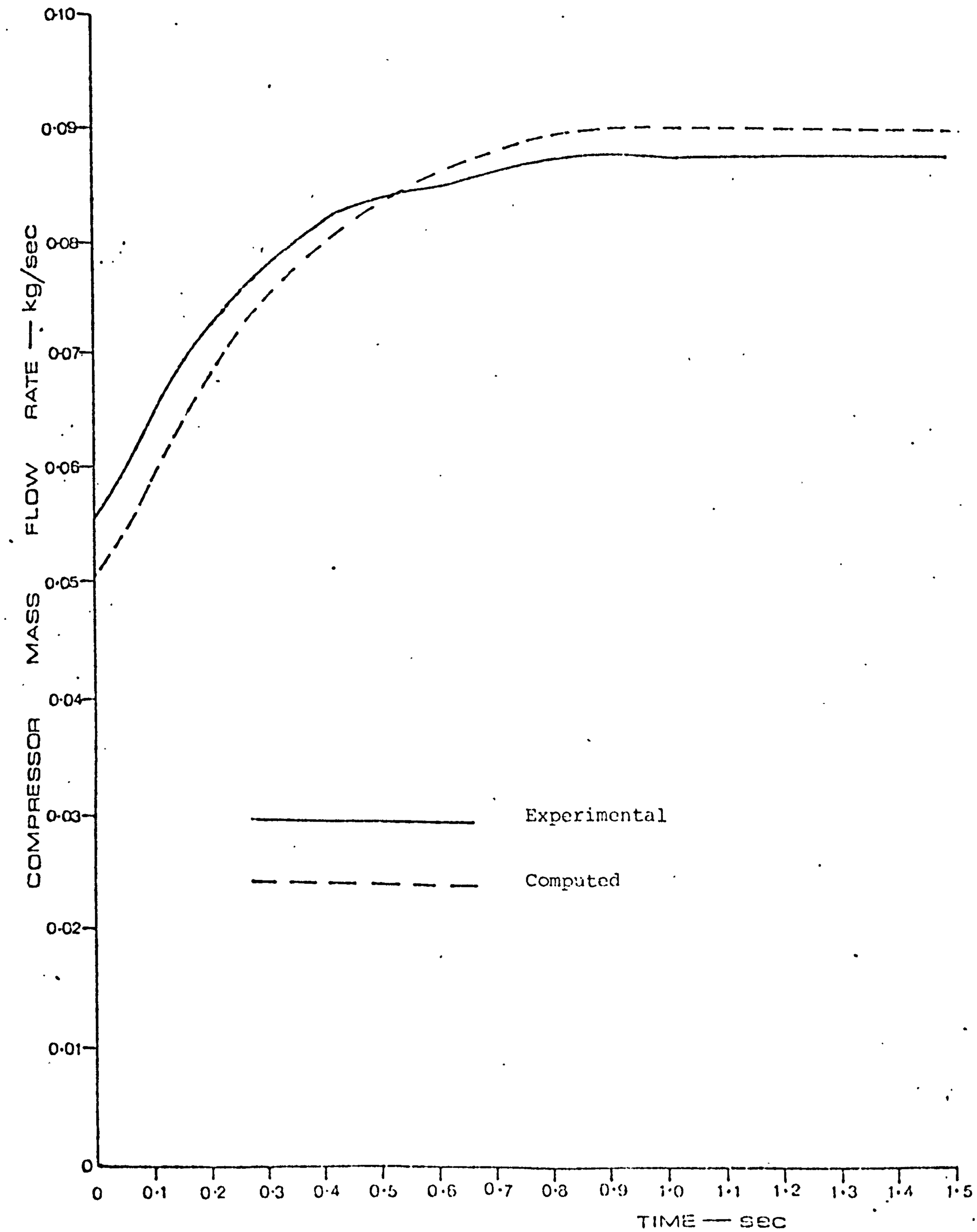

fig.(7.29) COMPRESSOR MASS FLOW RATE DURING PULSATING TRANSIENT

INITIAL SUPPLY PRESSURE = 1.676 bar

FINAL SUPPLY PRESSURE = 2.575 bar

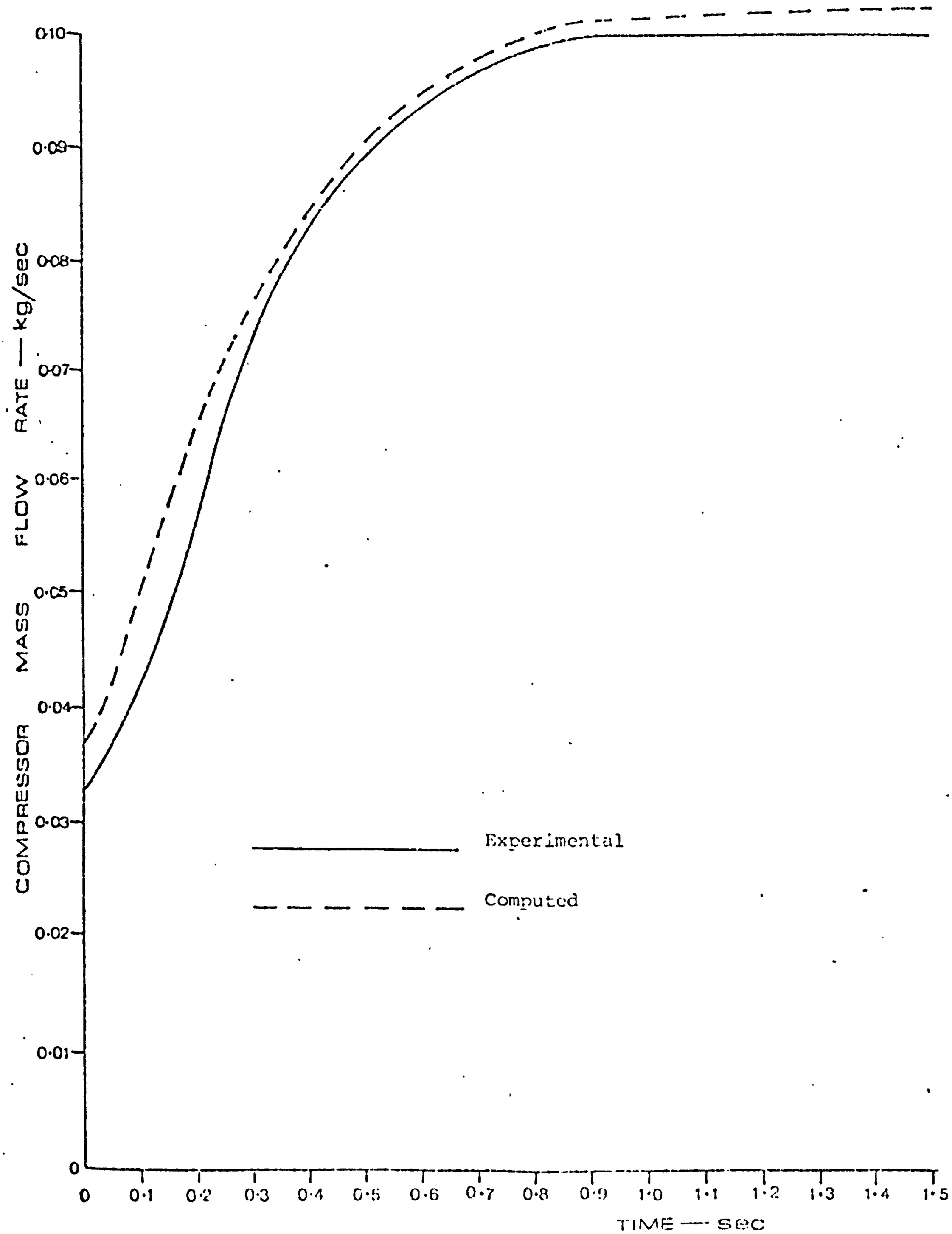

fig.(7.30) COMPRESSOR MASS FLOW RATE DURING PULSATING TRANSIENT

INITIAL SUPPLY PRESSURE = 1.241 bar

FINAL SUPPLY PRESSURE = 2.689 bar

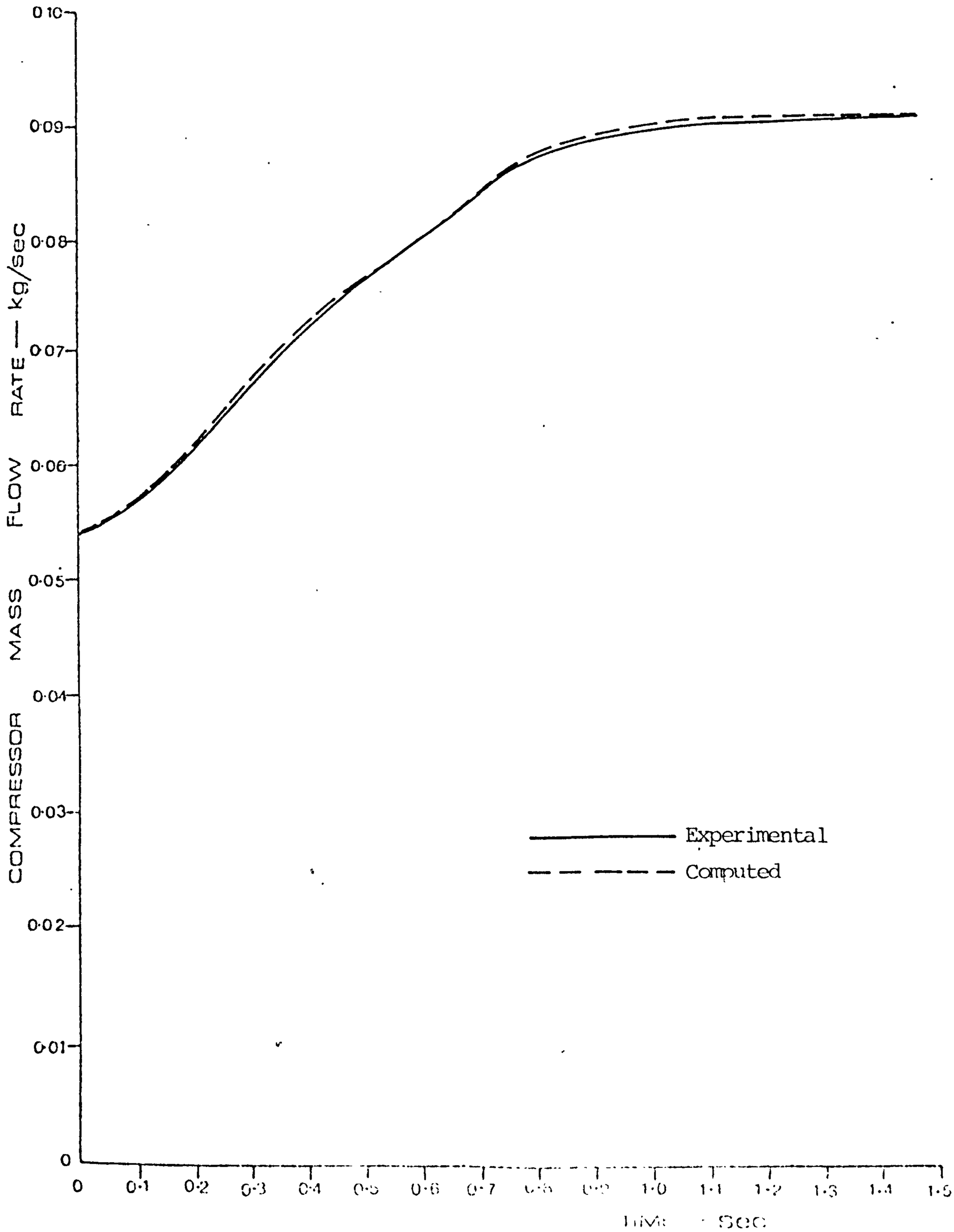

fig.(7.31). COMPRESSOR MASS FLOW RATE DURING NON-PULSATING TRANSIENT

INITIAL SUPPLY PRESSURE = 1.4 bar

FINAL SUPPLY PRESSURE = 2.021 bar

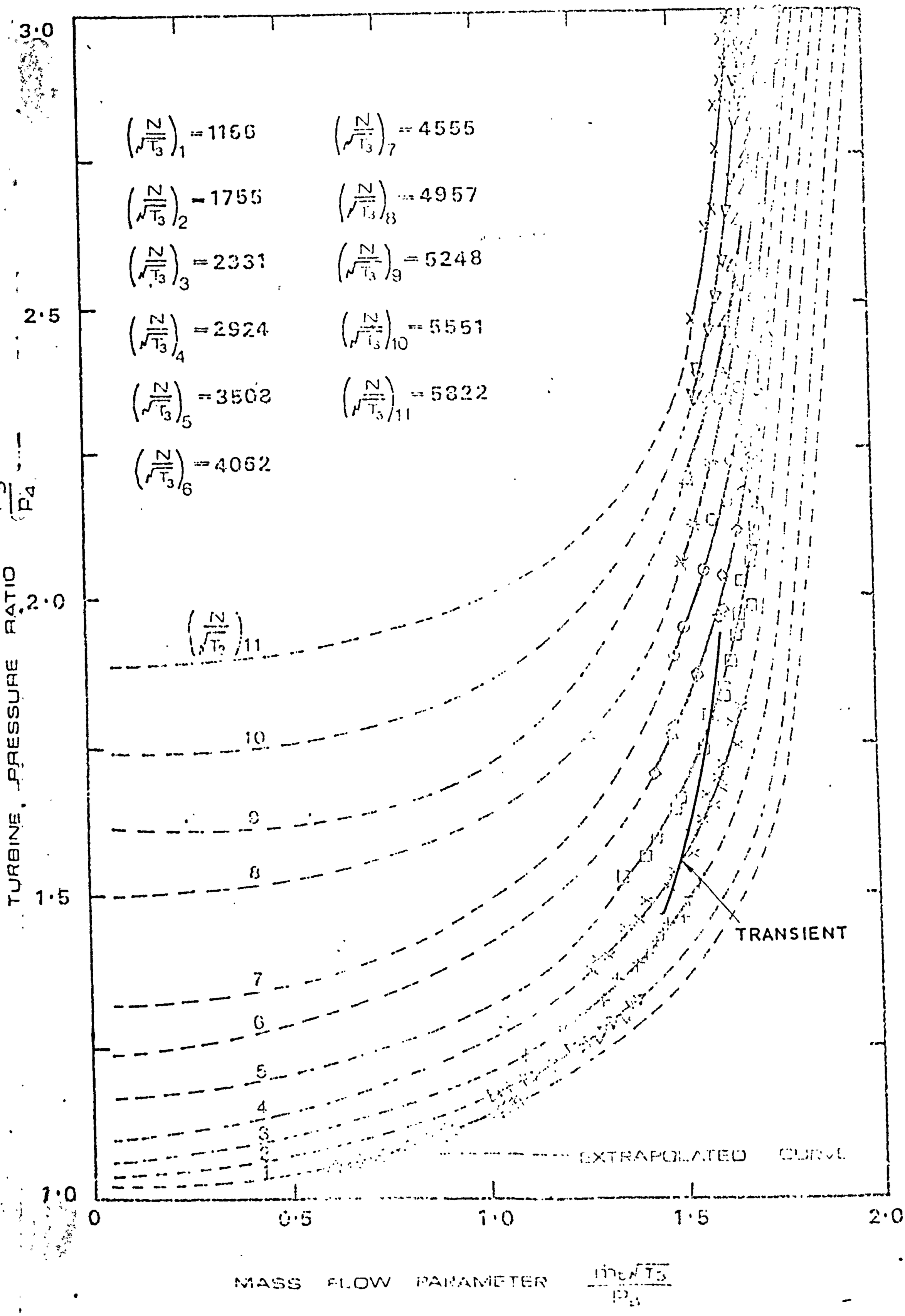

Fig. (7.31A) Superimposition of the transient shown in figs. (7.31), (7.34) (7.37) and (7.40) on turbine mass characteristics.

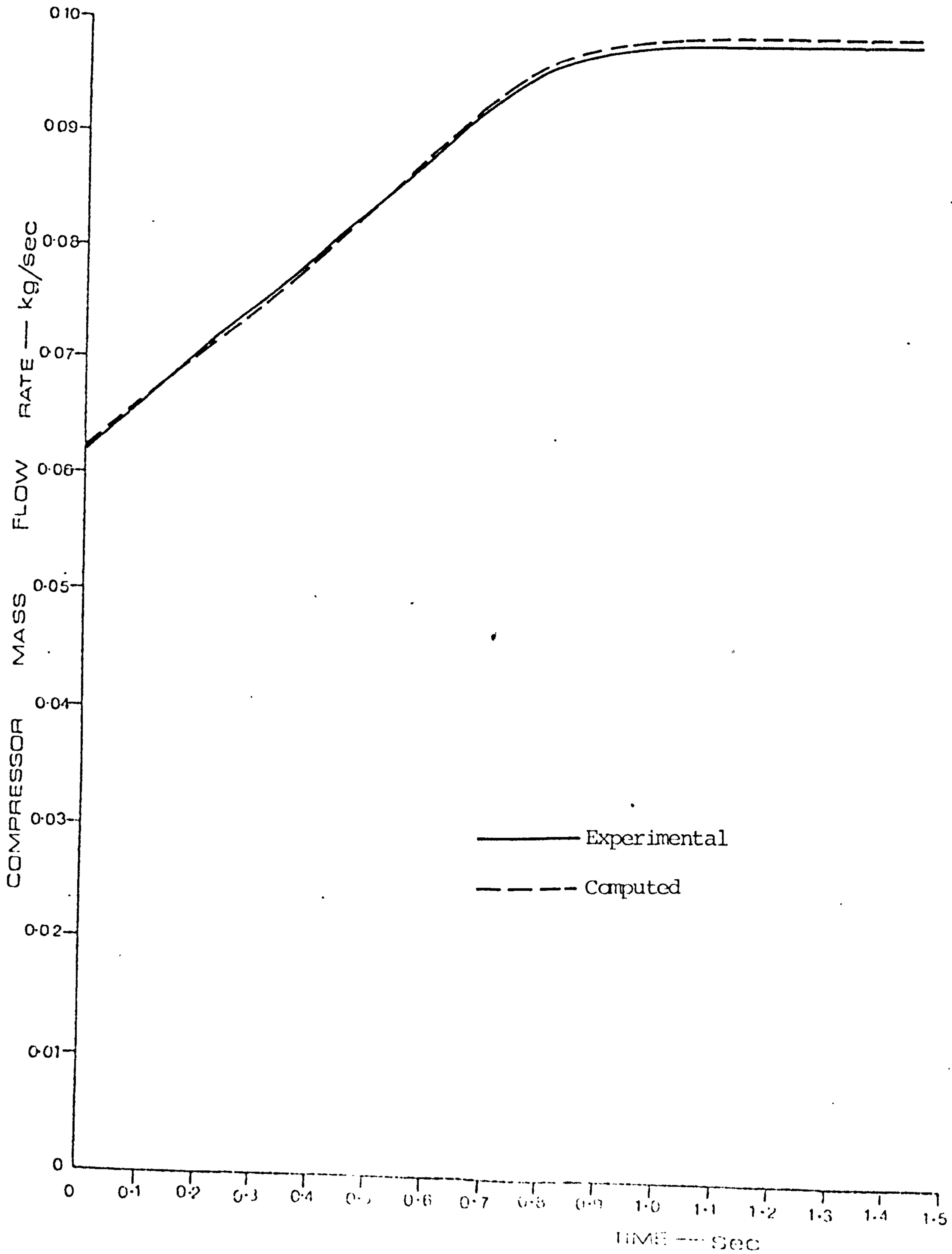

fig.(7.32). COMPRESSOR MASS FLOW RATE DURING NON-PULSATING TRANSIENT

INITIAL SUPPLY PRESSURE = 1.497 bar

FINAL SUPPLY PRESSURE = 2.269 bar

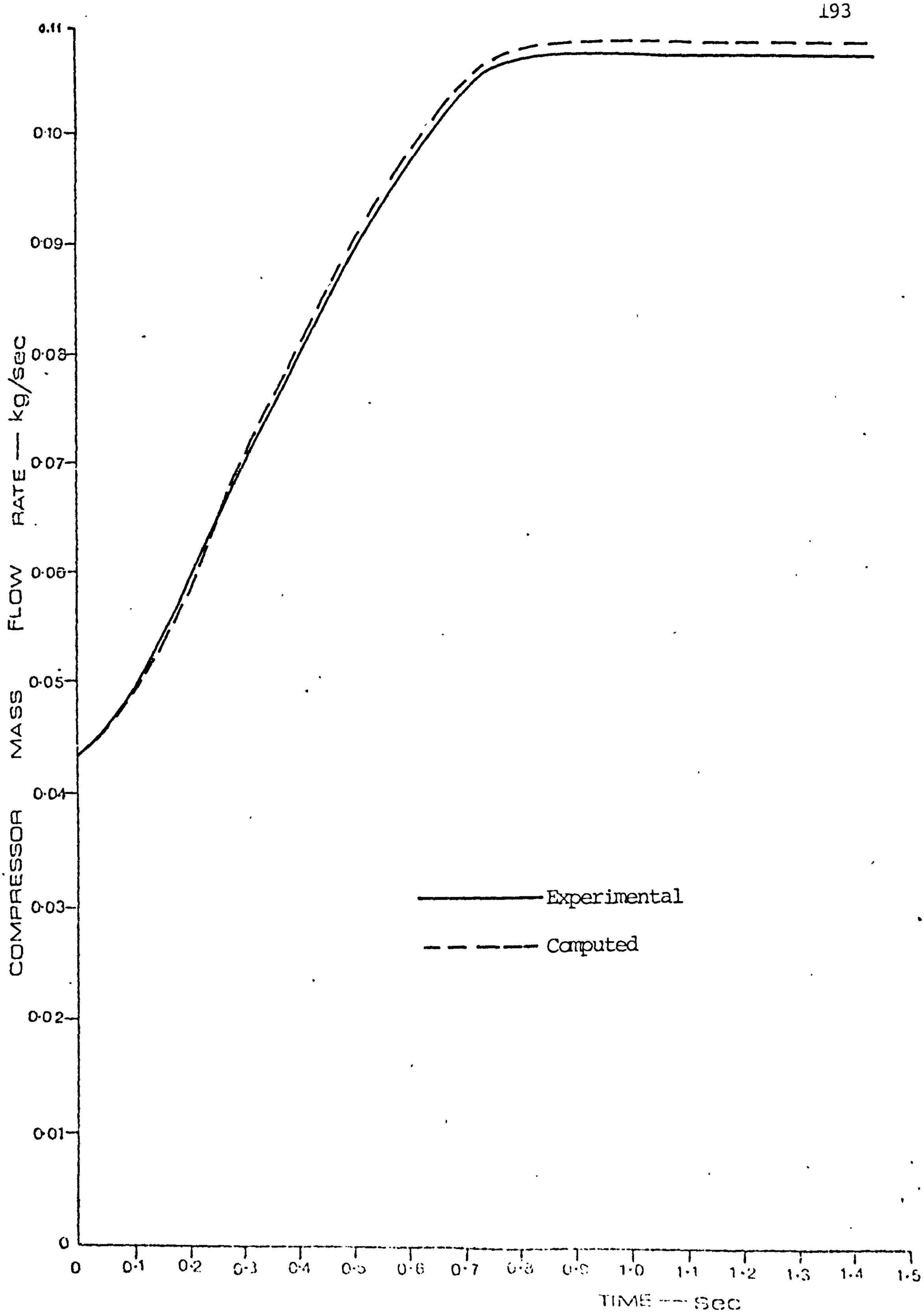

fig.(7.33). COMPRESSOR MASS FLOW RATE DURING NON-PULSATING TRANSIENT

INITIAL SUPPLY PRESSURE = 1.267 bar

FINAL SUPPLY PRESSURE = 2.674 bar

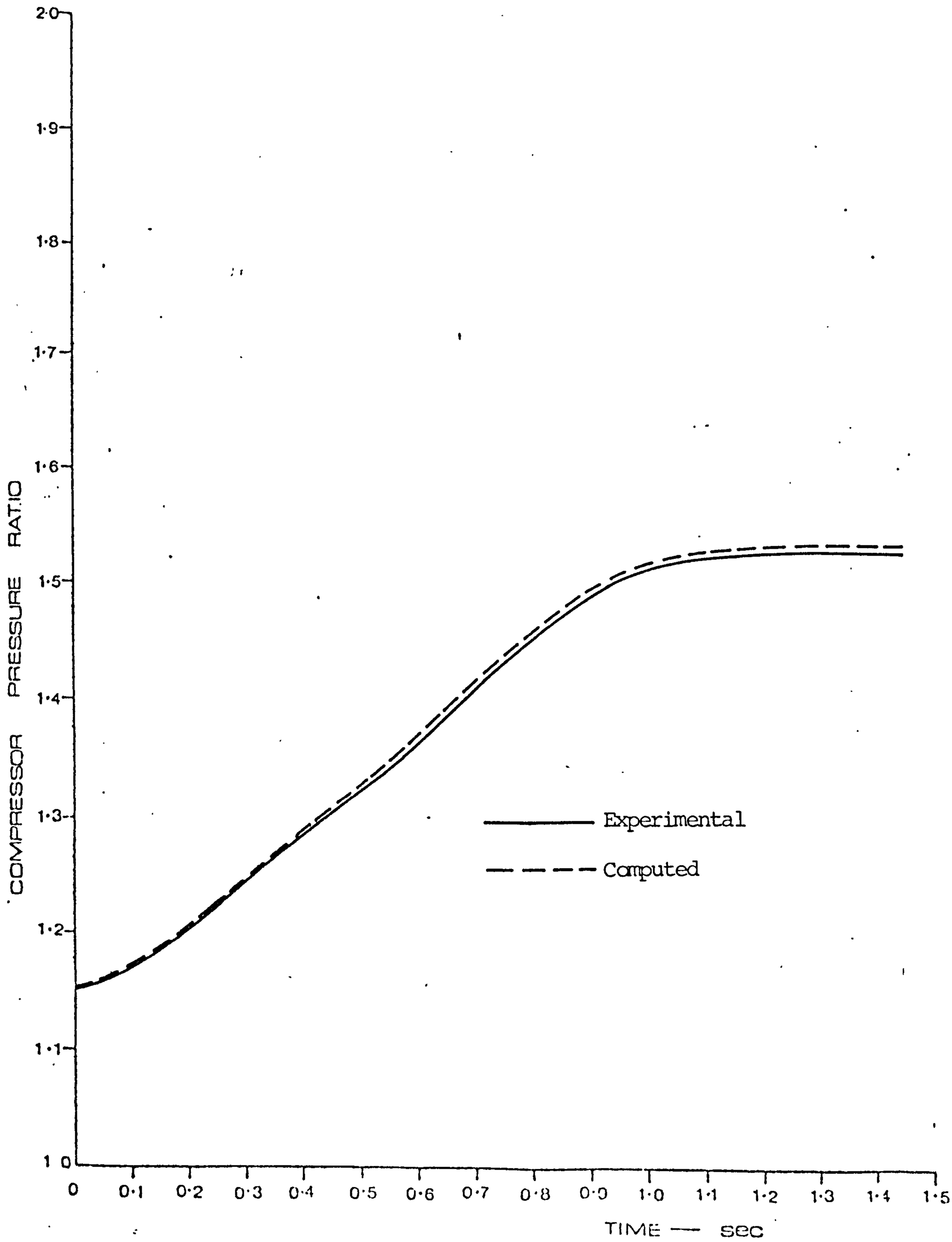

fig.(7.34).. COMPRESSOR PRESSURE RATIO

DURING NON-PULSATING TRANSIENT

INITIAL SUPPLY PRESSURE = 1.4 bar

FINAL SUPPLY PRESSURE = 2.021 bar

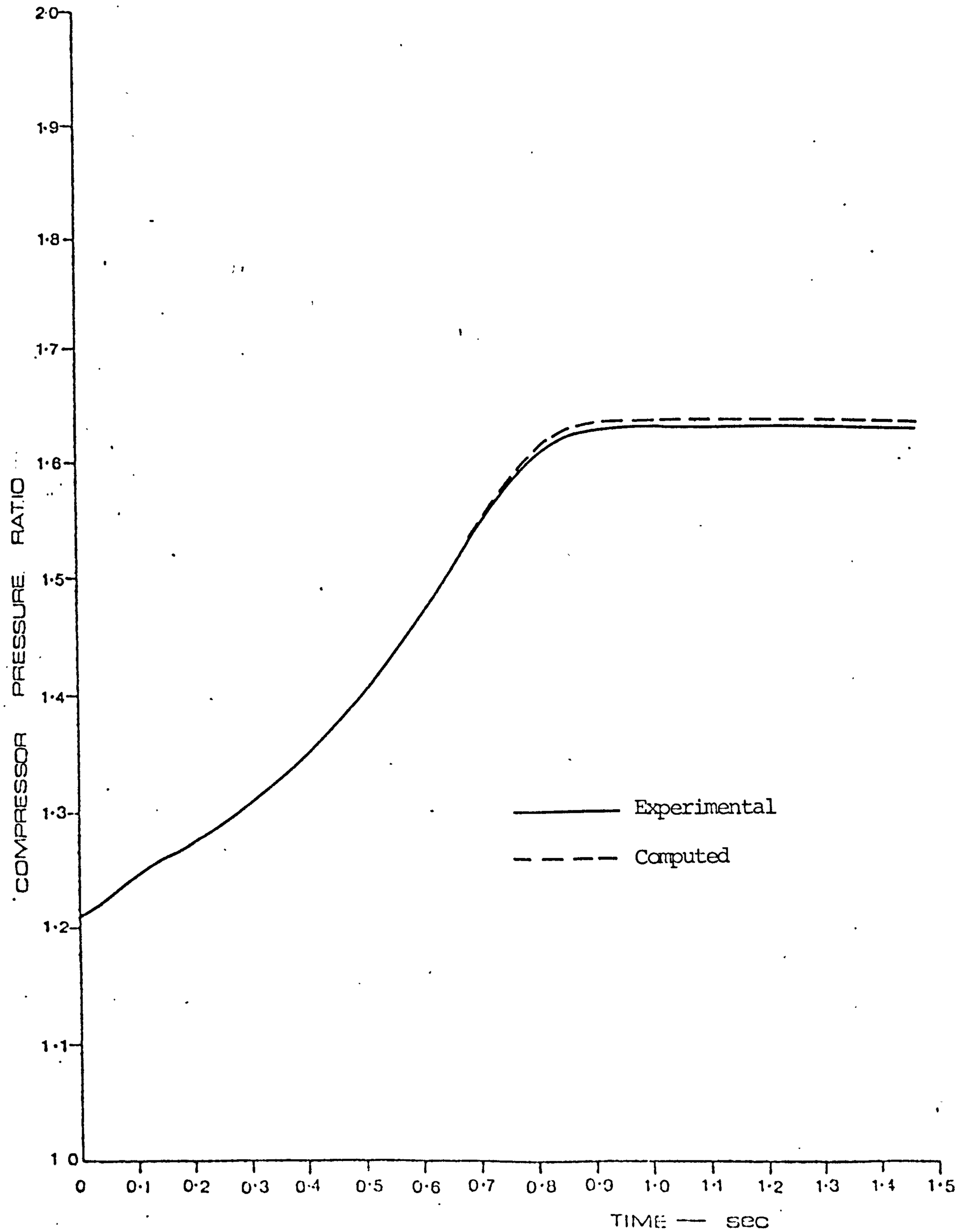

fig.(7.35).. COMPRESSOR PRESSURE RATIO

DURING NON-PULSATING TRANSIENT

INITIAL SUPPLY PRESSURE = 1.497 bar

FINAL SUPPLY PRESSURE = 2.269 bar

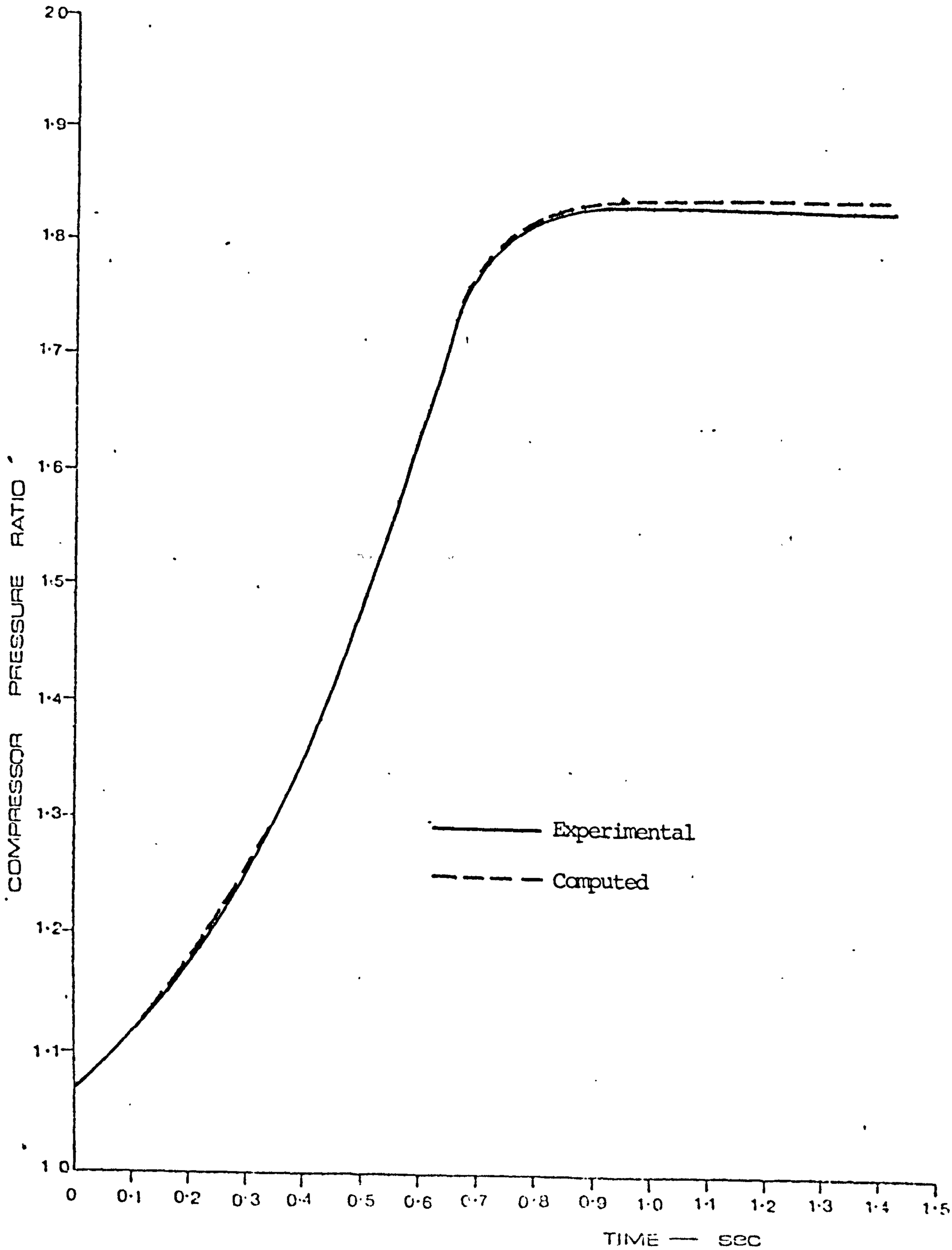

fig.(7.36).. COMPRESSOR PRESSURE RATIO

DURING NON-PULSATING TRANSIENT

INITIAL SUPPLY PRESSURE = 1.267 bar

FINAL SUPPLY PRESSURE = 2.674 bar

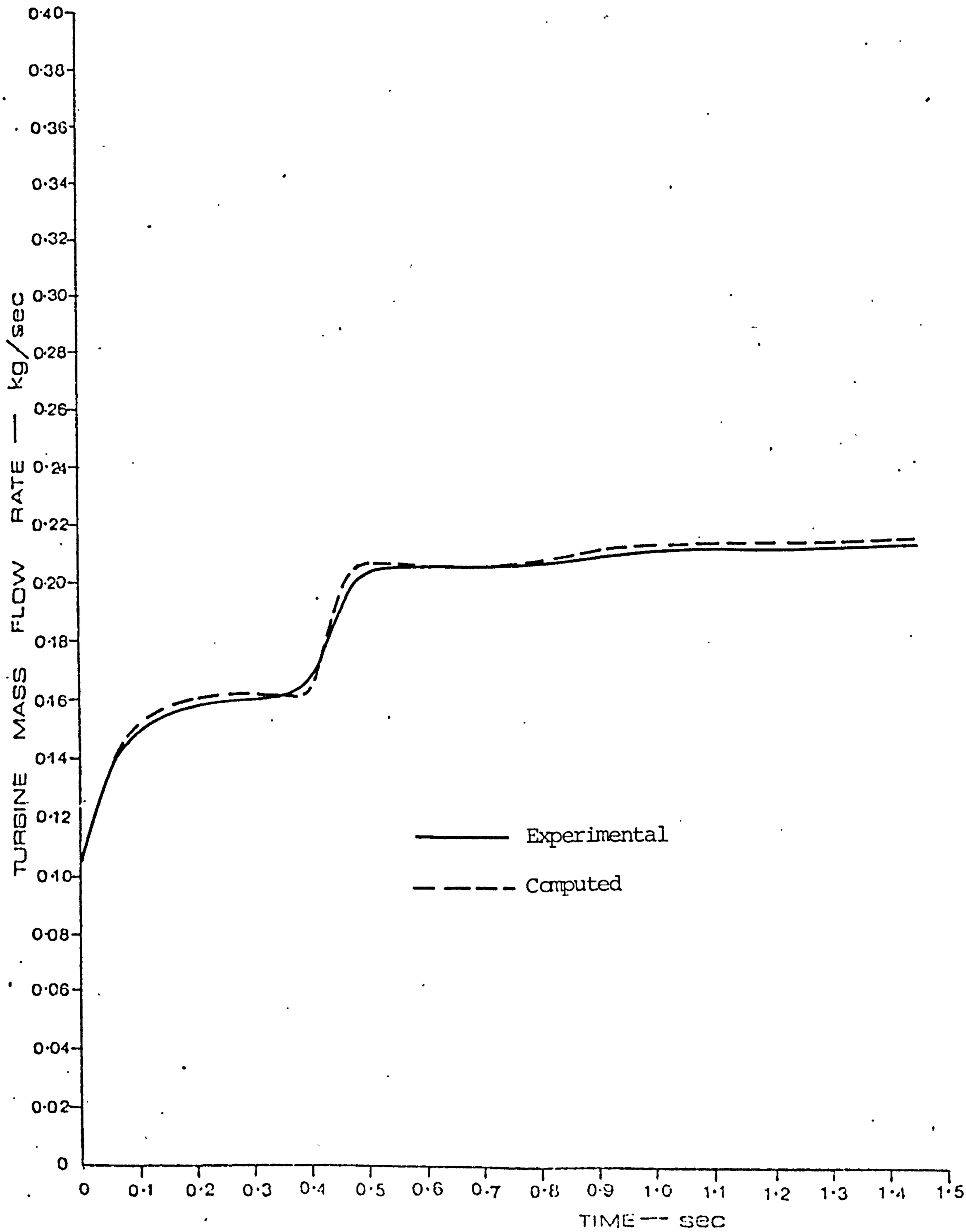

fig.(7.37). TURBINE MASS FLOW RATE

DURING NON - PULSATING TRANSIENT

INITIAL SUPPLY PRESSURE = 1.4 bar

FINAL SUPPLY PRESSURE = 2.021 bar

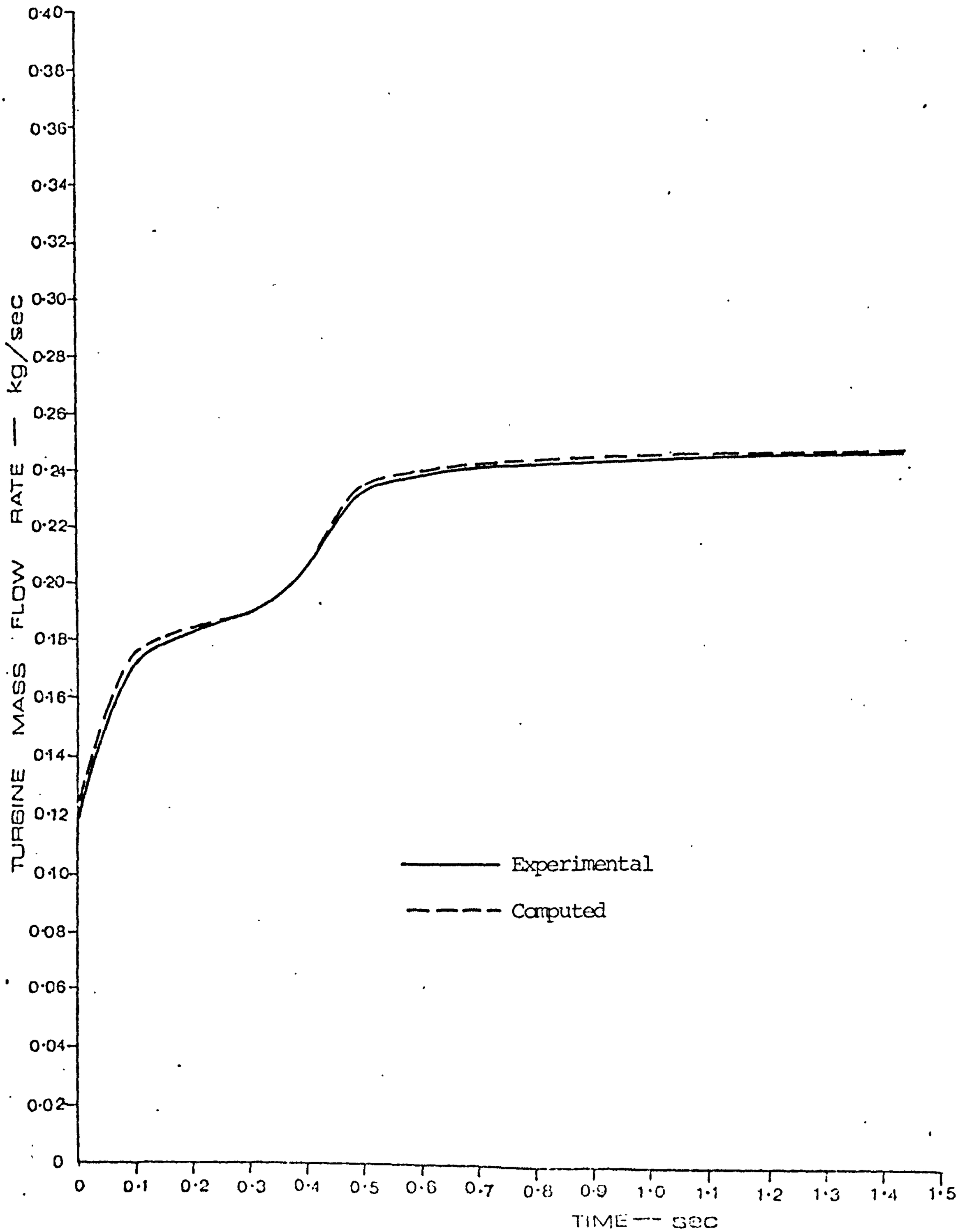

fig.(7.38). TURBINE MASS FLOW RATE

DURING NON - PULSATING TRANSIENT

INITIAL SUPPLY PRESSURE = 1.497 bar

FINAL SUPPLY PRESSURE = 2.269 bar

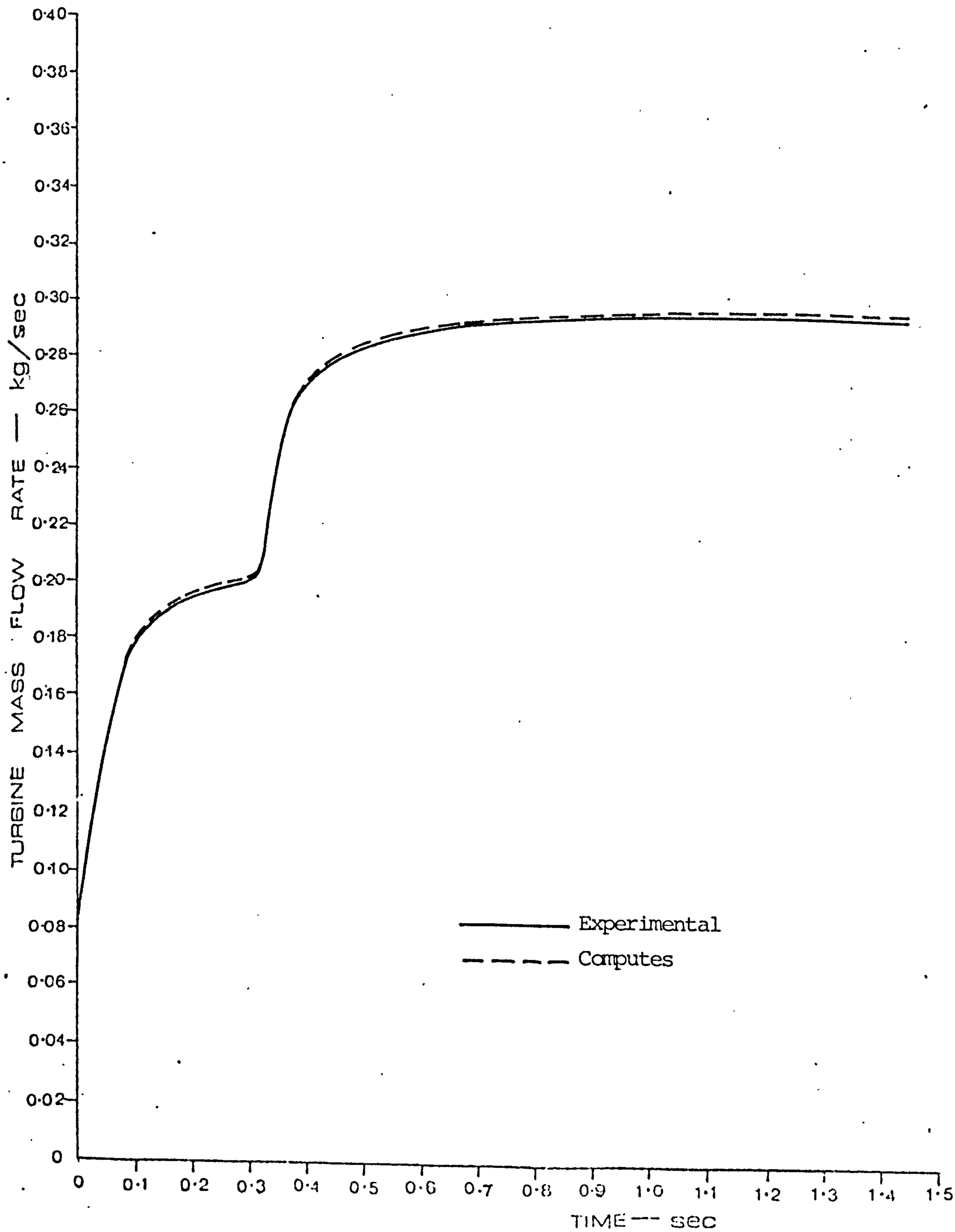

fig.(7.39). TURBINE MASS FLOW RATE

DURING NON - PULSATING TRANSIENT

INITIAL SUPPLY PRESSURE = 1.267 bar

FINAL SUPPLY PRESSURE = 2.674 bar

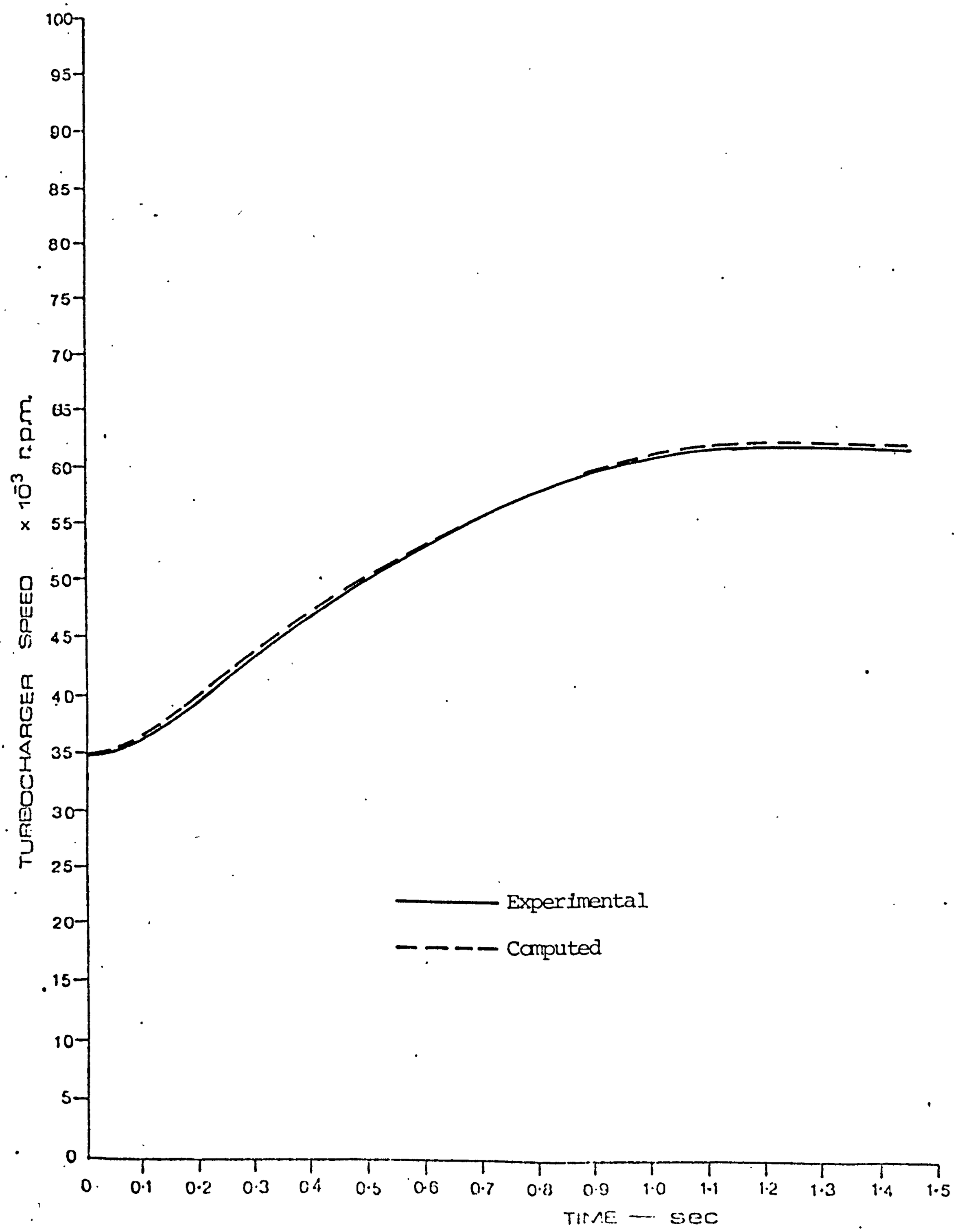

fig.(7.40). TURBOCHARGER SPEED DURING NON – PULSATING TRANSIENT

INITIAL SUPPLY PRESSURE = 1.4 bar

FINAL SUPPLY PRESSURE = 2.021 bar

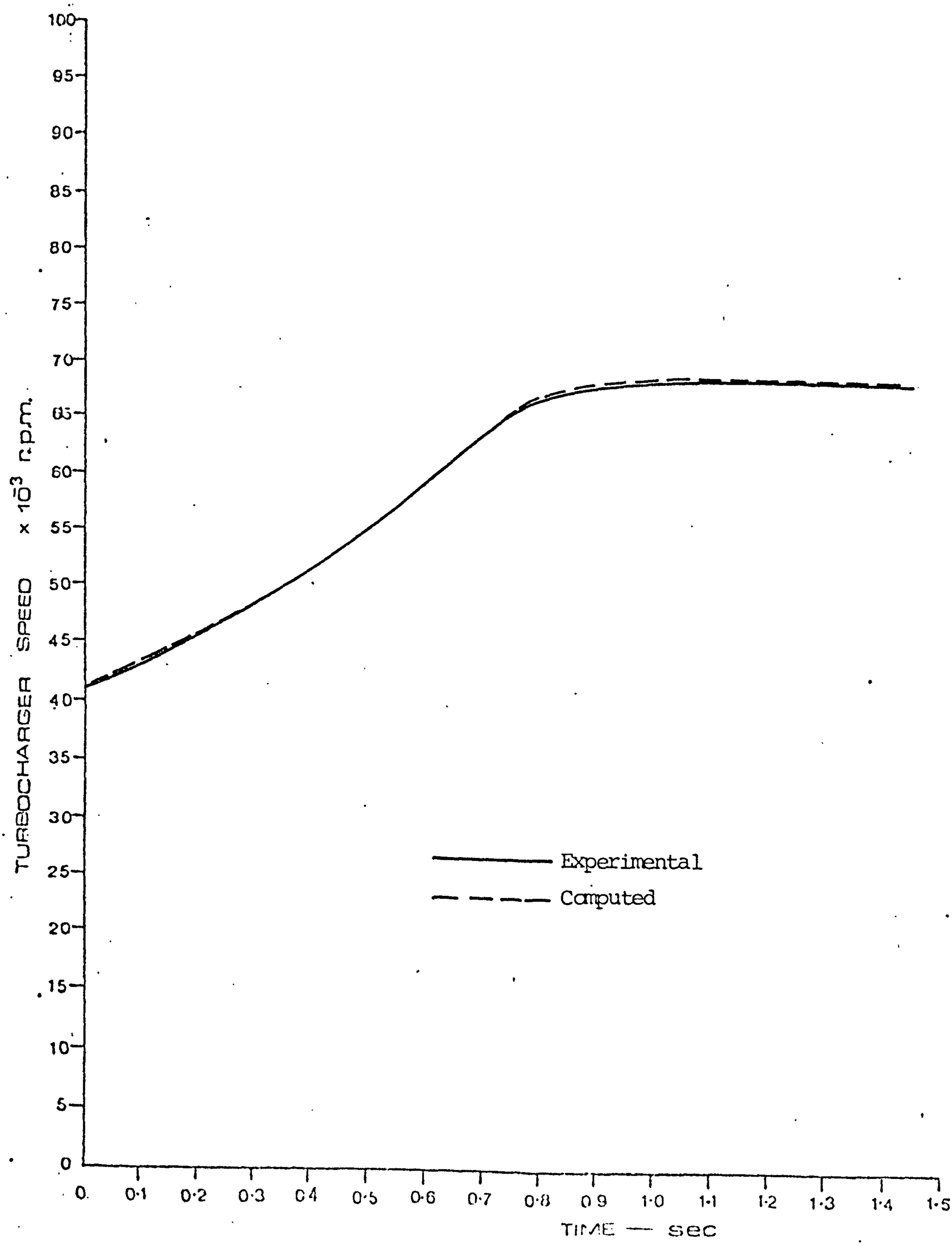

fig:(7.41). TURBOCHARGER SPEED DURING NON – PULSATING TRANSIENT

INITIAL SUPPLY PRESSURE = 1.497 bar

FINAL SUPPLY PRESSURE = 2.269 bar

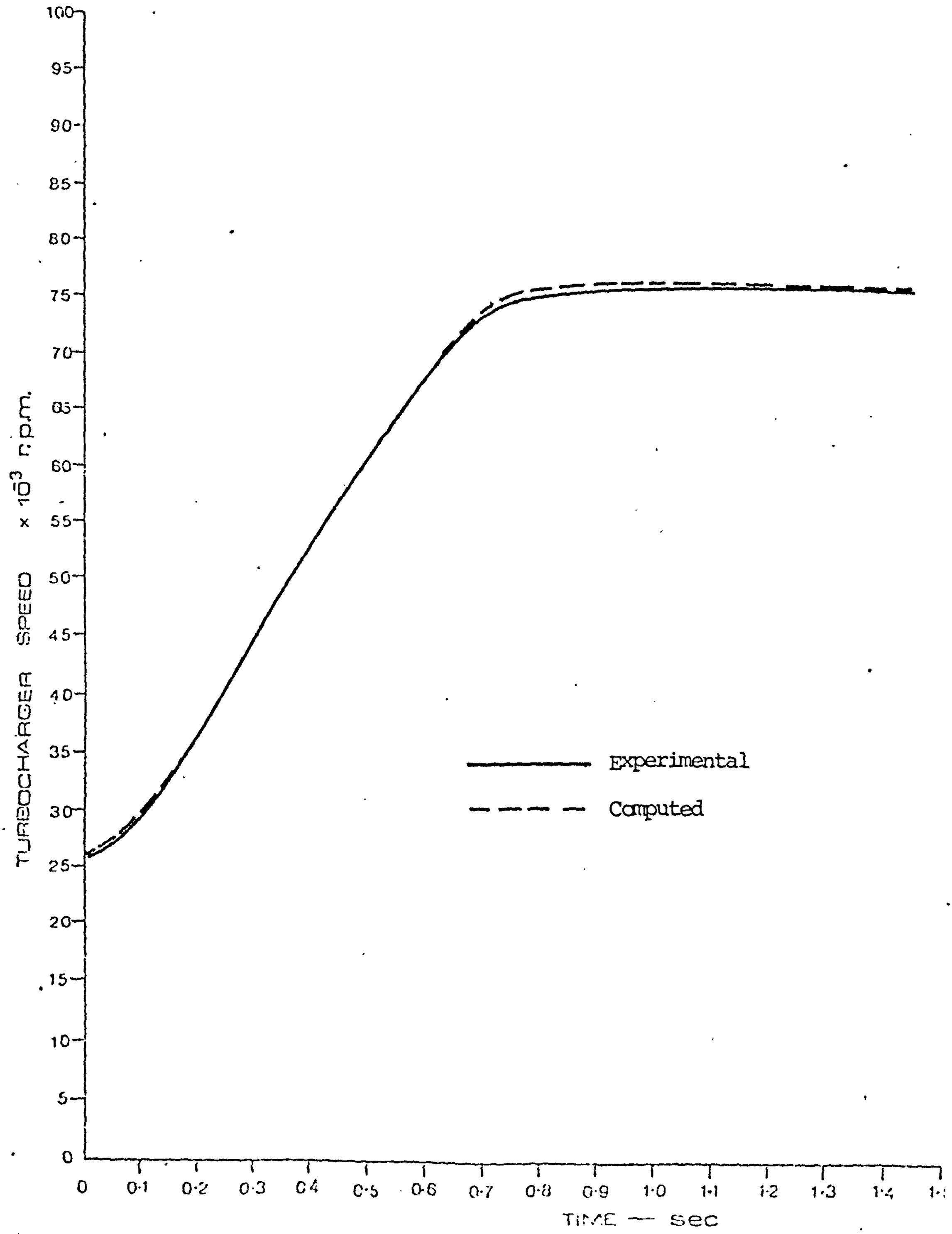

fig.(7.42). TURBOCHARGER SPEED DURING NON – PULSATING TRANSIENT

INITIAL SUPPLY PRESSURE = 1.267 bar

FINAL SUPPLY PRESSURE = 2.674 bar

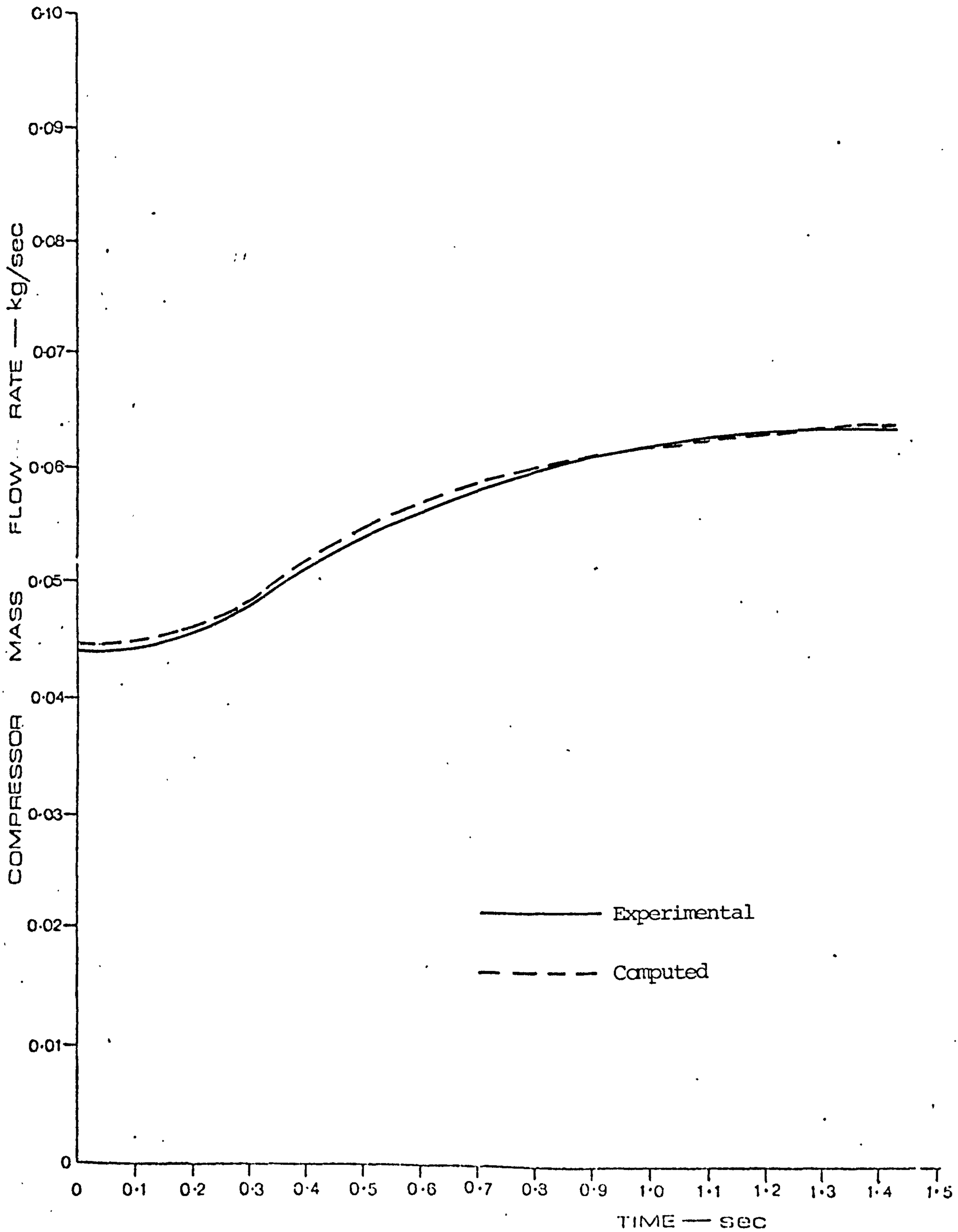

fig.(7.43). COMPRESSOR MASS FLOW RATE DURING PULSATING TRANSIENT

PULSE FREQUENCY = 25 pulses/sec

INITIAL SUPPLY PRESSURE == 1.293 bar

FINAL SUPPLY PRESSURE == 2.052 bar

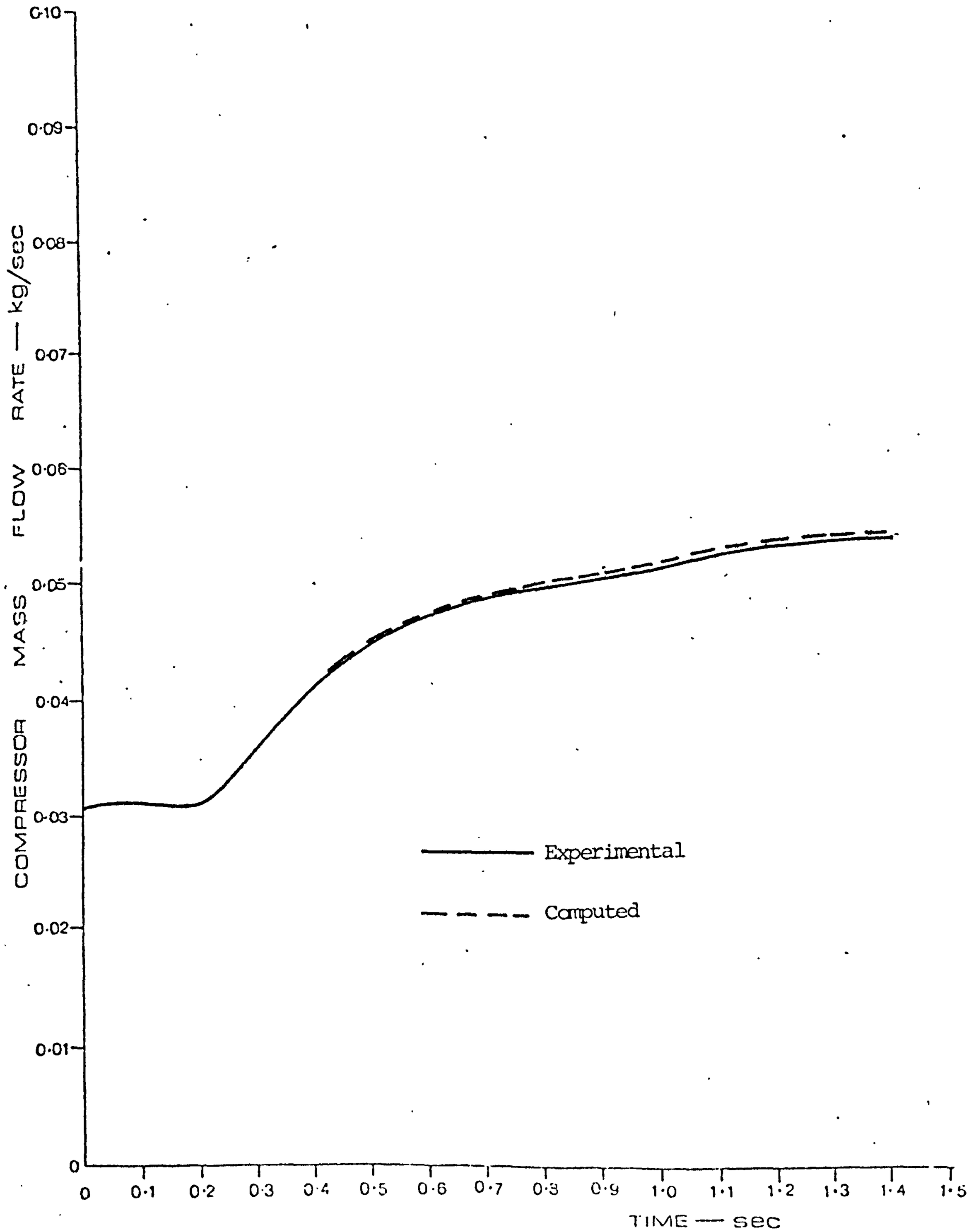

fig.(7.44). COMPRESSOR MASS FLOW RATE

DURING PULSATING TRANSIENT

PULSE FREQUENCY = 25 pulses/sec

INITIAL SUPPLY PRESSURE = 1.178 bar

FINAL SUPPLY PRESSURE = 1.854 bar

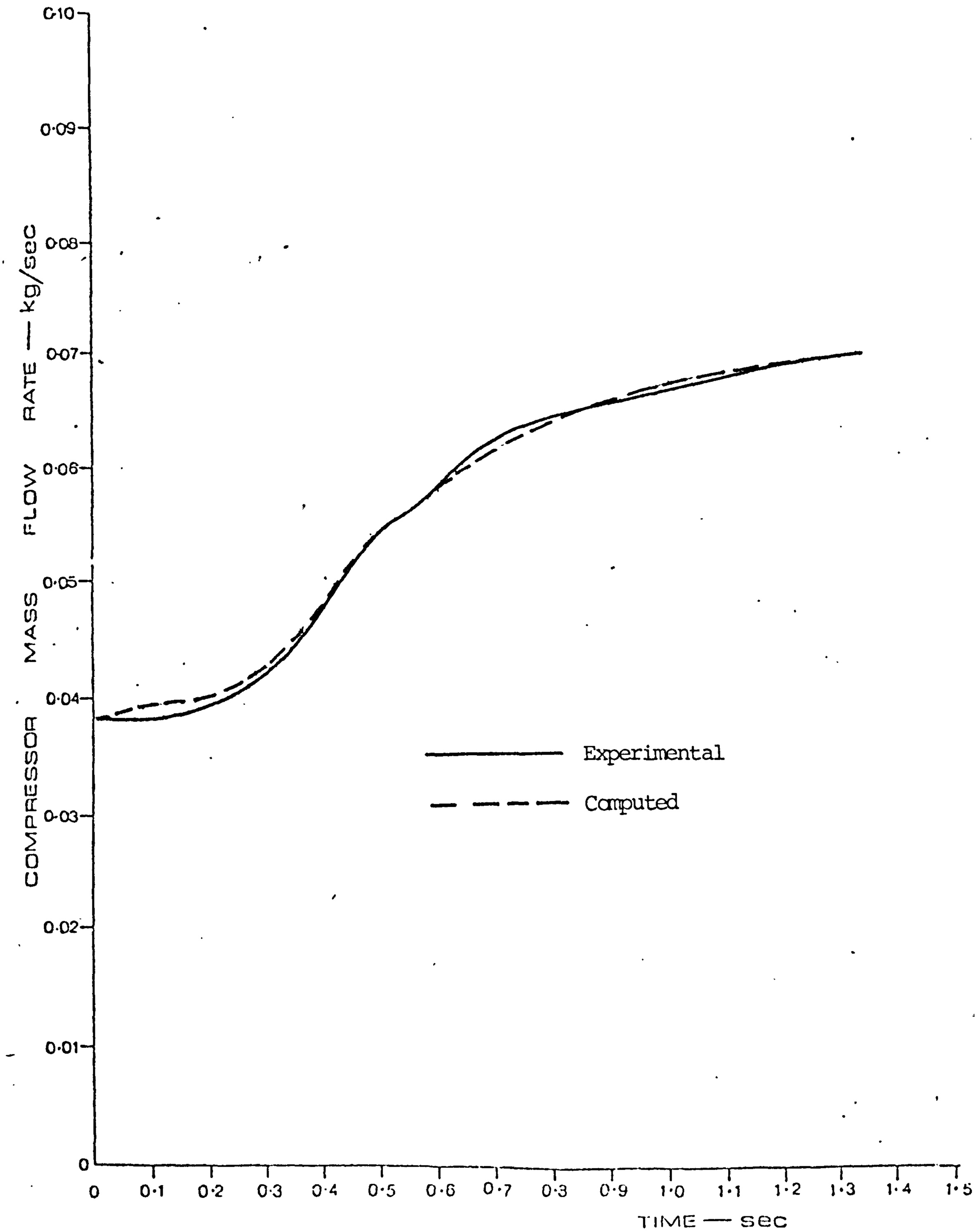

fig.(7.45). COMPRESSOR MASS FLOW RATE

DURING PULSATING TRANSIENT

PULSE FREQUENCY = 25 pulses/sec

INITIAL SUPPLY PRESSURE == 1.205 bar

FINAL SUPPLY PRESSURE == 2.183 bar

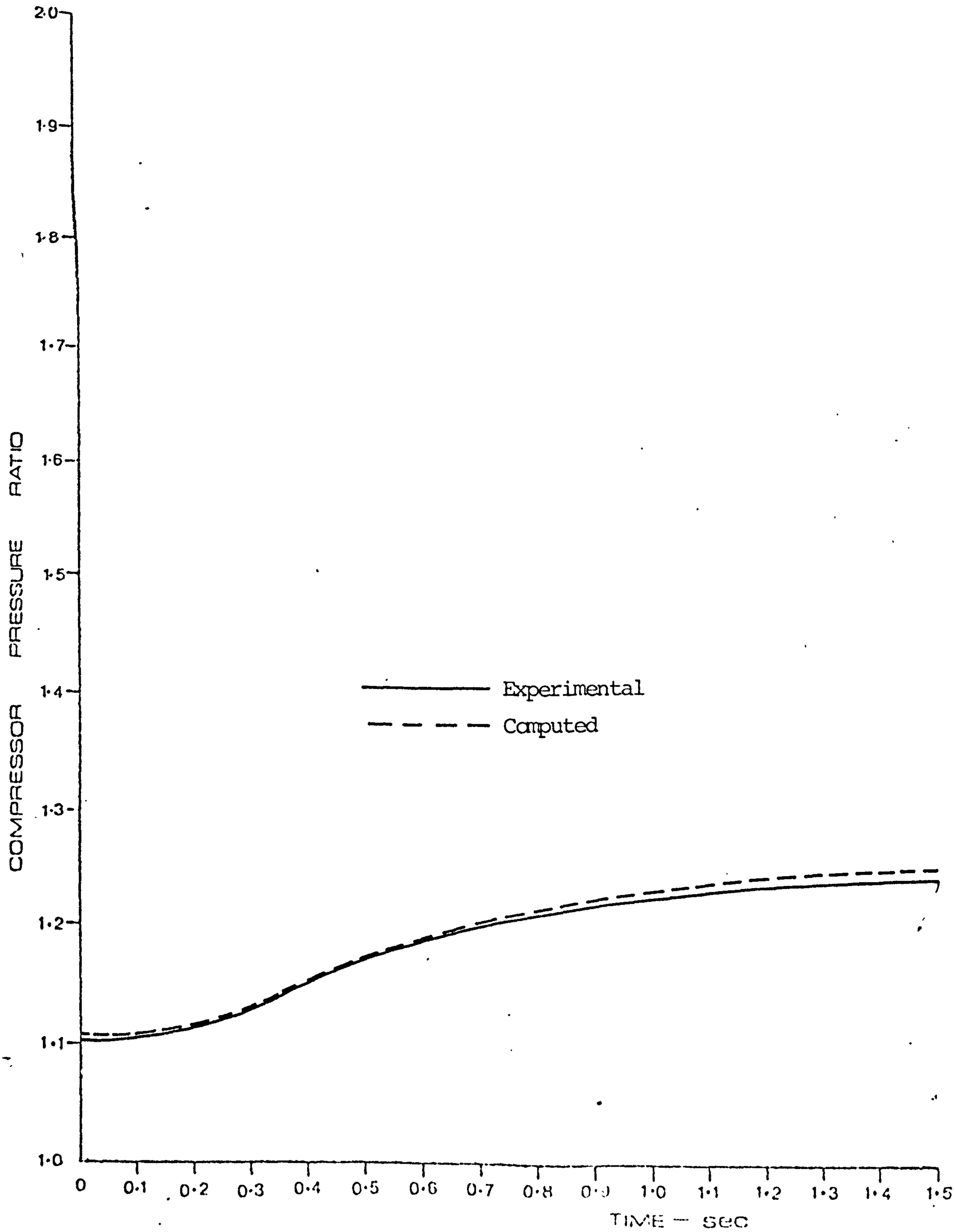

fig.(7.46). COMPRESSOR PRESSURE RATIO CURIN

PULSATING TRANSIENT

PULSE FREQUENCY = 25 pulses/sec

INITIAL SUPPLY PRESSURE = 1.293 bar

FINAL SUPPLY PRESSURE = 2.052 bar

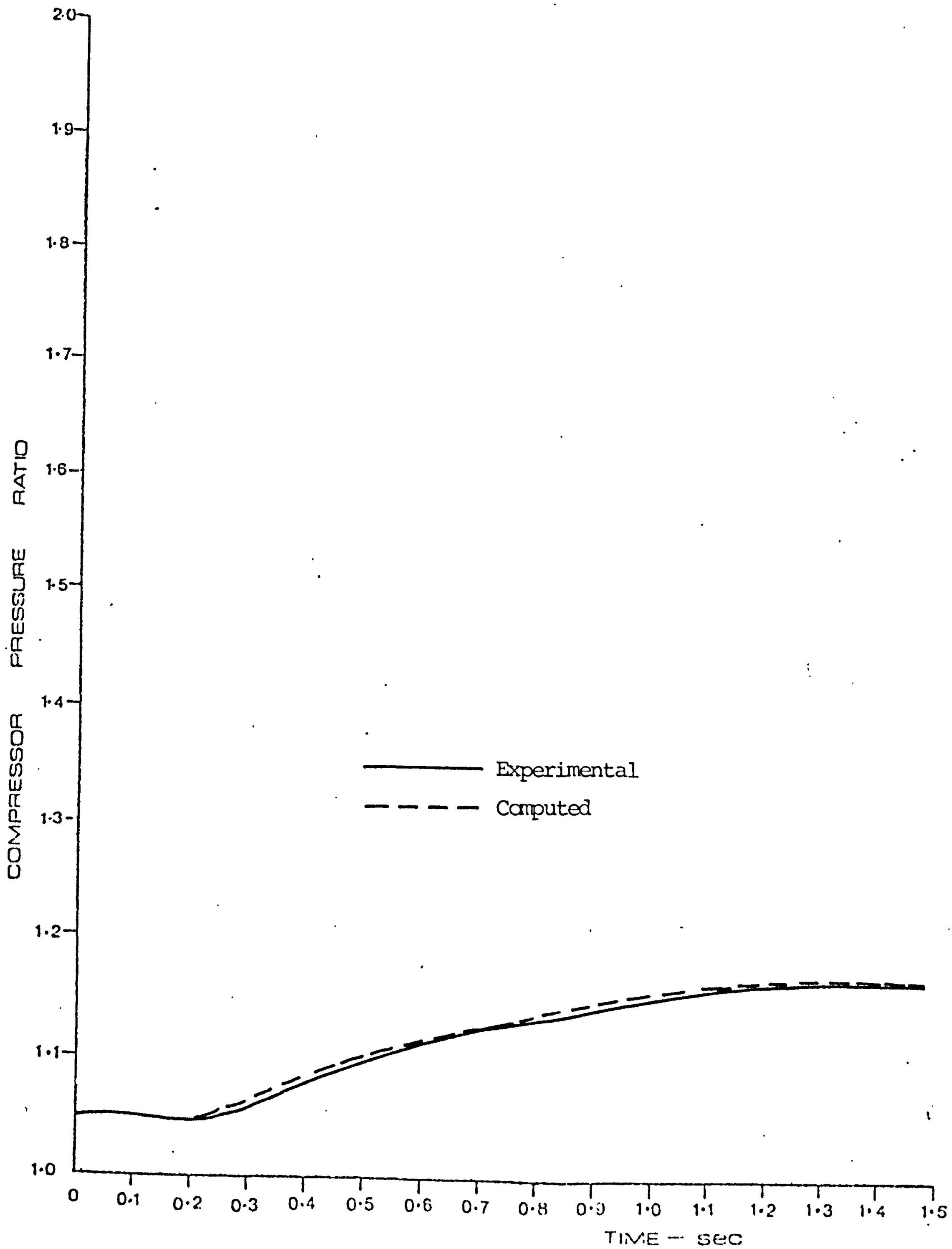

fig.(7.47).COMPRESSOR PRESSURE RATIO DURING

PULSATING TRANSIENT

PULSE FREQUENCY = 25 pulses/sec

INITIAL SUPPLY PRESSURE = 1.178 bar

FINAL SUPPLY PRESSURE = 1.854 bar

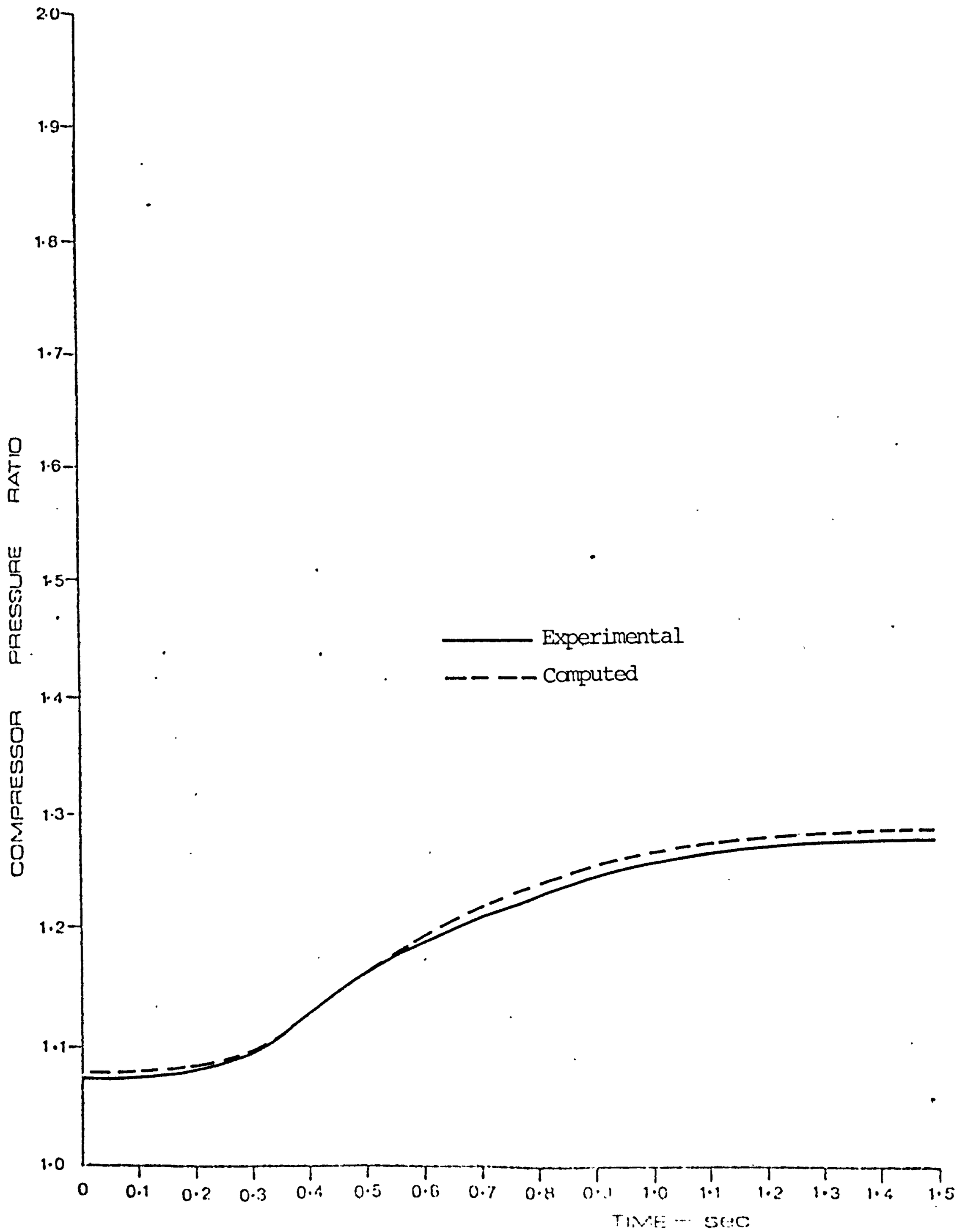

fig.(7.48). COMPRESSOR PRESSURE RATIO DURING

PULSATING TRANSIENT

PULSE FREQUENCY = 25 pulses/sec

INITIAL SUPPLY PRESSURE = 1.205 bar

FINAL SUPPLY PRESSURE = 2.183 bar

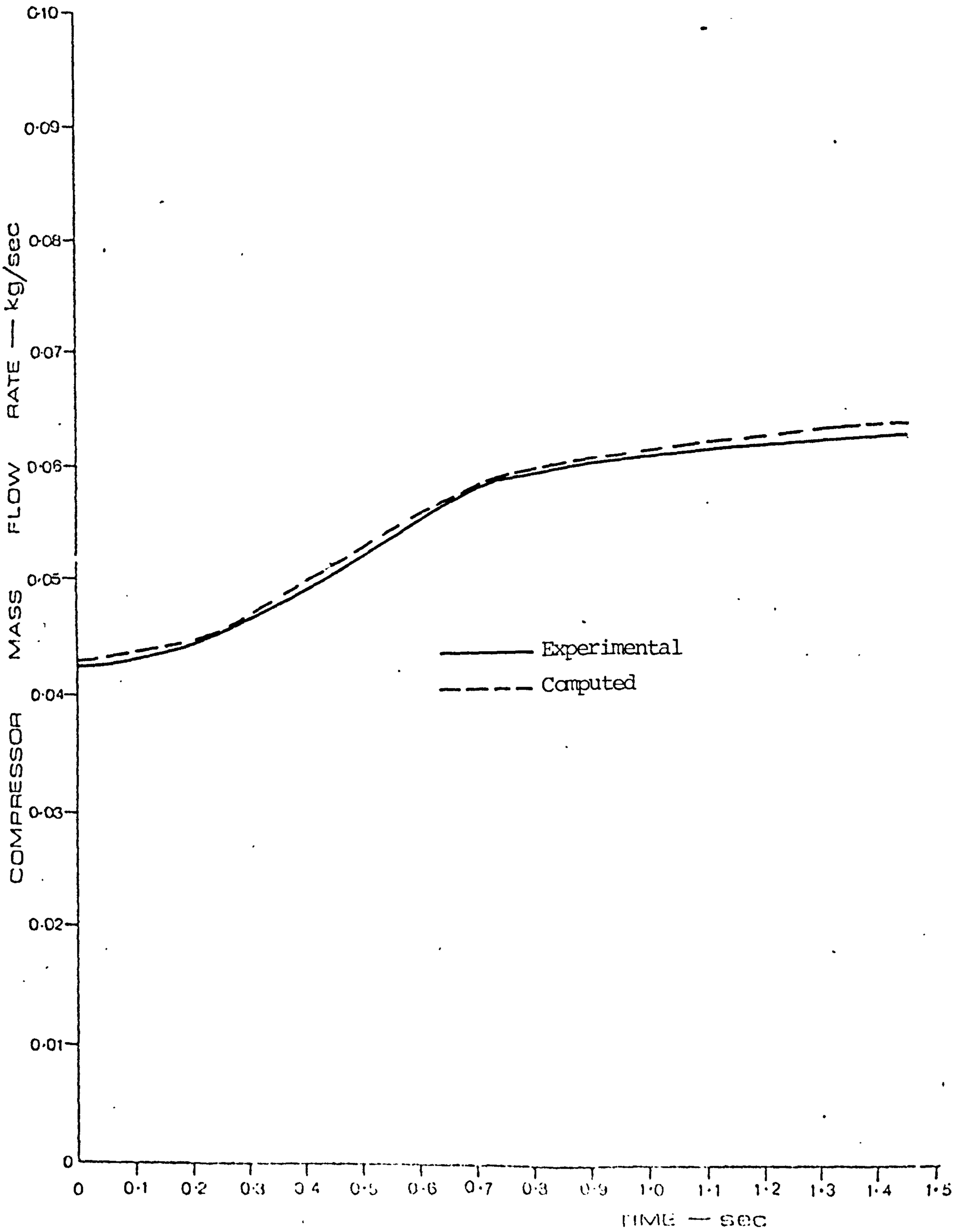

fig.(7.49). COMPRESSOR MASS FLOW RATE

DURING PULSATING TRANSIENT

PULSE FREQUENCY = 38 pulses/sec

INITIAL SUPPLY PRESSURE = 1.281 bar

FINAL SUPPLY PRESSURE = 1.791 bar

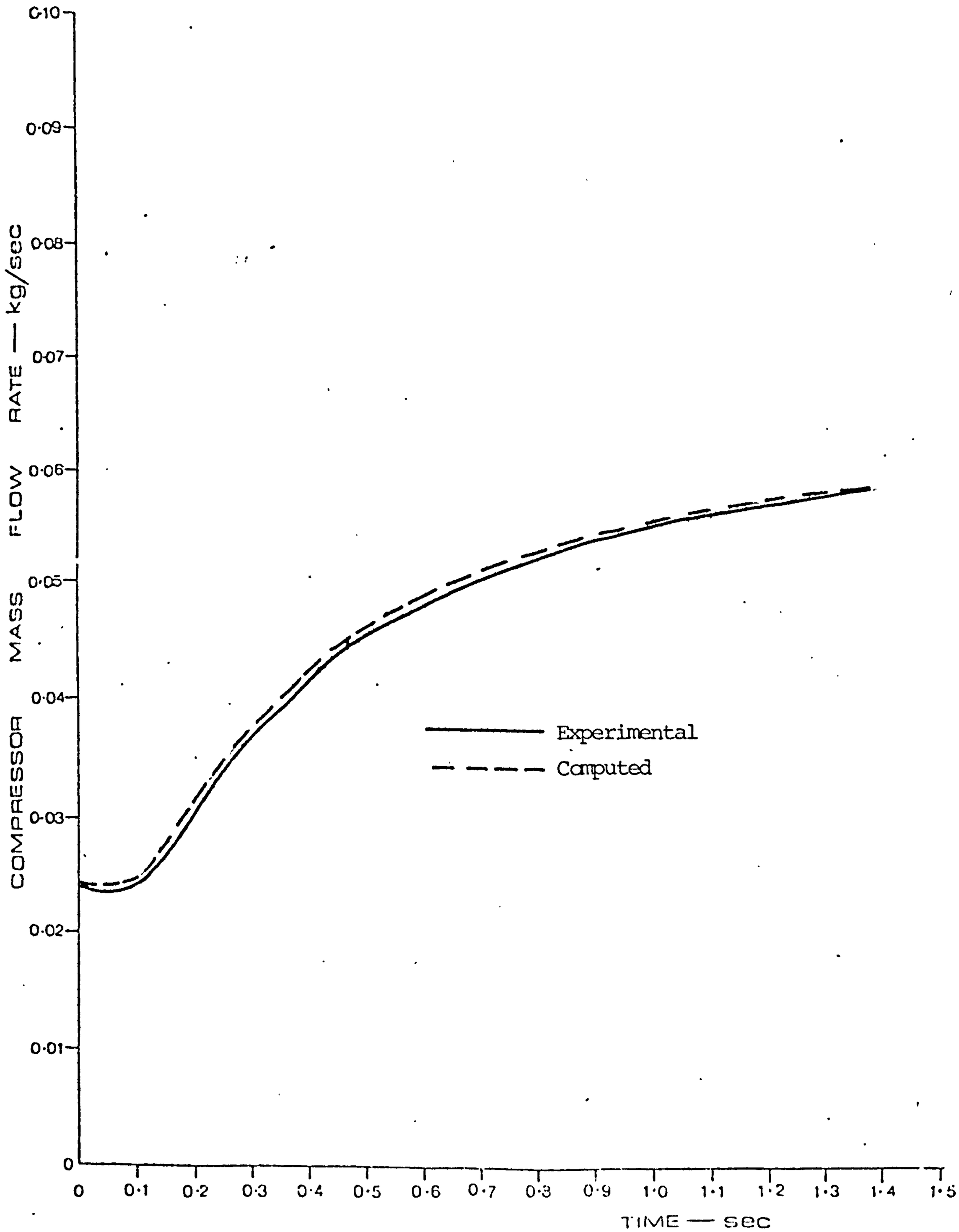

fig.(7.50). COMPRESSOR MASS FLOW RATE

DURING PULSATING TRANSIENT

PULSE FREQUENCY = 38 pulses/sec

INITIAL SUPPLY PRESSURE = 1.102 bar

FINAL SUPPLY PRESSURE = 1.764 bar

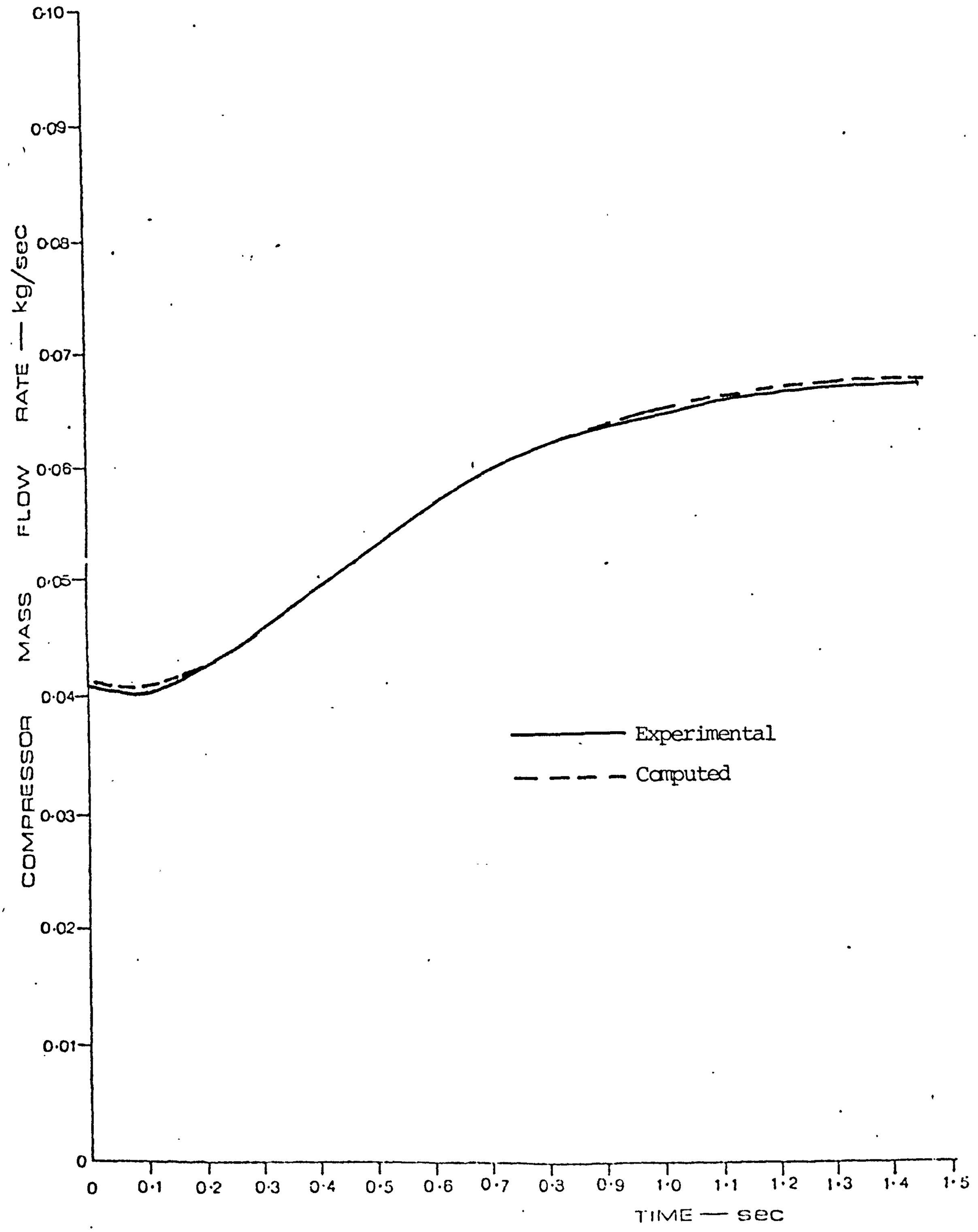

fig.(7.51). COMPRESSOR MASS FLOW RATE

DURING PULSATING TRANSIENT

PULSE FREQUENCY = 25 pulses/sec

INITIAL SUPPLY PRESSURE = 1.212 bar

FINAL SUPPLY PRESSURE = 2.108 bar

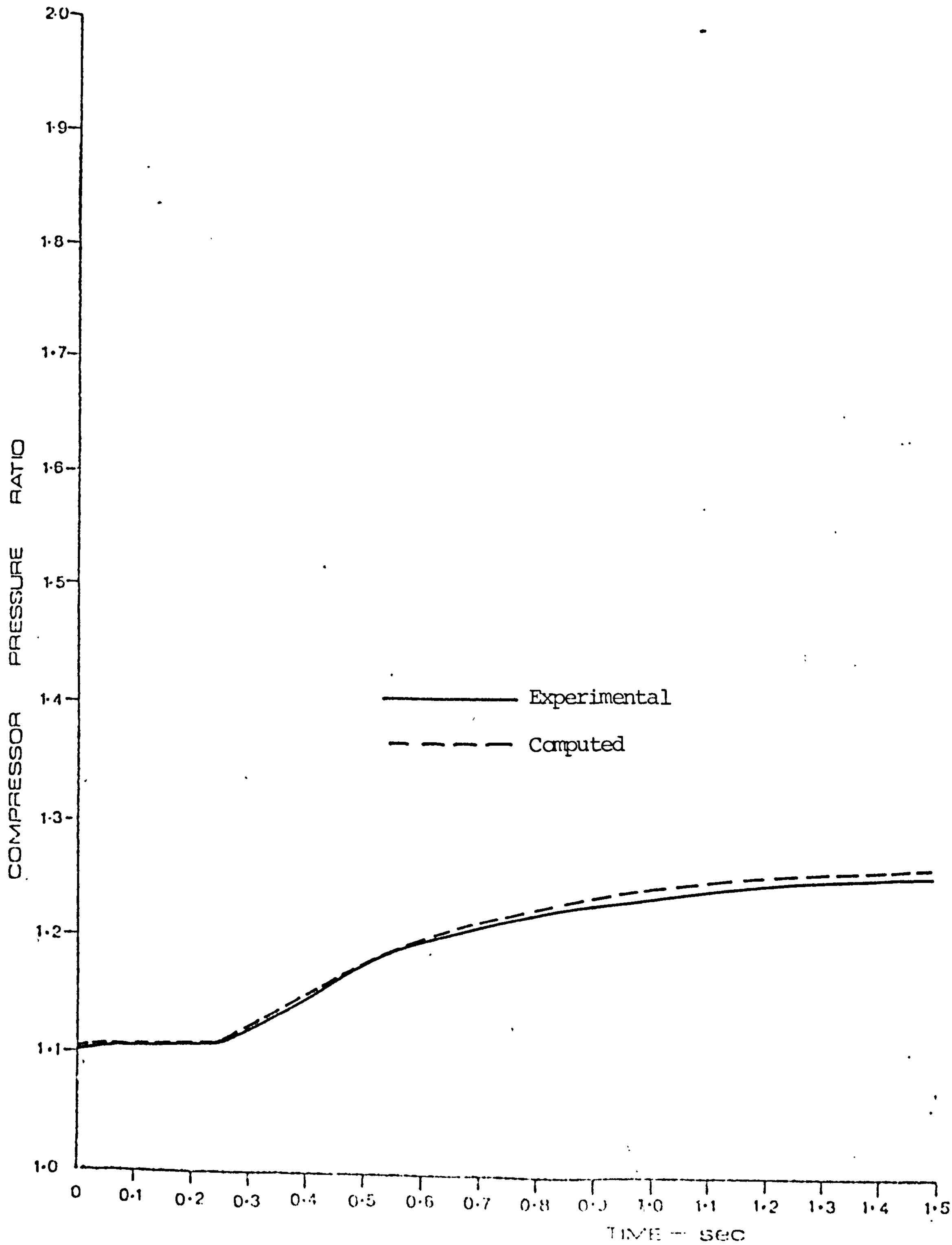

fig.(7.52). COMPRESSOR PRESSURE RATIO CURING

PULSATING TRANSIENT

PULSE FREQUENCY = 38 pulses/sec

INITIAL SUPPLY PRESSURE = 1.281 bar

FINAL SUPPLY PRESSURE = 1.791 bar

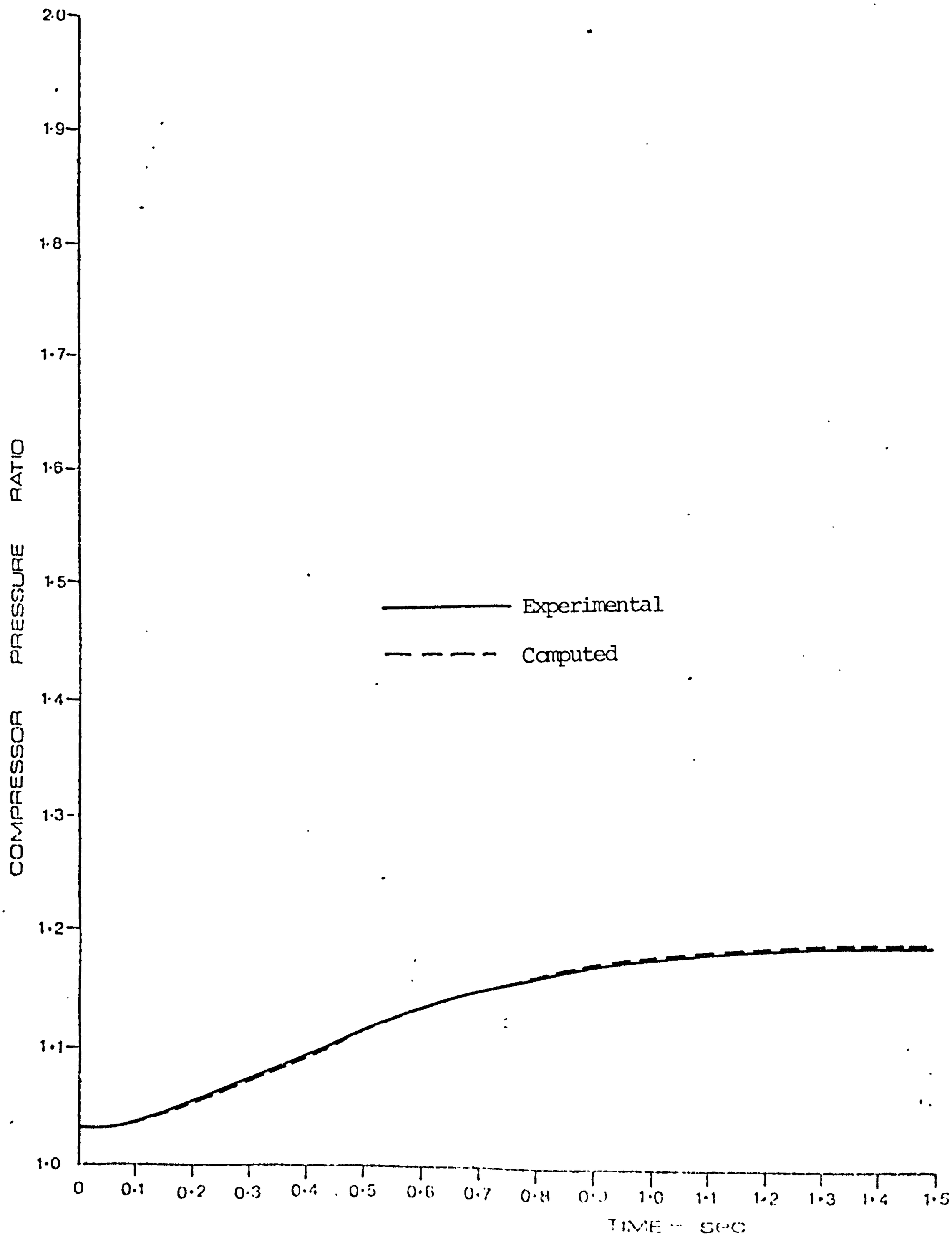

fig.(7.53). COMPRESSOR PRESSURE RATIO CURVE

PULSATING TRANSIENT

PULSE FREQUENCY = 38 pulses/sec

INITIAL SUPPLY PRESSURE = 1.102 bar

FINAL SUPPLY PRESSURE = 1.764 bar

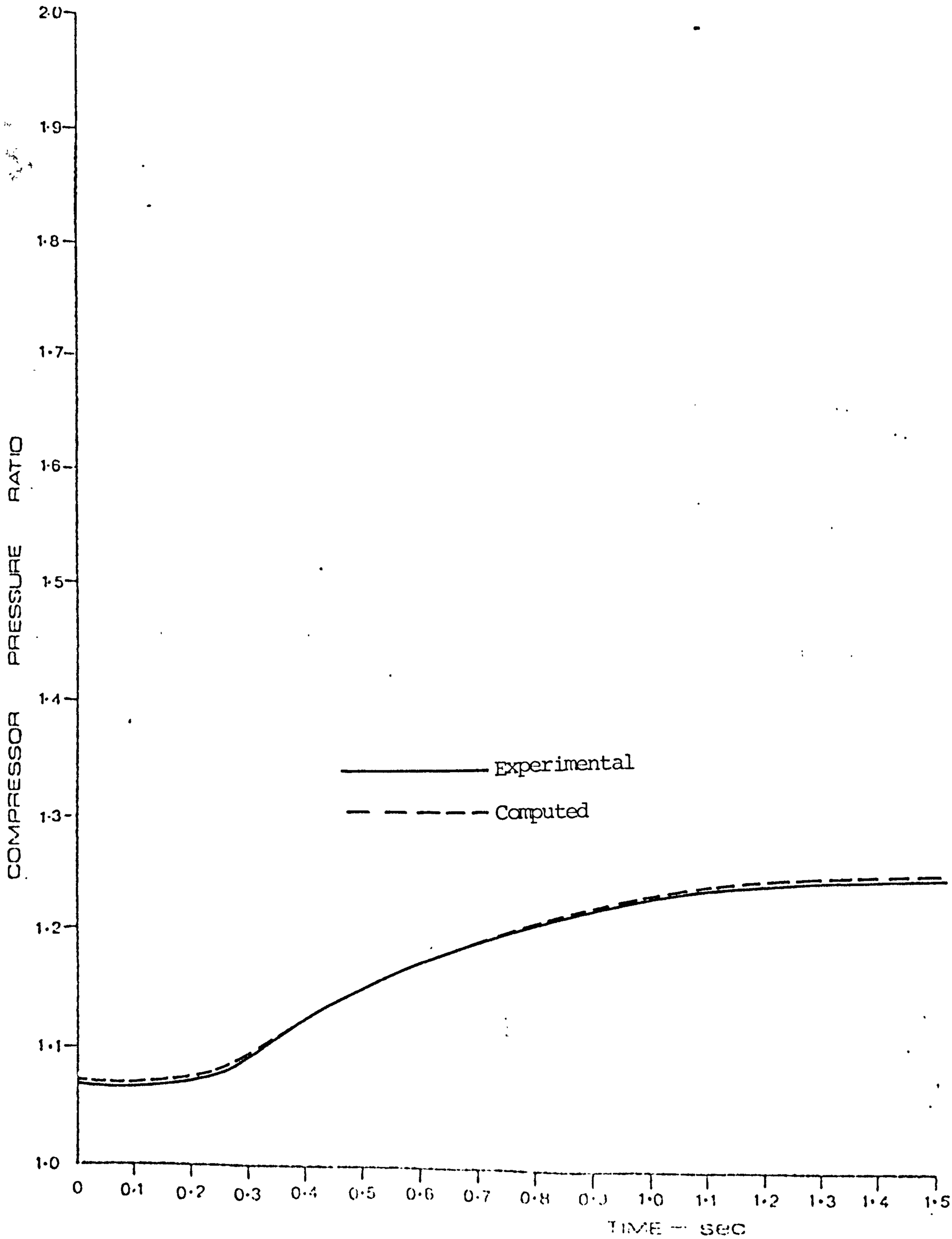

fig.(7.54). COMPRESSOR PRESSURE RATIO DURING PULSATING TRANSIENT

PULSE FREQUENCY=38 pulses/sec

INITIAL SUPPLY PRESSURE = 1.212 bar

FINAL SUPPLY PRESSURE = 2.108 bar

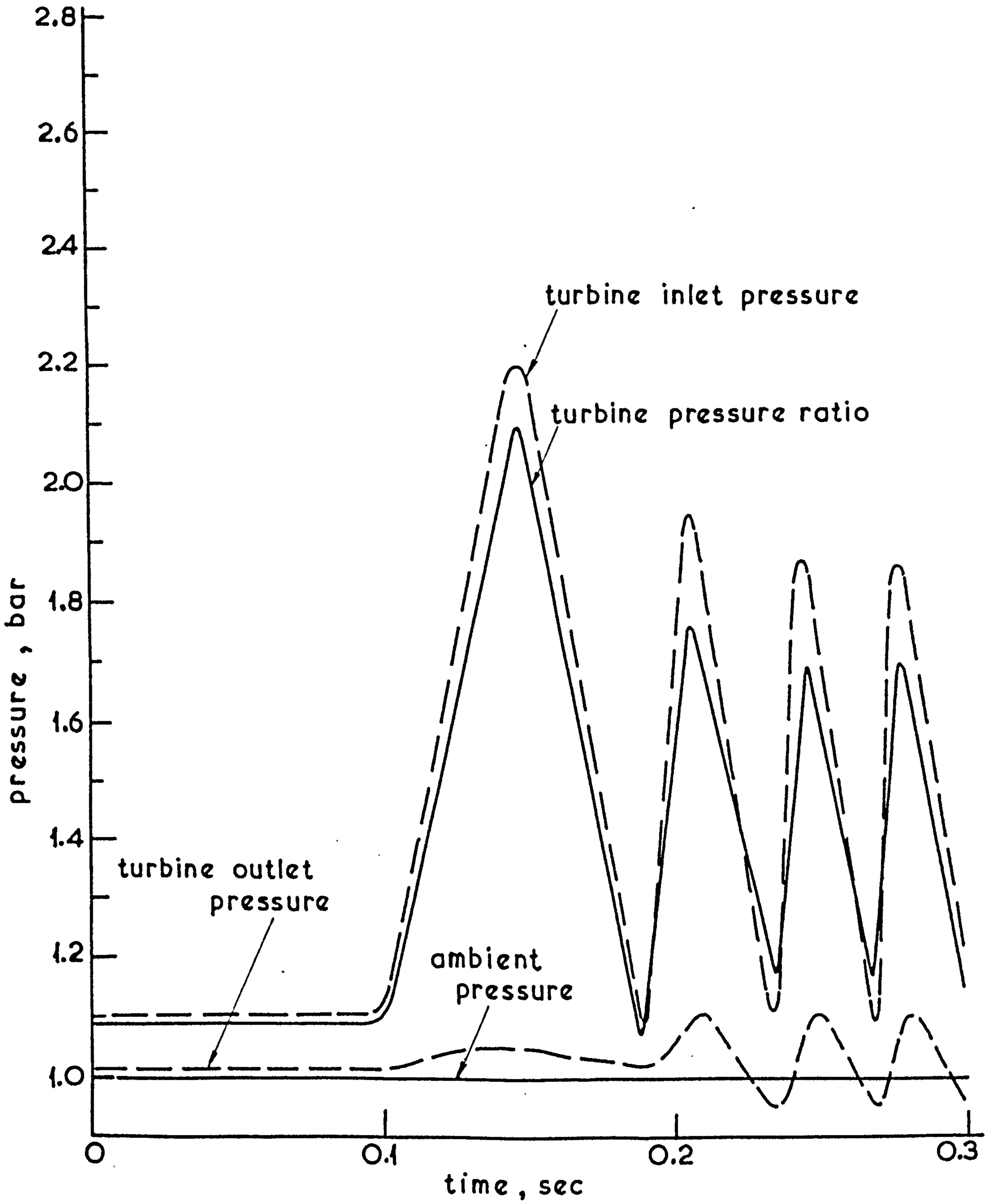

Fig. (7.54A) Turbine pressure during the initiation of the Transient.

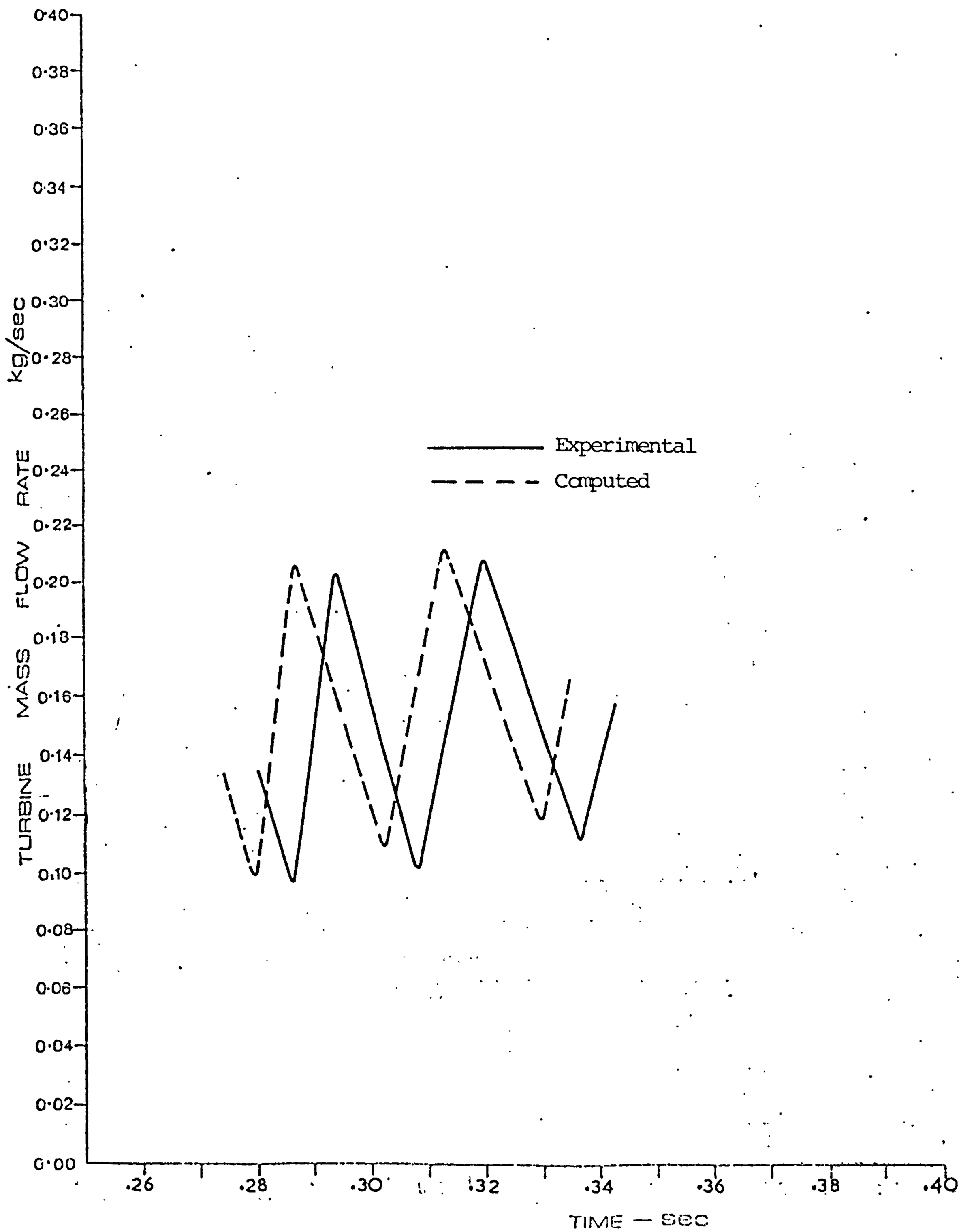

fig.(7.55) TURBINE MASS FLOW RATE DURING PULSATING TRANSIENT

PULSE FREQUENCY=38 pulses/sec

INITIAL SUPPLY PRESSURE == 1.212 bar

FINAL SUPPLY PRESSURE == 2.108 bar

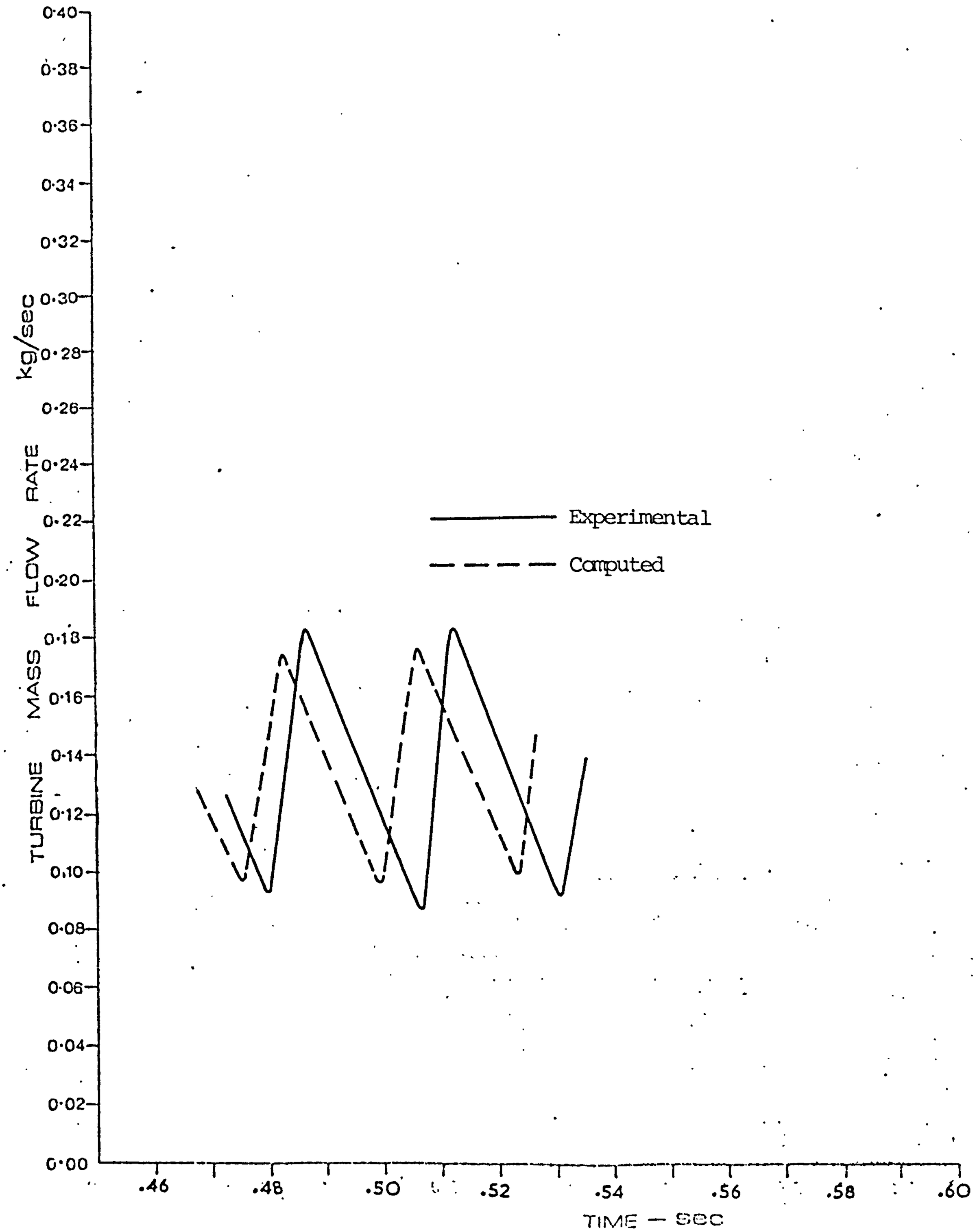

fig.(7.56) TURBINE MASS FLOW RATE DURING PULSATING TRANSIENT

PULSE FREQUENCY = 38 pulses/sec

INITIAL SUPPLY PRESSURE = 1.281 bar

FINAL SUPPLY PRESSURE = 1.791 bar

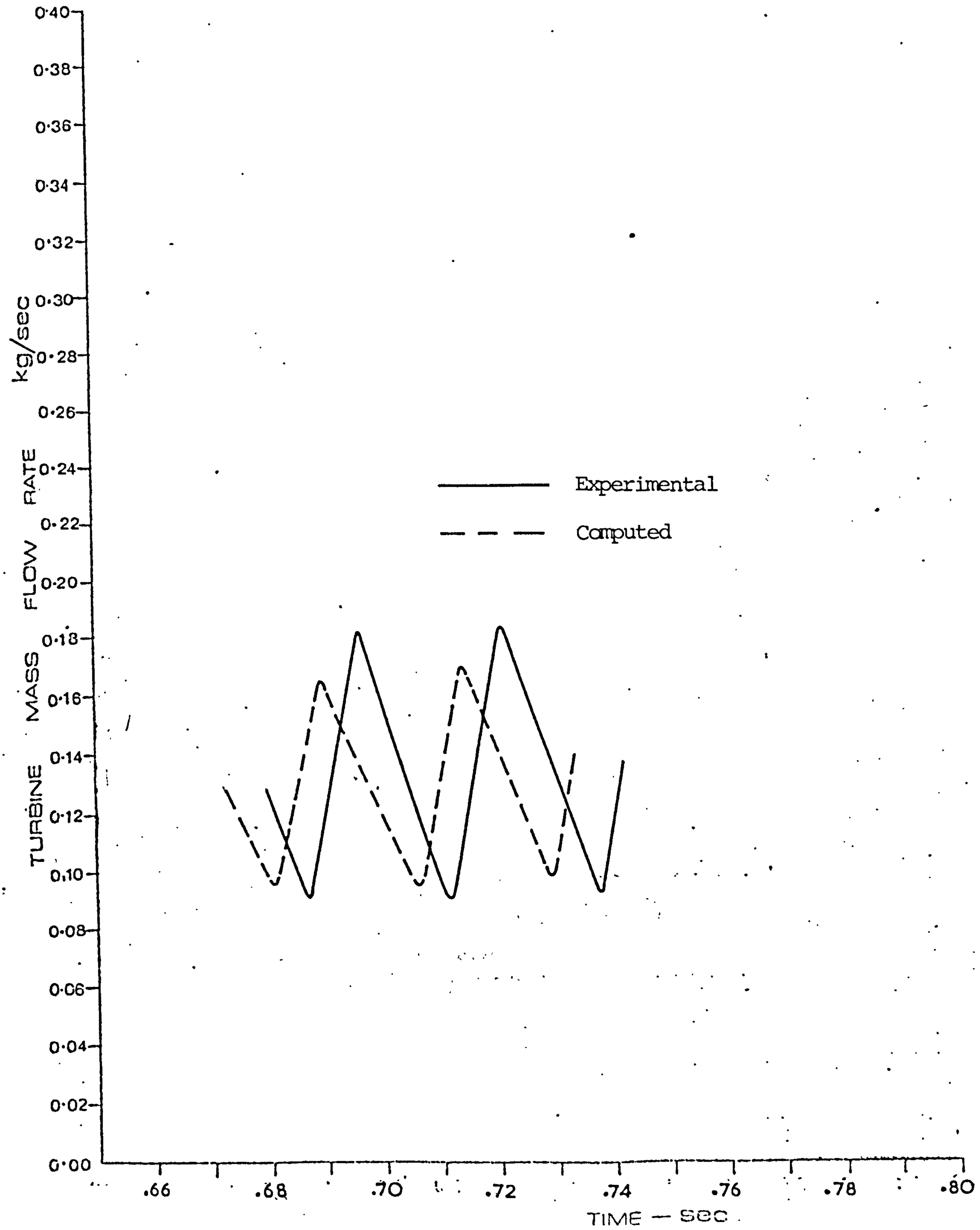

fig.(7.57) TURBINE MASS FLOW RATE DURING PULSATING TRANSIENT

PULSE FREQUENCY = 38 pulses/sec

INITIAL SUPPLY PRESSURE == 1.102 bar

FINAL SUPPLY PRESSURE == 1.764 bar

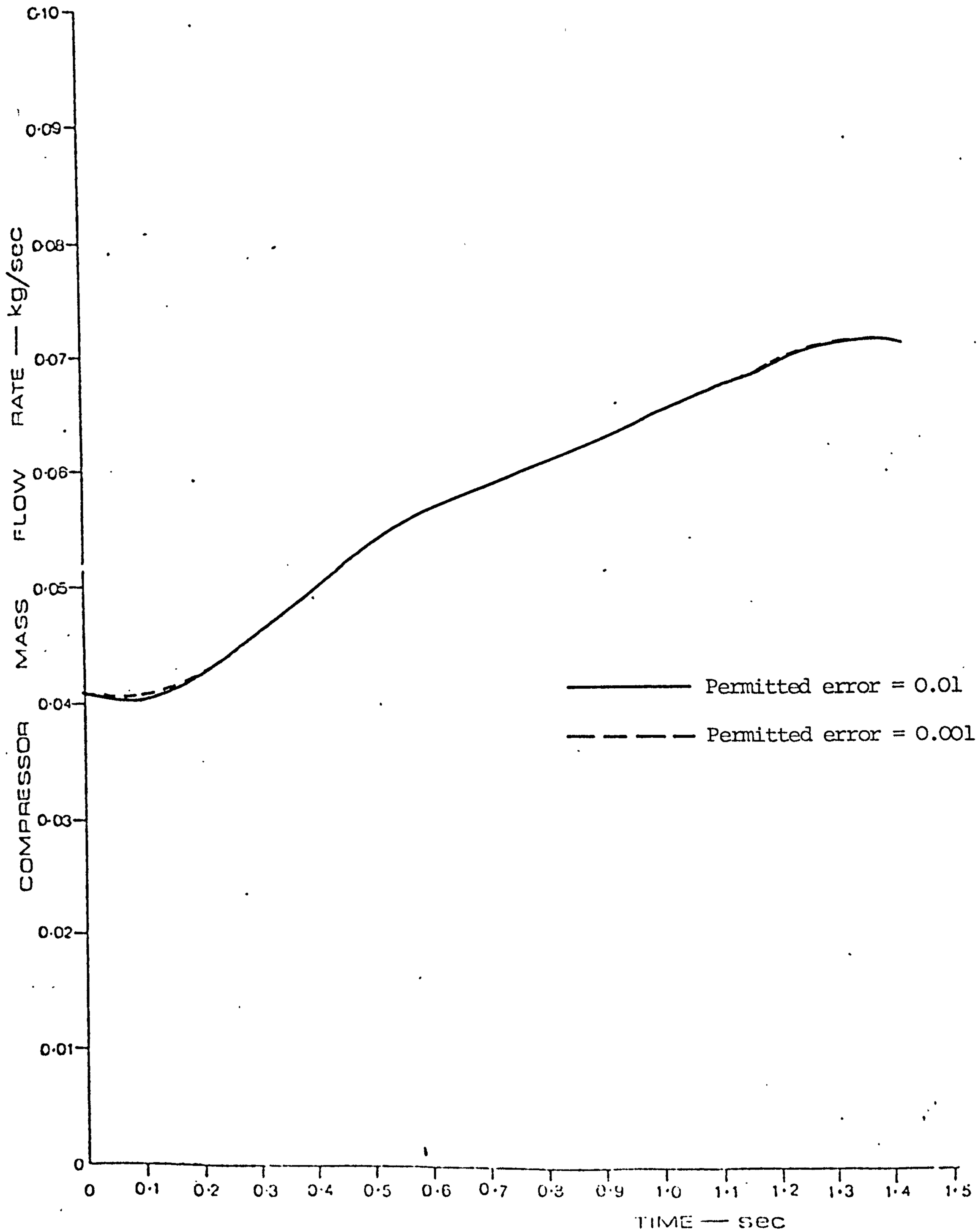

fig.(7.58). EFFECT OF CHANGING COMPUTER PROGRAM PERMITTED ERROR ON COMPRESSOR MASS FLOW RATE (PULSATING FLOW CONDITIONS)

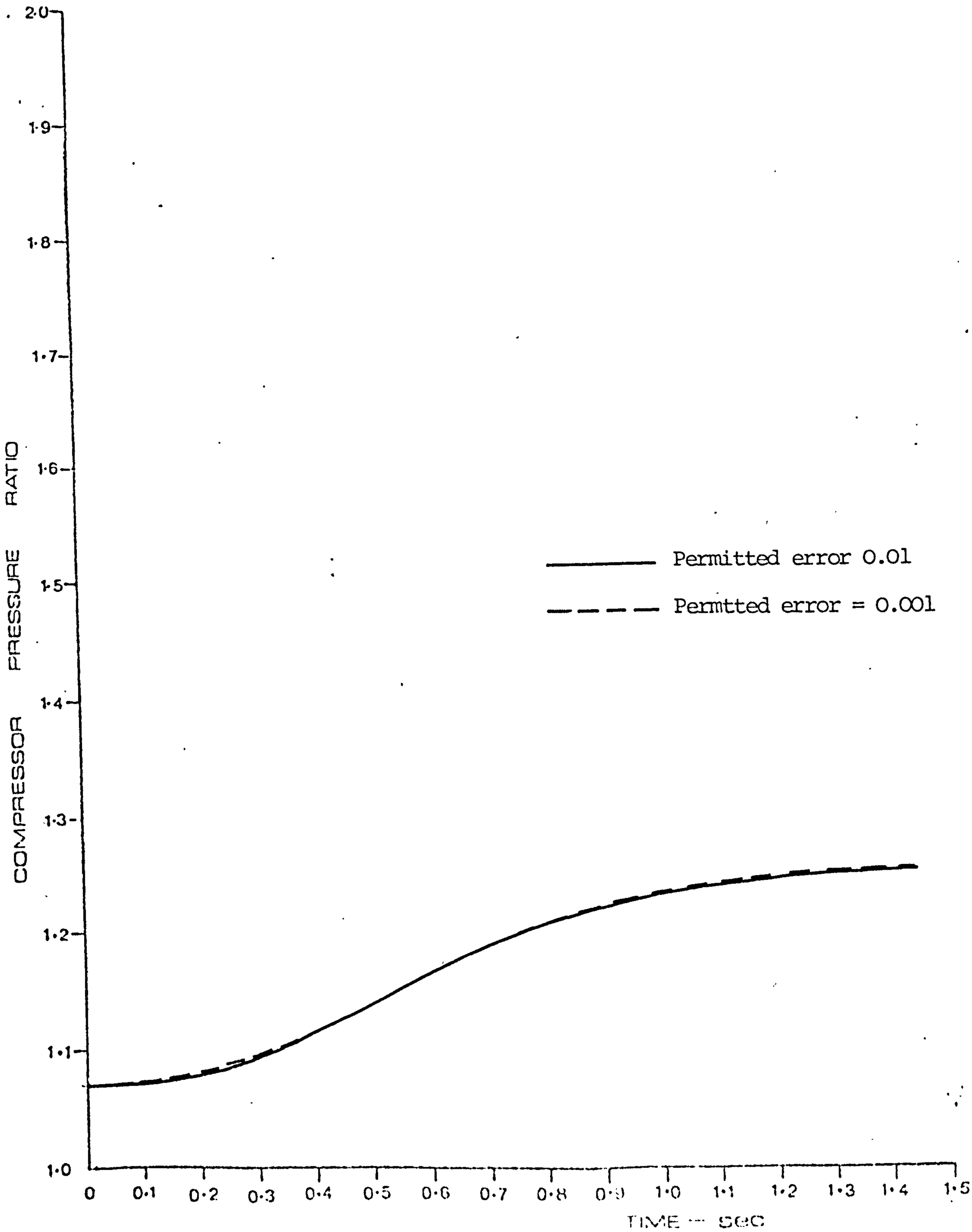

fig.(7.59) EFFECT OF CHANGING COMPUTER PROGRAM PERMITTED ERROR ON COMPRESSOR PRESSURE RATIO (PULSATING FLOW CONDITIONS)

CHAPTER EIGHT

CONCLUSIONS

1) Three computer programs to predict the transient performance of the turbocharger were developed. Comparisons between the experimental results and the theoretical predictions showed that two of the three programs, NON PULSATING and PULSATING2 gave reasonable accurate results to determine the transient response performanceof the turbocharger under both pulsating and non-pulsating flow conditions. The three programs could be run for any values of engine outlet temperature and pressure as long as the turbocharger characteristics were within the range of operation.

2) The programs assumed that the turbine and compressor operated during the transient in a quasi-steady manner. That is the steady characteristics applied instantaneously at all times. The correlation between the predicted and measured performances was sufficiently good to justify using the quasi-steady theory.

3) The programs can be used to obtain engine-turbocharger characteristics during the transient. The optimum performance of engine-turbocharger combination can then be evaluated.

4) As the compressor air mass flow rate is generally overestimated, the computed air flow should be reduced slightly in engine transient calculations.

5) The extension of the turbine and compressor steady state characteristics does not appear to introduce significant error.

6) The duration of the transient increased as the range of pressure was increased. The transient time varied from 0.5 seconds to 1.5 seconds.

7) The permitted error in the iteration process, which was used in the computer programs, was not critical.

CHAPTER NINE

RECOMMENDATIONS FOR FUTURE WORK

CHAPTER NINE

RECOMMENDATIONS FOR FUTURE WORK

1) The experimental rig could be improved by mechanising data storage during the transient by using the computer or a tape recorder to store the data for subsequent analysis instead of using a UV recorder.

2) The experimental programme could be extended by:
   i) carrying out transients at elevated temperatures;
   ii) finding the effect of turbine casing and blade design on the transient;
   iii) carrying out transients at lower and higher than pulse rates used.

3) The model used in the calculations could be improved by including variable specific heats to improve the accuracy at elevated temperatures.

REFERENCES

1. RICARDO, H R and HEMPSON, J G G — "The High Speed Internal Combustion Engine", Blackie and Son Ltd., London, 1968.

2. WALLACE, F J — "Theoretical Assessment of the Performance Characteristics of Inward Radial Flow Turbine", Proc. IMechE, Vol 172, 1958, pp 931-952.

3. WALLACE, F J, CAVE, P R and MILES, J — "Performance of Inward Radial Flow Turbine Under Steady Flow Conditions with Special Reference to High Pressure Ratios and Partial Admission", Proc. IMechE, Vol 184, Pt 1, 1969-70, p 1027.

4. BENSON, R S, GARG, R D and WOOLLATT, D — "A Numerical Solution of Unsteady Flow Problems", Int.J.Mech.Sci., 1964, Vol 6, No 1, pp 117-144.

5. BENSON, R S, WOODS, W A and WOOLLATT, D — "Unsteady Flow in Simple Branch Systems", Proc. IMechE, Vol 178, Pt 3I (iii), Paper 10, pp 24-49.

6. WHITE, D F — "A study of Turbine Performance in Non-Steady Field", Ph.D. Thesis, Penn. State University, 1958.

7. WALLACE, F J and ADGEY, J — "Theoretical Assessment of the Non-Steady Flow Performance of Inward Radial Flow Turbines", Proc. IMechE, Vol 182, Pt 3H, 1967-68, pp 22-35.

8. WALLACE, F.J., ADGEY, J and BLAIR, G P — "Performance of Inward Flow Turbines Under Non-Steady Flow Conditions", Proc. IMechE, Vol 184, Pt I, 1969-70, pp 183-195.

9. BENSON, R S and SCRIMSHAW, K H — "An Experimental Investigation of Non-Steady Flow in a Radial Gas Turbine", Proc. IMechE, Vol 180, Pt 3J, 1965-66, pp 74-85.

10. WALLACE, F J and BLAIR, G P — "The Pulsating Flow Performance of Inward Radial Flow Turbines", ASME, 65-GTP-21, 1965, ASME Gas Turbine Conference, Washington.

11. CRAIG, H R M
EDWARDS.K J
JANOTA, M
HORLOCK, J H
SHAW, R
and
WOODS, W A
"An Investigation of Steady and Unsteady Flow Through a Napier Turboblower Turbine Under Conditions of Full and Partial Admission", Proc. IMechE, Vol 183, Pt 1, No. 30, 1968-69, pp 615-626.

12. DANESHYAR, H
EDWARDS, F J
HORLOCK, J H
JANOTA, M
PEARSON, R D
and
SHAW, R
"A Comparison of the Performance of Three Model Axial Flow Turbines Tested Under Both Steady and Pulse Flow", Proc. IMechE, Vol 184, Pt 1, 1969-70, pp 1119-1131.

13. WHITEHOUSE, N D
STOTTER, A
and
JANOTA, M S
"Estimating the Effects of Altitude, Ambient Termperature and Turbochanger Match on Engine Performance", Proc. IMechE, Vol 178, Pt 1, No 19, 1963-64, pp 483-500.

14. WALLACE, F J
and
MILES, J
"Performance of Inward Flow Turbine Under Unsteady Flow Conditions with Full and Partial Admission", Proce. IMechE, Vol 185, 1970-71, pp 1091-1105.

15. MIYASHITA, T
TOMITA, T
and
ISHIHARA, D
"Performance of Inward Radial Flow Turbine Under Unsteady Flow Conditions - Influence of Pulse Frequency", IHI Engineering Review, Vol 7, No. 1 1974.

16. BENSON, R S
"Non-Steady Flow in a Turbocharger Nozzleless Radial Gas Turbine", National Combined Farm Construction & Industrial Machinery and Power Plant Meetings, Milwaukee, Wis., Sept 9-12, 1974, SAE Paper No. 740 739.

17. KASTNER, L J
and
BHINDER, F S
"A Method for Predicting the Performance of a Centripetal Gas Turbine Fitted with Nozzleless Volute Casing", ASME paper No. 75-GT-65, March 1975.

18. BHINDER, F S
and
GULATI, P S
"A Method for Predicting the Performance of Centripetal Turbines in Non-steady Flow", IMechE, Paper No. C77/78, April 1978.

19. SHAMSI, S S
"Experimental and Analytical Investigations of the Transient Performance of a Turbocharged Diesel Engine", M.Sc. Thesis, UMIST, 1974.

20. SHAMSI, S S — "Estimating the Influence of Pulsating Flow conditions on the Performance of a Turbine", SAE Spec. Publ. SP 442, Feb 26 - Mar 2, 1979.

21. WHITFIELD, A and WALLACE, F J — "A New Approach to the Problem of Predicting the Performance of Centrifugal Compressors", 2nd Int. JSME Symposium, Tokyo, 1972.

22. WHITFIELD, A and WALLACE, F J — "Performance Prediction for Automotive Turbocharger Compressors", Proc. IMechE, Vol 189, No 12, 1975, pp 59-67.

23. BENSON, R S and WHITFIELD, A — "Application of Non-Steady Flow in a Rotating Duct to Pulsating Flow in a Centrifugal Compressor", Proc. IMechE, Vol. 182, Pt 3H, 1967-68, pp 184-196.

24. BENSON, R S and WHITFIELD, A — "An Experimental Investigation of the Non-Steady Flow Characteristics of a Centrifugal Compressor", Proc. IMechE, Vol 180, Pt 1, No. 27, 1966, pp 641-660.

25. BENSON, R S and WHITFIELD, A — "A Quasi-Steady Flow Representation of Centrifugal Compressor Performance Characteristics in Non-Steady Flow Systems", Proc. IMechE, Vol 182, Pt 3H, 1967-68, pp 197-208.

26. LEDGER, J D BENSON, R S and FURUKAWA, H — "Performance Characteristics of a Centrifugal Compressor with Air Injection", Proc. IMechE, Vol 187, 1973, pp 425-434.

27. BENSON, R S LEDGER, J D and FURUKAWA, H — "Improvement in Transient Performance of a Turbocharged Diesel Engine by Air Injection into the Compressor", SAE, Paper No. 730, 665, 1973.

28. ABURWIN, A B — "The Transient Response Characteristics of an Exhaust Gas Turbocharger", M.Sc. Thesis, University of Salford, 1973.

29. STOCKTON, E C — "An Investigation into the Transient Response Characteristics of an Exhaust Gas Turbocharger", PhD Thesis, University of Salford, 1979.

30. BRITISH STANDARD 1042 — "Methods of Measurements of Fluid Flow in Pipes", Pt 1, 1964.

31. JENNEY, E — "Undimensional Transient Flow with Consideration of Friction, Heat Transfer and Change in Section", Brown Boveri Review, Vol 37, No 11, 1950, pp 447-461

32. WALLACE, F J and NASSIF, M H — "Air Flow in Naturally Aspirated Two Stroke Engine", Proc. IMechE, Vol 168, 1954, pp 515-535.

33. CONSIDINE — "Process Instruments and Controls Handbook", McGraw Hill, 1957.

34. BENSON, R S and BRUNDRETT, G W — "Development of a Resistance Wire for Measuring Transient Temperatures in Exhaust Systems of Internal Combustion Engines". Temperature, Its Measurement and Control in Science and Industry, Vol 3, Pt 2, Chapman Hall Ltd, London, 1962, pp 631-653.

35. BENSON, R S — "Measurement of Transient Exhaust Temperatures in I C Engines", The Engineer, Vol 217, 1964, pp 378-383.

36. WILLLIAMS, T J and COX, J B — "The Influence of Exhaust Poppet Valve Gas Flow on Reciprocating Engine Noise", Proc. IMechE, Vol 189, 1975, pp 461-469.

37. SCHLICHTING, H — "Boundary Layer Theory", McGraw Hill Co., New York, 1968.

38. BP TRADING LTD — "Lubrication Theory and its Application", Harrison and Son Ltd., High Wycombe, Bucks, 1969.

39. FREEMAN, P — "Lubrication and Friction", Sir Isaac Pitman & Sons Ltd, 1962.

40. CAMERON, A — "Basic Lubrication Theory", Longman, 1971.

41. SHELL UNITED KINGDOM OIL — Telegram Ref: UKL 060062 dated 7.8.1980.

42. LIST, H — "The Charging Processes of Internal Combustion Engines with Special Performance to the Two Stroke Cycle", Proc. IMechE, Auto Div, 1953-1954, pp 45-68.

43. EARNSHAW, S — "On the Mathematical Theory of Sound", Phil Trans Roy Soc, 150, 1860, pp 133-148.

44. SHAPIRO, A H — "The Dynamic and Thermodynamic of Compressible Fluid Flow", Ronald Press Co, 1953.

45. BENSON, R S GARG, R D and WOLLATT, D — "The Numerical Solution of Unsteady Flow Problems", International Journal of Mechanical Sciences, Vol 6, No 1, 1964, pp 117-144.

46. RYTI, M "Computing the Gas Exchange Process of pressure charged IC Engines", IMechE Symposium, Computers in IC Engine Design. Proc. IMechE, Vol 182, Pt 3L, 1967-68, pp 109-118.

47. EBERLE, M "Computation of Scavenging and Supercharging of Internal Combustion Engines", Proc. IMechE, Vol 182, Pt 3L, 1967-68, pp 119-128.

48. BARNA, P S "Fluid Mechanics for Engineers", 3rd Edition, Butterworths, London, 1971.

49. TRENGROUSE, G M IMRIE, B W and MALE, D H "Comparison of Unsteady Flow Discharge Coefficients for Sharp-Edged Orifice with Steady Flow Valves", Journal Mech Eng Science, Vol 8, No. 3, 1966, pp 322-329.

APPENDIX ONE

UNSTEADY FLOW DISCHARGE COEFFICIENT FOR ORIFICE PLATE

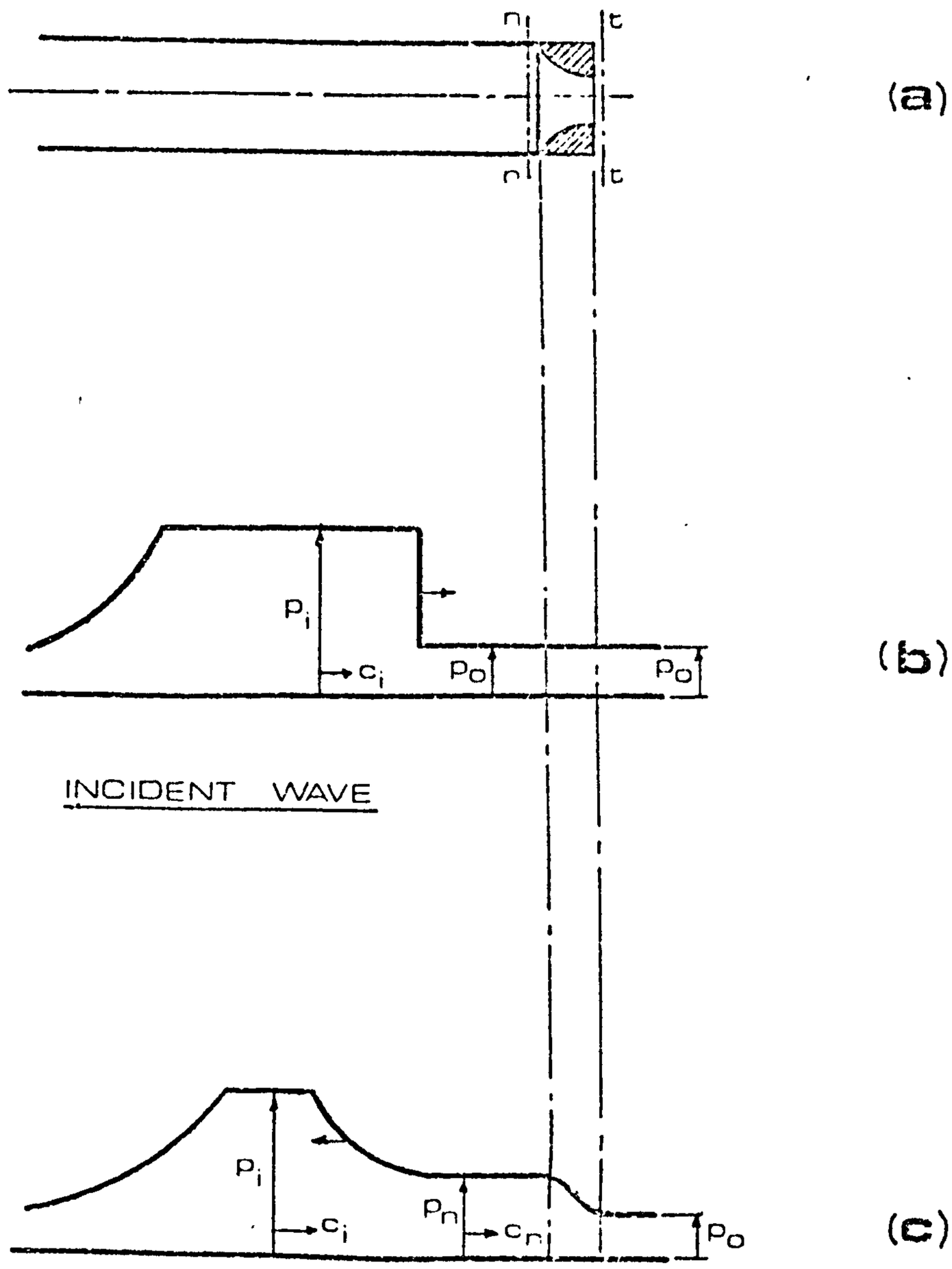

WAVE DIAGRAM DURING SUPERPOSITION

fig.(A1.1). SHOCK TUBE WAVE

Substituting equations (82) and (83) into equation (80),

$$\delta c = \frac{1}{\rho_o a_o} \left(\frac{P}{P_o}\right)^{-\left(\frac{\gamma+1}{2\gamma}\right)} \delta P \quad . \qquad \ldots \ldots \quad (84)$$

Integrating between P_o and P

$$c_i - c_o = \frac{1}{\rho_o a_o} \int_{P_o}^{P} \left(\frac{P}{P_o}\right)^{-\left(\frac{\gamma+1}{2\gamma}\right)} dP$$

$$= \frac{P_o}{a_o \rho_o} \times \frac{2\gamma}{\gamma-1} \left[\left(\frac{P}{P_o}\right)^{\frac{\gamma-1}{2\gamma}} - 1\right] . \qquad \ldots \ldots \quad (85)$$

When $P = P_o$ the particle velocity c will equal zero,

$$c_o = 0$$

$$c = \frac{P_o}{a_o \rho_o} \frac{2\gamma}{\gamma-1} \left[\left(\frac{P}{P_o}\right)^{\frac{\gamma-1}{2\gamma}} - 1\right] \qquad \ldots \ldots \quad (86)$$

but

$$a_o^2 = \frac{\gamma P_o}{\rho_o} \quad . \qquad \ldots \ldots \quad (87)$$

Substituting equation (87) into equation (86),

$$c = \frac{2}{\gamma-1} a_o \left[\left(\frac{P}{P_o}\right)^{\frac{\gamma-1}{2\gamma}} - 1\right] . \qquad \ldots \ldots \quad (88)$$

This is a particle velocity equation of a non-steep wave.

Consider two non-steep waves propagating towards each other through air having absolute pressure and acoustic velocity P_o and a_o respectively. Let the amplitude ratios of the two waves be $\frac{P_i}{P_o}$ and $\frac{P_r}{P_o}$ and the corresponding particle velocity be c_i and c_r respectively, and the resulted wave c_n, from equation (88),

$$c_i = \frac{2}{\gamma-1} a_o \left[\left(\frac{P_i}{P_o}\right)^{\frac{\gamma-1}{2\gamma}} - 1 \right] \qquad \ldots \quad \ldots \quad (89)$$

$$c_r = -\frac{2}{\gamma-1} a_o \left[\left(\frac{P_r}{P_o}\right)^{\frac{\gamma-1}{2\gamma}} - 1 \right] \qquad \ldots \quad \ldots \quad (90)$$

$$c_n = \frac{2}{\gamma-1} a_o \left[\left(\frac{P_n}{P_o}\right)^{\frac{\gamma-1}{2}} - 1 \right] \qquad \ldots \quad \ldots \quad (91)$$

but

$$c_n = c_i - c_o \ . \qquad \ldots \quad \ldots \quad (92)$$

Substituting equations (89),(90) and (91) into equation (92),

$$\left(\frac{P_n}{P_o}\right)^{\frac{\gamma-1}{2\gamma}} = \left(\frac{P_i}{P_o}\right)^{\frac{\gamma-1}{2\gamma}} - \left(\frac{P_r}{P_o}\right)^{\frac{\gamma-1}{2\gamma}} + 1 \ . \qquad \ldots \quad \ldots \quad (93)$$

Let

$$\left(\frac{P_n}{P_o}\right)^{\frac{\gamma-1}{2\gamma}} = X_n \qquad \ldots \quad \ldots \quad (94)$$

$$\left(\frac{P_i}{P_o}\right)^{\frac{\gamma-1}{2\gamma}} = X_i \qquad \ldots \quad \ldots \quad (95)$$

$$\left(\frac{P_r}{P_o}\right)^{\frac{\gamma-1}{2\gamma}} = X_r \quad . \qquad \ldots \quad \ldots \quad (96)$$

Substituting equations (94), (95), and (96) into equation (93),

$$X_n = X_i + X_r - 1 \quad . \qquad \ldots \quad \ldots \quad (97)$$

Similarly, consider the propagation of the wave of amplitude ratio $\frac{P_n}{P_o}$ .into gas already under the influence of a wave of amplitude ratio $\frac{P_i}{P_o}$,

$$c_n - c_i = - \frac{2}{\gamma-1} a_i \left[\left(\frac{P_n}{P_i}\right)^{\frac{\gamma-1}{2\gamma}} - 1 \right] . \qquad \ldots \quad \ldots \quad (98)$$

Substituting equation (89) into equation (98) and rearranging,

$$c_n = \frac{2}{\gamma-1} a_o \left[\left(\frac{P_i}{P_o}\right)^{\frac{\gamma-1}{2\gamma}} - 1 \right] - \frac{2}{\gamma-1} a_i \left[\left(\frac{P_n}{P_i}\right)^{\frac{\gamma-1}{2\gamma}} - 1 \; . \right]$$

$$\ldots \quad \ldots \quad (99)$$

Assuming the flow to be isentropic,

$$a_i = a_o \left(\frac{P_i}{P_o}\right)^{\frac{\gamma-1}{2\gamma}} . \qquad \ldots \quad \ldots \quad (100)$$

Let

$$\frac{c_n}{a_o} = Y_n \quad . \qquad \ldots \ldots \quad (101)$$

Then substituting equations (100), (101) into equation (99),

$$Y_n = \frac{2}{\gamma-1} (2\ X_i - X_n - 1) \quad . \qquad \ldots \ldots \quad (102)$$

Assuming that $\gamma = 1.4$,

$$Y_n = 5(2\ X_i - X_n - 1) \quad . \qquad \ldots \ldots \quad (103)$$

WAVE ACTION IN THE ORIFICE PLATE

The flow through the orifice plate during the period of wave superposition following the arrival of the wave at the orifice plate is assumed to be isentropic, one dimensional and quasi-steady. The maximum incident wave amplitudes to be considered are those giving sonic flow when the pressure at exit from the orifice plate is atmospheric. Referring to Fig (A1.1c), which shows the wave diagram during the quasi-steady flow period, and applying the equations of energy and mass continuity between station n in the pipe, immediately upstream of the orifice plate, and station t immediately

downstream from the orifice plate,

$$C_p T_n + \frac{c_n^2}{2} = C_p T_t + \frac{c_t^2}{2} \quad . \qquad \ldots \ldots \quad (104)$$

Let

$$\frac{c_t}{a_o} = y_t \quad . \qquad \ldots \ldots \quad (105)$$

Then substituting equations (101) and (105) into equation (104),

$$\frac{C_p T_n}{a_o^2} + y_n^2 = \frac{2C_p T_t}{a_o^2} + y_t^2 \qquad \ldots \ldots \quad (106)$$

but

$$P_n = \rho_n R T_n \qquad \ldots \ldots \quad (107)$$

$$P_t = \rho_t R T_t \qquad \ldots \ldots \quad (108)$$

and

$$C_p = \frac{\gamma R}{\gamma - 1} \quad . \qquad \ldots \ldots \quad (109)$$

Substituting equations (87), (107) and (109) into equation (106) ,

$$\frac{2}{\gamma-1}\,\frac{\frac{P_n}{P_o}}{\frac{\rho_n}{\rho_o}} + y_n^2 = \frac{2}{\gamma-1}\,\frac{\frac{P_t}{P_o}}{\frac{\rho_t}{\rho_o}} \quad . \qquad \ldots \quad \ldots \quad (110)$$

As the flow is assumed to be isentropic

$$\frac{\rho_n}{\rho_o} = \left(\frac{P_n}{P_o}\right)^{\frac{1}{\gamma}} \qquad \ldots \quad \ldots \quad (111)$$

$$\frac{\rho_t}{\rho_o} = \left(\frac{P_t}{P_o}\right)^{\frac{1}{\gamma}} \quad . \qquad \ldots \quad \ldots \quad (112)$$

Substituting equations (111) and (112) into equation (110),

$$\frac{2}{\gamma-1}\left(\frac{P_n}{P_o}\right)^{\frac{\gamma-1}{2\gamma}} + y_n^2 = \frac{2}{\gamma-1}\left(\frac{P_t}{P_o}\right)^{\frac{\gamma-1}{2\gamma}} + y_t^2 \quad . \qquad \ldots \quad \ldots \quad (113)$$

Let

$$\left(\frac{P_t}{P_o}\right)^{\frac{\gamma-1}{2\gamma}} = X_t \quad . \qquad \ldots \quad \ldots \quad (114)$$

Substituting equations (94) and (114) into equation (113), and assuming $\gamma = 1.4$,

$$5X_n^2 + y_n^2 = 5\,X_t^2 + y_t^2 \quad . \qquad \ldots \quad \ldots \quad (115)$$

The continuity equation gives

$$\rho_n\, c_n\, A_n = \rho_t\, c_t\, A_t \quad . \qquad \ldots \quad \ldots \quad (116)$$

Substituting equations (111) and (112) into (116),

$$\rho_o \left(\frac{P_n}{P_o}\right)^{\frac{1}{\gamma}} c_n A_n = \rho_o \left(\frac{P_t}{P_o}\right)^{\frac{1}{\gamma}} c_t A_t \ . \qquad \ldots \ldots \quad (117)$$

Let

$$\left(\frac{P_t}{P_o}\right)^{\frac{\gamma-1}{2\gamma}} = X_t \ . \qquad \ldots \ldots \quad (118)$$

Then substituting equations (94) and (118) into equation (117),

$$\frac{Y_n}{Y_t} = \left(\frac{A_t}{A_n}\right) \left(\frac{X_t}{X_n}\right)^{\frac{2}{\gamma-1}} \ . \qquad \ldots \ldots \quad (119)$$

Let $\frac{A_t}{A_n} = m_e$ the effective area ratio, then for $\gamma = 1.4$,

$$\frac{Y_n}{Y_t} = m_e \left(\frac{X_t}{X_n}\right)^5 \ . \qquad \ldots \ldots \quad (120)$$

If the flow at the orifice plate is subsonic, then

$$P_t = P_o \text{ and } X_t = 1.$$

Equations (115) and (120) become,

$$5\ X_n^2 + Y_n^2 = 5 + Y_t^2 \qquad \ldots \ldots \quad (121)$$

$$\frac{Y_n}{Y_t} \doteq \frac{m_e}{X_n^5} \ . \qquad \ldots \ldots \quad (122)$$

If the flow at the orifice plate is sonic, then the Mach number at the throat is equal 1, and $y_t = 1$.

Equation (115) and (120) then become

$$5\,x_n^2 + y_n^2 = 6 \qquad \text{.. .. (123)}$$

$$y_n = \frac{m_e}{x_n^{\,5}} \qquad \text{.. .. (124)}$$

DISCHARGE COEFFICIENTS

The discharge coefficient is calculated by measuring X_n and X_i (equations (94) and (95)), calculating y_n using equation (103), and evaluating y_t using equation (115), so that the effective area ratio m_e may be calculated from equation (120). The discharge coefficient can then be obtained by dividing the effective area m_e by the geometric area m

$$Cdp = \frac{m_e}{m} \; . \qquad \text{.. .. (125)}$$

As mentioned in section 4.2, standard BS1042[30] orifice plates with corner tappings were used to measure the mass flow rates through the turbine and compressor under the transient operation. A record of the variation of the upstream pressure and temperature as well as the pressure drop across the orifice plate was obtained from the UV recorder. Using these recorded values with the transient coefficient of discharge and applying the appropriate relationship the mass flow through the orifice plate was calculated as follows:

Applying the energy equation between the pipe (e) and the throat (a) gives

$$h_e + \frac{c_e^2}{2} = h_a + \frac{c_a^2}{2} \qquad \ldots\ldots (126)$$

$$1 + \frac{c_e^2}{2C_pT_a} = \frac{T_a}{T_e} + \frac{c_a^2}{2C_pT_e} . \qquad \ldots\ldots (127)$$

Applying the continuity equation between (e) and (a)

$$\rho_e F_e c_e = \rho_a F_a c_a$$

$$c_e = \frac{\rho_a F_a c_a}{\rho_e F_e} \qquad \ldots\ldots (128)$$

Substituting for c_e from equation (128) into equation (127) gives

$$1 + \left(\frac{\rho_a}{\rho_e}\right)^2 \left(\frac{F_a}{F_e}\right)^2 \frac{c_a^2}{2C_p T_e} = \frac{T_a}{T_e} + \frac{c_a^2}{2C_p T_a} \qquad \ldots\ldots (129)$$

The isentropic relations are

$$\frac{\rho_a}{\rho_e} = \left(\frac{P_a}{P_e}\right)^{\frac{1}{\gamma}} \qquad \ldots\ldots (130)$$

$$\frac{T_a}{T_e} = \left(\frac{P_a}{P_e}\right)^{\frac{\gamma-1}{\gamma}} \qquad \ldots\ldots (131)$$

Substituting for $\frac{\rho_a}{\rho_e}$ and $\frac{T_a}{T_e}$ from equations (130) and (131) into equation (129) to eliminate $\frac{\rho_a}{\rho_e}$ and $\frac{T_a}{T_e}$

$$1 + \left(\frac{P_a}{P_e}\right)^{\frac{2}{\gamma}} \left(\frac{F_a}{F_e}\right)^2 \frac{c_a^2}{2C_p T_e} = \left(\frac{P_a}{P_e}\right)^{\frac{\gamma-1}{\gamma}} + \frac{c_e^2}{2C_p T_a} \qquad \ldots\ldots (132)$$

Solving (132) for c_a

$$c_a = \left[\frac{2C_p T_e\left(\left(\frac{P_a}{P_e}\right)^{\frac{\gamma-1}{\gamma}} - 1\right)}{\left(\frac{P_a}{P_e}\right)^{\frac{2}{\gamma}} \left(\frac{F_a}{F_e}\right)^2 - 1}\right] \qquad \ldots\ldots (133)$$

since

$$\dot{m} = \rho_a c_a F_a \qquad \text{.. .. (134)}$$

$$\rho_e = \frac{P_e}{RT_e} \qquad \text{.. .. (135)}$$

$$C_p = \frac{\gamma}{\gamma-1} R \ . \qquad \text{.. .. (136)}$$

Substituting equations (130), (133),(135) and (136) into equation (134) gives

$$\dot{m} = \frac{p_e F_a \left[\frac{2\gamma}{\gamma-1} \frac{1}{RT_e} \left(\left(\frac{p_a}{p_e}\right)^{\frac{\gamma+1}{\gamma}} - \left(\frac{p_a}{p_e}\right)^{\frac{2}{\gamma}} \right)\right]^{\frac{1}{2}}}{\left[\left(\frac{p_a}{p_e}\right)^{\frac{2}{\gamma}} \left(\frac{F_a}{F_e}\right)^2 - 1\right]^{\frac{1}{2}}} \qquad \text{.. (137)}$$

Correcting equation (137) for the discharge coefficient, the mass flow rate is given by

$$m = \frac{Cdp\ P_e\ F_a \left[\frac{2\gamma}{\gamma-1} \frac{1}{RT_e} \left(\left(\frac{p_a}{p_e}\right)^{\frac{\gamma+1}{\gamma}} - \left(\frac{p_a}{p_e}\right)^{\frac{2}{\gamma}} \right)\right]^{\frac{1}{2}}}{\left[\left(\frac{p_a}{p_e}\right)^{\frac{2}{\gamma}} \left(\frac{F_a}{F_e}\right)^2 - 1\right]} \qquad \text{.. (138)}$$

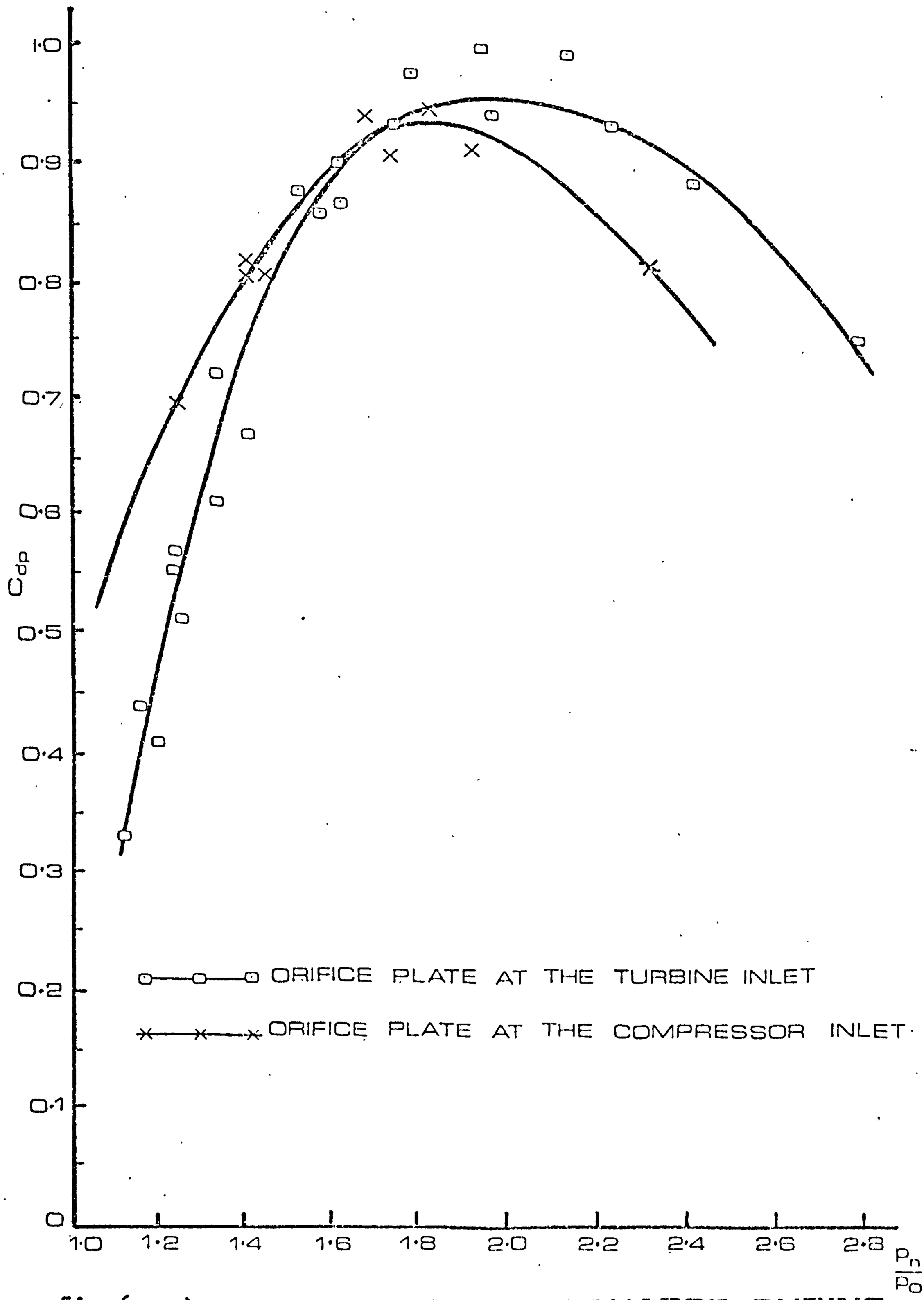

fig.(A1.2) COEFFICIENT OF DISCHARGE DURING UNSTEADY FLOW FOR THE ORIFICE PLATES

APPENDIX TWO

MEASURING MASS FLOW RATE BY BS 1042

APPENDIX 2

MEASURING MASS FLOW RATE BY BS1042

The British Standard method for calculating the mass flow rate through an orifice plate or a nozzle is explained in detail in BS1042[27]. The equations used are presented below with a brief explanation of the various factors.

$$W = 0.01252\ CZ\varepsilon Ed^2\sqrt{h\rho} \qquad \ldots \ldots \quad (128)$$

where		units
W	mass flow rate	kg/h
C	basic coefficient	
Z	correction factor which is the product of Z_R and Z_D where Z_R is Reynolds number correction factor and Z_D is pipe size correction factor	
ε	expansibility factor	
E	velocity of approach faster $= \frac{1}{\sqrt{1-m^2}}$ where $m = \frac{\text{orifice plate or throat area}}{\text{pipe area}}$	
d	diameter of the orifice plate or throat	mm
h	the difference between pressures at the upstream and downstream pressure tappings	mm H_2O
ρ	density of the fluid at the upstream pressure tapping .	kg/m^3

All the above factors are to be obtained from tables and graphs shown in BS1042[30].

APPENDIX 2

MEASURING MASS FLOW RATE BY BS1042

The British Standard method for calculating the mass flow rate through an orifice plate or a nozzle is explained in detail in BS1042[27]. The equations used are presented below with a brief explanation of the various factors.

$$W = 0.01252\ CZ\varepsilon Ed^2\sqrt{h\rho} \qquad \ldots \ldots \quad (128)$$

where		units
W	mass flow rate	kg/h
C	basic coefficient	
Z	correction factor which is the product of Z_R and Z_D where Z_R is Reynolds number correction factor and Z_D is pipe size correction factor	
ε	expansibility factor	
E	velocity of approach faster $= \frac{1}{\sqrt{1-m^2}}$ where $m = \frac{\text{orifice plate or throat area}}{\text{pipe area}}$	
d	diameter of the orifice plate or throat	mm
h	the difference between pressures at the upstream and downstream pressure tappings	mm H_2O
ρ	density of the fluid at the upstream pressure tapping .	kg/m^3

All the above factors are to be obtained from tables and graphs shown in BS1042[30].

APPENDIX THREE

TURBINE AND COMPRESSOR STEADY STATE CHARACTERISTICS

APPENDIX 3
TURBINE AND COMPRESSOR STEADY STATE CHARACTERISTICS

As the turbocharger manufacturers (Holset Engineering Company) could not supply turbine characteristics and the available compressor characteristics were very limited, an experimental data obtained by Stockton[29] to derive the characteristics of the turbine and compressor under cold conditions was used. In order to present this data in a suitable form for the computer programs of this thesis, the following points were observed:

(1) It was found that there was a little change in turbine inlet temperature T_3 for each turbocharger speed. Thus, it was assumed that the change could be neglected and average T_3 was taken to find the dimensionless speed parameter $\frac{N}{\sqrt{T_3}}$. In addition, the small change in the turbine speed during a constant speed test was neglected. Hence, $\frac{N}{\sqrt{T_3}}$ parameter was regarded as constant for calculation at a particular speed.

(2) Turbine mass flow parameter was presented in the form of normal pseudo non-dimensional parameter $\frac{\dot{m}_t \sqrt{T_3}}{P_3}$ and was presented as a function of pressure ratio.

(3) The experimental characteristics have been extended to cover the greater range of operation expected during the

transient flow tests. The standard shape of performance curves of radial turbine and compressor have been assumed for this purpose, the extended characteristics being shown by dotted curves, and the original characteristics by full curves. The turbine and compressor characteristics were plotted as shown in Figs (6.3), (6.4), (6.5), and (A3.1)

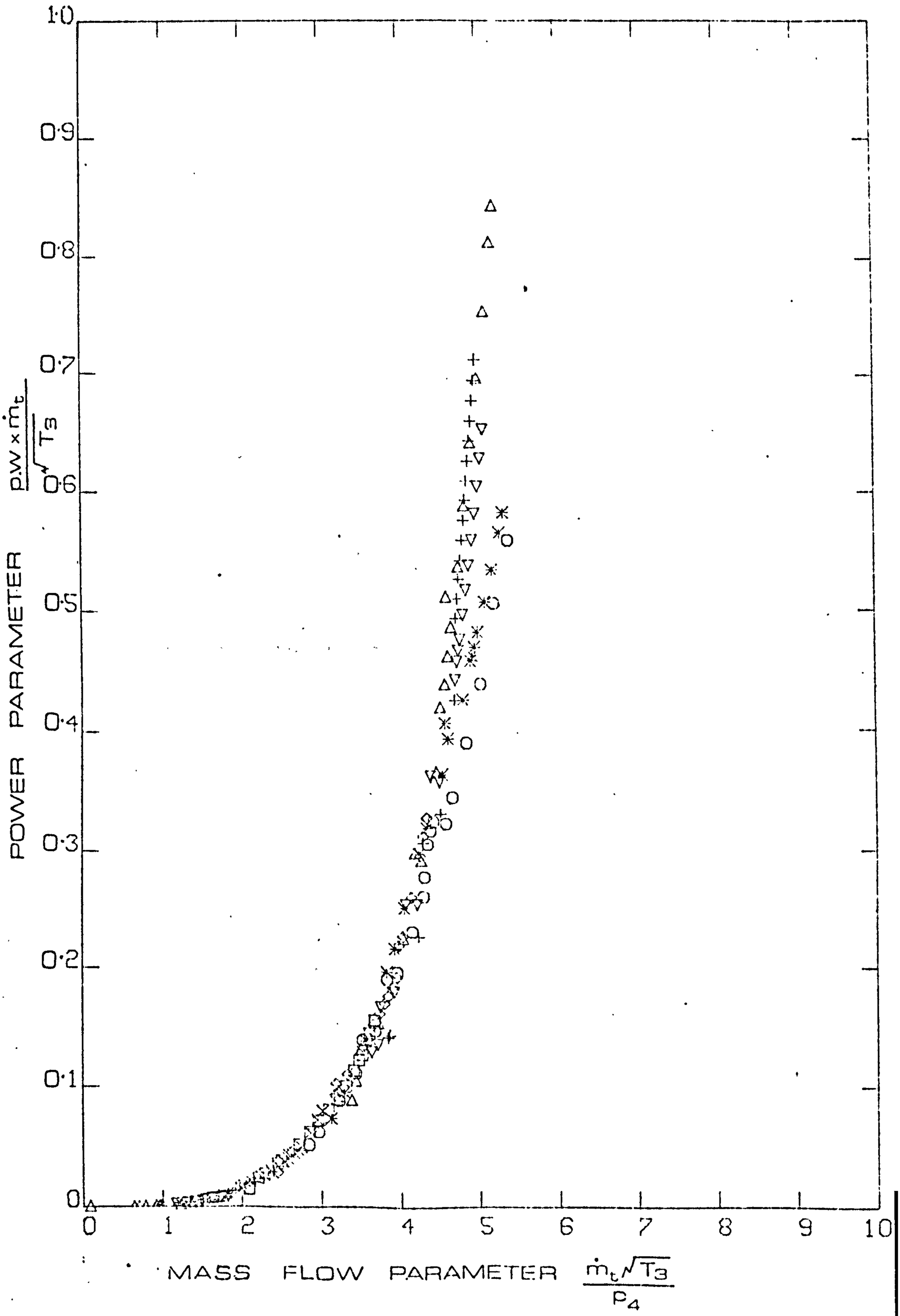

fig.(A3.1) TURBINE STEADY CHARACTERISTIC

APPENDIX FOUR

COMPRESSOR LOADING NOZZLE MASS FLOW RATE

APPENDIX 4

COMPRESSOR LOADING NOZZLE MASS FLOW RATE

In order to evaluate the mass flow rate through the compressor, a nozzle was designed, Fig (3.3), and then fitted at the compressor outlet to represent the engine. By assuming that the nozzle downstream pressure was constant, the nozzle mass flow rate through the nozzle could be calculated from the nozzle inlet conditions. The pressure change from the compressor outlet to the nozzle inlet was found to be very small and by assuming adiabatic flow, the compressor outlet conditions could be considered to be the same as the nozzle inlet conditions. A characteristic curve was drawn for the nozzle so that the mass flow rate through the nozzle could be predicted readily. To enable the characteristic curve to be used for varying supply conditions, the supply pressure was plotted against mass flow parameter $\frac{\dot{m}_z}{p_2^{\frac{1}{2}}}$. This characteristic curve, Fig (A4.1), was constructed as follows:

(a) Part AB-BS1042, Clause 78, was used to calculate the mass flow parameter for a pressure differential of up to 1.2 bar.

(b) Part CD-BS1042, Clauses 50 and 82, were used to calculate the mass flow parameter when the pressure ratio was greater than the critical pressure ratio which is 1.8.

(c) Part BC - The characteristics for Sections AB and CD were joined by a smooth curve as no data was available for this section of the characteristic.

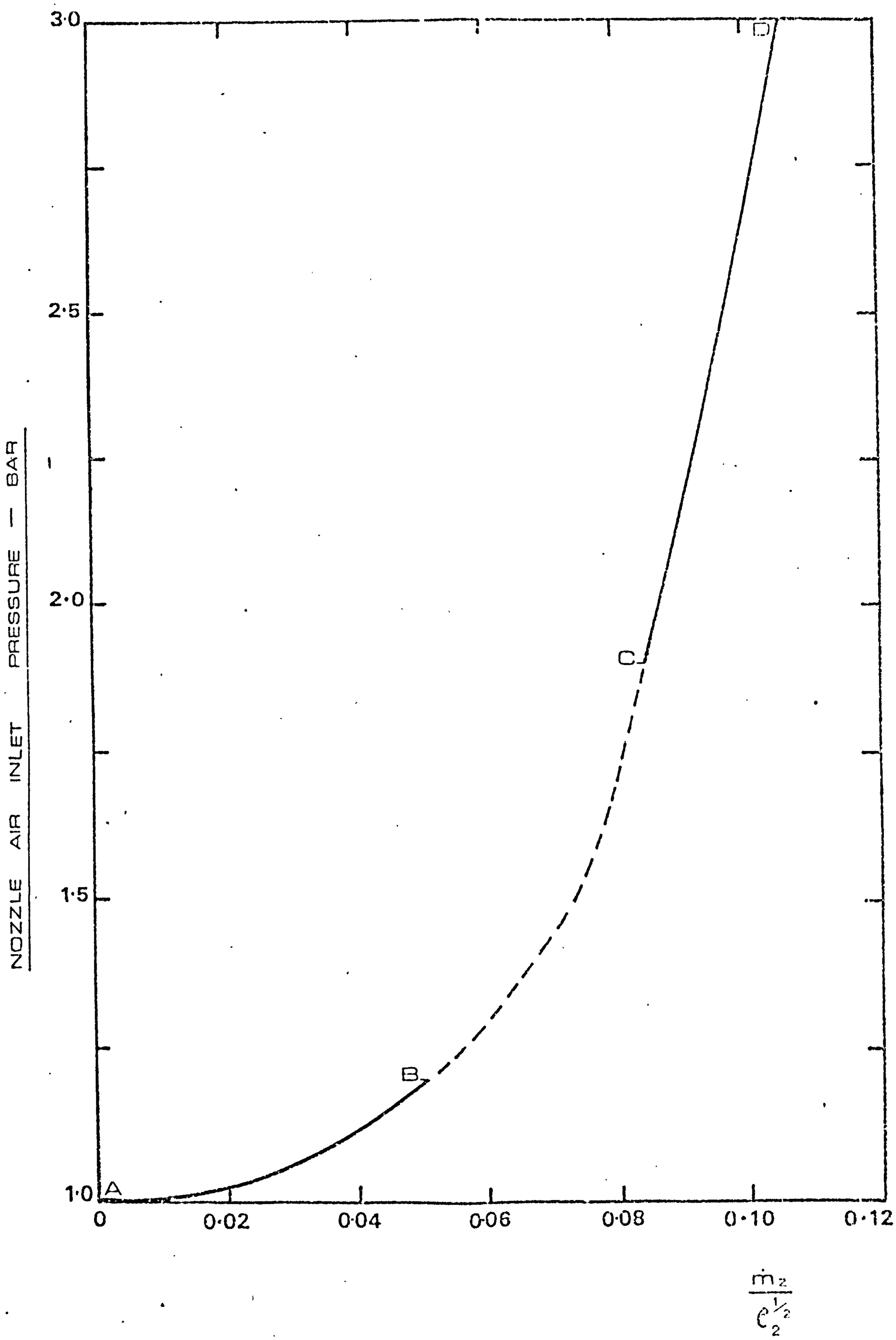

fig.(A4.1) NOZZLE MASS CHARACTERISTICS

APPENDIX FIVE

LAGRANGE INTERPOLATION

APPENDIX 5

LAGRANGE INTERPOLATION

A polynomial of degree n can be fitted exactly through n+1

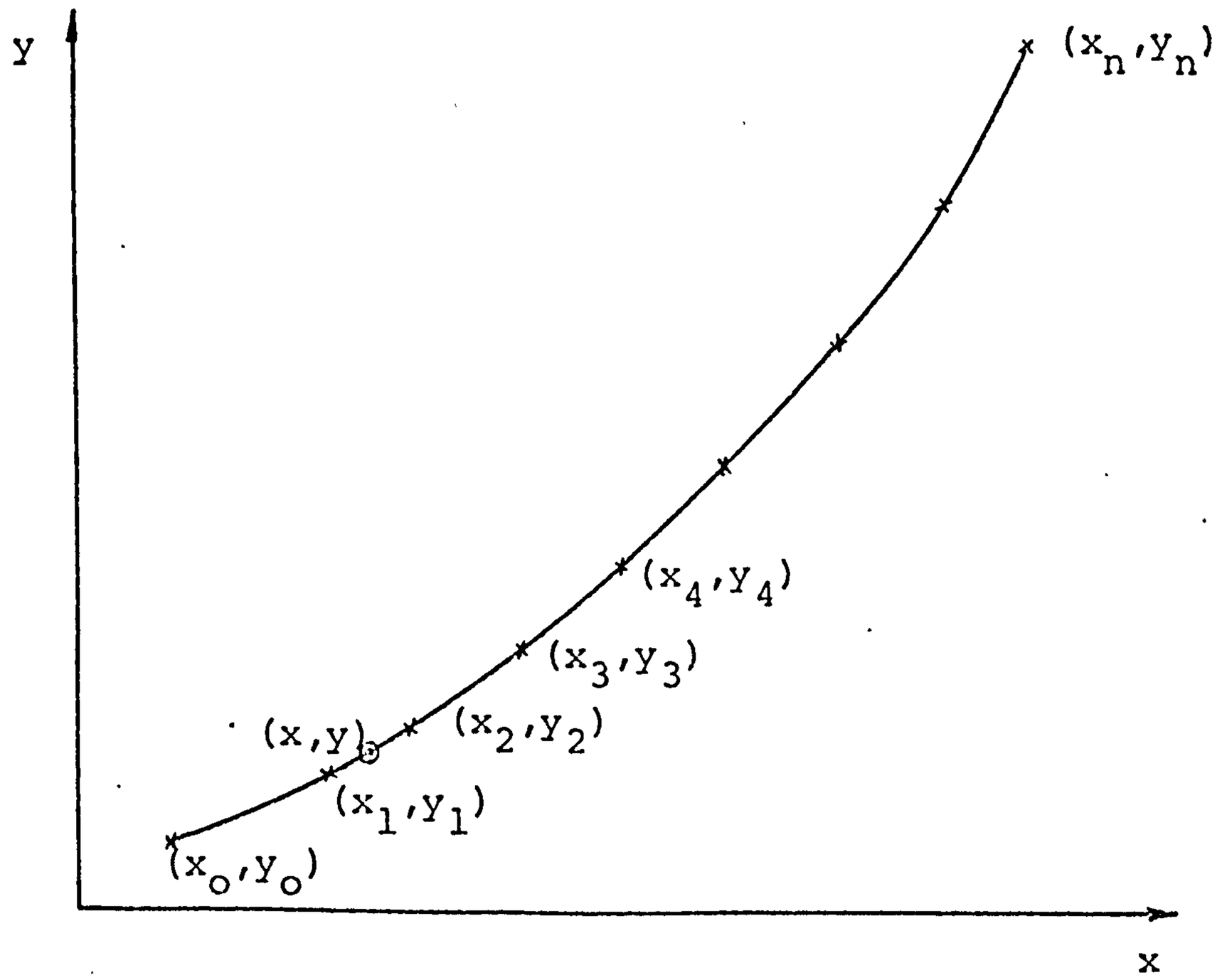

data points (x_o,y_o), (x_1,y_1), (x_2,y_2), ..., (x_n,y_n) and this may be written

$$y = \frac{(x-x_1)(x-x_2)\ldots\ldots(x-x_n)}{(x_o-x_1)(x_o-x_2)\ldots\ldots(x_o-x_n)}\, y_o + \frac{(x-x_o)(x-x_2)\ldots(x-x_n)}{(x_1-x_o)(x_1-x_2)\ldots(x_1-x_n)}\, y_1$$

$$+ \ldots\ldots\ldots + \ldots\ldots\ldots\ldots + \frac{(x-x_o)(x-x_1)\ldots\ldots(x-x_{n-1})}{(x_n-x_o)(x_n-x_1)\ldots(x_n-x_{n-1})}\, y_n \quad .$$

Therefore, an interpolated value of y can be found directly for a given value of x. This Lagrange polynomial was used to fit a curve through three points (quadratic fit) and find the

interpolated value of y for a given value of x as follows:

$$y = \frac{(x-x_1)(x-x_2)}{(x_o-x_1)(x_o-x_2)} y_o + \frac{(x-x_o)(x-x_2)}{(x_1-x_o)(x_1-x_2)} y_1 + \frac{(x-x_o)(x-x_1)}{(x_2-x_o)(x_2-x_1)} y_2 .$$

APPENDIX SIX

SUBROUTINES

APPENDIX 6

SUBROUTINES

A6.1 SUBROUTINE TSCHAR

When $N = 1$, the subroutine used Method B described in Section (6.7.2) to find the turbine speed parameter $\frac{N}{\sqrt{T_3}}$ from the known turbine mass flow parameter $\frac{\dot{m}_t\sqrt{T_3}}{P_3}$ and the turbine pressure ratio $\frac{P_3}{P_4}$, Fig (4.3). The special nomenclature for this case is as follows:

AMFP	$\frac{\dot{m}_t\sqrt{T_3}}{P_3}$
P3XN	$\frac{P_3}{P_4}$
ANSWER	$\frac{N}{\sqrt{T_3}}$
NN	Number of speed curves
NP	Number of data points on each speed curve

When $N = 2$, the subroutine used Method A explained in Section (6.7.1) to find turbine pressure ratio $\frac{P_3}{P_4}$ from the known turbine mass flow parameter $\frac{\dot{m}_t\sqrt{T_3}}{P_3}$ and the turbine speed parameter $\frac{N}{\sqrt{T_3}}$. The special nomenclature for this case is as follows:

AMFP	$\frac{\dot{m}_t\sqrt{T_3}}{P_3}$
P3XN	$\frac{N}{\sqrt{T_3}}$
ANSWER	$\frac{P_3}{P_4}$

NN	Number of speed curves
NP	Number of data points on each speed curve
DXA	Points on new speed curve for $\frac{\dot{m}_t\sqrt{T_3}}{P_3}$
DXP	Points on new speed curve for $\frac{P_3}{P_4}$

A6.2 SUBROUTINE TEFFCH

This subroutine used Method A described in section (6.7.1) to find the turbine efficiency η_t from a given turbine pressure ratio $\frac{P_3}{P_4}$ and turbine speed parameter $\frac{N}{\sqrt{T_3}}$, Fig (6.4). The special nomenclature for this subroutine was as follows:

AND	$\frac{N}{\sqrt{T_3}}$
P3D	$\frac{P_3}{P_4}$
ANSWER	η_t
NN	number of speed curves
NP	number of data points on each speed curve
DXP	points on new speed curve for pressure ratio $\frac{P_3}{P_4}$
DXT	points on new speed curve for efficiency η_t

A6.3 SUBROUTINE CCHAR

When $N = 1$, this subroutine was used to find the compressor initial mass flow rate in order to start the calculations.

When $N = 2$, the subroutine used Method A explained in section (6.7.1) to find the compressor pressure ratio $\frac{P_2}{P_1}$ and the compressor efficiency η_c from a given compressor mass flow rate $\dot{m}_c$ and the compressor speed N. The special nomenclature for this subroutine was as follows:

AMA	$\dot{m}_c$, compressor mass flow rate
CSPED	N, compressor speed
ANSE	η_c, compressor efficiency
ANSP	$\frac{P_2}{P_1}$, compressor pressure ratio
NN	number of speed curves
NP	number of data points on each speed curve
DXP	points on new speed curve for pressure ratio $\frac{P_2}{P_1}$
DXE	points on new speed curve for efficiency η_c
DXA	points on new speed curve for mass flow rate $\dot{m}_c$

A 6.4 SUBROUTINE PIPES

This subroutine used the Filling and Emptying method explained in section (6.5) to predict the flow in the exhaust system. The special nomenclature for this subroutine was as follows:

MS	$(m_s)_n$, initial mass of gas in the exhaust system
MV	$\dot{m}_v$, mass flow rate through the pulse generator valve
MVA	$\dot{m}_v$, actual mass flow rate entering the exhaust system through the three pulse generator valves
MSN	$(m_s)_{n+1}$, mass of gas in the exhaust system after a time step
P3NP1	$(P_3)_{n+1}$, exhaust system pressure after a time step
T3NP1	$(T_3)_{n+1}$, exhaust system temperature after a time step

A6.5 SUBROUTINE CFTINT

This subroutine was used to fit a quadratic curve through a set of date points with known X-axis and Y-axis parameters. It used the Lagrange interpolation method (see Appendix 5) to find the X-axis parameter for a point with known Y-axis parameter or vice versa.

This subroutine was used under two conditions:

(1) To find compressor loading nozzle mass flow parameter $\frac{\dot{m}_z}{\rho_2^{1/2}}$ for a given nozzle supply pressure P_2, see Fig (5.9). This special nomenclature for this case was as follows:

C	$\frac{\dot{m}_z}{\rho_2^{1/2}}$, the required nozzle mass flow parameter
X	array of input pressure data points
Y	array of input mass flow parameter data points
N	number of data points
FOP	actual nozzle supply pressure.

(2) To find the pulse generator valve coefficient of discharge for a given valve opening area, Fig (5.5). The nomenclature for this case was as follows:

C	Cd, the required coefficient of discharge of the valve
X	array of input valve opening areas
Y	array of input valve coefficient of discharge
N	number of data points
FOP	pulse generator valve coefficient of discharge.

A6.6 SUBROUTINE VAREA

This subroutine was used to fit three curves through three sets of data points with known X-axis and Y-axis parameters. It used the Lagrange interpolation method to find the Y-axis parameter from a known X-axis parameter. This subroutine was written to find the pulse generator valve opening area at a given time, Fig (5.5). The nomenclature was as follows:

PSI	opening area required at a given time
X	array of time data points
Y	array of valve opening area data points
N	number of data points
EX	the given time
L	number of pulse generator valves
TCYCLE	time required for one complete valve opening cycle

APPENDIX SEVEN

FLOW CHARTS

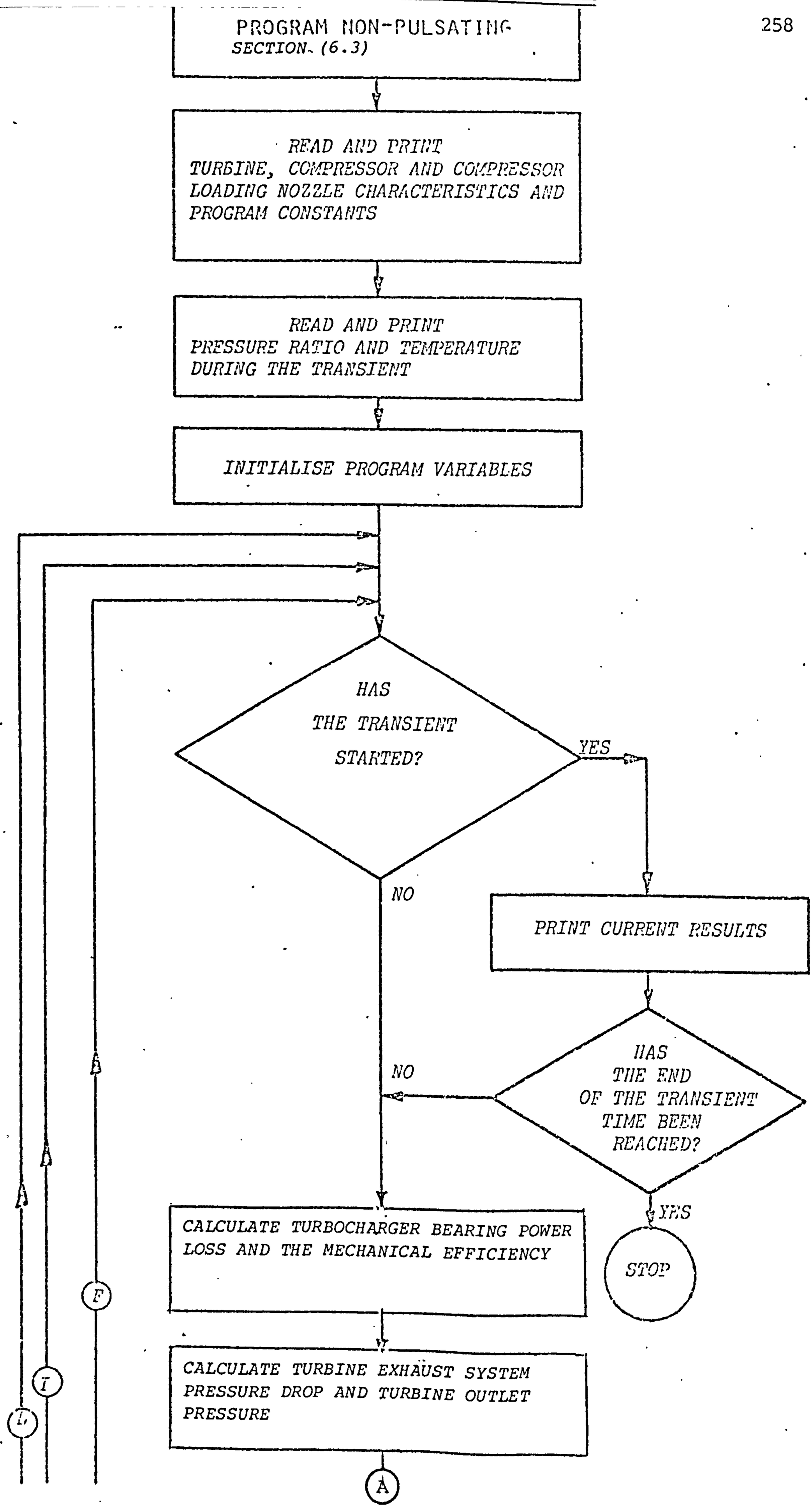
PROGRAM NON-PULSATING
SECTION (6.3)
READ AND PRINT
TURBINE, COMPRESSOR AND COMPRESSOR
LOADING NOZZLE CHARACTERISTICS AND
PROGRAM CONSTANTS
READ AND PRINT
PRESSURE RATIO AND TEMPERATURE
DURING THE TRANSIENT
INITIALISE PROGRAM VARIABLES
HAS
THE TRANSIENT
STARTED?
YES
NO
PRINT CURRENT RESULTS
HAS
THE END
OF THE TRANSIENT
TIME BEEN
REACHED?
NO
YES
STOP
CALCULATE TURBOCHARGER BEARING POWER
LOSS AND THE MECHANICAL EFFICIENCY
CALCULATE TURBINE EXHAUST SYSTEM
PRESSURE DROP AND TURBINE OUTLET
PRESSURE
A
F
I
L

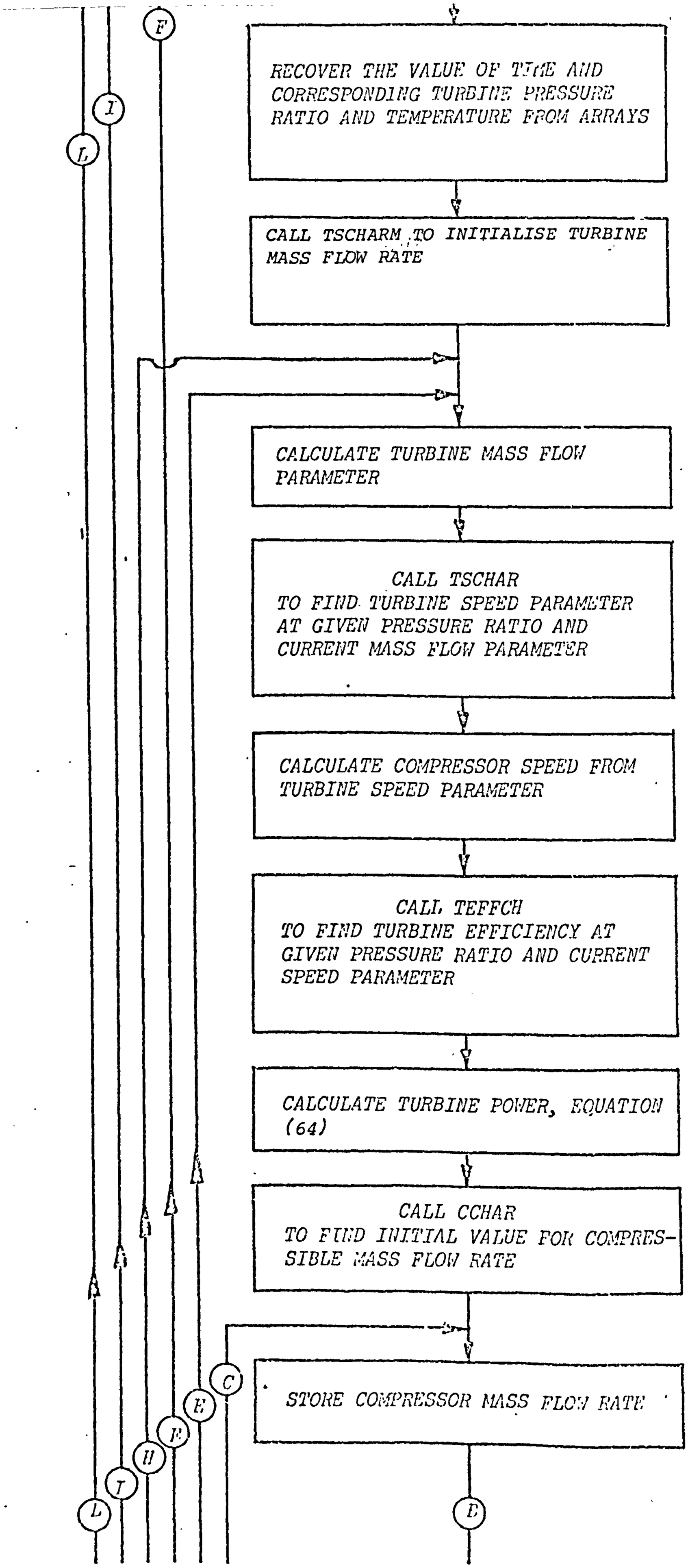
F
I
L
RECOVER THE VALUE OF TIME AND CORRESPONDING TURBINE PRESSURE RATIO AND TEMPERATURE FROM ARRAYS
CALL TSCHARM TO INITIALISE TURBINE MASS FLOW RATE
CALCULATE TURBINE MASS FLOW PARAMETER
CALL TSCHAR TO FIND TURBINE SPEED PARAMETER AT GIVEN PRESSURE RATIO AND CURRENT MASS FLOW PARAMETER
CALCULATE COMPRESSOR SPEED FROM TURBINE SPEED PARAMETER
CALL TEFFCH TO FIND TURBINE EFFICIENCY AT GIVEN PRESSURE RATIO AND CURRENT SPEED PARAMETER
CALCULATE TURBINE POWER, EQUATION (64)
CALL CCHAR TO FIND INITIAL VALUE FOR COMPRESSIBLE MASS FLOW RATE
STORE COMPRESSOR MASS FLOW RATE
C
E
B
H
T
L
E

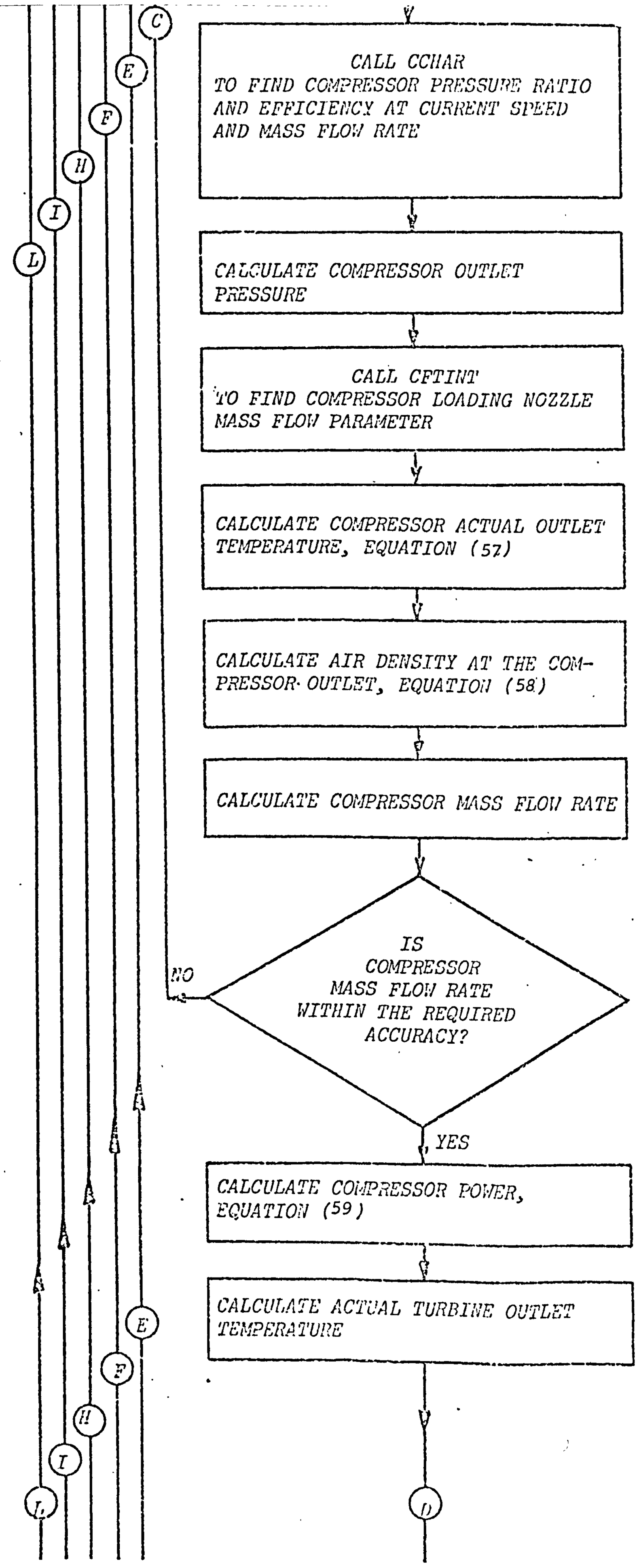
C
E
F
H
I
L
CALL CCHAR
TO FIND COMPRESSOR PRESSURE RATIO
AND EFFICIENCY AT CURRENT SPEED
AND MASS FLOW RATE
CALCULATE COMPRESSOR OUTLET
PRESSURE
CALL CFTINT
TO FIND COMPRESSOR LOADING NOZZLE
MASS FLOW PARAMETER
CALCULATE COMPRESSOR ACTUAL OUTLET
TEMPERATURE, EQUATION (57)
CALCULATE AIR DENSITY AT THE COM-
PRESSOR OUTLET, EQUATION (58)
CALCULATE COMPRESSOR MASS FLOW RATE
IS
COMPRESSOR
MASS FLOW RATE
WITHIN THE REQUIRED
ACCURACY?
NO
YES
CALCULATE COMPRESSOR POWER,
EQUATION (59)
CALCULATE ACTUAL TURBINE OUTLET
TEMPERATURE
D

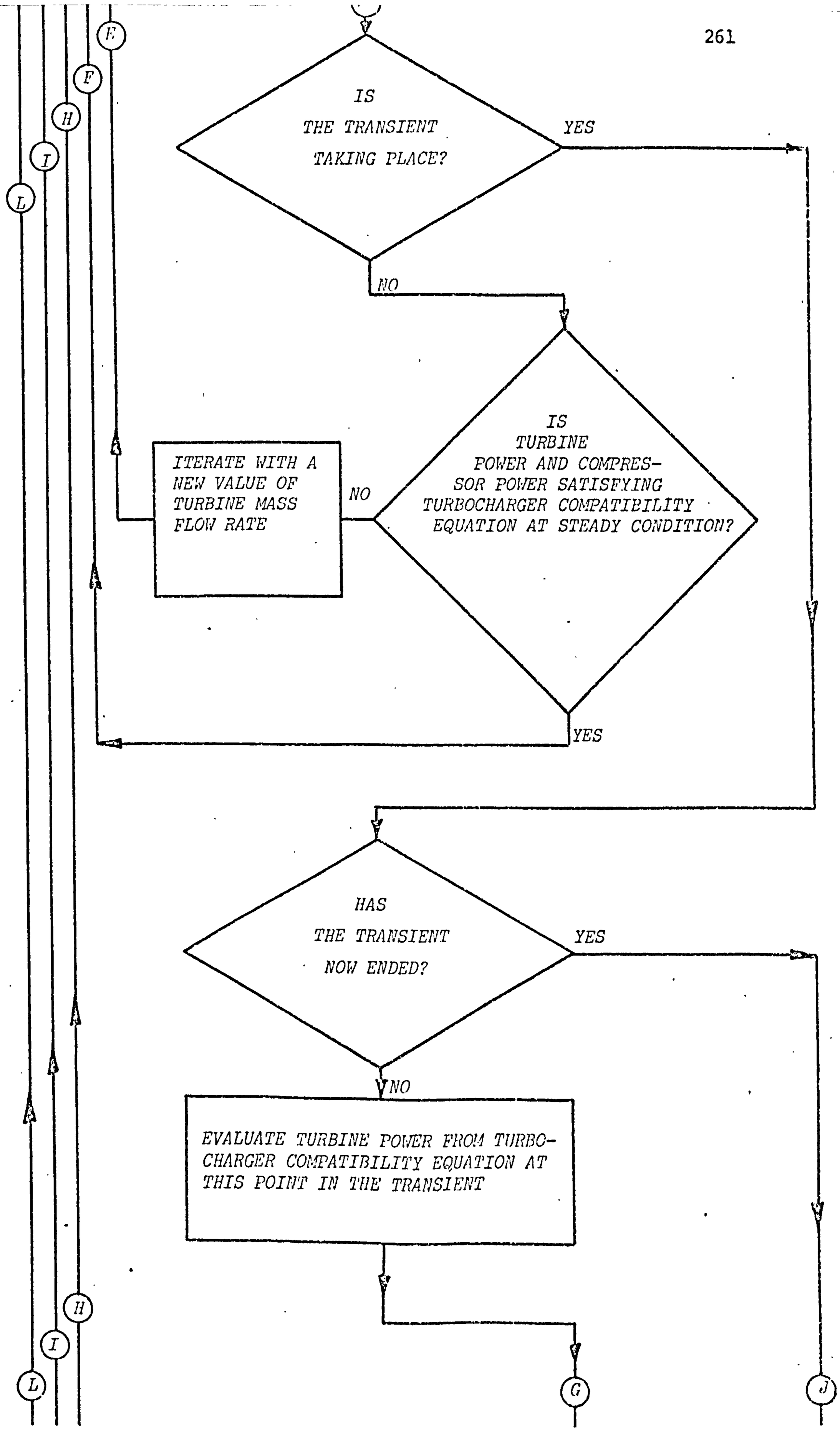
E
F
H
I
L
IS THE TRANSIENT TAKING PLACE?
YES
NO
IS TURBINE POWER AND COMPRESSOR POWER SATISFYING TURBOCHARGER COMPATIBILITY EQUATION AT STEADY CONDITION?
NO
ITERATE WITH A NEW VALUE OF TURBINE MASS FLOW RATE
YES
HAS THE TRANSIENT NOW ENDED?
YES
NO
EVALUATE TURBINE POWER FROM TURBOCHARGER COMPATIBILITY EQUATION AT THIS POINT IN THE TRANSIENT
G
J
H
I
L

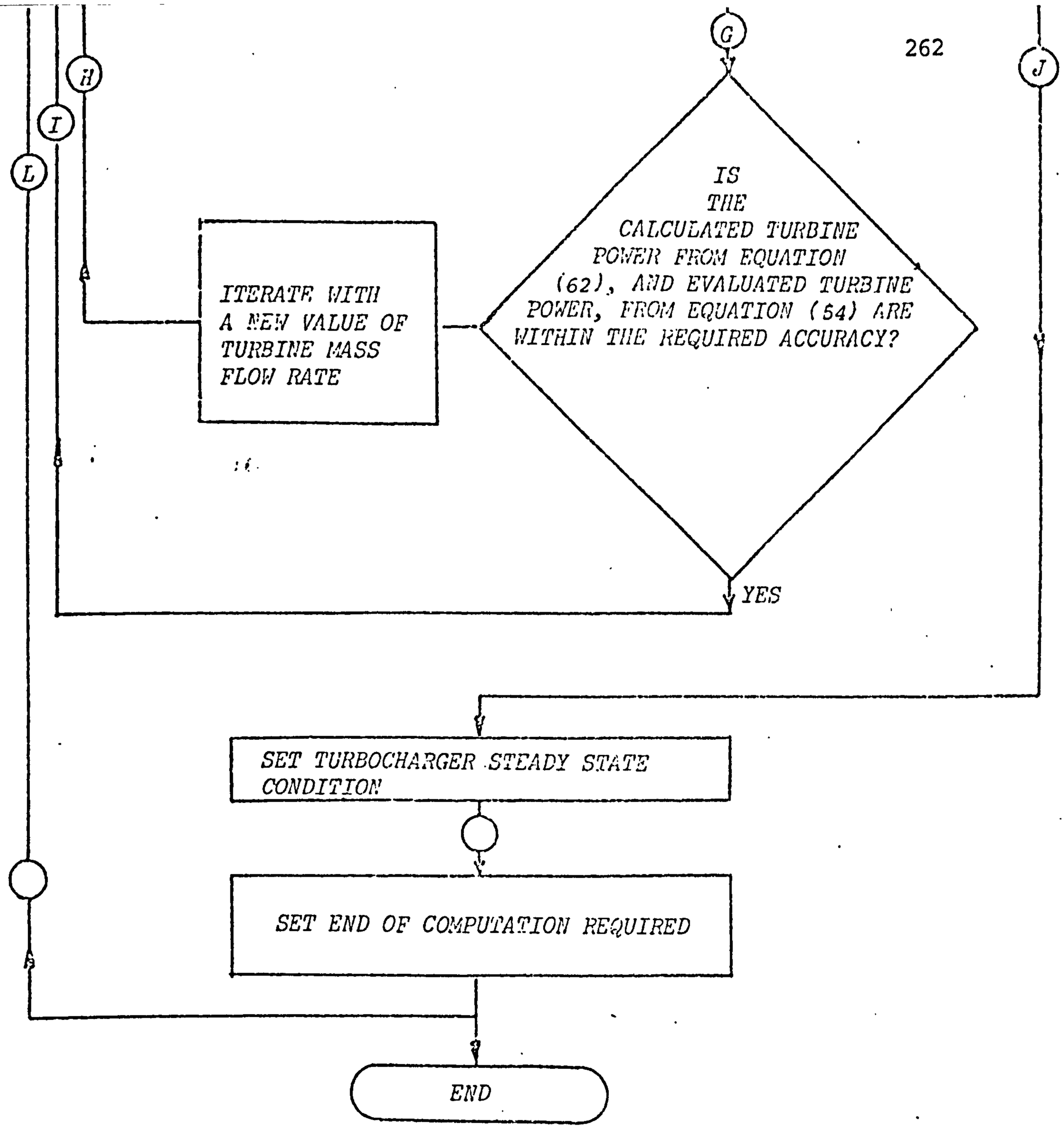
G
J
H
I
L
IS THE CALCULATED TURBINE POWER FROM EQUATION (62), AND EVALUATED TURBINE POWER, FROM EQUATION (54) ARE WITHIN THE REQUIRED ACCURACY?
ITERATE WITH A NEW VALUE OF TURBINE MASS FLOW RATE
YES
SET TURBOCHARGER STEADY STATE CONDITION
SET END OF COMPUTATION REQUIRED
END

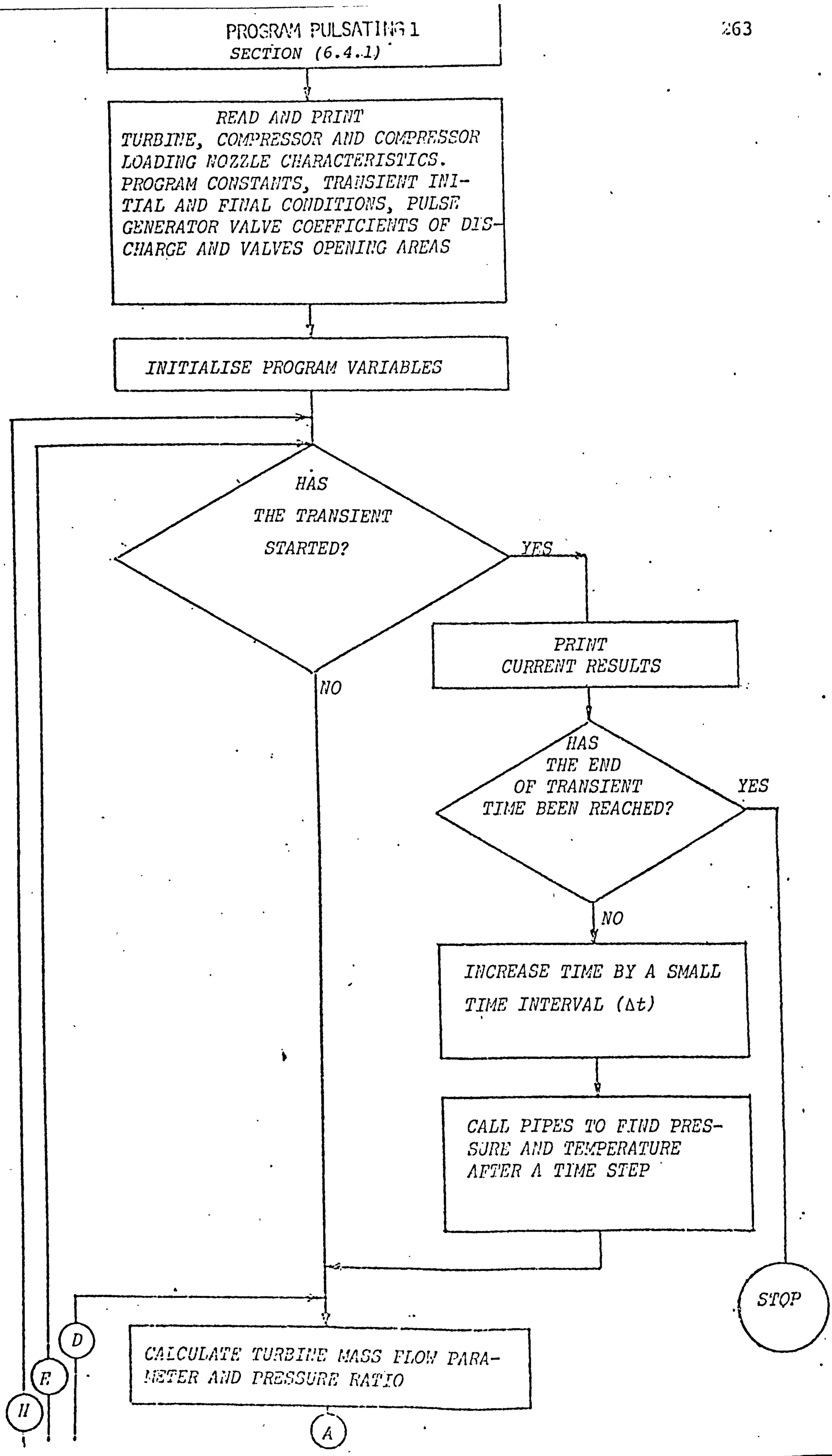
PROGRAM PULSATING 1
SECTION (6.4.1)
READ AND PRINT
TURBINE, COMPRESSOR AND COMPRESSOR LOADING NOZZLE CHARACTERISTICS. PROGRAM CONSTANTS, TRANSIENT INITIAL AND FINAL CONDITIONS, PULSE GENERATOR VALVE COEFFICIENTS OF DISCHARGE AND VALVES OPENING AREAS
INITIALISE PROGRAM VARIABLES
HAS THE TRANSIENT STARTED?
YES
NO
PRINT CURRENT RESULTS
HAS THE END OF TRANSIENT TIME BEEN REACHED?
YES
NO
INCREASE TIME BY A SMALL TIME INTERVAL (Δt)
CALL PIPES TO FIND PRESSURE AND TEMPERATURE AFTER A TIME STEP
STOP
CALCULATE TURBINE MASS FLOW PARAMETER AND PRESSURE RATIO
D
E
H
A

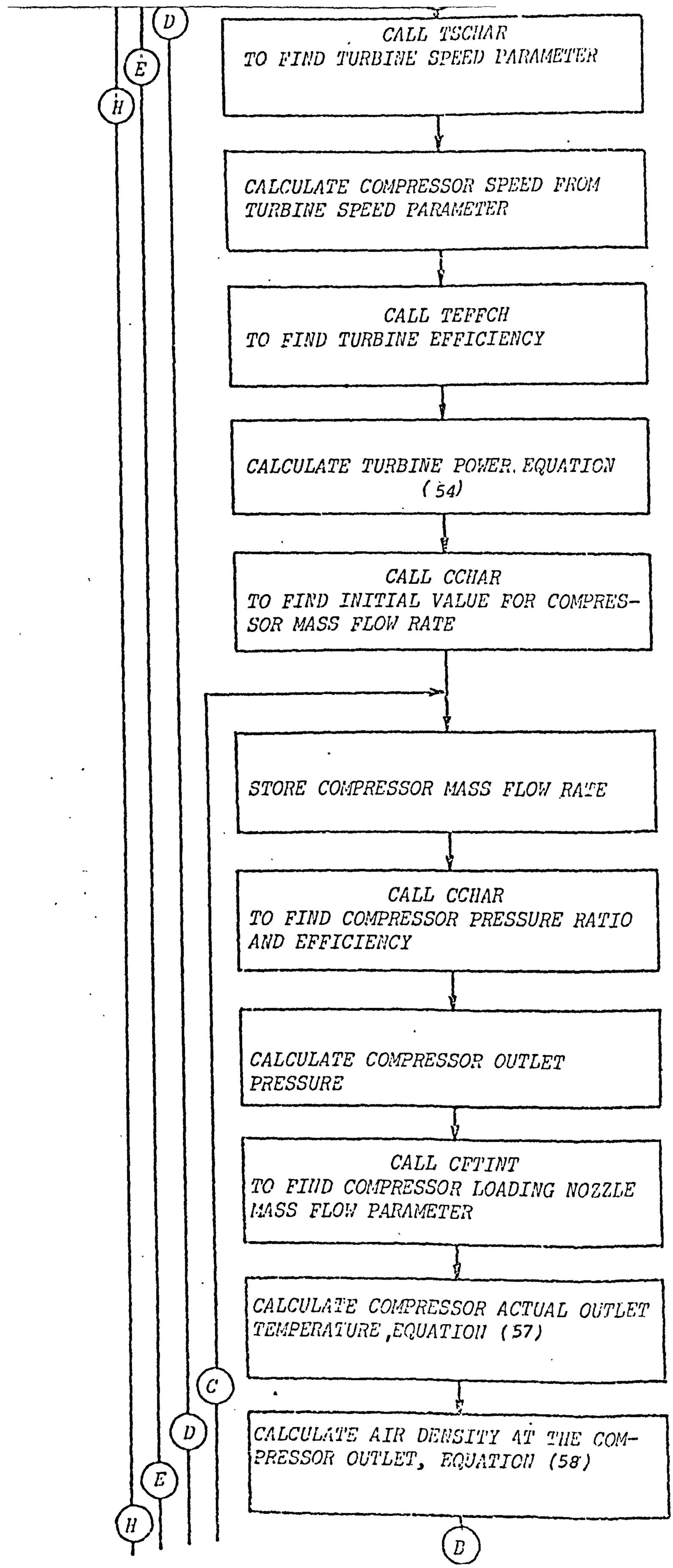
D
E
H
CALL TSCHAR
TO FIND TURBINE SPEED PARAMETER
CALCULATE COMPRESSOR SPEED FROM
TURBINE SPEED PARAMETER
CALL TEFFCH
TO FIND TURBINE EFFICIENCY
CALCULATE TURBINE POWER, EQUATION
(54)
CALL CCHAR
TO FIND INITIAL VALUE FOR COMPRES-
SOR MASS FLOW RATE
STORE COMPRESSOR MASS FLOW RATE
CALL CCHAR
TO FIND COMPRESSOR PRESSURE RATIO
AND EFFICIENCY
CALCULATE COMPRESSOR OUTLET
PRESSURE
CALL CFTINT
TO FIND COMPRESSOR LOADING NOZZLE
MASS FLOW PARAMETER
CALCULATE COMPRESSOR ACTUAL OUTLET
TEMPERATURE, EQUATION (57)
C
D
E
H
CALCULATE AIR DENSITY AT THE COM-
PRESSOR OUTLET, EQUATION (58)
B

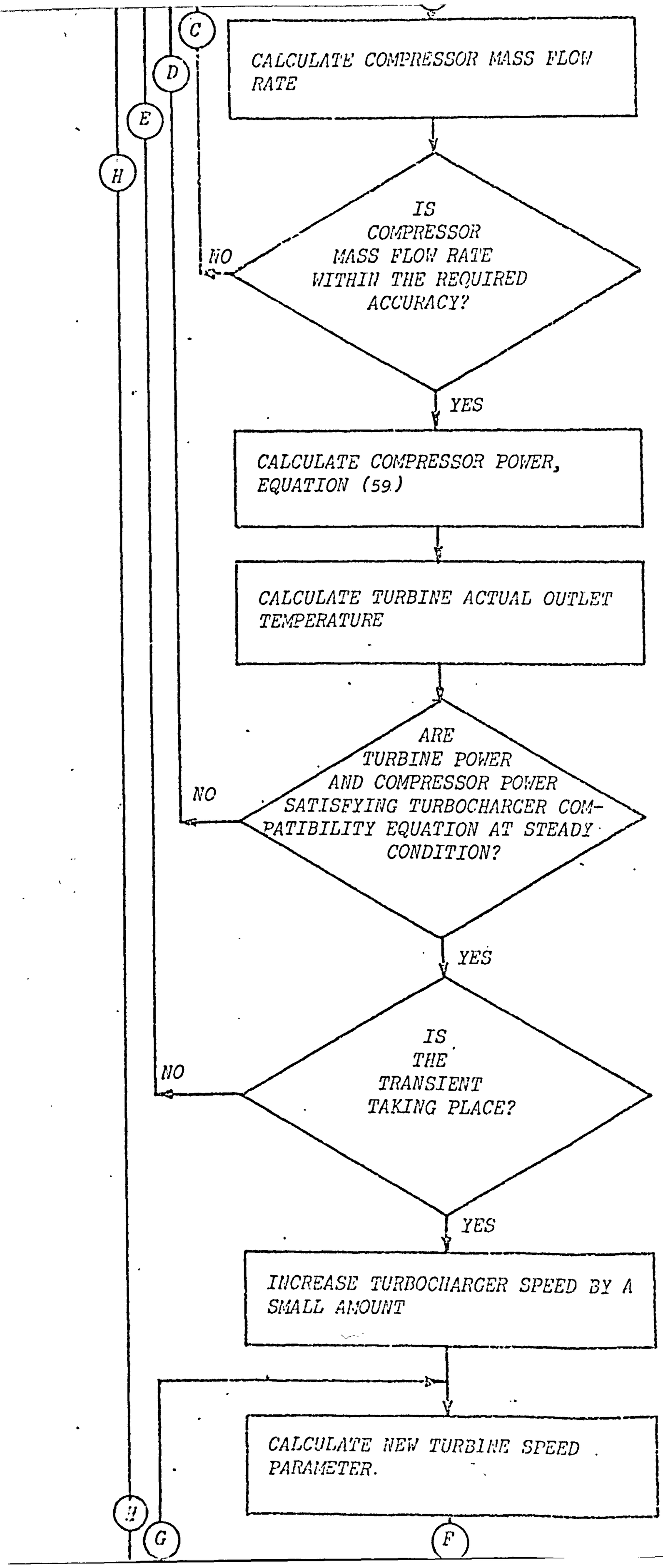
C
D
E
H
CALCULATE COMPRESSOR MASS FLOW RATE
IS COMPRESSOR MASS FLOW RATE WITHIN THE REQUIRED ACCURACY?
NO
YES
CALCULATE COMPRESSOR POWER, EQUATION (59)
CALCULATE TURBINE ACTUAL OUTLET TEMPERATURE
ARE TURBINE POWER AND COMPRESSOR POWER SATISFYING TURBOCHARGER COMPATIBILITY EQUATION AT STEADY CONDITION?
NO
YES
IS THE TRANSIENT TAKING PLACE?
NO
YES
INCREASE TURBOCHARGER SPEED BY A SMALL AMOUNT
CALCULATE NEW TURBINE SPEED PARAMETER.
H
G
F

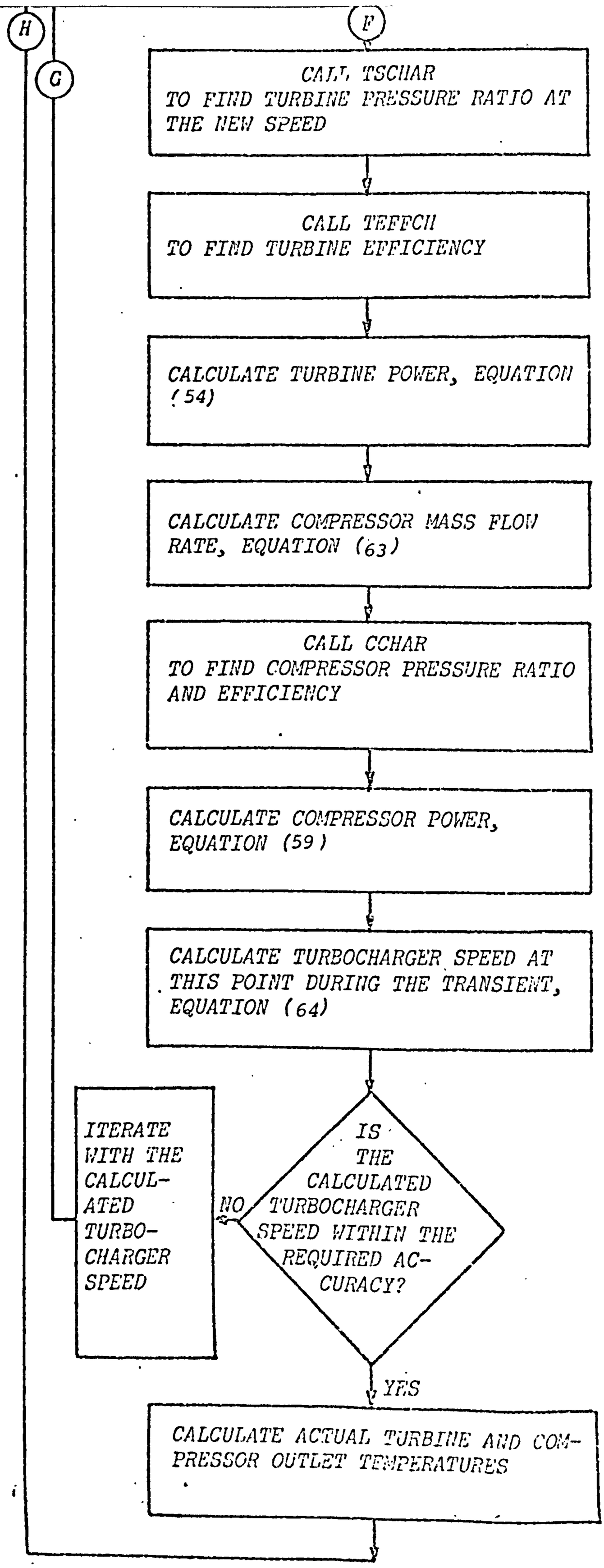
H
G
F
CALL TSCHAR
TO FIND TURBINE PRESSURE RATIO AT THE NEW SPEED
CALL TEFFCH
TO FIND TURBINE EFFICIENCY
CALCULATE TURBINE POWER, EQUATION (54)
CALCULATE COMPRESSOR MASS FLOW RATE, EQUATION (63)
CALL CCHAR
TO FIND COMPRESSOR PRESSURE RATIO AND EFFICIENCY
CALCULATE COMPRESSOR POWER, EQUATION (59)
CALCULATE TURBOCHARGER SPEED AT THIS POINT DURING THE TRANSIENT, EQUATION (64)
IS THE CALCULATED TURBOCHARGER SPEED WITHIN THE REQUIRED ACCURACY?
NO
ITERATE WITH THE CALCULATED TURBOCHARGER SPEED
YES
CALCULATE ACTUAL TURBINE AND COMPRESSOR OUTLET TEMPERATURES

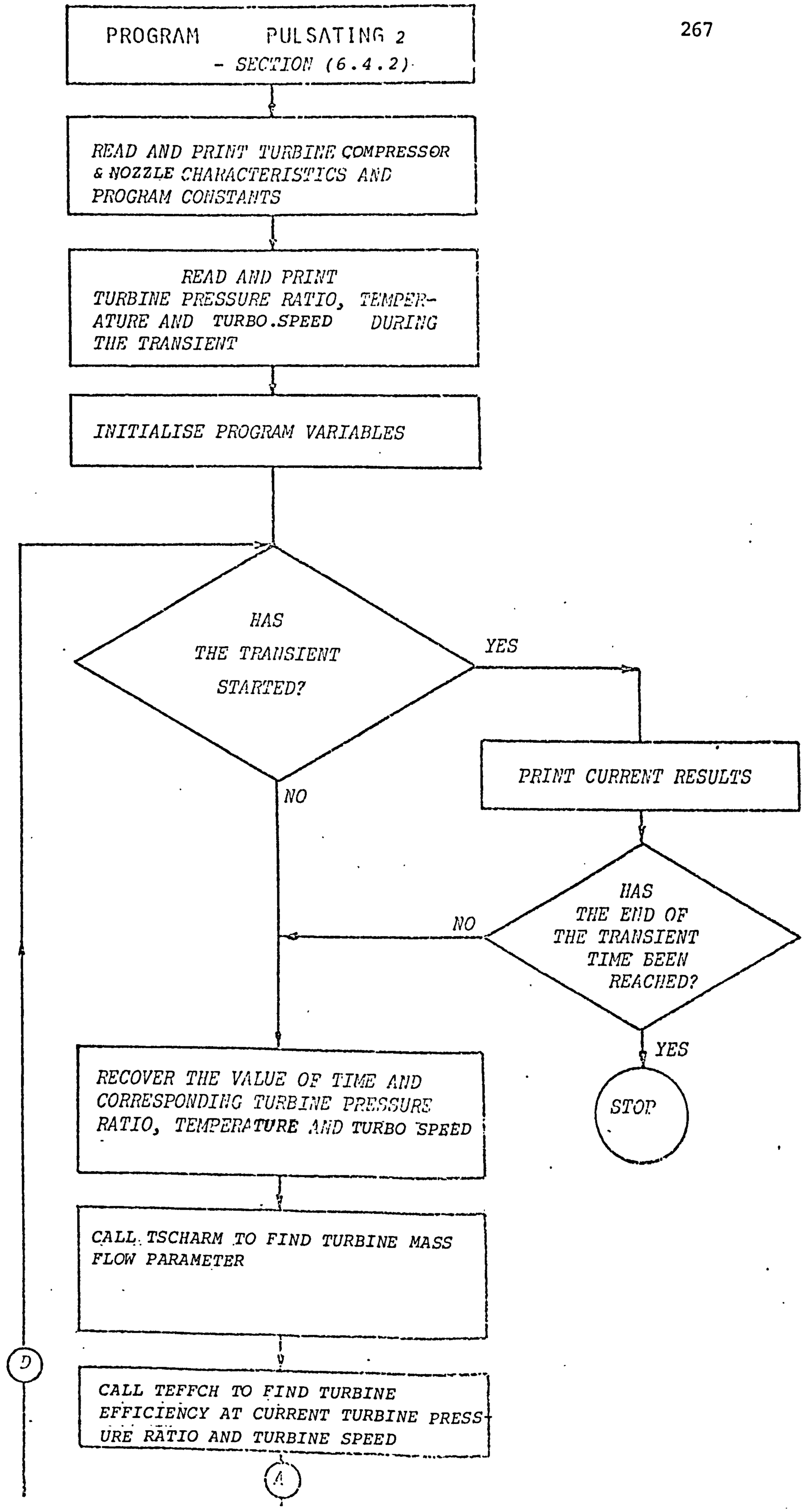
PROGRAM PULSATING 2
- SECTION (6.4.2)
READ AND PRINT TURBINE COMPRESSOR & NOZZLE CHARACTERISTICS AND PROGRAM CONSTANTS
READ AND PRINT TURBINE PRESSURE RATIO, TEMPERATURE AND TURBO.SPEED DURING THE TRANSIENT
INITIALISE PROGRAM VARIABLES
HAS THE TRANSIENT STARTED?
YES
NO
PRINT CURRENT RESULTS
HAS THE END OF THE TRANSIENT TIME BEEN REACHED?
NO
YES
STOP
RECOVER THE VALUE OF TIME AND CORRESPONDING TURBINE PRESSURE RATIO, TEMPERATURE AND TURBO SPEED
CALL TSCHARM TO FIND TURBINE MASS FLOW PARAMETER
D
CALL TEFFCH TO FIND TURBINE EFFICIENCY AT CURRENT TURBINE PRESSURE RATIO AND TURBINE SPEED
A

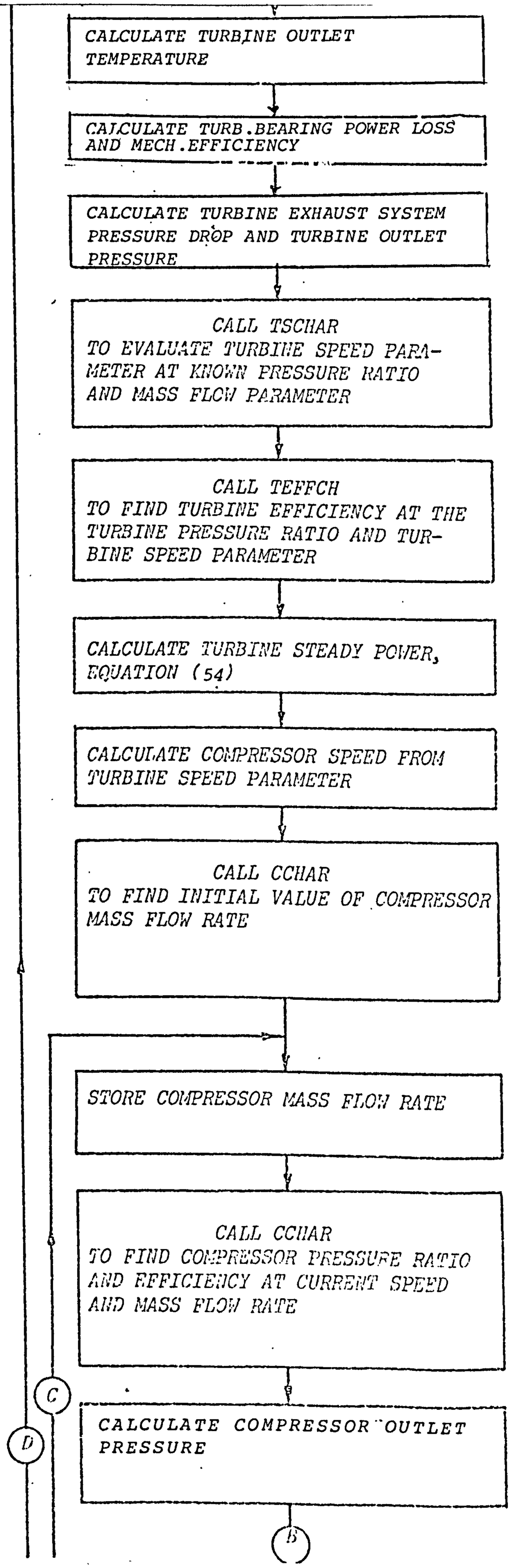
CALCULATE TURBINE OUTLET TEMPERATURE
CALCULATE TURB.BEARING POWER LOSS AND MECH.EFFICIENCY
CALCULATE TURBINE EXHAUST SYSTEM PRESSURE DROP AND TURBINE OUTLET PRESSURE
CALL TSCHAR TO EVALUATE TURBINE SPEED PARAMETER AT KNOWN PRESSURE RATIO AND MASS FLOW PARAMETER
CALL TEFFCH TO FIND TURBINE EFFICIENCY AT THE TURBINE PRESSURE RATIO AND TURBINE SPEED PARAMETER
CALCULATE TURBINE STEADY POWER, EQUATION (54)
CALCULATE COMPRESSOR SPEED FROM TURBINE SPEED PARAMETER
CALL CCHAR TO FIND INITIAL VALUE OF COMPRESSOR MASS FLOW RATE
STORE COMPRESSOR MASS FLOW RATE
CALL CCHAR TO FIND COMPRESSOR PRESSURE RATIO AND EFFICIENCY AT CURRENT SPEED AND MASS FLOW RATE
C
D
CALCULATE COMPRESSOR OUTLET PRESSURE
B

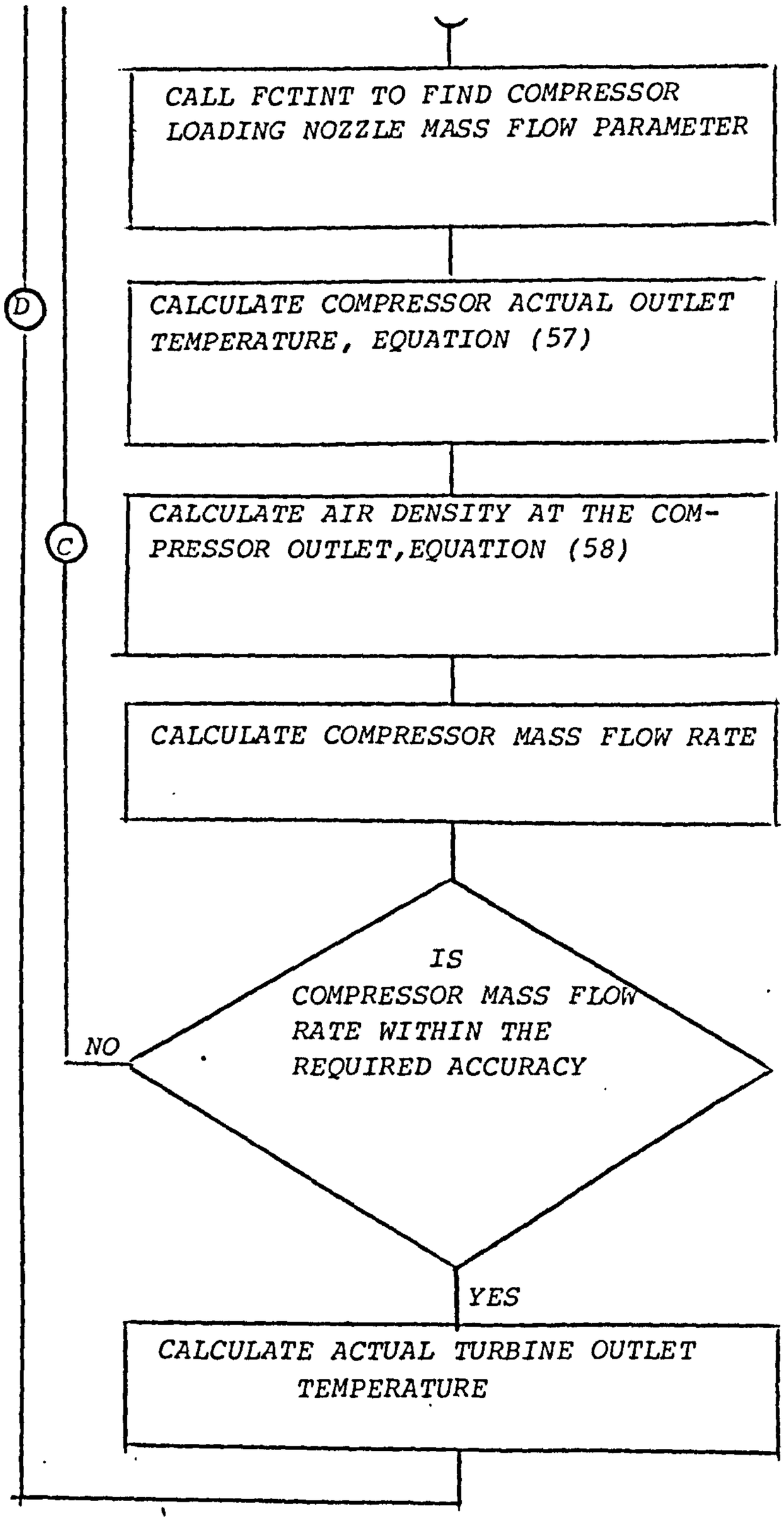
CALL FCTINT TO FIND COMPRESSOR LOADING NOZZLE MASS FLOW PARAMETER
D
CALCULATE COMPRESSOR ACTUAL OUTLET TEMPERATURE, EQUATION (57)
C
CALCULATE AIR DENSITY AT THE COMPRESSOR OUTLET,EQUATION (58)
CALCULATE COMPRESSOR MASS FLOW RATE
IS COMPRESSOR MASS FLOW RATE WITHIN THE REQUIRED ACCURACY
NO
YES
CALCULATE ACTUAL TURBINE OUTLET TEMPERATURE

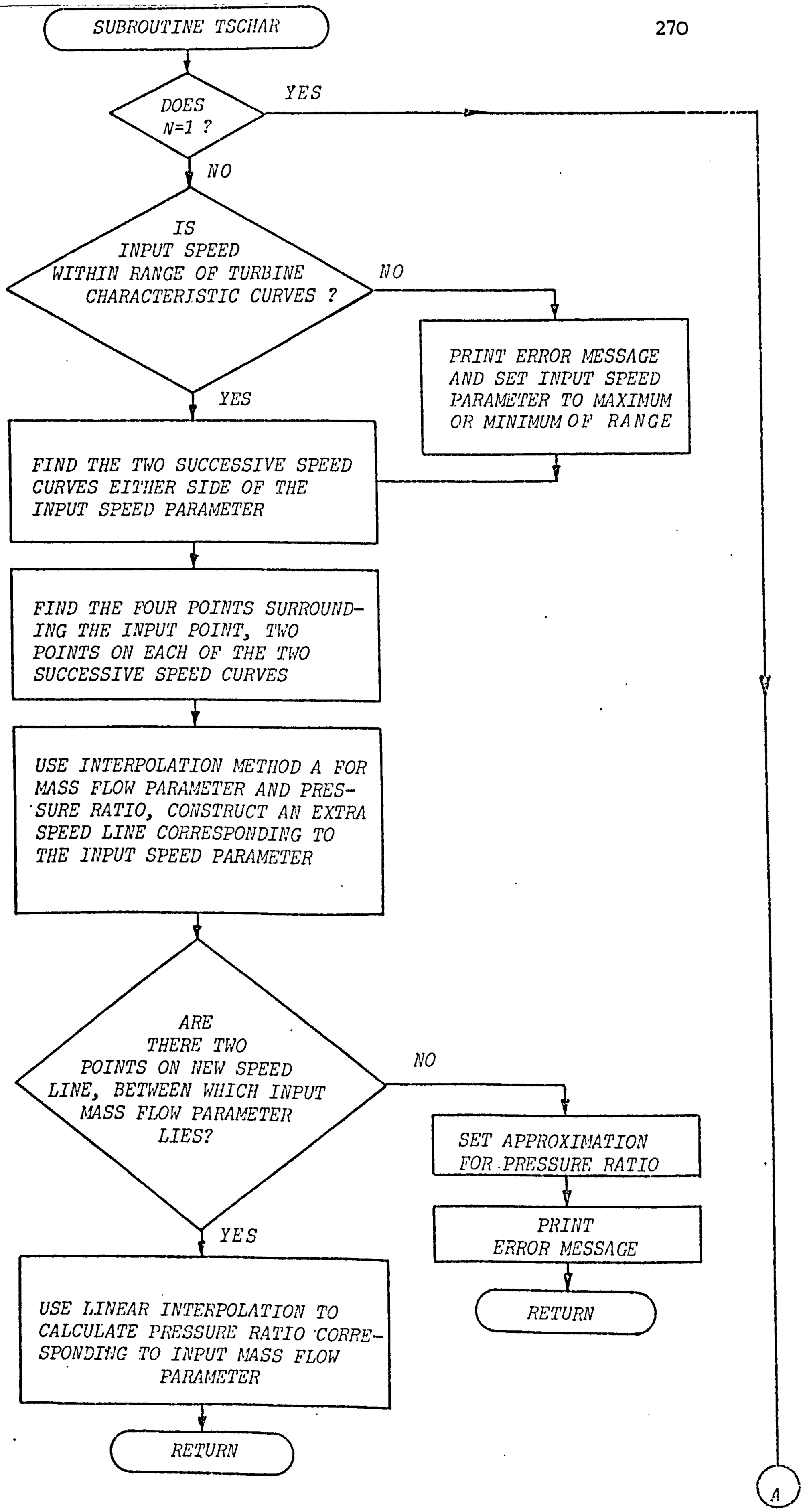
SUBROUTINE TSCHAR
DOES N=1 ?
YES
NO
IS INPUT SPEED WITHIN RANGE OF TURBINE CHARACTERISTIC CURVES ?
NO
PRINT ERROR MESSAGE AND SET INPUT SPEED PARAMETER TO MAXIMUM OR MINIMUM OF RANGE
YES
FIND THE TWO SUCCESSIVE SPEED CURVES EITHER SIDE OF THE INPUT SPEED PARAMETER
FIND THE FOUR POINTS SURROUNDING THE INPUT POINT, TWO POINTS ON EACH OF THE TWO SUCCESSIVE SPEED CURVES
USE INTERPOLATION METHOD A FOR MASS FLOW PARAMETER AND PRESSURE RATIO, CONSTRUCT AN EXTRA SPEED LINE CORRESPONDING TO THE INPUT SPEED PARAMETER
ARE THERE TWO POINTS ON NEW SPEED LINE, BETWEEN WHICH INPUT MASS FLOW PARAMETER LIES?
NO
SET APPROXIMATION FOR PRESSURE RATIO
PRINT ERROR MESSAGE
RETURN
YES
USE LINEAR INTERPOLATION TO CALCULATE PRESSURE RATIO CORRESPONDING TO INPUT MASS FLOW PARAMETER
RETURN
A

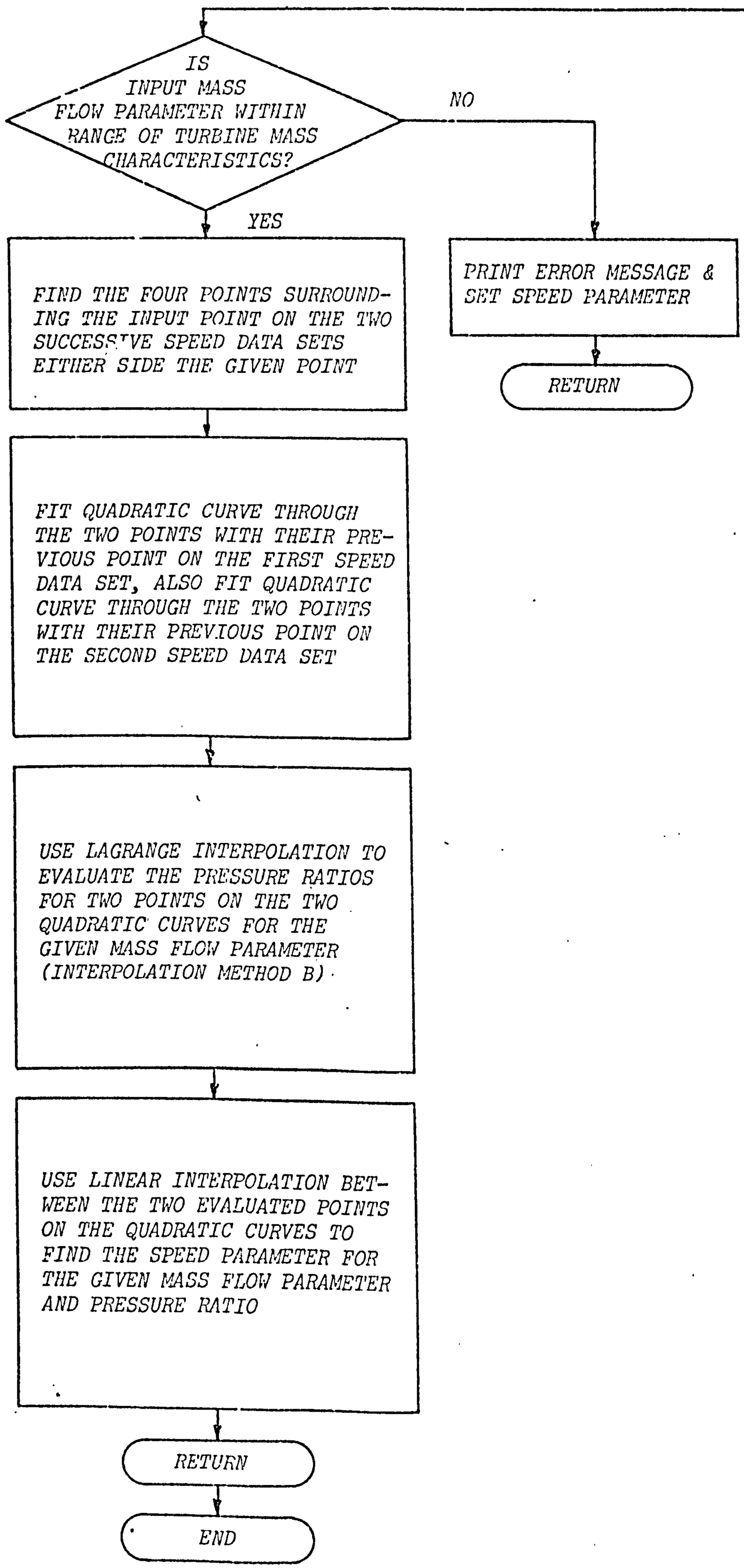
A
IS INPUT MASS FLOW PARAMETER WITHIN RANGE OF TURBINE MASS CHARACTERISTICS?
NO
YES
PRINT ERROR MESSAGE & SET SPEED PARAMETER
RETURN
FIND THE FOUR POINTS SURROUNDING THE INPUT POINT ON THE TWO SUCCESSIVE SPEED DATA SETS EITHER SIDE THE GIVEN POINT
FIT QUADRATIC CURVE THROUGH THE TWO POINTS WITH THEIR PREVIOUS POINT ON THE FIRST SPEED DATA SET, ALSO FIT QUADRATIC CURVE THROUGH THE TWO POINTS WITH THEIR PREVIOUS POINT ON THE SECOND SPEED DATA SET
USE LAGRANGE INTERPOLATION TO EVALUATE THE PRESSURE RATIOS FOR TWO POINTS ON THE TWO QUADRATIC CURVES FOR THE GIVEN MASS FLOW PARAMETER (INTERPOLATION METHOD B)
USE LINEAR INTERPOLATION BETWEEN THE TWO EVALUATED POINTS ON THE QUADRATIC CURVES TO FIND THE SPEED PARAMETER FOR THE GIVEN MASS FLOW PARAMETER AND PRESSURE RATIO
RETURN
END

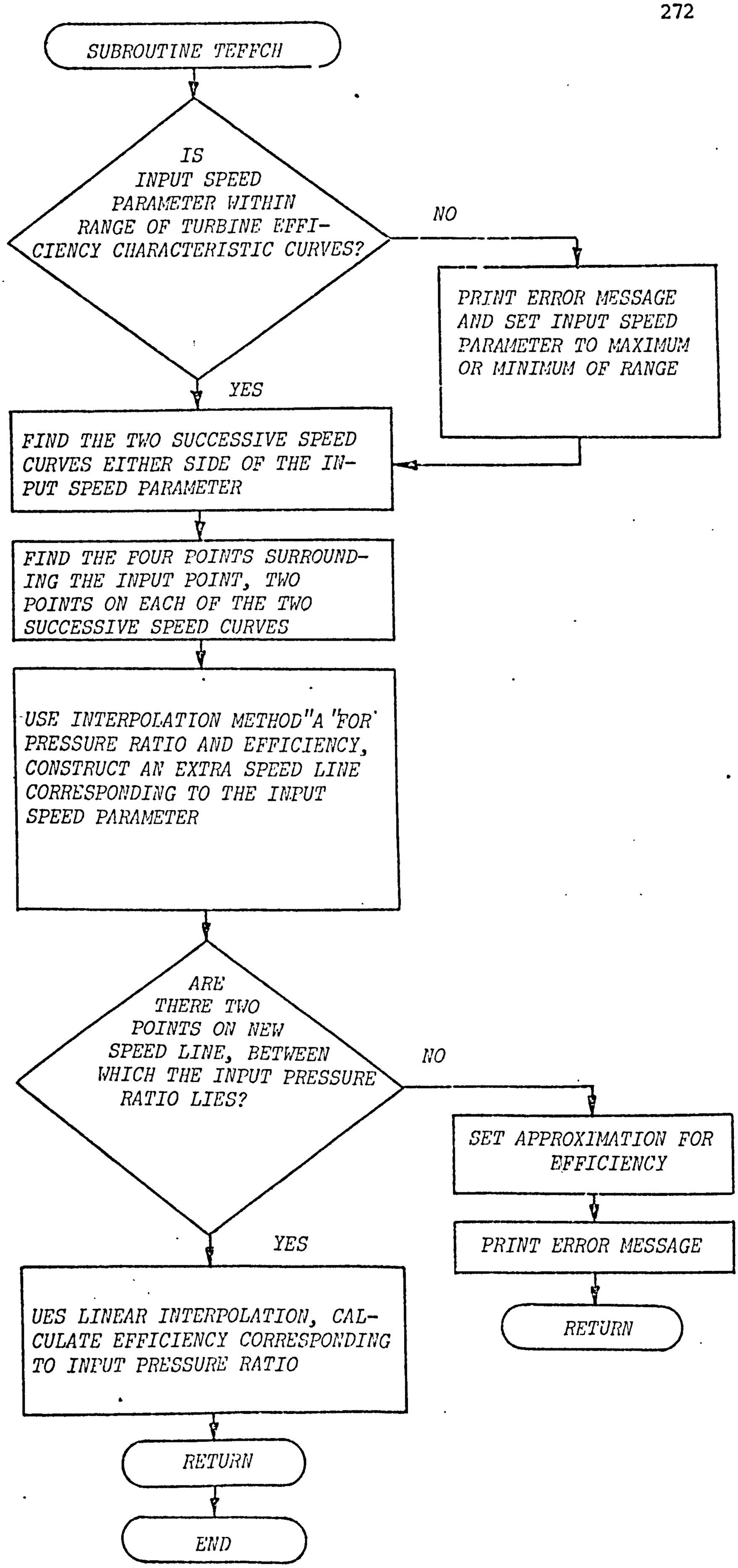
SUBROUTINE TEFFCH
IS INPUT SPEED PARAMETER WITHIN RANGE OF TURBINE EFFICIENCY CHARACTERISTIC CURVES?
NO
PRINT ERROR MESSAGE AND SET INPUT SPEED PARAMETER TO MAXIMUM OR MINIMUM OF RANGE
YES
FIND THE TWO SUCCESSIVE SPEED CURVES EITHER SIDE OF THE INPUT SPEED PARAMETER
FIND THE FOUR POINTS SURROUNDING THE INPUT POINT, TWO POINTS ON EACH OF THE TWO SUCCESSIVE SPEED CURVES
USE INTERPOLATION METHOD "A" FOR PRESSURE RATIO AND EFFICIENCY, CONSTRUCT AN EXTRA SPEED LINE CORRESPONDING TO THE INPUT SPEED PARAMETER
ARE THERE TWO POINTS ON NEW SPEED LINE, BETWEEN WHICH THE INPUT PRESSURE RATIO LIES?
NO
SET APPROXIMATION FOR EFFICIENCY
PRINT ERROR MESSAGE
RETURN
YES
UES LINEAR INTERPOLATION, CALCULATE EFFICIENCY CORRESPONDING TO INPUT PRESSURE RATIO
RETURN
END

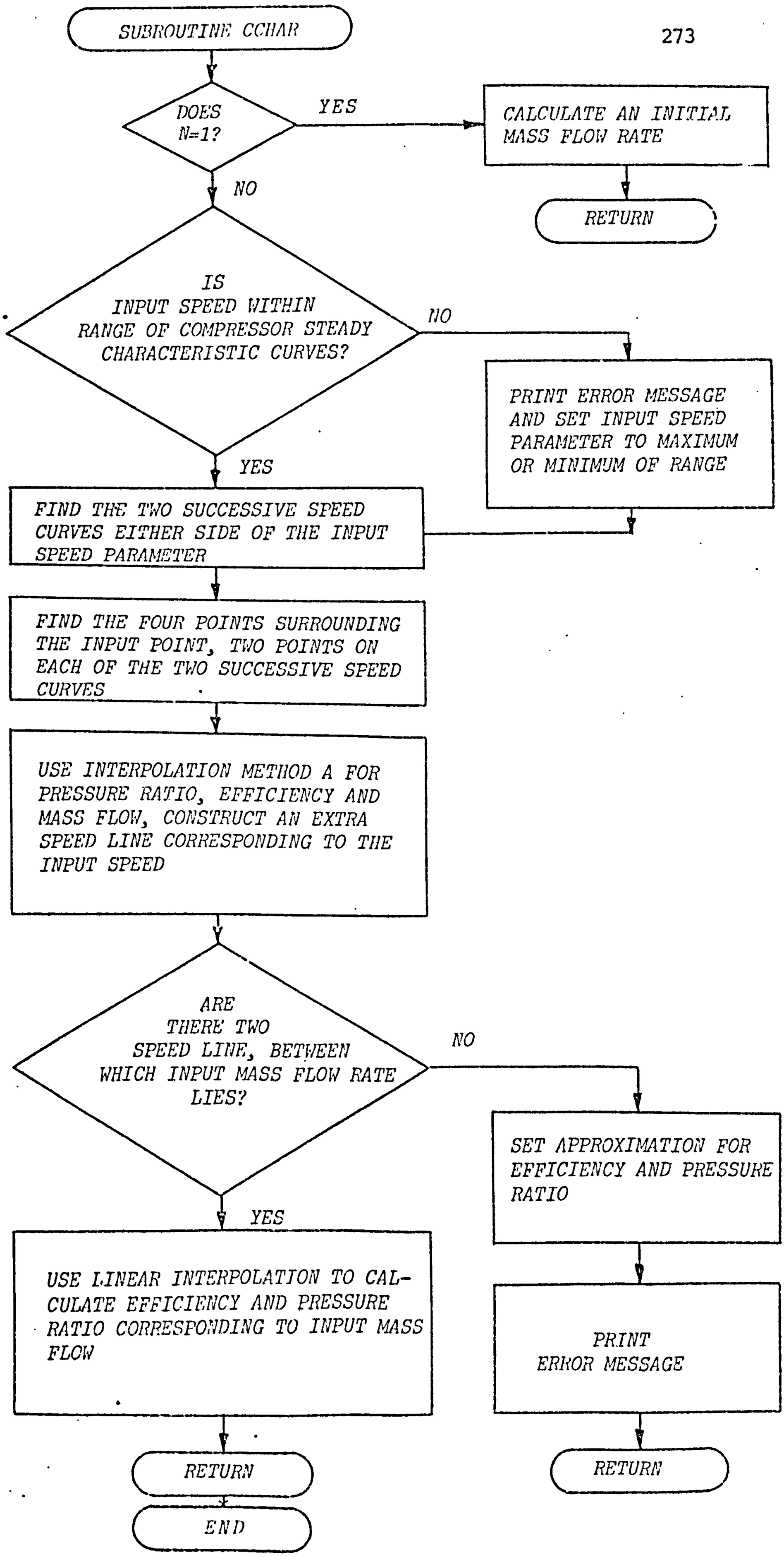
SUBROUTINE CCHAR
DOES N=1?
YES
CALCULATE AN INITIAL MASS FLOW RATE
RETURN
NO
IS INPUT SPEED WITHIN RANGE OF COMPRESSOR STEADY CHARACTERISTIC CURVES?
NO
PRINT ERROR MESSAGE AND SET INPUT SPEED PARAMETER TO MAXIMUM OR MINIMUM OF RANGE
YES
FIND THE TWO SUCCESSIVE SPEED CURVES EITHER SIDE OF THE INPUT SPEED PARAMETER
FIND THE FOUR POINTS SURROUNDING THE INPUT POINT, TWO POINTS ON EACH OF THE TWO SUCCESSIVE SPEED CURVES
USE INTERPOLATION METHOD A FOR PRESSURE RATIO, EFFICIENCY AND MASS FLOW, CONSTRUCT AN EXTRA SPEED LINE CORRESPONDING TO THE INPUT SPEED
ARE THERE TWO SPEED LINE, BETWEEN WHICH INPUT MASS FLOW RATE LIES?
NO
SET APPROXIMATION FOR EFFICIENCY AND PRESSURE RATIO
YES
USE LINEAR INTERPOLATION TO CALCULATE EFFICIENCY AND PRESSURE RATIO CORRESPONDING TO INPUT MASS FLOW
PRINT ERROR MESSAGE
RETURN
RETURN
END

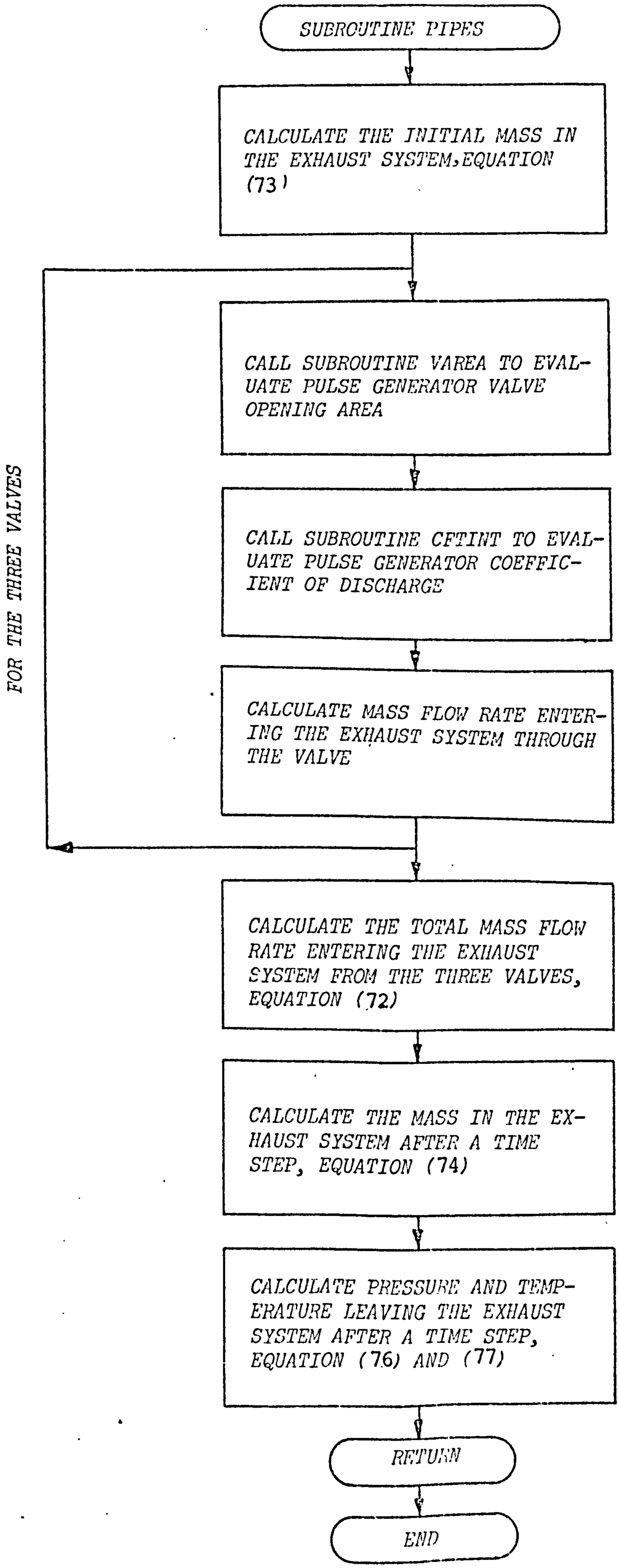
SUBROUTINE PIPES
CALCULATE THE INITIAL MASS IN THE EXHAUST SYSTEM, EQUATION (73)
CALL SUBROUTINE VAREA TO EVALUATE PULSE GENERATOR VALVE OPENING AREA
CALL SUBROUTINE CFTINT TO EVALUATE PULSE GENERATOR COEFFICIENT OF DISCHARGE
CALCULATE MASS FLOW RATE ENTERING THE EXHAUST SYSTEM THROUGH THE VALVE
FOR THE THREE VALVES
CALCULATE THE TOTAL MASS FLOW RATE ENTERING THE EXHAUST SYSTEM FROM THE THREE VALVES, EQUATION (72)
CALCULATE THE MASS IN THE EXHAUST SYSTEM AFTER A TIME STEP, EQUATION (74)
CALCULATE PRESSURE AND TEMPERATURE LEAVING THE EXHAUST SYSTEM AFTER A TIME STEP, EQUATION (76) AND (77)
RETURN
END

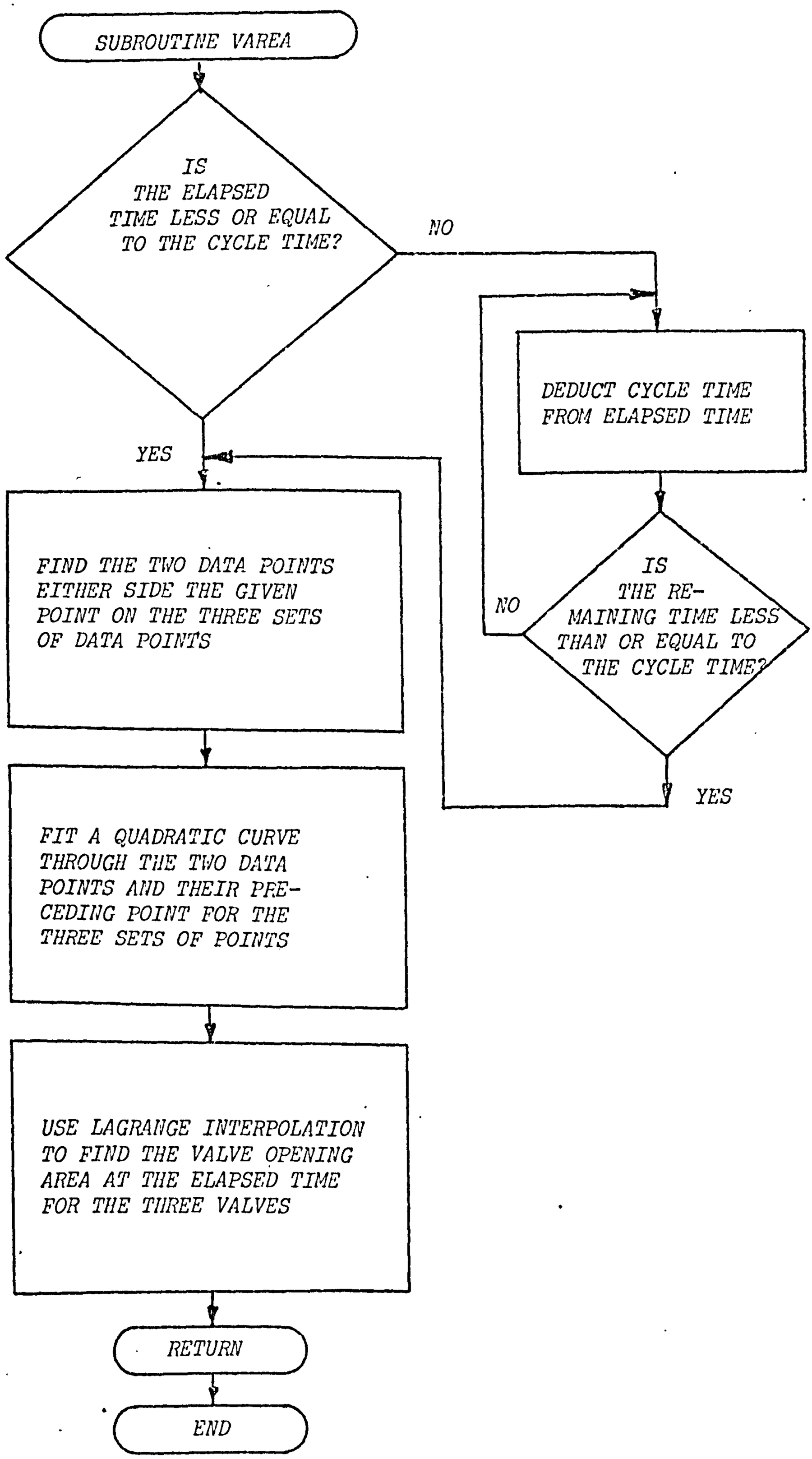
SUBROUTINE VAREA
IS THE ELAPSED TIME LESS OR EQUAL TO THE CYCLE TIME?
NO
YES
DEDUCT CYCLE TIME FROM ELAPSED TIME
IS THE RE-MAINING TIME LESS THAN OR EQUAL TO THE CYCLE TIME?
NO
YES
FIND THE TWO DATA POINTS EITHER SIDE THE GIVEN POINT ON THE THREE SETS OF DATA POINTS
FIT A QUADRATIC CURVE THROUGH THE TWO DATA POINTS AND THEIR PRE-CEDING POINT FOR THE THREE SETS OF POINTS
USE LAGRANGE INTERPOLATION TO FIND THE VALVE OPENING AREA AT THE ELAPSED TIME FOR THE THREE VALVES
RETURN
END

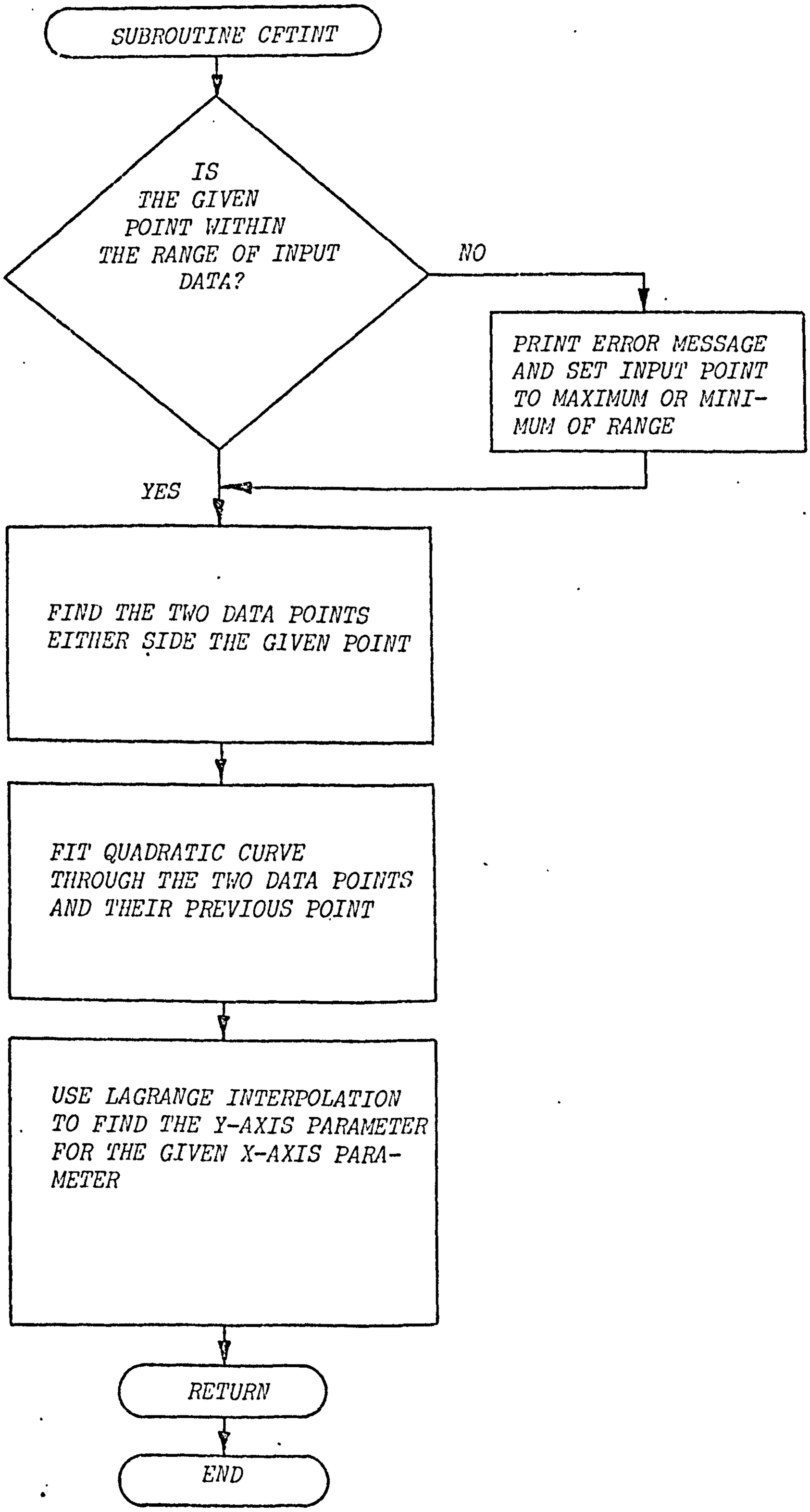
SUBROUTINE CFTINT
IS THE GIVEN POINT WITHIN THE RANGE OF INPUT DATA?
NO
PRINT ERROR MESSAGE AND SET INPUT POINT TO MAXIMUM OR MINIMUM OF RANGE
YES
FIND THE TWO DATA POINTS EITHER SIDE THE GIVEN POINT
FIT QUADRATIC CURVE THROUGH THE TWO DATA POINTS AND THEIR PREVIOUS POINT
USE LAGRANGE INTERPOLATION TO FIND THE Y-AXIS PARAMETER FOR THE GIVEN X-AXIS PARAMETER
RETURN
END

APPENDIX EIGHT

LISTINGS OF THE PROGRAMS AND SUBROUTINES

PROGRAM NON-PULSATING

```
      DIMENSION XAMFP(35,11),XP3DPO(35,11),XNRT3(11)
      DIMENSION XN(11),XP(35,11),XT(35,11)
      DIMENSION XCS(11),XA(20,11),XPC(20,11),XCE(20,11)
      DIMENSION XP2(23),XAMD(23)
      DIMENSION AMGTEST(3000),AMGST(100)
      DIMENSION TA(4),TP(4),TC(4),TL(4),TE(4),TF(4)
      REAL MEFF
      COMMON/MTS/XAMFP,XP3DPO,XNRT3
      COMMON/MTE/XN,XP,XT
      COMMON/MCC/XCS,XA,XPC,XCE
      COMMON/MTP/XP2,XAMD
      COMMON/TT1/TIMED(1000),AMGL(1000),P3DPOL(1000),T3D(1000),POD(1000)
      WRITE(2,183)
  183 FORMAT(1H1)
      READ(1,530)(XNRT3(I),I=1,11)
      WRITE(2,530)(XNRT3(I),I=1,11)
      DO 21 J=1,11
      READ(1,505)(XAMFP(I,J),I=1,35)
      WRITE(2,505)(XAMFP(I,J),I=1,35)
   21 CONTINUE
      DO 22 J=1,11
      READ(1,505)(XP3DPO(I,J),I=1,35)
      WRITE(2,505)(XP3DPO(I,J),I=1,35)
   22 CONTINUE
      READ(1,530)(XN(I),I=1,11)
      WRITE(2,530)(XN(I),I=1,11)
      DO 31 J=1,11
      READ(1,505)(XP(I,J),I=1,35)
      WRITE(2,505)(XP(I,J),I=1,35)
   31 CONTINUE
      DO 32 J=1,11
      READ(1,505)(XT(I,J),I=1,35)
      WRITE(2,505)(XT(I,J),I=1,35)
   32 CONTINUE
      READ(1,540)(XCS(I),I=1,11)
      WRITE(2,540)(XCS(I),I=1,11)
      DO 41 J=1,11
      READ(1,500)(XA(I,J),I=1,20)
      WRITE(2,500)(XA(I,J),I=1,20)
   41 CONTINUE
      DO 42 J=1,11
      READ(1,500)(XPC(I,J),I=1,20)
      WRITE(2,500)(XPC(I,J),I=1,20)
   42 CONTINUE
      DO 43 J=1,11
      READ(1,500)(XCE(I,J),I=1,20)
      WRITE(2,500)(XCE(I,J),I=1,20)
   43 CONTINUE
      READ(1,182)(XP2(I),I=1,23)
      WRITE(2,182)(XP2(I),I=1,23)
      READ(1,182)(XAMD(I),I=1,23)
      WRITE(2,182)(XAMD(I),I=1,23)
      WRITE(2,183)
      WRITE(2,1103)
```

```
1103 FORMAT(////24H TURBOCHARGER INPUT DATA/24H-----------------------
    1)
     READ(1,101)T1,AI,CP,GAM,ERROR
     READ(1,101)P0,P4
     READ(1,101)ERROR1
 101 FORMAT(6E12.4)
     WRITE(2,107)
     WRITE(2,102)
     WRITE(2,108)T1
     WRITE(2,109)AI
     WRITE(2,110)CP
     WRITE(2,111)GAM
     WRITE(2,113)ERROR
 555 FORMAT(7E11.4/7E11.4/7E11.4)
 102 FORMAT(13H -----------------)
 107 FORMAT(////13H PROGRAM CONSTANTS)
 108 FORMAT(/31H COMPRESSOR INLET TEMPERATURE =,E12.4)
 109 FORMAT(/33H TURBOCHARGER MOMENT OF INERTIA =,E12.4)
 110 FORMAT(/37H SPECIFIC HEAT AT CONSTANT PRESSURE =,E12.4)
 111 FORMAT(/26H RATIO OF SPECIFIC HEATS =,E12.4)
 113 FORMAT(/35H ACCURACY OF ITERATIVE PROCEDURES =,E12.4)
     WRITE(2,103)
 103 FORMAT(////11H INPUT DATA/11H ----------)
 500 FORMAT(10F8.5)
 510 FORMAT(8F10.5)
 520 FORMAT(10F8.2)
 530 FORMAT(10F8.2/F8.2)
 540 FORMAT(8F10.2/3F10.2)
 550 FORMAT(F10.2,F10.5,F10.2,F10.5,F10.5)
 505 FORMAT(5F8.5/10F8.5/10F8.5/10F8.5)
 182 FORMAT(11F7.4/11F7.4/F7.4)
 900 FORMAT(8E12.6)
     JJ=1
     K=0
   4 K=K+1
     READ(1,550)TIMED(K),P3DP0D(K),T3D(K)
     IF(TIMED(K).GT.1.0E+04)GOTO 7
     WRITE(2,105)TIMED(K),P3DP0D(K),T3D(K)
 105 FORMAT(F12.4,8X,F12.4,12X,F12.4,4X,F12.4)
     GOTO 4
   7 GAM1=GAM-1.0
     MEFF=1.0
     STEP1=0.001
     STEP2=0.0001
     PTS=0.0
     AMG=0.08
     CSPED=0.0
     AC1=0.0
     J=0
     WRITE(2,106)
 106 FORMAT(1H1////12H OUTPUT DATA/12H -----------)
     WRITE(2,114)
 114 FORMAT(2X,5H TIME,7X,6H SPEED,4X,12H T MASS FLOW,7X,6H T EFF,6X,8
    1H T POWER,4X,12H C MASS FLOW,2X,14H C PRESS RATIO,3X,6H C EFF,6X,8
```

```
LF NPMR,FR108,TC162
   1H C POWER/)
  5 PTNP1=PCNP1
    SPDNP1=CSPED
  2 J=J+1
    MM=0.0
    IF(J.EQ.1)GOTO 6
    WRITE(2,115)T,SPDNP1,AMG,TEFF,PTNP1,AMA,P2DP1,CEFF,PCNP1
115 FORMAT(9E13.4)
    IF(TIMED(J).GT.1.0E+04)STOP
    A1=-0.4931214E-02
    B1=0.1118452E-05
    C1=0.2185368E-09
    D1=-0.8979711E-15
    PWB=((D1*SPDNP1+C1)*SPDNP1+B1)*SPDNP1+A1
    PTNP=AMG*CP*T3*TEFF*(1.0-(1.0/P3DP0)**(GAM1/GAM))
    MEFF=(PTNP-PWB)/PTNP
    DEN4=348.4321*P4/T4
    VOLFR4=AMG/DEN4
    A2=0.5591953E-03
    B2=-0.1066845E+00
    C2=0.2463249E+01
    D2=-0.2496935E+00
    DPL=((D2*VOLFR4+C2)*VOLFR4+B2)*VOLFR4+A2
    P4=DPL+P4
  6 T=TIMED(J)
    P3DP0=P3DP0D(J)
    P3=P3DP0*P4
    T3=T3D(J)
    RT3=SQRT(T3)
245 SPDN=SPDNP1
    PTN=PTNP1
    IF(P3DP0D(J).GT.P3DP0D(J-1))GO TO 11
    CALL TSCHARM(P3DP0,ANDRT3,AMFP)
    AMG=AMFP*P3/RT3
    PCN=PCNP1
 11 JJ=JJ+1
    AMFP=AMG*RT3/P3
    IF(AMFP.GT.(0.22E+01))STOP
    CALL TSCHAR(AMFP,P3DP0,ANDRT3)
    CSPED=ANDRT3*RT3
    CALL TEFFCH(ANDRT3,P3DP0,TEFF)
    PW=AMG*CP*T3*TEFF*MEFF*(1.0-1.0/P3DP0**(GAM1
   1/GAM))
    IF(J.GT.1)GO TO 15
    CALL CCHAR(1,AMA,CSPED,CEFF,P2DP1)
 15 AMASTO=AMA
    CALL CCHAR(2,AMA,CSPED,CEFF,P2DP1)
    PR2=P2DP1*P0
    CALL CFTINT(AMA,XP2,XAMD,23,PR2)
    T2P=T1*(P2DP1)**(GAM1/GAM)
    T2=(T2P-T1)/CEFF+T1
    DEN=348.4321*PR2/T2
    DENR=SQRT(DEN)
    AMA=AMA*DENR
    IF(ABS((AMA-AMASTO)/AMA).LE.ERROR)GO TO 61
```

```
      GO TO 15
   61 PCNP1=AMA*CP*T1*(P2DP1**(GAM1/GAM)-1.0)/CEFF
      T4P=T3/P3DP0**(GAM1/GAM)
      T4=T3-TEFF*(T3-T4P)
      AMGTEST(JJ)=AMG
      IF(J.GT.1)GO TO 14
      IF(PCNP1.LT.PW.AND.MM.EQ.1)GO TO 5
      IF(PCNP1.GT.PW)GO TO 52
      IF(ABS((PW-PCNP1)/PW).LE.ERROR)GO TO 5
      AMG=AMGTEST(JJ-1)+STEP2
      MM=1
      GO TO 11
   52 AMG=AMGTEST(JJ)+STEP1
      GO TO 11
   14 DT=TIMED(J)-TIMED(J-1)
      SPDNP1=CSPED
      PA1=(SPDNP1**2-SPDN**2)*AI/(DT*0.91139E+05)
      PTNP1=PCNP1+PA1+PCN-PTN
      AMGTEST(JJ)=AMG
      IF(P3DP0D(J).LT.P3DP0D(J-1))GO TO 246
      IF(PTNP1.LT.PW.AND.MM.EQ.1)GO TO 2
      IF(PTNP1.GT.PW)GO TO 82
      IF(ABS((PW-PTNP1)/PW).LE.ERROR)GO TO 2
      AMG=AMGTEST(JJ-1)+STEP2
      MM=1
      GO TO 11
   82 AMG=AMGTEST(JJ)+STEP1
      GO TO 11
  246 IF(PW.LT.PTNP1.AND.MM.EQ.1)GO TO 2
      IF(PW.GT.PTNP1)GO TO 83
      IF(ABS((PTNP1-PW)/PTNP1).LE.ERROR)GO TO 2
      AMG=AMGTEST(JJ-1)-STEP2
      MM=1
      GO TO 11
   83 AMG=AMGTEST(JJ)-STEP1
      GO TO 11
  280 PTNP1=AMG*CP*T3*TEFF*MEFF*(1.0-1.0/P3DP0**
     1(GAM1/GAM))
      PCNP1=PTNP1
      CEFF=AMA*CP*T1*(P2DP1**(GAM1/GAM)-1.0)/PCNP1
      AC1=1.0
      GO TO 2
   50 STOP
      END
```

```
PROGRAM PULSATING1

      DIMENSION XAMFP(35,11),XP3DP0(35,11),XNRT3(11)
      DIMENSION XN(11),XP(35,11),XT(35,11)
      DIMENSION XCS(11),XA(20,11),XPC(20,11),XCE(20,11)
      DIMENSION XP2(23),XAMO(23)
      DIMENSION AMGTEST(3000)
      REAL MEFF
      COMMON/MTS/XAMFP,XP3DP0,XNRT3
      COMMON/MTE/XN,XP,XT
      COMMON/MCC/XCS,XA,XPC,XCE
      COMMON/MTP/XP2,XAMO
      COMMON/MDP/VS,GASR,PG,GAM,TG,BTIME(37),BFG(3,37)
     1,NTN,TCYCLE,DT,AFG(12),ACDG(12),NTM
      WRITE(2,1)
    1 FORMAT(1H1)
      READ(1,15)(XNRT3(I),I=1,11)
      WRITE(2,15)(XNRT3(I),I=1,11)
      DO 2 J=1,11
      READ(1,18)(XAMFP(I,J),I=1,35)
      WRITE(2,18)(XAMFP(I,J),I=1,35)
    2 CONTINUE
      DO 3 J=1,11
      READ(1,18)(XP3DP0(I,J),I=1,35)
      WRITE(2,18)(XP3DP0(I,J),I=1,35)
    3 CONTINUE
      READ(1,15)(XN(I),I=1,11)
      WRITE(2,15)(XN(I),I=1,11)
      DO 4 J=1,11
      READ(1,18)(XP(I,J),I=1,35)
      WRITE(2,18)(XP(I,J),I=1,35)
    4 CONTINUE
      DO 5 J=1,11
      READ(1,18)(XT(I,J),I=1,35)
      WRITE(2,18)(XT(I,J),I=1,35)
    5 CONTINUE
      READ(1,16)(XCS(I),I=1,11)
      WRITE(2,16)(XCS(I),I=1,11)
      DO 6 J=1,11
      READ(1,12)(XA(I,J),I=1,20)
      WRITE(2,12)(XA(I,J),I=1,20)
    6 CONTINUE
      DO 7 J=1,11
      READ(1,12)(XPC(I,J),I=1,20)
      WRITE(2,12)(XPC(I,J),I=1,20)
    7 CONTINUE
      DO 8 J=1,11
```

```
      READ(1,12)(XCE(I,J),I=1,20)
      WRITE(2,12)(XCE(I,J),I=1,20)
    8 CONTINUE
      READ(1,19)(XP2(I),I=1,23)
      WRITE(2,19)(XP2(I),I=1,23)
      READ(1,19)(XAMO(I),I=1,23)
      WRITE(2,19)(XAMO(I),I=1,23)
      WRITE(2,1)
      WRITE(2,9)
    9 FORMAT(////24H TURBOCHARGER INPUT DATA/24H------------------------
     1)
      READ(1,21)T1,AI,CP,GAM,P0,ERROR
      READ(1,20)MEFF
      READ(1,21)PG,TG,GASR,VS,T3,P3
      READ(1,21)DT,TMAX
      READ(1,39)NTM
      DO 10 N=1,NTM
      READ(1,11)AFG(N),ACDG(N)
      WRITE(2,11)AFG(N),ACDG(N)
   10 CONTINUE
   11 FORMAT(E14.6,E10.2)
      READ(1,39)NTN
      WRITE(2,23)
      WRITE(2,22)
      WRITE(2,24)T1
      WRITE(2,25)AI
      WRITE(2,26)CP
      WRITE(2,27)GAM
      WRITE(2,28)P0
      WRITE(2,29)ERROR
      WRITE(2,30)MEFF
      WRITE(2,31)PG
      WRITE(2,32)TG
      WRITE(2,33)GASR
      WRITE(2,34)VS
      WRITE(2,35)T3
      WRITE(2,36)P3
      WRITE(2,37)DT
      WRITE(2,38)TMAX
   12 FORMAT(10F8.5)
   13 FORMAT(8F10.5)
   14 FORMAT(10F8.2)
   15 FORMAT(10F8.2/F8.2)
   16 FORMAT(8F10.2/3F10.2)
   17 FORMAT(F10.2,F10.5,F10.2,F10.5,F10.5)
   18 FORMAT(5F8.5/10F8.5/10F8.5/10F8.5)
   19 FORMAT(11F7.4)
   20 FORMAT(3E12.5)
   21 FORMAT(6E12.4)
   22 FORMAT(18H ------------------)
```

```
23 FORMAT(1H1////18H PROGRAM CONSTANTS)
24 FORMAT(/26H ATMOSPHERIC TEMPERATURE =,E12.4)
25 FORMAT(/33H TURBOCHARGER MOMENT OF INERTIA =,E12.4)
26 FORMAT(/37H SPECIFIC HEAT AT CONSTANT PRESSURE =,E12.4)
27 FORMAT(/26H RATIO OF SPECIFIC HEATS =,E12.4)
28 FORMAT(/23H ATMOSPHERIC PRESSURE =,E12.4)
29 FORMAT(/35H ACCURACY OF ITERATIVE PROCEDURES =,E12.4)
30 FORMAT(/24H MECHANICAL EFFICIENCY =,E12.4)
31 FORMAT(/21H P C INPUT PRESSURE =,E12.4)
32 FORMAT(/24H P C INPUT TEMPERATURE =,E12.4)
33 FORMAT(/15H GAS CONSTANT =,E12.4)
34 FORMAT(/15H PIPES VOLUME =,E12.4)
35 FORMAT(/21H STEADY TEMPERATURE =,E12.4)
36 FORMAT(/18H STEADY PRESSURE =,E12.4)
37 FORMAT(/12H TIME STEP =,E12.4)
38 FORMAT(/28H CALCULATION TIME REQUIRED =,E12.4)
39 FORMAT(I6)
   DO 41 N=1,NTN
   READ(1,40)BTIME(N),BFG(1,N),BFG(2,N),BFG(3,N)
   BTIME(N)=BTIME(N)*2000.00/2950.00
   WRITE(2,40)BTIME(N),BFG(1,N),BFG(2,N),BFG(3,N)
40 FORMAT(5E12.4)
41 CONTINUE
42 FORMAT(11F7.1)
43 FORMAT(12F6.4)
44 FORMAT(11F7.4)
45 FORMAT(8F9.1)
46 FORMAT(13F6.4)
47 FORMAT(10E11.4)
48 GAM1=GAM-1.0
   PTS=0.0
   CSPED=0.0
   AMG=0.05
   M=1
   J=0
   WRITE(2,49)
49 FORMAT(////12H OUTPUT DATA/12H ------------)
   WRITE(2,50)
50 FORMAT(/'       TIM    SPDNP1      AMG     TEFF      T3      T4    P3DP0
  1    PTNP1      AMA     CEFF      T2    P2DP1     PCNP1')
51 PTNP1=PCNP1
   SPDNP1=CSPED
   TSTART=BTIME(1)
   TCYCLE=BTIME(NTN)
   TIM=TSTART
52 SPDN=SPDNP1
   PCN=PCNP1
   PTN=PTNP1
   DM=0.001
53 J=J+1
```

```
      IF(J.EQ.1)GOTO 57
      WRITE(2,54)TIM,SPDNP1,AMG,TEFF,T3,T4,P3DP0,PTNP1
     1,AMA,CEFF,T2,P2DP1,PCNP1
   54 FORMAT(F10.5,F9.2,2F8.5,2F7.2,F8.5,F9.5,2F8.5,
     1F7.2,F8.5,F9.5)
      IF(TIM.GT.TMAX)GO TO 67
   55 TIM=TIM+DT
   56 CALL PIPES(P3,13,AMG,TIM,P3NP1,T3NP1)
      P3=P3NP1
      T3=T3NP1
   57 P3DP0=P3/P0
      RT3=SQRT(T3)
   58 M=M+1
      AMFP=AMG*RT3/P3
      CALL TSCHAR(1,AMFP,P3DP0,ANDRT3)
      CSPED=ANDRT3*RT3
      CALL TEFFCH(ANDRT3,P3DP0,TEFF)
      PW=AMG*CP*T3*TEFF*MEFF*(1.0-1.0/P3DP0**(GAM1
     1/GAM))
      CALL CCHAR(1,AMA,CSPED,CEFF,P2DP1)
   59 AMASTO=AMA
      CALL CCHAR(2,AMA,CSPED,CEFF,P2DP1)
      PR2=P2DP1*P0
      CALL CFTINT(AMA,XP2,XAMO,23,PR2)
      T2P=T1*(P2DP1)**(GAM1/GAM)
      T2=(T2P-T1)/CEFF+T1
      DEN=348.4321*PR2/T2
      DENR=SQRT(DEN)
      AMA=AMA*DENR
      IF(ABS((AMA-AMASTO)/AMA).LT.ERROR)GO TO 60
      GO TO 59
   60 PCNP1=AMA*CP*T1*(P2DP1**(GAM1/GAM)-1.0)/CEFF
      T4P=T3/P3DP0**(GAM1/GAM)
      T4=T3-TEFF*(T3-T4P)
      AMGTEST(M)=AMG
      IF(PCNP1.LE.PW)GO TO 62
   61 AMG=AMG+DM
      GO TO 58
   62 IF(J.GT.1)GO TO 64
   63 IF(ABS((PW-PCNP1)/PW).LE.ERROR)GO TO 51
      DM=DM/10.0
      AMG=AMGTEST(M-1)+DM
      GO TO 58
   64 CSPEDN=CSPED
      CSPED=CSPED+500
   65 ANDRT3=CSPED/RT3
      CALL TSCHAR(2,AMFP,ANDRT3,P3DP0)
      CALL TEFFCH(ANDRT3,P3DP0,TEFF)
      PTNP1=AMG*CP*T3*TEFF*(1.0-(1.0/P3DP0)**(GAM1/GAM))*MEFF
      AMAP=AMA*CSPED/CSPEDN
```

```
      CALL CCHAR(2,AMAP,CSPED,CEFF,P2DP1)
      PCNP1=AMAP*CP*T1*(P2DP1**(GAM1/GAM)-1.0)/CEFF
      PA1=0.91189E+05*DT*(PTNP1+PTN-PCNP1-PCN)/AI
      SPDNP1=SQRT(SPDN**2+PA1)
      IF(ABS((SPDNP1-CSPED)/SPDNP1).LT.ERROR)GO TO 66
      CSPED=SPDNP1
      GO TO 65
   66 AMA=AMAP
      T2P=T1*(P2DP1)**(GAM1/GAM)
      T2=(T2P-T1)/CEFF+T1
      T4P=T3/P3DP**(GAM1/GAM)
      T4=T3-TEFF*(T3-T4P)
      GO TO 52
   67 STOP
      END
```

PROGRAM PULSATING2

```
      DIMENSION XAMFP(35,11),XP3LP0(35,11),XNRT3(11)
      DIMENSION XN(11),XP(35,11),XT(35,11)
      DIMENSION XCS(11),XA(20,11),XPC(20,11),XCE(20,11)
      COMMON/MTS/XAMFP,XP3LP0,XNRT3
      DIMENSION XP2(23),XAMC(23)
      COMMON/MTE/XN,XP,XT
      COMMON/MCC/XCS,XA,XPC,XCE
      COMMON/TTI/TIMED(1000),P3DPOD(1000),T3D(1000),CSPEDD(1000)
      REAL MEFF
      WRITE(2,183)
  183 FORMAT(1H1)
      READ(1,530)(XNRT3(I),I=1,11)
      WRITE(2,530)(XNRT3(I),I=1,11)
      DO 21 J=1,11
      READ(1,505)(XAMFP(I,J),I=1,35)
      WRITE(2,505)(XAMFP(I,J),I=1,35)
   21 CONTINUE
      DO 22 J=1,11
      READ(1,505)(XP3LP0(I,J),I=1,35)
      WRITE(2,505)(XP3LP0(I,J),I=1,35)
   22 CONTINUE
      READ(1,530)(XN(I),I=1,11)
      WRITE(2,530)(XN(I),I=1,11)
      DO 31 J=1,11
      READ(1,505)(XP(I,J),I=1,35)
      WRITE(2,505)(XP(I,J),I=1,35)
   31 CONTINUE
      DO 32 J=1,11
      READ(1,505)(XT(I,J),I=1,35)
      WRITE(2,505)(XT(I,J),I=1,35)
   32 CONTINUE
      READ(1,540)(XCS(I),I=1,11)
      WRITE(2,540)(XCS(I),I=1,11)
      DO 41 J=1,11
      READ(1,500)(XA(I,J),I=1,20)
      WRITE(2,500)(XA(I,J),I=1,20)
   41 CONTINUE
      DO 42 J=1,11
      READ(1,500)(XPC(I,J),I=1,20)
      WRITE(2,500)(XPC(I,J),I=1,20)
   42 CONTINUE
      DO 43 J=1,11
      READ(1,500)(XCE(I,J),I=1,20)
      WRITE(2,500)(XCE(I,J),I=1,20)
   43 CONTINUE
      READ(1,132)(XP2(I),I=1,23)
      WRITE(2,132)(XP2(I),I=1,23)
      READ(1,132)(XAMC(I),I=1,23)
      WRITE(2,132)(XAMC(I),I=1,23)
      WRITE(2,183)
      READ(1,101)T1,AI,CP,GAM,ERROR
      READ(1,101)P0,P4
  101 FORMAT(6E12.4)
      WRITE(2,183)
```

```
      WRITE(2,107)
      WRITE(2,102)
      WRITE(2,108)T1
      WRITE(2,109)AI
      WRITE(2,110)CP
      WRITE(2,111)GAM
      WRITE(2,113)ERROR
  102 FORMAT(13H ------------------)
  107 FORMAT(1H1////13H PROGRAM CONSTANTS)
  108 FORMAT(/31H COMPRESSOR INLET TEMPERATURE =,E12.4)
  109 FORMAT(/33H TURBOCHARGER MOMENT OF INERTIA =,E12.4)
  110 FORMAT(/37H SPECIFIC HEAT AT CONSTANT PRESSURE =,E12.4)
  111 FORMAT(/26H RATIO OF SPECIFIC HEATS =,E12.4)
  113 FORMAT(/35H ACCURACY OF ITERATIVE PROCEDURES =,E12.4)
      WRITE(2,103)
  103 FORMAT(////11H INPUT DATA/11H ----------)
  500 FORMAT(10F8.5)
  510 FORMAT(8F10.5)
  520 FORMAT(10F8.2)
  991 FORMAT(F8.4)
  530 FORMAT(10F8.2/F8.2)
  540 FORMAT(8F10.2/3F10.2)
  550 FORMAT(F10.2,F10.5,F10.2,F10.5,F10.5)
  559 FORMAT(2F8.3,F9.2)
  505 FORMAT(5F8.5/10F8.5/10F8.5/10F8.5)
  182 FORMAT(11F7.4/11F7.4/F7.4)
  900 FORMAT(8F12.6)
      K=0
    4 K=K+1
      READ(1,539)TIMED(K),P3DPOD(K),T3D(K),CSPEED(K)
      IF (TIMED(K).GT.1.0E+02) GO TO 7
      WRITE(2,589)TIMED(K),P3DPOD(K),T3D(K),CSPEED(K)
  105 FORMAT(1H ,F12.4,8X,F12.4,12X,F12.4,4X,F12.4,5X,F12.4)
  539 FORMAT(2F8.3,F9.2,F11.2)
      GO TO 4
    7 GAM1=GAM-1.0
      CSPED=32000
      J=0
      WRITE(2,106)
  106 FORMAT(////12H OUTPUT DATA/12H -----------)
      WRITE(2,183)
      WRITE(2,114)
  114 FORMAT(/4X,5H TIME,9X,6H T MAS,9X,6H T EFF,8X,8H T POWER,6X,12H C
     1MASS FLOW,3X,14H C PRESS RATIO,5X,6H C EFF,9X,8H C POWER/)
    2 J=J+1
      IF (J.EQ.1) GO TO 6
      WRITE(2,115)T,AMG,TEFF,PTNPI,AMA,P2DPI,CEFF,PCNPI
  115 FORMAT(4(E12.4,3X),E12.4,4X,E12.4,4X,E12.4,4X,E12.4)
      IF (TIMED(J).GT.1.0E+02) STOP
    6 T=TIMED(J)
      IF(T.EQ.10)STOP
      CSPED=CSPEED(J)
      P3DPO=P3DPOD(J)
      T3=T3D(J)
```

```
      RT3=SQRT(T3)
      P3=P3DP0*P4
      ANDRT3=CSPED/RT3
      CALL TSCHARM(P3DP0,ANDRT3,AMFP)
      AMG=AMFP*P3/RT3
      CALL TEFFCH(ANDRT3,P3DP0,TEFF)
      T4P=T3/P3DP0**(GAM1/GAM)
      T4=T3-TEFF*(T3-T4P)
      A1=-0.4931214E-02
      B1=0.1113452E-05
      C1=0.2185368E-09
      D1=-0.3979711E-15
      PWB=((D1*CSPED+C1)*CSPED+B1)*CSPED+A1
      PTNP=AMG*CP*T3*TEFF*(1.0-(1.0/P3DP0)**(GAM1/GAM))
      MEFF=(PTNP-PWB)/PTNP
      DEN4=348.4321*P4/T4
      VDLFR4=AMG/DEN4
      A2=0.5591953E-03
      B2=-0.1066345E+00
      C2=0.2468249E+01
      D2=-0.2496935E+00
      DPL=((D2*VDLFR4+C2)*VDLFR4+B2)*VDLFR4+A2
      P4=DPL+P4
      PTNP1=AMG*CP*T3*TEFF*MEFF*(1.0-1.0/P3DP0**(GAM1
     1/GAM))
      CALL CCHAR(1,AMA,CSPED,CEFF,P2DP1)
   15 AMASTD=AMA
      CALL CCHAR(2,AMA,CSPED,CEFF,P2DP1)
      PR2=P2DP1*P0
      CALL CFTINT(AMA,XP2,XAMD,23,PR2)
      T2P=T1*(P2DP1)**(GAM1/GAM)
      T2=(T2P-T1)/CEFF+T1
      DEN=348.4321*PR2/T2
      DENR=SQRT(DEN)
      AMA=AMA*DENR
      IF(ABS((AMA-AMASTD)/AMA).LE.ERR)GO TO 61
      GO TO 15
   61 PCNP1=AMA*CP*T1*(P2DP1**(GAM1/GAM)-1.0)/CEFF
      GO TO 2
      END
```

```
      SUBROUTINE TSCHAR(N,AMFP,P3XN,ANSWER)
      DIMENSION XAMFP(35,11),XP3DP0(35,11),XNRT3(11),DXA(35),DXP(35),
     1X(35),Y(35),Z(2)
      COMMON/MTS/XAMFP,XP3DP0,XNRT3
      NN=11
      NP=35
      IF (N.EQ.1) GO TO 13
       IF (P3XN-XNRT3(1)) 1,3,3
    1 WRITE(2,2)P3XN
    2 FORMAT(///,41H SPEED PARAMETER OUT OF RANGE IN TSCHAR =,E12.4)
      P3XN=XNRT3(1)
      GO TO 5
    3 IF (P3XN-XNRT3(NN)) 5,5,4
    4 WRITE(2,2)P3XN
      P3XN=XNRT3(NN)
    5 DO 6 J=2,NN
      PA1=P3XN-XNRT3(J-1)
      PA2=P3XN-XNRT3(J)
      K=J-1
      IF (PA1*PA2.LE.0.0) GO TO 7
    6 CONTINUE
    7 DO 8 I=1,NP
      PA1=(P3XN-XNRT3(K))/(XNRT3(K+1)-XNRT3(K))
      DXA(I)=XAMFP(I,K)+PA1*(XAMFP(I,K+1)-XAMFP(I,K))
      DXP(I)=XP3DP0(I,K)+PA1*(XP3DP0(I,K+1)-XP3DP0(I,K))
    8 CONTINUE
      DO 9 I=2,NP
      PA1=AMFP-DXA(I-1)
      PA2=AMFP-DXA(I)
      K=I-1
      IF (PA1*PA2.LE.0.0) GO TO 12
    9 CONTINUE
      ANSWER=DXP(1)
      IF (AMFP.GT.DXA(NP)) ANSWER=DXP(NP)
      WRITE(2,10)AMFP,P3XN
      WRITE(2,11)ANSWER
   10 FORMAT(////34H PARAMETERS OUT OF RANGE IN TSCHAR/22H MASS FLOW PAR
     1AMETER =,E12.4/18H SPEED PARAMETER =,E12.4)
   11 FORMAT(//41H APPROXIMATION FOR PRESSURE RATIO TAKEN =,E12.4)
      RETURN
   12 PA1=(AMFP-DXA(K))/(DXA(K+1)-DXA(K))
      ANSWER=DXP(K)+PA1*(DXP(K+1)-DXP(K))
      RETURN
   13 J=0
   14 M=0
   15  M=M+1
      J=J+1
      IF (J.GT.NN) GO TO 23
      DO 16 I=2,NP
      PA1=AMFP-XAMFP(I-1,J)
```

```
      PA2=AMFP-XAMFP(I,J)
      K=I-1
      IF (PA1*PA2.LE.0.0) GO TO 17
   16 CONTINUE
      GO TO 14
   17 IF (K.EQ.1) K=K-1
      IF (K.GT.1) K=K-2
      DO 18 L=1,3
      K=K+1
      X(L)=XAMFP(K,J)
      Y(L)=XP3DP0(K,J)
   18 CONTINUE
      PA1=0.0
      DO 20 I=1,3
      PA2=1.0
      DO 19 K=1,3
      IF (I.EQ.K) GO TO 19
      PA2=PA2*(AMFP-X(K))/(X(I)-X(K))
   19 CONTINUE
      PA1=PA1+PA2*Y(I)
   20 CONTINUE
      Z(M)=PA1
      IF (M.EQ.1) GO TO 15
   21 IF ((P3XN-Z(1))*(P3XN-Z(2)).LE.0.0) GO TO 22
      Z(1)=Z(2)
      M=1
      GO TO 15
   22 PA1=(P3XN-Z(1))/(Z(2)-Z(1))
      ANSWER=XNRT3(J-1)+PA1*(XNRT3(J)-XNRT3(J-1))
      RETURN
C
   23 ANSWER=XNRT3(INT(FLOAT(NN)/2.0))
      WRITE(2,24)AMFP,P3XN
      WRITE(2,25)ANSWER
   24 FORMAT(////34H PARAMETERS OUT OF RANGE IN TSCHAR/22H MASS FLOW PAR
     1AMETER =,E12.4/17H PRESSURE RATIO =,E12.4)
   25 FORMAT(//42H APPROXIMATION FOR SPEED PARAMETER TAKEN =,E12.4)
      RETURN
      END
```

```
      SUBROUTINE TEFFCH(AND,P3D,ANSWER)
      DIMENSION XN(11),XP(35,11),XT(35,11),DXP(35),DXT(35)
      COMMON/MTE/XN,XP,XT
      NN=11
      NP=35
      IF (AND-XN(1)) 1,3,3
    1 WRITE(2,2)AND
    2 FORMAT(////41H SPEED PARAMETER OUT OF RANGE IN TEFFCH =,E12.4)
      AND=XN(1)
      GO TO 5
    3 IF (AND-XN(NN)) 5,5,4
    4 WRITE(2,2)AND
      AND=XN(NN)
    5 DO 6 J=2,NN
      PA1=AND-XN(J-1)
      PA2=AND-XN(J)
      K=J-1
      IF (PA1*PA2.LE.0.0) GO TO 7
    6 CONTINUE
    7 DO 8 I=1,NP
      PA1=(AND-XN(K))/(XN(K+1)-XN(K))
      DXP(I)=XP(I,K)+PA1*(XP(I,K+1)-XP(I,K))
      DXT(I)=XT(I,K)+PA1*(XT(I,K+1)-XT(I,K))
    8 CONTINUE
      DO 9 I=2,NP
      PA1=P3D-DXP(I-1)
      PA2=P3D-DXP(I)
      K=I-1
      IF (PA1*PA2.LE.0.0) GO TO 12
    9 CONTINUE
      ANSWER=DXT(1)
      IF (P3D.GT.DXP(NP)) ANSWER=DXT(NP)
      WRITE(2,10)AND,P3D
      WRITE(2,11)ANSWER
   10 FORMAT(////34H PARAMETERS OUT OF RANGE IN TEFFCH/18H SPEED PARAMET
     1ER =,E12.4/17H PRESSURE RATIO =,E12.4)
   11 FORMAT(//37H APPROXIMATION FOR EFFICIENCY TAKEN =,E12.4)
      RETURN
   12 PA1=(P3D-DXP(K))/(DXP(K+1)-DXP(K))
      ANSWER=DXT(K)+PA1*(DXT(K+1)-DXT(K))
      RETURN
      END
```

```
      SUBROUTINE CCHAR(N,AMA,CSPED,ANSE,ANSP)
      DIMENSION XCS(11),XA(20,11),XPC(20,11),XCE(20,11),
     1          DXP(20),DXE(20),DXA(20)
      COMMON/MCC/XGS,XA,XPC,XCE
      NN=11
      NP=20
      IF (N.GT.1) GO TO 7
      IF(CSPED-XCS(1))1,2,2
    1 CSPED=XCS(1)
      GO TO 4
    2 IF (CSPED-XCS(NN))4,4,3
    3 CSPED=XCS(NN)
    4 DO 5 J=2,NN
      PA1=CSPED-XCS(J-1)
      PA2=CSPED-XCS(J)
      K=J-1
      IF(PA1*PA2.LE.0.0)GO TO 6
    5 CONTINUE
    6 AMA=XA(1,K+1)+0.001
      RETURN
    7 IF (CSPED-XCS(1)) 8,9,9
    8 CSPED=XCS(1)
      GO TO 11
    9 IF (CSPED-XCS(NN)) 11,11,10
   10 CSPED=XCS(NN)
   11 DO 12 J=2,NN
      PA1=CSPED-XCS(J-1)
      PA2=CSPED-XCS(J)
      K=J-1
      IF (PA1*PA2.LE.0.0) GO TO 13
   12 CONTINUE
   13 DO 14 I=1,NP
      PA1=(CSPED-XCS(K))/(XCS(K+1)-XCS(K))
      DXP(I)=XPC(I,K)+PA1*(XPC(I,K+1)-XPC(I,K))
      DXE(I)=XCE(I,K)+PA1*(XCE(I,K+1)-XCE(I,K))
      DXA(I)=XA(I,K)+PA1*(XA(I,K+1)-XA(I,K))
   14 CONTINUE
      DO 15 I=2,NP
      PA1=AMA-DXA(I-1)
      PA2=AMA-DXA(I)
      K=I-1
      IF (PA1*PA2.LE.0.0) GO TO 17
   15 CONTINUE
      ANSE=DXE(1)
      ANSP=DXP(1)
      IF (AMA.LT.DXA(1)) GO TO 16
      ANSE=DXE(NP)
      ANSP=DXP(NP)
   16 RETURN
   17 PA1=(AMA-DXA(K))/(DXA(K+1)-DXA(K))
```

```
ANSE=DXE(K)+PA1*(DXE(K+1)-DXE(K))
ANSP=DXP(K)+PA1*(DXP(K+1)-DXP(K))
RETURN
END
```

```
      SUBROUTINE PIPES(P3,T3,AMG,TIM,P3NP1,T3NP1)
      COMMON/MDP/US,GASR,PG,GAM,TG,BTIME(37),BFG(3,37)
     1,NTN,TCYCLE,DT,AFG(12),ACDG(12),NTM
      DIMENSION FG(3),MU(3),CDG(3)
      REAL MS,MU,MUA,MSN
      MS=(P3*US*1.0E+02)/(GASR*T3)
      COEFF1=1.0-(P3/PG)**((GAM-1.0)/GAM)
      COEFF1=(2.0*GAM/(TG*GASR*(GAM-1.0)))*COEFF1
      COEFF1=PG*1.0E+05*((P3/PG)**(1.0/GAM))*SQRT(COEFF1/1.0E+03)
      DO 1 J=1,3
      CALL VAREA(FG(J),BTIME,BFG,NTN,TIM,J,TCYCLE)
      CALL CFTINT(CDG(J),AFG,ACDG,NTM,FG(J))
      MU(J)=COEFF1*FG(J)*CDG(J)
    1 CONTINUE
      MUA=(MU(1)+MU(2)+MU(3))
      MSN=MS+DT*(MUA-AMG)
      COEFF2=DT*(MUA*TG-AMG*T3)
      P3NP1=P3+GAM*GASR*COEFF2/(US*1.0E+02)
      T3NP1=P3NP1*US*1.0E+02/(MSN*GASR)
      RETURN
      END
```

```
      SUBROUTINE VAREA(PSI,X,Y,N,EX,I,TCYCLE)
      DIMENSION X(37),Y(3,37),FX(3),FY(3)
      IF (EX.LT.X(N)) GO TO 2
      DO 1 I=1,N
      X(I)=X(I)+TCYCLE
    1 CONTINUE
    2 I=1
    3 I=I+1
      IF (X(I).LT.EX) GO TO 3
      IF (I.EQ.N) I=N-1
      DO 4 J=1,3
      K=I+J-2
      FX(J)=X(K)
      FY(J)=Y(I,K)
    4 CONTINUE
      PSI=0.0
      DO 6 I=1,3
      PR=1.0
      DO 5 J=1,3
      IF (I.EQ.J) GO TO 5
      PR=PR*(EX-FX(J))/(FX(I)-FX(J))
    5 CONTINUE
      PSI=PSI+PR*FY(I)
    6 CONTINUE
      RETURN
      END
```

```
      SUBROUTINE CFTINT(C,X,Y,N,FOP)
      DIMENSION X(N),Y(N),FX(3),FY(3)
      IF (FOP.GE.X(1).AND.FOP.LE.X(N)) GO TO 1
      IF (FOP.LT.X(1)) FOP=X(1)
      IF (FOP.GT.X(N)) FOP=X(N)
    1 I=1
    2 I=I+1
      IF (X(I).LT.FOP) GO TO 2
      IF (I.EQ.N) I=N-1
      DO 3 J=1,3
      K=I+J-2
      FX(J)=X(K)
      FY(J)=Y(K)
    3 CONTINUE
      C=0.0
      DO 5 I=1,3
      PR=1.0
      DO 4 J=1,3
      IF (I.EQ.J) GO TO 4
      PR=PR*(FOP-FX(J))/(FX(I)-FX(J))
    4 CONTINUE
      C=C+PR*FY(I)
    5 CONTINUE
      RETURN
      END
```

```
      SUBROUTINE TSCHARM(P3DP0,P3XN,ANSWER)
      DIMENSION XAMFP(35,11),XP3DP0(35,11),XNRT3(11),DXA(35),DXP(35),
     1X(35),Y(35),Z(2)
      COMMON/MTS/XAMFP,XP3DP0,XNRT3
      NN=11
      NP=35
       IF (P3XN-XNRT3(1)) 15,16,16
   15 WRITE(2,103)P3XN
  103 FORMAT(////41H SPEED PARAMETER OUT OF RANGE IN TSCHAR =,E12.4)
      P3XN=XNRT3(1)
      GO TO 14
   16 IF (P3XN-XNRT3(NN)) 14,14,17
   17 WRITE(2,103)P3XN
      P3XN=XNRT3(NN)
   14 DO 2 J=2,NN
      PA1=P3XN-XNRT3(J-1)
      PA2=P3XN-XNRT3(J)
      K=J-1
      IF (PA1*PA2.LE.0.0) GO TO 7
    2 CONTINUE
    7 DO 18 I=1,NP
      PA1=(P3XN-XNRT3(K))/(XNRT3(K+1)-XNRT3(K))
      DXA(I)=XAMFP(I,K)+PA1*(XAMFP(I,K+1)-XAMFP(I,K))
      DXP(I)=XP3DP0(I,K)+PA1*(XP3DP0(I,K+1)-XP3DP0(I,K))
   18 CONTINUE
      DO 19 I=2,NP
      PA1=P3DP0-DXP(I-1)
      PA2=P3DP0-DXP(I)
      K=I-1
      IF (PA1*PA2.LE.0.0) GO TO 20
   19 CONTINUE
      ANSWER=DXA(1)
      IF (P3DP0.GT.DXP(NP)) ANSWER=DXA(NP)
      WRITE(2,104)P3DP0,P3XN
      WRITE(2,105)ANSWER
  104 FORMAT(////34H PARAMETERS OUT OF RANGE IN TSCHAR/11H PRESSURE =,
     1 E12.4/18H SPEED PARAMETER =,E12.4)
  105 FORMAT(//41H APPROXIMATION FOR MASS FLOW PARA TAKEN =,E12.4)
      RETURN
   20 PA1=(P3DP0-DXP(K))/(DXP(K+1)-DXP(K))
      ANSWER=DXA(K)+PA1*(DXA(K+1)-DXA(K))
      RETURN
```

APPENDIX NINE

COMPUTER PROGRAMS INPUT DATA

APPENDIX 9

COMPUTER PROGRAMS INPUT DATA

The explanation of the terms of the input data of each program starting from left to right is given immediately after the relevant data.

PROGRAM 'PULSATING 1 INPUT DATA:

Line No										
1.	1166.90	1755.77	2331.46	2921.63	3509.47	4062.22	4555.96	4957.72	5248.55	5551.00
2.	5922.60									
3.	0.02500	0.15000	0.30000	0.40000	0.55000					
4.	0.60500	0.66000	0.72500	0.78772	0.83318	0.85700	0.86000	0.87000	0.87750	0.88500
5.	0.90000	1.00000	1.02500	1.03000	1.03500	1.04600	1.04900	1.05200	1.05600	1.06000
6.	1.17000	1.39200	1.54100	1.64500	1.71100	1.76000	1.80500	1.87500	1.93000	1.99000
7.	0.02500	0.30000	0.50000	0.60000	0.90000					
8.	1.00000	1.01260	1.05000	1.09144	1.10000	1.15985	1.21800	1.23210	1.25500	1.27500
9.	1.28000	1.29500	1.30600	1.30400	1.32320	1.33320	1.34000	1.35000	1.35900	1.37600
10.	1.48500	1.58500	1.66700	1.76200	1.80000	1.84000	1.86500	1.89000	1.91600	1.94000
11.	0.02500	0.30000	0.45000	0.65000	0.90000					
12.	1.08500	1.16000	1.17500	1.20500	1.22000	1.27500	1.33000	1.37662	1.40000	1.43000
13.	1.43500	1.44500	1.45000	1.46200	1.47000	1.47200	1.47500	1.51200	1.53400	1.55500
14.	1.60500	1.67200	1.71500	1.74500	1.76500	1.79000	1.82000	1.84500	1.87200	1.90000
15.	0.02500	0.35000	0.65000	0.85000	1.05000					
16.	1.11700	1.29200	1.30100	1.37000	1.38900	1.42500	1.46500	1.48000	1.50500	1.53000
17.	1.55000	1.56300	1.56500	1.57500	1.58200	1.59500	1.60500	1.63200	1.64700	1.65900
18.	1.68500	1.71200	1.73000	1.74500	1.76300	1.78000	1.79600	1.81500	1.84500	1.87500
19.	0.02500	0.45000	0.80000	1.05000	1.20000					
20.	1.36000	1.40165	1.43000	1.48291	1.49500	1.55500	1.57800	1.60650	1.61000	1.63000
21.	1.64500	1.65000	1.65500	1.66200	1.67750	1.68200	1.69000	1.69400	1.69600	1.70500
22.	1.72000	1.73000	1.74000	1.75500	1.76600	1.78300	1.79700	1.81300	1.82600	1.84200
23.	0.02500	0.35000	0.65000	1.05000	1.23000					
24.	1.43000	1.48000	1.49000	1.54800	1.60200	1.60500	1.63000	1.65700	1.67000	1.68200
25.	1.68800	1.69500	1.70000	1.70400	1.70469	1.71000	1.71800	1.72800	1.73000	1.73500
26.	1.74500	1.75500	1.76100	1.77000	1.78000	1.79100	1.79600	1.80600	1.81600	1.83000
27.	0.02500	0.40000	0.74500	1.10000	1.20000					
28.	1.24875	1.26000	1.27000	1.29200	1.31500	1.33500	1.36036	1.38800	1.42400	1.44914
29.	1.49000	1.52000	1.57200	1.60700	1.62114	1.64000	1.66500	1.67000	1.69800	1.71000
30.	1.71200	1.71500	1.71761	1.72190	1.73000	1.73500	1.75000	1.76500	1.77600	1.79000
31.	0.02500	0.65000	1.05000	1.17000	1.25000					
32.	1.31605	1.32500	1.33200	1.34740	1.36600	1.39200	1.42269	1.43500	1.45500	1.47839
33.	1.51400	1.54500	1.59000	1.63000	1.64119	1.65500	1.66939	1.68500	1.70500	1.70990
34.	1.71000	1.72500	1.73500	1.73600	1.73900	1.74200	1.75000	1.75800	1.76600	1.77000
35.	0.02500	0.60000	1.01300	1.20000	1.32800					
36.	1.35000	1.36000	1.36700	1.38730	1.39600	1.42000	1.43940	1.45200	1.47500	1.49680
37.	1.53000	1.54000	1.55065	1.58500	1.63000	1.65120	1.65700	1.68000	1.68500	1.69000
38.	1.69200	1.69600	1.70000	1.70600	1.71000	1.71600	1.72200	1.72900	1.73300	1.73500
39.	0.02500	0.85000	1.20000	1.25000	1.30000					
40.	1.32500	1.33200	1.34000	1.37300	1.41000	1.43000	1.46200	1.48000	1.50500	1.52500
41.	1.54600	1.56000	1.56500	1.59200	1.61192	1.63000	1.64500	1.65500	1.67000	1.6730
42.	1.67400	1.67500	1.67700	1.68000	1.68200	1.68400	1.68500	1.68600	1.68700	1.68800
43.	0.02500	0.65000	1.10000	1.20000	1.25000					
44.	1.28000	1.30000	1.34500	1.36700	1.39500	1.42500	1.46825	1.49000	1.50500	1.52500
45.	1.55020	1.55500	1.60000	1.60500	1.62500	1.63800	1.64000	1.64100	1.64200	1.64500
46.	1.64600	1.64800	1.64900	1.65000	1.65100	1.65200	1.65300	1.65400	1.65500	1.65600
47.	1.01700	1.02200	1.02800	1.03600	1.05200					
48.	1.05900	1.06700	1.07900	1.09100	1.10000	1.10300	1.10800	1.11000	1.11250	1.11500
49.	1.11800	1.14900	1.15400	1.15600	1.15700	1.16000	1.16100	1.16200	1.16300	1.1640
50.	1.20000	1.30000	1.40000	1.50000	1.60000	1.70000	1.90000	2.20000	2.00000	3.00000
51.	1.04200	1.05600	1.07000	1.11800	1.14200					
52.	1.17000	1.17200	1.18460	1.19900	1.20270	1.22300	1.24200	1.25400	1.26200	1.27040
53.	1.27640	1.28040	1.12800	1.29000	1.29500	1.30000	1.30500	1.31000	1.31500	1.3260
54.	1.40000	1.50000	1.60000	1.80000	2.00000	2.20000	2.40000	2.60000	2.80000	3.00000
55.	1.06200	1.07800	1.09200	1.11900	1.17600					
56.	1.23900	1.27010	1.28000	1.29300	1.30250	1.33110	1.36130	1.38960	1.40500	1.42650

57.	1.43160	1.44110	1.44890	1.45200	1.45730	1.46000	1.46600	1.50000	1.52000	1.5420
58.	1.60000	1.70000	1.80200	1.90000	2.00000	2.20000	2.40000	2.60000	2.80000	3.00000
59.	1.09100	1.11800	1.16200	1.20600	1.27600					
60.	1.38600	1.39760	1.40300	1.44830	1.45920	1.49320	1.52800	1.54350	1.57210	1.60350
61.	1.63050	1.65040	1.65300	1.67230	1.67980	1.69720	1.71210	1.75000	1.79000	1.81600
62.	1.90000	2.00000	2.10000	2.20000	2.30000	2.40000	2.50000	2.60000	2.80000	3.00000
63.	1.15800	1.18600	1.25300	1.34000	1.41900					
64.	1.53400	1.57000	1.59840	1.64700	1.66740	1.74450	1.80440	1.83900	1.85140	1.89190
65.	1.93760	1.95260	1.97210	1.98820	2.02800	2.06000	2.08000	2.10000	2.12000	2.14600
66.	2.20000	2.25000	2.30000	2.40000	2.50000	2.60000	2.70000	2.80000	2.90000	3.00000
67.	1.24000	1.26200	1.30000	1.42200	1.52000					
68.	1.71000	1.77100	1.78200	1.87000	1.97300	1.98200	2.03800	2.11600	2.18100	2.21700
69.	2.24100	2.26100	2.28500	2.31300	2.32500	2.35000	2.40000	2.45000	2.47000	2.49000
70.	2.55000	2.60000	2.65000	2.70000	2.75000	2.80000	2.85000	2.90000	2.95000	3.00300
71.	1.34200	1.36200	1.41000	1.52800	1.58200					
72.	1.61000	1.62000	1.63000	1.64900	1.67000	1.69000	1.71500	1.75000	1.80000	1.84700
73.	1.90400	1.94850	2.04850	2.13250	2.16400	2.23560	2.29000	2.36130	2.43660	2.50140
74.	2.50670	2.52600	2.54300	2.55700	2.64000	2.68200	2.76000	2.84000	2.92000	3.00000
75.	1.50400	1.53800	1.63300	1.68000	1.72300					
76.	1.77100	1.78000	1.79000	1.80500	1.83000	1.86000	1.90700	1.93000	1.96000	1.99500
77.	2.05800	2.12170	2.23090	2.33750	2.38200	2.43660	2.52700	2.56460	2.65240	2.66660
78.	2.68840	2.77620	2.81700	2.82900	2.84000	2.86000	2.90000	2.94000	2.98000	3.00000
79.	1.62000	1.64300	1.72000	1.78400	1.86000					
80.	1.87900	1.89000	1.90000	1.91700	1.94000	1.97000	2.01900	2.03000	2.08000	2.12600
81.	2.20500	2.22770	2.24800	2.34010	2.46850	2.52600	2.56530	2.64350	2.67300	2.70000
82.	2.72000	2.74000	2.76000	2.78000	2.82000	2.86000	2.90000	2.94000	2.98000	3.00000
83.	1.74000	1.80000	1.90400	1.92800	1.95700					
84.	1.97600	1.98000	1.99000	2.02100	2.07000	2.10000	2.14100	2.18000	2.23000	2.27300
85.	2.34000	2.37260	2.38600	2.45640	2.51300	2.57490	2.65900	2.71100	2.81080	2.82000
86.	2.83000	2.84000	2.86000	2.88000	2.90000	2.92000	2.94000	2.96000	2.98000	3.00000
87.	1.88000	1.93300	2.02900	2.06700	2.08900					
88.	2.10400	2.12000	2.14000	2.15300	2.17500	2.20000	2.26200	2.30000	2.34000	2.39400
89.	2.47000	2.47550	2.63360	2.66100	2.76710	2.85950	2.87000	2.88000	2.89000	2.9000
90.	2.91000	2.92000	2.93000	2.94000	2.95000	2.96000	2.97000	2.98000	2.99000	3.00000
91.	1166.80	1755.77	2331.46	2924.63	3508.47	4062.22	4555.95	4957.72	5248.55	5551.00
92.	5822.62									
93.	1.01700	1.02200	1.02800	1.03600	1.05200					
94.	1.05900	1.06700	1.07900	1.09120	1.10000	1.10300	1.10800	1.11000	1.11250	1.11500
95.	1.11800	1.14900	1.15400	1.15600	1.15700	1.16000	1.16100	1.16200	1.16300	1.1640
96.	1.20000	1.30000	1.40000	1.50000	1.60000	1.70000	1.90000	2.20000	2.60000	3.00000
97.	1.04200	1.05600	1.07000	1.11800	1.14200					
98.	1.17000	1.17200	1.18460	1.19900	1.20270	1.22300	1.24200	1.25400	1.26200	1.27040
99.	1.27640	1.28040	1.12650	1.29000	1.29500	1.30000	1.30500	1.31000	1.31500	1.3260
100.	1.40000	1.50000	1.60000	1.80000	2.00000	2.20000	2.40000	2.60000	2.80000	3.00000
101.	1.06200	1.07800	1.09200	1.11900	1.17600					
102.	1.23900	1.27010	1.28000	1.29300	1.30250	1.33110	1.36130	1.38960	1.40500	1.42650
103.	1.43160	1.44110	1.44890	1.45200	1.45730	1.46000	1.46600	1.50000	1.52000	1.5420
104.	1.60000	1.70200	1.80000	1.90000	2.00000	2.20000	2.40000	2.60000	2.80000	3.00000
105.	1.09100	1.11800	1.16200	1.20600	1.27600					
106.	1.38600	1.39760	1.40300	1.44830	1.45900	1.49320	1.52800	1.54350	1.57210	1.60350
107.	1.63050	1.65040	1.65300	1.67230	1.67980	1.69720	1.71210	1.75000	1.79000	1.81600
108.	1.90000	2.00000	2.10000	2.20000	2.30000	2.40000	2.50000	2.60000	2.80000	3.00000
109.	1.15800	1.18600	1.25300	1.34000	1.41900					
110.	1.53400	1.57000	1.59840	1.64700	1.66740	1.74450	1.80440	1.83900	1.85140	1.89190
111.	1.93760	1.95260	1.97210	1.98820	2.02800	2.06000	2.08000	2.10000	2.12000	2.14600
112.	2.20000	2.25000	2.30000	2.40000	2.50000	2.60000	2.70000	2.80000	2.90000	3.00000

113.	1.24000	1.26200	1.30000	1.42200	1.52000					
114.	1.71000	1.77100	1.78200	1.87000	1.97300	1.98200	2.03600	2.11600	2.18100	2.21700
115.	2.24100	2.26100	2.28500	2.31300	2.32500	2.35000	2.40000	2.45000	2.47000	2.49000
116.	2.55000	2.60200	2.65000	2.70000	2.75000	2.80000	2.85000	2.90000	2.95000	3.00000
117.	1.34200	1.36200	1.41000	1.52800	1.58000					
118.	1.61000	1.62000	1.63000	1.64000	1.67000	1.69000	1.71500	1.75000	1.80000	1.84700
119.	1.90400	1.94850	2.04850	2.13250	2.16400	2.23560	2.29000	2.36130	2.43060	2.50140
120.	2.50670	2.52600	2.54300	2.55700	2.64000	2.68000	2.76000	2.84000	2.92000	3.00000
121.	1.50400	1.53800	1.63300	1.68000	1.72300					
122.	1.77100	1.78000	1.79000	1.80500	1.83000	1.86000	1.90700	1.93000	1.96000	1.99500
123.	2.05800	2.12170	2.23090	2.33750	2.38200	2.43660	2.52700	2.56460	2.65240	2.66660
124.	2.68840	2.77620	2.81700	2.82980	2.84000	2.86000	2.90000	2.94000	2.98000	3.00000
125.	1.62000	1.64300	1.72000	1.78400	1.86000					
126.	1.87900	1.89000	1.98000	1.91700	1.94000	1.97020	2.01900	2.03000	2.06000	2.12600
127.	2.20500	2.22770	2.24800	2.34010	2.46850	2.52600	2.56530	2.64350	2.67300	2.70000
128.	2.72000	2.74000	2.76000	2.78000	2.82000	2.86000	2.90000	2.94000	2.98000	3.00000
129.	1.74000	1.82000	1.90400	1.92800	1.95700					
130.	1.97600	1.98800	1.99000	2.02100	2.07000	2.10000	2.14100	2.18000	2.23000	2.27300
131.	2.34000	2.37260	2.38600	2.45640	2.51300	2.57490	2.65900	2.71100	2.81080	2.82000
132.	2.83000	2.84000	2.86000	2.88000	2.90000	2.92000	2.94000	2.96000	2.98000	3.00000
133.	1.88000	1.93300	2.02900	2.06700	2.08900					
134.	2.10400	2.12000	2.14000	2.15300	2.17500	2.20000	2.26200	2.30000	2.34000	2.39400
135.	2.47000	2.47550	2.63360	2.66100	2.76710	2.85090	2.87000	2.88000	2.89200	2.9000
136.	2.91000	2.92000	2.93000	2.94000	2.95000	2.96000	2.97000	2.98000	2.99000	3.00000
137.	0.10000	0.16000	0.23000	0.32000	0.51000					
138.	0.58661	0.61000	0.63700	0.65225	0.65600	0.66000	0.66100	0.66200	0.66300	0.66400
139.	0.66500	0.66900	0.66790	0.66780	0.66770	0.66750	0.66740	0.66730	0.66720	0.6671
140.	0.66550	0.65500	0.64150	0.62700	0.61550	0.60550	0.59750	0.56700	0.55450	0.55000
141.	0.10000	0.16500	0.23500	0.47000	0.58000					
142.	0.63000	0.63162	0.64000	0.64900	0.65100	0.65842	0.66000	0.66755	0.67000	0.6710
143.	0.67150	0.67200	0.67250	0.67280	0.67270	0.67500	0.67230	0.67200	0.67180	0.67090
144.	0.66050	0.64350	0.62750	0.60400	0.58650	0.57350	0.56400	0.55800	0.55520	0.55200
145.	0.10000	0.14700	0.18600	0.25200	0.40000					
146.	0.56200	0.61300	0.52000	0.62850	0.63400	0.64750	0.65800	0.66600	0.65900	0.67300
147.	0.67400	0.67500	0.67600	0.67691	0.67700	0.67784	0.67800	0.68000	0.67900	0.67850
148.	0.67300	0.65400	0.63400	0.62000	0.60800	0.58500	0.56950	0.56220	0.55950	0.55700
149.	0.10000	0.14300	0.21000	0.27600	0.36400					
150.	0.55200	0.56250	0.57106	0.60800	0.61500	0.63400	0.65150	0.65800	0.66750	0.67600
151.	0.68100	0.68200	0.68395	0.68500	0.68600	0.68580	0.68520	0.68300	0.67600	0.67000
152.	0.64820	0.62700	0.61300	0.60300	0.59300	0.58400	0.57800	0.57350	0.56970	0.56900
153.	0.10000	0.13600	0.21500	0.31800	0.41120					
154.	0.54800	0.58100	0.60200	0.62950	0.63800	0.66000	0.67300	0.67846	0.68000	0.68550
155.	0.68900	0.68880	0.68850	0.68810	0.68151	0.67120	0.66400	0.65500	0.64600	0.63400
156.	0.63300	0.62400	0.61640	0.60450	0.59450	0.58700	0.58270	0.57950	0.57800	0.57650
157.	0.10000	0.11900	0.15200	0.25800	0.34300					
158.	0.50750	0.55100	0.55800	0.60950	0.65100	0.65300	0.66900	0.68400	0.69000	0.68950
159.	0.68800	0.68500	0.68150	0.67650	0.67300	0.66650	0.65500	0.64150	0.63520	0.62900
160.	0.61550	0.60750	0.60250	0.59850	0.59550	0.59300	0.59150	0.59000	0.58850	0.58690
161.	0.10000	0.11300	0.14800	0.23300	0.27000					
162.	0.29100	0.29850	0.30550	0.31950	0.33400	0.34820	0.36650	0.39150	0.42700	0.46000
163.	0.50100	0.52900	0.57900	0.60000	0.61900	0.63550	0.65300	0.66750	0.67900	0.68600
164.	0.68800	0.68960	0.69150	0.69300	0.69900	0.69700	0.69200	0.68250	0.66950	0.65200
165.	0.10000	0.12500	0.19100	0.22500	0.25550					
166.	0.29000	0.29600	0.30300	0.31350	0.33200	0.35300	0.38600	0.40250	0.42350	0.44850
167.	0.49300	0.53700	0.59600	0.62900	0.64100	0.65400	0.67268	0.67950	0.69100	0.69286
168.	0.69400	0.69800	0.69850	0.69842	0.69820	0.69600	0.69350	0.69100	0.69400	0.67920

169.	0.10000	0.11500	0.16550	0.20700	0.25700					
170.	0.27000	0.27750	0.28400	0.29500	0.31000	0.32950	0.36200	0.36900	0.40200	0.43200
171.	0.48350	0.49050	0.51300	0.56650	0.62200	0.63965	0.64800	0.66350	0.66880	0.67300
172.	0.67620	0.67900	0.68120	0.68310	0.68710	0.69100	0.69420	0.69750	0.69950	0.70000
173.	0.10000	0.13650	0.19950	0.21400	0.23150					
174.	0.24300	0.24550	0.25150	0.27000	0.30000	0.31850	0.34350	0.36700	0.39700	0.42350
175.	0.46350	0.46700	0.49362	0.53800	0.57088	0.60000	0.63369	0.65000	0.67450	0.67600
176.	0.67800	0.68200	0.63300	0.68590	0.68800	0.69000	0.69150	0.69250	0.69310	0.6940
177.	0.10000	0.13000	0.18300	0.20400	0.21600					
178.	0.22400	0.23300	0.24450	0.25150	0.26400	0.27750	0.31150	0.33250	0.35450	0.38550
179.	0.42550	0.42850	0.51600	0.53000	0.55100	0.62300	0.62800	0.63200	0.63650	0.64120
180.	0.64500	0.64950	0.65350	0.65800	0.66250	0.66650	0.67100	0.67510	0.67920	0.6832
181.	20000.00	30000.00	40000.00	50000.00	60000.00	70000.00	78000.00	85000.00		
182.	90000.00	95000.00	100000.00							
183.	0.01409	0.01450	0.01680	0.02100	0.02303	0.02360	0.02493	0.02540	0.02571	0.02600
184.	0.02690	0.03176	0.03709	0.03802	0.04100	0.04200	0.04300	0.04400	0.04500	0.04600
185.	0.01631	0.01700	0.01905	0.02700	0.02781	0.03699	0.04964	0.05493	0.05901	0.06307
186.	0.06449	0.06613	0.06900	0.07100	0.07300	0.07500	0.07700	0.07900	0.08200	0.08550
187.	0.01751	0.02288	0.02600	0.03040	0.03436	0.04548	0.05660	0.06639	0.06936	0.07734
188.	0.08002	0.08285	0.08435	0.08500	0.08562	0.08680	0.08741	0.09980	0.10600	0.11400
189.	0.01855	0.02576	0.02700	0.03715	0.04380	0.05410	0.06520	0.06753	0.07817	0.08547
190.	0.09286	0.09827	0.09840	0.10248	0.10520	0.10823	0.11020	0.12820	0.14140	0.15070
191.	0.02230	0.03660	0.04258	0.05580	0.06024	0.07785	0.09187	0.10160	0.10278	0.11230
192.	0.12181	0.12527	0.12871	0.13169	0.14450	0.15120	0.15440	0.16240	0.16640	0.17300
193.	0.02966	0.04380	0.04594	0.06396	0.08364	0.08840	0.10098	0.11615	0.12837	0.13653
194.	0.14234	0.14611	0.15047	0.15409	0.16180	0.16960	0.18400	0.20000	0.20560	0.21150
195.	0.03686	0.04410	0.06199	0.07820	0.09600	0.09892	0.11150	0.12104	0.13464	0.14690
196.	0.15522	0.16260	0.16600	0.16760	0.17080	0.17780	0.19100	0.20500	0.21840	0.23200
197.	0.03795	0.04841	0.06776	0.09168	0.09880	0.10836	0.12580	0.12904	0.14438	0.15230
198.	0.15421	0.16413	0.17090	0.17260	0.17460	0.17770	0.18380	0.19020	0.19620	0.19980
199.	0.03756	0.04414	0.05160	0.06494	0.08943	0.10740	0.10918	0.13004	0.14020	0.14750
200.	0.15330	0.15910	0.16480	0.17050	0.18160	0.19320	0.20590	0.21640	0.22770	0.23340
201.	0.04305	0.04644	0.05300	0.06302	0.07880	0.08323	0.10860	0.10917	0.12990	0.13210
202.	0.13410	0.13610	0.14010	0.14400	0.14800	0.15210	0.15600	0.16010	0.16400	0.16820
203.	0.04515	0.04614	0.06717	0.07540	0.08610	0.10615	0.11640	0.11930	0.12220	0.12510
204.	0.12800	0.13090	0.13380	0.13670	0.13950	0.14240	0.14530	0.14820	0.15110	0.15400
205.	1.01700	1.02200	1.02600	1.03000	1.03300	1.03400	1.03560	1.03620	1.03700	1.03770
206.	1.03800	1.04500	1.03800	1.03200	1.02500	1.02000	1.01700	1.01300	1.00800	1.00200
207.	1.09970	1.09950	1.10000	1.10950	1.11020	1.11710	1.09900	1.09020	1.07940	1.06780
208.	1.06350	1.05860	1.05000	1.04400	1.03800	1.03200	1.02600	1.02000	1.01100	1.00200
209.	1.17720	1.21700	1.22300	1.22500	1.22600	1.21760	1.20320	1.18080	1.17070	1.14890
210.	1.13380	1.12380	1.11890	1.11400	1.11260	1.11000	1.10940	1.05600	1.03200	1.00200
211.	1.27740	1.35220	1.35400	1.36390	1.36280	1.35760	1.33900	1.33510	1.30550	1.27440
212.	1.24280	1.22130	1.22000	1.20320	1.19650	1.18340	1.18060	1.09300	1.03700	1.00200
213.	1.41100	1.53200	1.54560	1.54500	1.54090	1.50800	1.46600	1.42200	1.41610	1.36440
214.	1.30790	1.29100	1.27400	1.26400	1.17200	1.13300	1.11300	1.10660	1.04300	1.00200
215.	1.70400	1.77500	1.78100	1.77800	1.72800	1.70600	1.66000	1.59300	1.52600	1.47900
216.	1.44600	1.42300	1.40400	1.38800	1.32800	1.27600	1.18200	1.07400	1.03800	1.00400
217.	1.92100	2.00630	2.01430	1.97440	1.90600	1.89470	1.83400	1.78800	1.70950	1.63970
218.	1.58980	1.53200	1.50800	1.49700	1.47700	1.43120	1.34600	1.28600	1.17100	1.08200
219.	2.12900	2.26830	2.24890	2.16000	2.10200	2.04590	1.93400	1.91360	1.80730	1.75500
220.	1.74310	1.69050	1.62900	1.61700	1.60400	1.58300	1.54200	1.49800	1.45800	1.43400
221.	2.26600	2.43800	2.45700	2.45900	2.37100	2.24800	2.23900	2.08100	2.00600	1.94900
222.	1.90600	1.86200	1.82000	1.77920	1.69400	1.61000	1.51600	1.43700	1.35400	1.30800
223.	2.54400	2.63500	2.66000	2.66800	2.61800	2.58600	2.38400	2.37900	2.20300	2.18600
224.	2.17100	2.15600	2.12500	2.09500	2.06600	2.03300	2.00400	1.97100	1.94200	1.91000

225. 2.75300 2.96900 2.96200 2.91600 2.72600 2.53200 2.46800 2.44400 2.41000 2.39400
226. 2.37000 2.34700 2.32200 2.29600 2.27200 2.24900 2.22400 2.20000 2.17600 2.15200
227. 0.20051 0.20673 0.20804 0.23251 0.24303 0.24623 0.25017 0.24973 0.24949 0.24916
228. 0.24830 0.23402 0.22100 0.18180 0.15720 0.12595 0.10809 0.08439 0.05871 0.01339
229. 0.24277 0.24465 0.24491 0.32758 0.32954 0.39234 0.39597 0.36933 0.33089 0.29124
230. 0.27113 0.24923 0.21934 0.19655 0.17100 0.14609 0.11950 0.09318 0.05220 0.01920
231. 0.30834 0.37619 0.41981 0.43920 0.47583 0.51716 0.51525 0.47495 0.44134 0.39541
232. 0.36933 0.34273 0.32696 0.30788 0.30325 0.29506 0.29245 0.15578 0.29986 0.08574
233. 0.29562 0.41827 0.42239 0.47134 0.52144 0.56002 0.55220 0.54917 0.53270 0.48569
234. 0.44148 0.40869 0.39431 0.37254 0.36257 0.33564 0.32591 0.17745 0.07635 0.00299
235. 0.32459 0.48787 0.52195 0.56424 0.57682 0.57512 0.55327 0.51487 0.50844 0.46032
236. 0.40738 0.38834 0.36686 0.35255 0.24079 0.18828 0.16141 0.15280 0.06342 0.00301
237. 0.45971 0.54216 0.55958 0.59574 0.57780 0.57274 0.56643 0.52059 0.47694 0.44899
238. 0.42664 0.40912 0.39516 0.38062 0.33069 0.29551 0.19607 0.08422 0.04383 0.00470
239. 0.49713 0.54363 0.59587 0.62215 0.62832 0.59813 0.54765 0.54174 0.49881 0.45987
240. 0.43929 0.39920 0.38367 0.37464 0.36281 0.33252 0.27386 0.23165 0.14376 0.07108
241. 0.47910 0.54158 0.57143 0.58315 0.56063 0.54773 0.50701 0.48300 0.45060 0.43157
242. 0.42819 0.40694 0.37346 0.37243 0.36668 0.35643 0.33643 0.31441 0.29292 0.29059
243. 0.45019 0.51522 0.53994 0.57761 0.58386 0.56193 0.55947 0.52268 0.50003 0.48195
244. 0.46762 0.45212 0.43650 0.42068 0.38591 0.34911 0.30671 0.26582 0.22179 0.19608
245. 0.49390 0.52106 0.54341 0.57767 0.57704 0.57368 0.54390 0.53897 0.50063 0.49657
246. 0.49283 0.48900 0.48034 0.47143 0.46298 0.45321 0.44309 0.43371 0.42409 0.41375
247. 0.54917 0.57263 0.58775 0.55319 0.54925 0.52453 0.51109 0.50663 0.50147 0.49659
248. 0.49176 0.48695 0.48145 0.47574 0.46990 0.46456 0.45852 0.45264 0.44664 0.43992
249. 1.0000 1.0500 1.1000 1.1500 1.2000 1.3000 1.4000 1.5000 1.6000 1.7000 1.8000
250. 1.9000 2.0000 2.1000 2.2000 2.3000 2.4000 2.5000 2.6000 2.7000 2.8000 2.9000
251. 3.0000
252. 0.0000 0.0274 0.0377 0.0451 0.0507 0.0559 0.0674 0.0729 0.0797 0.0796 0.0820
253. 0.0840 0.0862 0.0883 0.0904 0.0924 0.0943 0.0963 0.0982 0.1001 0.1019 0.1037
254. 0.1055
255. 0.2912E+03 0.1104E-03 0.1205E+01 0.1400E+01 0.1000E+01 0.1200E-01
256. 0.95000E+00
257. 0.2689E+01 0.2942E+03 0.2870E+00 0.1059E-01 0.2842E+03 0.1193E+01
258. 0.1000E-02 0.1500E+01
259. 12
260. 0.077571E-06 0.85E+00
261. 0.071281E-03 0.69E+00
262. 0.144391E-03 0.59E+00
263. 0.219328E-03 0.51E+00
264. 0.296092E-03 0.43E+00
265. 0.374684E-03 0.36E+00
266. 0.455104E-03 0.30E+00
267. 0.537260E-03 0.25E+00
268. 0.320110E-02 0.22E+00
269. 0.418590E-02 0.20E+00
270. 0.536623E-02 0.18E+00
271. 0.674469E-02 0.17E+00
272. 37
273. 0.0000E+00 0.7760E-06 0.1821E-04 0.3450E-04
274. 0.8300E-03 0.8530E-06 0.9247E-05 0.2154E-03
275. 0.1670E-02 0.8530E-06 0.2872E-05 0.4298E-03
276. 0.2500E-02 0.8530E-06 0.7750E-06 0.3108E-02
277. 0.3330E-02 0.8530E-06 0.6210E-06 0.4254E-02
278. 0.4170E-02 0.9530E-06 0.6980E-06 0.5995E-02
279. 0.5000E-02 0.7760E-06 0.6210E-06 0.6405E-02
280. 0.5830E-02 0.6980E-06 0.6980E-06 0.5870E-02

281.	0.6670E-02	0.1009E-05	0.8530E-06	0.4549E-02
282.	0.7500E-02	0.4114E-05	0.9310E-06	0.2908E-02
283.	0.8330E-02	0.1041E-04	0.9310E-06	0.4056E-03
284.	0.9170E-02	0.2126E-04	0.7760E-06	0.1891E-03
285.	0.1000E-01	0.3450E-04	0.7760E-06	0.2674E-04
286.	0.1083E-01	0.2154E-03	0.8530E-06	0.1821E-04
287.	0.1167E-01	0.4298E-03	0.8530E-06	0.9247E-05
288.	0.1250E-01	0.3108E-02	0.8530E-06	0.2872E-05
289.	0.1333E-01	0.4754E-02	0.8530E-06	0.7760E-06
290.	0.1417E-01	0.5985E-02	0.8530E-06	0.6210E 06
291.	0.1500E-01	0.6405E-02	0.7760E-06	0.6980E-06
292.	0.1583E-01	0.5870E-02	0.6980E-06	0.6212E-06
293.	0.1667E-01	0.4549E-02	0.1009E-05	0.6980E-06
294.	0.1750E-01	0.2908E-02	0.4114E-05	0.8530E-06
295.	0.1833E-01	0.4056E-03	0.1041E-04	0.9310E-06
296.	0.1917E-01	0.1891E-03	0.2126E-04	0.9310E-06
297.	0.2000E-01	0.2674E-04	0.3450E-04	0.7760E-06
298.	0.2083E-01	0.1821E-04	0.2154E-03	0.7760E-06
299.	0.2167E-01	0.9247E-05	0.4298E-03	0.8530E-06
300.	0.2250E-01	0.2872E-05	0.3108E-02	0.8530E-06
301.	0.2333E-01	0.7760E-06	0.4754E-02	0.8530E-06
302.	0.2417E-01	0.6210E-06	0.5985E-02	0.8530E-06
303.	0.2500E-01	0.6980E-06	0.6405E-02	0.8530E-06
304.	0.2583E-01	0.6210E-06	0.5870E-02	0.7760E-06
305.	0.2667E-01	0.6980E+06	0.4549E-02	0.6980E-06
306.	0.2750E-01	0.8530E-06	0.2908E-02	0.1009E-05
307.	0.2833E-01	0.9310E-06	0.4056E-03	0.4114E-05
308.	0.2917E-01	0.9310E-06	0.1891E-03	0.1041E-04
309.	0.3000E-01	0.7760E-06	0.2674E-04	0.2126E-04

MISSING

PRINT

Line No	Nomen-clature	Definition	Units	Value in Sample
		Turbine Mass Characteristics (Fig 6.3)		
1&2	XNRT3	$\frac{N}{\sqrt{T_3}}$, turbocharger speed parameter	rpm/$\sqrt{K}$	Array
3-46	XAMFP	$\frac{\dot{m}_t\sqrt{T_3}}{P_3}$, turbine mass parameter	$\frac{kg\sqrt{K}}{sec\ bar}$	Array
47-90	XP3DPO	$\frac{P_3}{P_4}$, turbine pressure ratio	-	Array
		Turbine Efficiency Characteristics (Fig 6.4)		
91&92	XN	$\frac{N}{\sqrt{T_3}}$, turbocharger speed parameter	rpm/$\sqrt{K}$	Array
93-136	XP	$\frac{P_3}{P_4}$, turbine pressure ratio	-	Array
137-180	XT	η_t, turbine efficiency	-	Array
		Compressor Steady Characteristics (Fig 6.5)		
181&182	XCS	N, turbocharger speed	rpm	Array
183-204	XA	$\dot{m}_c$, compressor mass flow rate	kg/sec	Array
205-226	XPC	$\frac{P_2}{P_1}$, compressor pressure ratio	-	Array
227-248	XCE	η_c, compressor efficiency	-	Array
		Compressor Loading Nozzle Characteristics (Fig 5.9)		
249-251	XP2	P_2, compressor loading nozzle inlet pressure	bar	Array
252-254	XAMO	$\frac{\dot{m}_z}{\rho_2^{1/2}}$, compressor loading nozzle mass flow rate divided by square root of density	$\frac{kg}{sec\sqrt{kg/m^3}}$	Array
255	T1	T_1, compressor inlet temperature	K	292.2
"	AI	I, turbocharger moment of	$kg.m^2$	0.1104×10^{-3}

Line No	Nomen clature	Definition	Units	Value in Sample
255	CP	C_p, specific heat at constant pressure	kJ/kg.K	1.005
"	GAM	γ, ratio of specific heats	-	1.4
"	PO	P_o, atmospheric pressure	bar	1.0
"	ERROR	Permitted error of iterative procedure	-	0.01
256	MEFF	η_m, turbocharger mechanical efficiency		0.95
257	PG	P_u, pulse generator input pressure	bar	2.689
"	TG	T_u, pulse generator input pressure	K	284.2
"	GASR	R, characteristic gas constant	kJ/kg.k	0.287
"	VS	V_s, exhaust system volume	m^3	0.1099×10^{-1}
"	T3	T_3, turbine initial inlet temperature	K	284.2
"	P3	P_3, turbine initial inlet pressure	bar	1.193
258	DT	Δt, time step	sec	0.001
"	TMAX	t_{max}, calculation time required	sec	1.5
259	NTM	Number of data points for valve opening areas against valve coefficients of discharge	-	12
260-271	AFG	Pulse generator valve opening area	m^2	Array
	ACDG	C_d, pulse generator valve coefficient of discharge	-	Array
272	NTN	Number of data points for pulse generator valves cycle time against pulse generator valves opening areas, (Fig 3.15)	-	Array

Line No	Nomen-clature	Definition	Units	Value in Sample
273-309	BTIME	Pulse generator valve cycle time, (Fig 5.3)	sec	Array
	BFG(1)	First pulse generator valve opening area, (Fig 5.3)	m^2	Array
	BFG(2)	Second pulse generator valve opening area, (Fig 5.3)	m^2	Array
	BFG(3)	Third pulse generator valve opening area, (Fig 5.3)	m^2	Array

PROGRAM PULSATING2 INPUT DATA

Line No.				
1-254	As in program Pulsating1 input data (page 299)			
255	0.2964E+03	0.1104E-03	0.1005E+01	0.1400E+01	0.1000E-01
256	0.1027E+01	0.1050E+01		
257	0.000	1.195	293.70	25715.00
258	0.050	1.155	292.95	25715.00
259	0.100	1.101	292.95	25715.00
260	0.150	1.101	300.60	25715.00
261	0.158	1.344	305.40	25715.00
262	0.200	1.693	303.60	26062.00
263	0.223	1.227	234.70	26410.00
264	0.223	1.704	302.70	26410.00
265	0.253	1.251	283.30	26757.00
266	0.257	1.775	303.60	27105.00
267	0.280	1.224	234.40	27300.00
268	0.288	1.763	302.70	28495.00
269	0.306	1.259	284.70	28342.00
270	0.315	1.741	302.40	29190.00
271	0.334	1.279	284.70	29190.00
272	0.340	1.720	302.70	29537.00
273	0.358	1.287	284.70	30232.00
274	0.365	1.709	302.40	30580.00
275	0.382	1.290	285.00	31275.00
276	0.390	1.691	302.10	31622.00
277	0.406	1.302	285.30	31970.00
278	0.415	1.697	301.30	31970.00
279	0.432	1.302	235.00	32317.00
280	0.439	1.697	301.30	32665.00
281	0.455	1.302	235.00	33012.00
282	0.462	1.697	301.80	33360.00
283	0.478	1.316	235.00	33707.00
284	0.487	1.696	301.50	34055.00
285	0.503	1.312	285.00	34750.00
286	0.510	1.683	301.20	34750.00
287	0.526	1.312	235.00	35097.00
288	0.535	1.683	301.20	35445.00
289	0.550	1.312	235.00	35792.00
290	0.558	1.683	301.50	36140.00
291	0.573	1.312	235.00	36487.00
292	0.580	1.696	301.50	36835.00
293	0.596	1.312	235.00	37182.00
294	0.605	1.696	301.20	37530.00
295	0.622	1.312	235.00	37877.00
296	0.628	1.696	301.20	38225.00
297	0.645	1.312	235.00	38225.00
298	0.651	1.696	301.20	38572.00
299	0.668	1.312	235.00	38572.00
300	0.675	1.696	301.20	38920.00
301	0.692	1.312	235.00	39267.00
302	0.698	1.696	301.20	39267.00
303	0.713	1.325	235.00	39615.00
304	0.722	1.696	301.20	39962.00
305	0.738	1.325	235.00	39962.00
306	0.745	1.696	301.20	40310.00
307	0.759	1.339	235.00	40310.00
308	0.768	1.696	301.20	40657.00

309	0.775	1.339	235.00	41005.00
310	0.782	1.696	301.20	41005.00
311	0.808	1.339	235.00	41005.00
312	0.816	1.696	301.20	41352.00
313	0.830	1.339	235.00	41352.00
314	0.838	1.696	301.20	41352.00
315	0.855	1.339	235.00	41352.00
316	0.862	1.696	301.20	41352.00
317	0.878	1.339	235.00	42047.00
318	0.885	1.696	301.20	42047.00
319	0.902	1.339	235.00	42395.00
320	0.908	1.696	301.20	42395.00
321	0.924	1.339	235.00	42395.00
322	0.931	1.696	301.20	42395.00
323	0.948	1.339	235.00	42742.00
324	0.955	1.696	301.20	43090.00
325	0.970	1.339	235.00	43090.00
326	0.978	1.696	301.20	43090.00
327	0.994	1.339	235.00	43437.00
328	1.002	1.696	301.20	43437.00
329	1.018	1.339	235.00	43785.00
330	1.025	1.696	301.20	43785.00
331	1.041	1.339	235.00	43785.00
332	1.049	1.696	301.20	43785.00
333	1.065	1.339	235.00	43785.00
334	1.070	1.696	301.20	43785.00
335	1.088	1.339	235.00	43785.00
336	1.095	1.696	301.20	43785.00
337	1.110	1.339	235.00	43785.00
338	1.118	1.696	301.20	43785.00
339	1.134	1.339	235.00	44132.00
340	1.140	1.696	301.20	44480.00
341	1.158	1.339	235.00	44480.00
342	1.164	1.696	301.20	44480.00
343	1.181	1.339	235.00	44480.00
344	1.188	1.696	301.20	44480.00
345	1.204	1.339	235.00	44480.00
346	1.210	1.696	301.20	44480.00
347	1.228	1.339	235.00	44480.00
348	1.234	1.696	301.20	44480.00
349	1.252	1.339	235.00	44480.00
350	1.258	1.696	301.20	44480.00
351	1.274	1.339	235.00	44827.00
352	1.282	1.696	301.20	44827.00
353	1.298	1.339	235.00	44827.00
354	1.308	1.696	301.20	44827.00
355	1.322	1.339	235.00	44827.00
356	1.328	1.696	301.20	44827.00
357	1.343	1.339	235.00	44827.00

Line No	Nomen-calture	Definition	Units	Value in Sample
1-254		as in PROGRAM-PULSATING1 INPUT DATA	-	-
255	T1	T_1, compressor inlet temperature	K	296.4
"	AI	I, turbocharger moment of inertia	$kg.m^2$	0.1104×10^{-3}
"	CP	C_p, specific heat at constant pressure	kJ/kg.K	1.005
"	GAM	γ, ratio of specific heats	-	1.4
"	ERROR	Permitted error of iterative procedures	-	0.01
256	PO	P_o, Atmospheric pressure	bar	1.027
"	P4	P_4, Initial turbine exhaust pressure	bar	1.050
257-357	TIMED	t, time	sec	Array
	P3DPOD	$\frac{P_3}{P_4}$, turbine pressure ratio	-	Array
	T3D	T_3, turbine inlet temperature	K	Array
	CSPEDD	N, turbocharger speed	rpm	Array

PROGRAM NON-PULSATING INPUT DATA

Line No.					
1-254	As in Program Pulsatingl Input Data				
255	0.2959E+03	0.1104E-03	0.1005E+01	0.1400E+01	0.1000E-01
256	0.1036E+01	0.1043E+01			
257	0.0010E+00				
258	0.00	1.27500	281.30		
259	0.10	1.60300	232.60		
260	0.20	1.66700	280.60		
261	0.30	1.69400	232.60		
262	0.40	1.99200	233.20		
263	0.50	2.02000	230.60		
264	0.60	1.99300	273.60		
265	0.70	1.93600	273.60		
266	0.80	1.93200	273.60		
267	0.90	1.97900	273.60		
268	900000.00				

Line No	Nomen-clature	Definition	Units	Value in Sample
1-254		as in PROGRAM-PULSATING1 INPUT DATA	-	-
255	T1	T_1, compressor inlet temperature	K	295.9
	A1	I, turbocharger moment of inertia	$kg.m^2$	0.1104×10^{-3}
	CP	C_p, specific heat at constant pressure	kJ/kg.K	1.005
	GAM	γ, ratio of specific heats	-	1.4
	ERROR	Permitted error of iterative procedures	-	0.01
256	PO	P_o, Atmospheric pressure	bar	1.036
	P4	P_4, Initial turbine exhaust pressure	bar	1.048
257	ERROR1	Permitted error of iterative procedures		0.001
258-267	TIMED	t, time	sec	Array
	P3DPOD	$\frac{P_3}{P_4}$, turbine pressure ratio	-	Array
	T3D	T_3, turbine inlet temperature	K	Array